UNIVERSIDAD AUTÓNOMA DE BARCELONA

FACULTAD DE CIENCIAS

Departamento de Genética y Microbiología

IMPACTO DEL PETRÓLEO EN LA DISTRIBUCIÓN Y BIOMASA DE LAS CIANOBACTERIAS EN ECOSISTEMAS NATURALES Y ARTIFICIALES

Elia Diestra Villanueva

2005

UNIVERSIDAD AUTÓNOMA DE BARCELONA

FACULTAD DE CIENCIAS

Departamento de Genética y Microbiología

IMPACTO DEL PETRÓLEO EN LA DISTRIBUCIÓN Y BIOMASA DE LAS CIANOBACTERIAS EN ECOSISTEMAS NATURALES Y ARTIFICIALES

Memoria redactada para optar al Grado de Doctor en Biotecnología por la universidad Autónoma de Barcelona, por Elia Diestra Villanueva.

VºBº de los Directores de Tesis

Dra. Isabel Esteve Martínez

Dr. Antonio Solé i Cornellà

Bellaterra, Octubre del 2005

La ciencia, a pesar de sus progresos increíbles, no puede ni nunca podrá explicarlo todo. Cada vez ganará nuevas zonas a lo que hoy parece inexplicable. Pero las rayas fronterizas del saber, por muy lejos que se eleven, tendrán siempre delante un infinito mundo de misterio.

Gregorio Marañón

ÍNDICE

Índice

Resumen

En el presente trabajo se ha estudiado el efecto del petróleo en las cianobacterias, bacterias fototróficas oxigénicas que forman las poblaciones dominantes de los tapetes microbianos. Se trata de ambientes bentónicos estratificados situados en costas litorales y que se encuentran en ocasiones expuestos a los vertidos accidentales de petróleo. El papel de las cianobacterias en la bioreparación del crudo es un tema que suscita mucho interés, aunque no se han dado, hasta el presente momento, datos concluyentes sobre si la degradación del petróleo se produce exclusivamente por un tipo de cianobacteria o por un consorcio de microorganismos.

Considerando el objetivo anteriormente expuesto, se ha analizado la diversidad, y determinado los perfiles de biomasa individual y total de las cianobacterias, mediante microscopio láser confocal (CLSM) en los ambientes naturales contaminados y no contaminados por petróleo (delta del Ebro, Salins-de-Giraud, Colònia de Sant Jordi, Waulkmill bay, Swanbister bay y Etang de Bêrre) y en ecosistemas artificiales (mesocosmos).

Así mismo, se ha aislado e identificado un consorcio de microorganismos con capacidad para degradar el petróleo.

En los tapetes microbianos estudiados, se observan cambios tanto en la diversidad de las cianobacterias, como en su biomasa total. En los ambientes no contaminados se han identificado cianobacterias filamentosas como *Microcoleus chthonoplastes*, *Oscillatoria* sp., *Lyngbya* sp., *Limnothrix* sp. y cianobacterias unicelulares como *Gloeocapsa* sp., *Chroococcus* sp., *Synechocystis* sp., localizándose la concentración máxima de biomasa total principalmente en la capa óxica de los tapetes. En los ecosistemas poco contaminados, se han identificado principalmente cianobacterias unicelulares correspondientes al grupo *Pleurocapsa*, siguiendo la biomasa total de estos microorganismos un perfil parecido al de los ambientes anteriormente mencionados. En los muy contaminados, se identificaron exclusivamente cianobacterias del tipo filamentoso, observándose una reducción de la biomasa total a lo largo del tapete.

En los ecosistemas artificiales (mesocosmos), las cianobacterias del tipo unicelular se detectaron solo en los contaminados por petróleo (aunque a muy baja concentración de biomasa), mientras que *Microcoleus chthonoplastes* fue la cianobacteria dominante, tanto en las muestras control, como en las contaminadas por el crudo.

Dada la ubicuidad de esta cianobacteria en los diferentes tipos de ambientes estudiados, y por su reconocido papel en la estabilización de los sedimentos, el objetivo anterior se complementó con un análisis de la distribución de los perfiles de biomasa de este microorganismo durante un ciclo día-noche en los tapetes microbianos de Salins-de-Giraud. El estudio demostró la versatilidad metabólica de esta cianobacteria, al presentar máximos de biomasa, en capas sometidas a parámetros ambientales muy distintos: presencia de luz y O_2 (31.22 mgC/cm^3 de sedimento), presencia de luz y H_2S (28.91 mgC/cm^3 de sedimento).

Finalmente, uno de los principales objetivos del trabajo, fue el aislamiento de *Microcoleus* sp. en cultivos de laboratorio para analizar el efecto sobre el crecimiento de este microorganismo, de dos tipos de petróleo: el Casablanca (con alto contenido de hidrocarburos alifáticos) y el Maya (rico en azufre y en compuestos aromáticos) y muy tóxico. A partir de dichos cultivos se aisló un consorcio de microorganismos, al que se denominó *Microcoleus* consorcio.

La caracterización de este consorcio, se realizó utilizando técnicas microscópicas de alta resolución. El CLSM, permitió caracterizar e identificar a la cianobacteria filamentosa, mientras que la caracterización de las bacterias heterotróficas que formaban parte del consorcio, se realizó mediante microscopía electrónica de transmisión (TEM) y de barrido (SEM). La identificación de las bacterias antes mencionadas se efectuó además mediante técnicas moleculares (Reacción en Cadena de la Polimerasa-Electroforesis en Gel de Gradiente Desnaturalizante).

Los resultados obtenidos mostraban que el consorcio estaba formado por una cianobacteria, *Microcoleus chthonoplastes* y diferentes bacterias heterotróficas incluidas en la envuelta de exopolisacáridos de la cianobacteria. Las bacterias heterotróficas identificadas, fueron en su mayoría fijadoras de nitrógeno y pertenecían a diferentes grupos filogenéticos como a las α, β y γ, subclases de Proteobacteria, y al grupo CFB.

Es importante mencionar, que el análisis químico del petróleo, después del crecimiento del consorcio, demostró que éste degradaba el crudo Maya; principalmente los alquiltianos, alquiltiolanos y carbazoles, lo que podría tener un gran interés en estudios futuros de ecotoxicidad.

Summary

The present work studies the effect of oil on cyanobacteria, oxygenic phototrophic bacteria that form the dominant populations of microbial mats. These are stratified benthonic environments located in coastal sites and that are sometimes exposed to accidental oil spills. The role of the cyanobacteria in the biorepair of oil is an issue that has raised considerable interest, although to date no conclusive data has been forthcoming on whether the degradation of oil is exclusively produced by a given cyanobacterium or by a consortium of micro-organisms.

Bearing in mind the objective raised above, we have analysed the diversity—and determined the profiles—of individual and total cyanobacteria biomass, through confocal laser microscopy (CLSM), in natural environments (the Ebro delta, Salins-de-Giraud, Colònia de Sant Jordi, Waulkmill bay, Swanbister bay and Etang de Bêrre) and in artificial environments (mesocosms).

At the same time, we have isolated and identified a consortium of micro-organisms capable of degrading oil.

In the microbial mats studied, changes are observed both in the diversity of the cyanobacteria and in their total biomass. In the non-polluted environments, we have observed filamentous cyanobacteria such as *Microcoleus chthonoplastes*, *Oscillatoria* sp., *Lyngbya* sp., *Limnothrix* sp. and unicellular cyanobacteria such as *Gloeocapsa* sp., *Chroococcus* sp., *Synechocystis* sp., situating the maximum concentration of total biomass basically in the oxic layer of the mats. In those environments that are only slightly polluted, we have principally identified unicellular cyanobacteria corresponding to the *Pleurocapsa* group, the total biomass of these micro-organisms following a profile similar to that of the above-mentioned environments. In heavily polluted environments, we exclusively identify cyanobacteria of the filamentous type, observing a reduction in total biomass throughout the mat.

In artificial ecosystems (mesocosmos), unicellular type cyanobacteria are only detected in oil contaminants (although at very low biomass concentrations), whilst *Microcoleus chthonoplastes* was the dominant cyanobacterium, both in control samples as well as in oil contaminants.

Given the ubiquity of this cyanobacterium in the various environment types studied, and because of its recognised role in sediment stabilization, our earlier objective has been complemented with an analysis of the biomass-profile distribution for this micro-

organism during the day-night cycle in the Salins-de-Giraud microbial mats. The study demonstrated the metabolic versatility of this cyanobacterium, on showing biomass maximums, in those layers subjected to very distinct environmental parameters, namely, the presence of light and O_2 (31.22 mgC/cm^3 of sediment), the presence of light and H_2S (28.91 mgC/cm^3 of sediment).

Finally, one of the principal objectives of this work was that of isolating *Microcoleus* sp. In laboratory cultures so as to analyse the effect on the growth of this micro-organism of two types of oil: Casablanca (with a high content of aliphatic hydrocarbons) and Maya (rich in sulphur and aromatic compounds) and highly toxic. On the basis of these cultures, a consortium of micro-organisms was then isolated, which was given the name of the *Microcoleus* consortium.

The characterization of this consortium was undertaken by high-resolution microscope techniques. CLSM allows the characterization and identification of the filamentous cyanobacterium, whilst characterization of the heterotrophic bacteria that formed part of the consortium was undertaken by transmission-electronic microscopy (TEM) and sweep microscopy (SEM). Identification of the above-mentioned bacteria was additionally carried out through molecular techniques (Polymerase-Electrophoresis Chain Reaction in Denaturalizing Gradient Gel).

The results obtained show that the consortium was formed by a cyanobacterium, *Microcoleus chthonoplastes*, and different heterotrophic bacteria included within the exopolisaccharide sheath of the cyanobacterium. The heterotrophic bacteria identified were, in their majority, nitrogen fixers belonging to different phylogenetic groups such as α, β and γ—subclasses of Proteobacteria—and the CFB group.

It is of importance to observe that the chemical analysis of oil, after the growth of the consortium, showed that the consortium degraded the Maya oil, principally alkylthiolanes, alkylthianes and carbazoles, which could be of considerable interest to future studies of ecotoxicity.

CAPÍTULO I: INTRODUCCIÓN

Diversidad, Ecofisiología e Importancia Evolutiva de las Cianobacterias

1. Ecofisiología de las Cianobacterias
2. Taxonomía y Diversidad de las Cianobacterias
3. Las Cianobacterias y su Papel en la Degradación del Petróleo

Introducción:

Diversidad, Ecofisiología e Importancia Evolutiva de las Cianobacterias

En este primer capítulo se expone una introducción global a las cianobacterias. Se las ubica taxonómica y filogenéticamente en el dominio Eubacteria y se resalta su importancia en la evolución de la vida sobre la tierra.

Al tratarse de un grupo muy diverso de bacterias, con una extraordinaria capacidad adaptativa a distintos ecosistemas y en general muy extremos para la vida, se destacan los resultados obtenidos por diferentes investigadores para explicar dicha adaptabilidad.

Finalmente, aunque son muchas las aplicaciones biotecnológicas de las cianobacterias, se destaca su tolerancia e incluso la utilización de algunos contaminantes, como el petróleo, lo que ha incrementado el interés sobre estos microorganismos en su posible papel biorreparador de los ecosistemas naturales.

1. Ecofisiología de las Cianobacterias:

Las cianobacterias, son bacterias fototróficas oxigénicas que utilizan la luz como fuente de energía, el CO_2 como fuente de carbono y el agua como fuente de poder reductor. Es importante mencionar que parte del éxito del desarrollo de estos microorganismos en diferentes tipos de hábitats, tanto acuáticos como terrestres, se debe a su larga historia evolutiva (Margulis et al. 1986, García-Pichel et al. 1996). Las cianobacterias son capaces de colonizar ambientes muy distintos y en muchos casos muy limitantes para la vida como son los tapetes microbianos, ecosistemas estratificados bentónicos de pocos milímetros de grosor. Los tapetes microbianos salinos ubicados en zonas litorales protegidas desarrollan poblaciones de microorganismos que se disponen en capas de distintos colores en función de los parámetros ambientales, principalmente luz, oxígeno y sulfhídrico. Los tapetes microbianos y las cianobacterias que los constituyen se han tomado como modelo para el estudio de los estromatolitos, que son estructuras órgano-sedimentarias, ampliamente

distribuidas en la tierra durante el Arqueozoico y el Proterozoico (Grotzinger y Knoll, 1999) (Figura 1). Se han encontrado semejanzas entre los microfósiles preservados y las cianobacterias actuales de los tapetes microbianos y también a nivel geoquímico y geológico (Schopf J. W., 2000) (Figura 2).

Figura 1: División geológica de la tierra desde sus orígenes y localización de las cianobacterias.
http:// homepage .mac.com/uriarte/tcianobaterias.html

Figura 2: Estromatolitos de Shark Bay (Australia).
http:// homepage .mac.com/uriarte/testromatolitos.html

La historia de la tierra ha estado condicionada por los eventos geoquímicos volcánicos y tectónicos, el impacto de la temperatura global y de la irradiación (incluyendo la luz ultravioleta), la desecación, la disponibilidad de nutrientes y la composición iónica (salinidad). Actualmente estas condiciones se dan en hábitats muy extremos para la vida y en los que normalmente se encuentran cianobacterias. Éstas son capaces de colonizar ambientes marinos costeros (Mir et al. 1991, Caumette et al. 1994, Esteve et al. 1994, Benlloch et al. 2002), ambientes hipersalinos (Giani et al. 1989, Demergasso et al. 2003, Fourçans et al. 2004), fuentes termales (Ferris et al., 1996) y lagos alcalinos (Brock T. D., 1978) (Tabla 1).

En ambientes litorales, salinos e hipersalinos y normalmente protegidos por una barrera de dunas se encuentran los tapetes microbianos. Éstos, como se ha dicho con anterioridad, están constituidos por comunidades bentónicas verticalmente estratificadas en capas. De manera general la disposición de las distintas poblaciones (desde la superficie hasta la capa más profunda) es la siguiente (Figura 3): diatomeas (capa amarilla-parduzca), cianobacterias (capa verde), bacterias rojas del azufre (capa rojiza), bacterias verdes del azufre, que no suelen formar una lámina de color evidente, aunque se han detectado debajo de la capa roja en cultivos de enriquecimiento. Finalmente y por debajo de la zona pigmentada se encuentra un sedimento negruzco debido a la actividad de las bacterias sulfato reductoras, que producen H_2S al utilizar el sulfato como aceptor final de electrones. Los sulfuros de hierro que forman al reaccionar el sulfhídrico con el hierro son principalmente los responsables de dicha coloración.

Tabla 1: Diversidad de cianobacterias en diferentes ambientes extremos, tanto acuáticos como terrestres (Paerl et al., 2000).

Habitat/location/stresses	Dominant genera	N_2-fixing capabilities
Aquatic		
Planktonic		
Oligotrophic tropical and subtropical ocean (N, I)	*Trichodesmium, Richelia*	+, +
Eutrophic lakes, rivers and some estuaries (I, P)	*Microcystis, Oscillatoria*	−, most −
	Anabaena, Aphanizomenon	+, +
	Nodularia, Gloeotrichia	+, +
Benthic/intertidal mats		
Temperate mud/sandflats (T, I, D, P, N, H)	*Microcoleus, Phormidium*	−, −-
	Lyngbya, Oscillatoria	some +, some +
	Anabaena, Calothrix	+, +
Saltmarshes (T, I, D, P, N, H)	*Microcoleus, Lyngbya*	− , some +
	Oscillatoria, Phormidium	some +, −
tropical mud/sandflats (T, I, D, P, N, H)	*Microcoleus, Phormidium*	−, −
	Lyngbya, Oscillatoria	some +, some +
	Schizothrix, Scytonema	?, +
	Calothrix, Plectonema	+, +
	Synechococcus	most −-
Hypersaline lagoons, ponds (T, I, D, P, N, H)	*Microcoleus, Lyngbya*	− , most +
	Synechococcus, Phormidium	most −-, −-
	Calothrix, Scytonema	+, +
	Schizothrix, Spirulina	?, −-
Tropical mangrove swamps (T, D, P, N)	*Aphanocapsa, Chroococcus*	?, −
	Scytonema, Synechococcus	+, some +
	Lyngbya, Oscillatoria	+, +
Temp./trop. seagrass beds (I, P, N)	*Lyngbya, Oscillatoria*	some +, some +
	Gloeotrichia, Nostoc	+, +
	Calothrix, Anabaena	+, +
Coral reefs (I, P, N)	*Calothrix, Lyngbya*	+, some +
	Scytonema, Anabaena	+, +
Stromatolites (T, I, D, P, N, H)	*Scytonema, Calothrix*	+, +
	Calothrix, Schizothrix	+,?
	Phormidium, Synechococcus	−, most −
Terrestrial		
Endoliths (tropical to polar) (T, D, N)	*Hyella, Mastigocladus*	?, +
	Synechococcus, Synechocystis	some +, some +
Soils		
Temperate epiliths, temperate mats (T, I, D, N)	*Nostoc, Scytonema, Anabaena*	+, +, +
	Microcoleus, Oscillatoria	− , some +
	Lyngbya, Phormidium	some +, −
	Synechocystis, Synechococcus	−, most −
Desert soil mats, all climes (T, I, D, N, H)	*Microcoleus, Nostoc, Anabaena*	− ,+ , +
	Phormidium, Lyngbya, Oscillatoria	−, some +, some +
Lichens (tropical to polar) (T, I, D, N)	*Nostoc, Scytonema*	+, +
	Synechocystis, Synechococcus	−, some +
	Phormidium, Chroococcus	−, −

Estrés físico: temperaturas extremas (T), irradiación excesiva (I), desecación (D).
Estrés químico: agotamiento de nutrientes (N), pH extremos (P) e hipersalinidad (H).

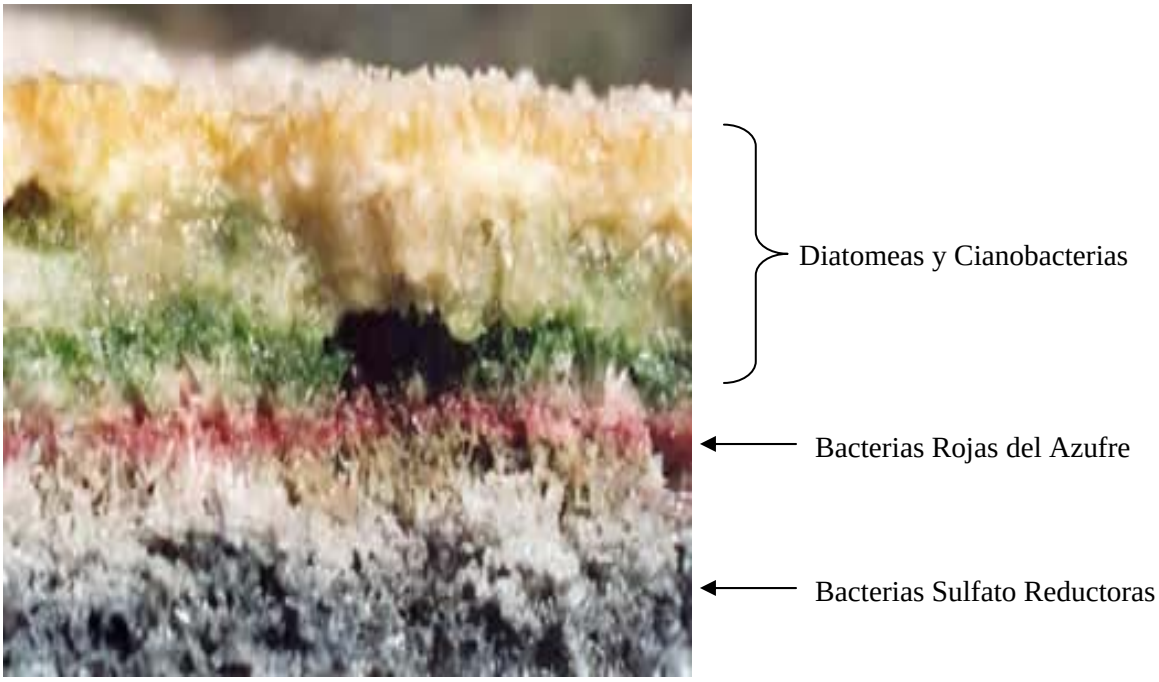

Figura 3: Disposición de las distintas poblaciones en un tapete microbiano típico.

En todos estos ambientes las cianobacterias suelen realizar una fotosíntesis oxigénica en la capa verde, siendo la clorofila *a* su principal pigmento fotosintético. Es importante mencionar que muchas veces la capa verde, que contiene a las cianobacterias, se encuentra recubierta por una capa de arena o una capa de mucílago orgánico, el cual contiene un pigmento llamado escitonemina, de color marrón amarillento. Este pigmento está producido por las cianobacterias que están expuestas a elevadas intensidades de luz y que por lo tanto tiene un papel protector frente la excesiva irradiación ultravioleta (García Pichel y Castenholz, 1991). La escitonemina se encuentra principalmente en las vainas exopolisacáridas y se caracteriza por ser altamente recalcitrante, por lo que se la puede encontrar en las vainas mucilaginosas vacías, eliminadas por las cianobacterias. Otros pigmentos accesorios son las ficobilinas: la ficocianina, que es de color azul y que junto al verde de la clorofila *a* son los pigmentos responsables del color azul verdoso de estos microorganismos (también conocidos como algas verde-azuladas) y la ficoeritrina, una ficobilina roja que da un color rojizo a las especies que la producen. Las ficobilinas se localizan dentro de los tilacoides, estructuras intracelulares del aparato fotosintético de las cianobacterias.

Se ha demostrado que algunas cianobacterias también pueden realizar una fotosíntesis anoxigénica. Se pueden distinguir dos grupos de cianobacterias con respecto a la capacidad de realizar fotosíntesis anoxigénica. Un grupo se caracteriza porque la fotosíntesis oxigénica se inhibe a bajas concentraciones de sulfhídrico, induciéndose en este caso la fotosíntesis anoxigénica. El otro grupo presenta ambos tipos de fotosíntesis que pueden llevarse a cabo al mismo tiempo; a bajas concentraciones de sulfhídrico la fotosíntesis oxigénica es la más importante (Cohen y Rosenberg 1989, Canfield y Des Marais 1991, Moezelaar et al. 1996). En ambos grupos de cianobacterias, la fotosíntesis anoxigénica es inducida y depende exclusivamente de la concentración de sulfhídrico y del espectro de luz que éstas reciben. Los microorganismos que han demostrado tener la capacidad de realizar los dos tipos de fotosíntesis, como es el caso de *Microcoleus chthonoplastes*, tienen una gran ventaja ecológica, puesto que en aquellos ambientes en los que las concentraciones de sulfhídrico fluctúen, pueden colonizar un mayor espacio.
Diferentes estudios indican que las cianobacterias poseen en ocasiones metabolismo alternativos ya que han sido encontradas en capas anóxicas, en las que probablemente realizan un metabolismo fermentativo en la oscuridad.

Esta capacidad metabólica fue descrita en *Oscillatoria limnetica* en los tapetes microbianos de Solar Lake (Sinaí) (Oren y Shilo 1979). Esta cianobacteria filamentosa se caracteriza porque fermenta el glicógeno produciendo lactato. Stal y Moezelaar (1997) realizaron una serie de estudios que demuestran que existen diferentes posibilidades de metabolismo fermentativo en las cianobacterias (Tabla 2).

Tabla 2: Diferentes tipos de metabolismos fermentativos (Stal y Moezelaar 1997).

ORGANISMO	ORIGEN/CEPA	VÍA DE FERMENTACIÓN	PRODUCTOS*
Anabaena azollae AaL	Simbionte de *Azolla caroliniana*	Homoacetato	Acetato (lactato, CO_2, H_2)
Anabaena azollae AaN	Simbionte de *Azolla caroliniana*	Homoacetato	Acetato (lactato, CO_2, H_2)
Anabaena azollae AaS	Simbionte de *Azolla filuculoides*	Homoacetato	Acetato (lactato, CO_2, H_2)
Anabaena siamensis Aa1	Arrozales	Homoacetato	Acetato (CO_2, H_2)
Cyanothece	PCC 7822 (Inst. Pasteur)	Ácido Mixta	H_2, etanol, lactato, formato, acetato
Microcoleus chthonoplastes	Tapete microbiano	Ácido Mixta	H_2, etanol, lactato, formato, acetato
Microcystis aeruginosa	PCC 7806 (Inst. Pasteur)	Ácido Mixta	H_2, etanol, acetato
Nostoc sp. Cc	Simbionte de *Cycas circinalis*	Homoacetato	Acetato (lactato, CO_2, H_2)
Nostoc sp. A12	Simbionte de *Anthoceros laevis*	Homoacetato	Acetato (lactato, CO_2, H_2)
Nostoc sp. Ef1	Simbionte de *Encephalartos ferox*	Homoacetato	Acetato (lactato, CO_2, H_2)
Nostoc sp. MAC	Simbionte de *Macrozamia lucida*	Homoacetato	Acetato (lactato, CO_2, H_2)
Nostoc sp. Mm1	Simbionte de *Macrozamia moorei*	Homoacetato	Acetato (lactato, CO_2, H_2)
Nostoc sp. M1	Simbionte de *Macrozamia* sp.	Homoacetato	Acetato (CO_2, H_2)
Nostoc sp. Gm	Simbionte de *Gunnera manicata*	Homoacetato	Acetato (lactato)
Nostoc sp. T1	Arrozales	Homoacetato	Acetato (formato, CO_2, H_2)
Nostoc sp. Bali	Arrozales	Homoacetato	Acetato (CO_2, H_2)
Oscillatoria limnetica	Hipolimnio del Solar Lake	Homoacetato	Lactato
Oscillatoria limosa	Tapete Microbiano	Heteroláctica Homoacetato	Lactato, etanol, acetato
Oscillatoria sp.	Tapete microbiano	Desconocido	Lactato, etanol, acetato, formato
Oscillatoria terebriformis	Tapete microbiano	Homoláctica?	?
Spirulina platensis	Desconocido	Ácido Mixta	H_2, etanol, acetato, formato, lactato
Spirulina mimosa	Desconocido	Desconocido	Lactato, acetato

* Los productos entre paréntesis son producidos en cantidades pequeñas.

Con respecto a la capacidad de las cianobacterias de fijar nitrógeno, se ha estudiado que muchas de ellas pueden fijarlo (Bergman et al. 1997). Además algunos miembros pueden hacerlo (Tabla 1), usando células especiales llamadas heterocistos. Así mismo, son capaces de producir un compuesto nitrogenado conocido como cianoficina, que está formada por un polímero de arginina y ácido aspártico. La cianoficina, puede representar hasta el 8% del peso seco celular y es un reservorio de nitrógeno. Las cianobacterias son capaces de utilizar el N_2 como única fuente de nitrógeno para su crecimiento. Estos microorganismos se pueden dividir en tres grupos, dependiendo de su capacidad para fijar nitrógeno: Grupo I, corresponde a los microorganismos filamentosos que presentan heterocistos. La fijación del nitrógeno, en este caso se lleva a cabo gracias a la presencia de una enzima compleja llamada nitrogenasa. Grupo II, está comprendida por cianobacterias filamentosas y unicelulares y que no presentan heterocistos, siendo capaces de llevar a cabo la fijación del N_2 en condiciones anóxicas, en diversos ambientes incluyendo los tapetes microbianos. Las condiciones anóxicas se dan cuando existen elevadas concentraciones de sulfhídrico, y que por lo tanto inhibe la fotosíntesis oxigénica. Se ha descrito en este caso que, las cianobacterias pueden crecer diazotróficamente cuando el sulfuro de hidrógeno este presente en los tapetes microbianos (Villbrandt y Stal, 1996). Grupo III, comprende a las cianobacterias filamentosas y unicelulares que no tienen heterocistos y que fijan nitrógeno atmosférico aeróbicamente.

Por otra parte muchas de las cianobacterias estudiadas poseen la capacidad de producir exopolisacáridos (Decho A. W., 1990). Las estructuras mucilaginosas, excreciones extracelulares de sustancias poliméricas (EPS), que algunas cianobacterias poseen, aglutinan las partículas del suelo, retienen la humedad y la protegen de factores negativos externos. Las cianobacterias filamentosas son las que principalmente forman una red, que envolviéndose de una matriz polisacárida consolidan el sedimento (d'Amelio et al. 1987). Los EPS, se caracterizan además por ser un gran reservorio de agua, ya que cuando éstos están completamente hidratados, retienen hasta el 99%. Finalmente, los EPS también evitan la difusión de diferentes metales tóxicos; cuya presencia genera a veces una excesiva producción de sustancias poliméricas (de Philippis et al. 1998).

Es importante mencionar que se conoce poco acerca de los EPS en los tapetes microbianos. Además, algunos polisacáridos parecen ser recalcitrantes a la degradación microbiológica, mientras que otros no lo son.

2. Taxonomía y Diversidad de las Cianobacterias:

Las cianobacterias son un grupo filogenético en el dominio Bacteria (Woese C.R., 1987) (Figura 4). Es uno de los grupos más amplios entre los procariotas (Casamayor et al. 2002), con aproximadamente 56 géneros descritos y más de 1000 especies. Difieren de los otros organismos procariotas en la composición de los ácidos grasos. Las otras bacterias contienen casi exclusivamente ácidos grasos saturados y no saturados con un doble enlace mientras que en las cianobacterias es fácil encontrar ácidos grasos con dos o más dobles enlaces. La pared de las cianobacterias tiene características similares a la de las bacterias Gram negativas.

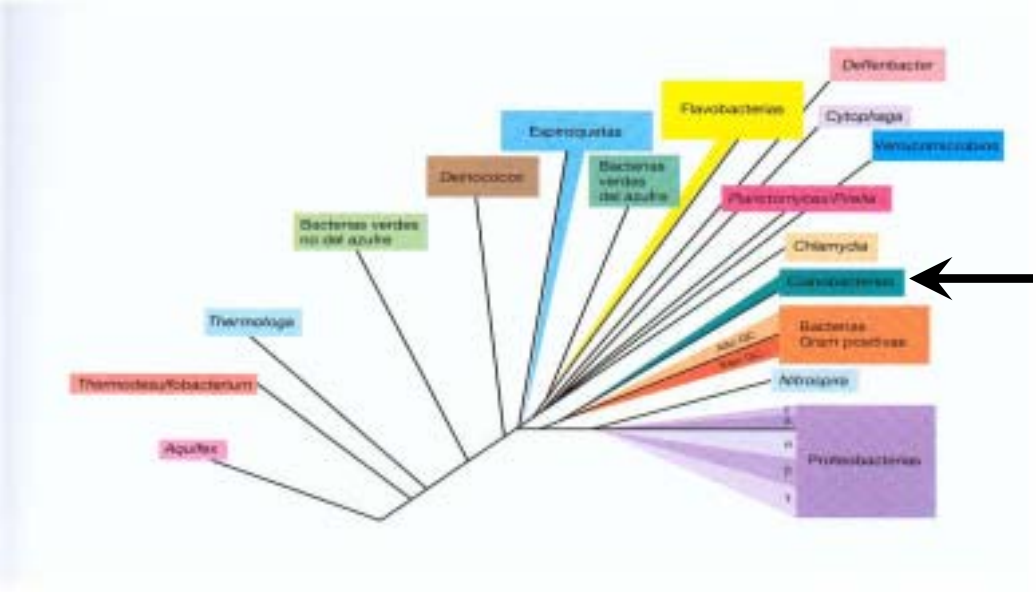

Figura 4: Árbol filogenético construido a partir de las secuencias del RNA ribosómico 16S. *Datos obtenidos del Proyecto de Secuenciación del Ribosoma (Ribosomal Database Project)*. http://rdp.cme.msu.edu

Estos microorganismos, tal como se ha expuesto en el apartado anterior, son un grupo muy diverso tanto morfológica como fisiológicamente. Castenholz et al. (2001) las clasifica en cinco órdenes: A) Orden Chroococcales, formado por microorganismos unicelulares que se reproducen por fisión binaria o por gemación, la división puede ocurrir en uno, dos o tres planos. El diámetro de la célula varía entre 0.5 y 30 μm y suelen presentar una vaina que envuelve grupos de células. B) Orden Pleurocapsales, microorganismos que se reproducen por fisión múltiple, cuyas células se caracterizan por su diversidad en formas y tamaños. C) Orden Oscillatoriales, bacterias filamentosas que presentan una división celular por fisión binaria y en un solo plano, reproduciéndose por fragmentación del tricoma (cadena de células sin la envuelta mucopolisacárida). Las células presentan un diámetro variable, entre 0.5 y 100 μm; y muestran dos tipos de morfología: alargada (célula más larga que ancha) y forma de disco (célula más ancha que larga). Las células de la especie *Oscillatoria princeps* son las mayores conocidas dentro de las cianobacterias**.** D) Orden Nostocales, son organismos filamentosos, que se dividen exclusivamente por fisión binaria; el diámetro de su tricoma varía entre 2 y 15 μm, además se caracterizan principalmente por presentar células diferenciadas, unas llamadas heterocistos (en las que se fija el nitrógeno), y otras acinetos (que las hace resistentes a los cambios de temperatura) y finalmente, E) Orden Stigonematales, las células de estos filamentos se dividen por fisión binaria en múltiples planos, lo que origina que los filamentos presenten ramificaciones a lo largo de su tricoma.

El conocimiento de la diversidad de las cianobacterias, que habitan los ecosistemas anteriormente mencionados, se ha realizado en gran parte gracias a la aplicación de técnicas clásicas de cultivo y aislamiento; de análisis microscópico y del contenido específico de pigmentos a partir de cultivos aislados de muestras naturales. No obstante en los últimos años, se ha ampliado mucho el conocimiento sobre su biodiversidad, aplicando las técnicas moleculares y las de microscopía de alta resolución. Las primeras se han utilizado para hacer estudios filogenéticos de estos microorganismos (García-Pichel et al. 2001).

No obstante la aplicación de técnicas moleculares (en tapetes microbianos) para la identificación de cianobacterias tiene también su dificultad, puesto que los EPS, que muchas de ellas producen, dificultan en ocasiones la extracción de los ácidos nucleicos (López-Cortés et al. 2001).

Entre las técnicas microscópicas de alta resolución, se han utilizado con el mismo objetivo la microscopía electrónica (TEM y SEM) y la microscopía láser confocal (CLSM). El TEM permite visualizar la ultraestructura de estos microorganismos; mientras que el SEM es útil para caracterizar los diferentes morfotipos permitiendo estudiar tanto la distribución vertical de los microorganismos en muestras intactas como las interacciones entre ellos y las partículas de sedimento (Mir y Esteve, 1992). Es importante mencionar que estas técnicas de microscopía electrónica necesitan exhaustivos protocolos para la preparación de las muestras (Esteve et al. 1992). También la microscopía de fluorescencia convencional se ha utilizado con éxito en muestras procedentes de ambientes acuáticos; pero en tapetes microbianos, donde abundan las cianobacterias filamentosas en interacción con el sedimento, dicha microscopía ofrece una menor resolución.

Nuestro grupo de trabajo aplicó el CLSM en tapetes microbianos (Solé et al. 1998) para obviar las dificultades anteriormente expuestas. El CLSM permite que las cianobacterias puedan ser observadas “in vivo”. Debido a que estos microorganismos emiten fluorescencia natural, por poseer pigmentos fotosintéticos, se evita la aplicación de tinciones específicas. Este microscopio permite obtener diferentes secciones ópticas con elevado poder de resolución, a partir de una muestra gruesa de tapete. Es por ello, que hoy en día el uso del CLSM, proporciona nueva y valiosa información referente a la estructura y composición de los tapetes microbianos, ayudando en la caracterización e identificación de los microorganismos (Johnson I. 1999, Solé et al. 2001). También su aplicación proporciona importantes resultados en la determinación de la biomasa de las cianobacterias (Solé et al. 2003) pudiéndose hacer un seguimiento individualizado de cada una de ellas en profundidad dentro de una muestra de tapete.

Actualmente y gracias a la aplicación, sobre *stacks* de imágenes (ver material y métodos), del programa *Image J* de análisis de imagen, pueden analizarse además un número elevado de muestras en muy poco tiempo, lo que proporciona un mayor número de datos (Solé et al., enviado a *Journal of Microscopy*).

3. Las Cianobacterias y su Papel en la Degradación del Petróleo:

En la actualidad se ha incrementado el interés por el estudio de las cianobacterias con respecto al papel que pueden desempeñar en la posible biorreparación de ambientes contaminados, en especial por petróleo, ya que los tapetes microbianos de las costas litorales afectadas, se ven recubiertos al poco tiempo por las cianobacterias.

El petróleo es una sustancia aceitosa de color oscuro formada básicamente por: Carbono (84-87%), Hidrógeno (11-14%), Azufre (0-2%) y Nitrógeno (0.2%), generando tres fracciones principales: los hidrocarburos alifático aromáticos, las resinas o compuestos polares y los asfaltenos (García de Oteyza T. 2003).

Los hidrocarburos pueden estar en estado líquido o en estado gaseoso. En el primer caso es un aceite al que se le denomina crudo. En el segundo caso se le conoce como gas natural.

El origen del petróleo y del gas natural es de tipo orgánico y sedimentario, por lo que el petróleo es el resultado de un complejo proceso físico-químico producido en el interior de la tierra, y donde debido a la alta presión y temperatura, se produce la descomposición de enormes cantidades de materia orgánica en aceite y gas. Aunque es mucha la información que se tiene sobre la capacidad de diferentes microorganismos para degradar el petróleo (Mejharaj et al. 2000, Medina et al. 2005, Menezes et al. 2005), en realidad se conoce muy poco sobre el papel de las cianobacterias en la degradación de este compuesto orgánico.

En los últimos años ha crecido el interés por estos microorganismos debido a los frecuentes desastres ecológicos, que producen los vertidos de petróleo desde los buques de transporte en las zonas litorales. Los mencionados vertidos llegan en muchas ocasiones a las costas litorales y contaminan los tapetes microbianos formados mayoritariamente por cianobacterias. Diferentes estudios demuestran la capacidad de persistencia de las cianobacterias en tapetes microbianos contaminados (Al-Hasan et al. 1994, 1998, 2001). También se han realizado experimentos de laboratorio con cultivos axénicos de algunas cianobacterias, como *Oscillatoria* sp. y *Phormidium* sp. (Cohen Y. 2002) analizando su papel en la degradación del petróleo pero los datos en forma generalizada no son muy concluyentes.

Microcoleus sp. es la cianobacteria más abundante en la mayoría de los tapetes microbianos analizados en el presente trabajo. Aún cuando algunos de ellos han sufrido en los últimos años contaminación por petróleo, su papel en la utilización del crudo ha sido muy cuestionado. Una de las principales cuestiones planteadas es si la degradación finalmente observada, es debido a la actividad de esta cianobacteria, o a la de los microorganismos heterotróficos que frecuentemente se asocian a *Microcoleus* sp.

El objetivo global del presente trabajo, ha sido analizar el efecto que el petróleo puede causar en las poblaciones de microorganismos fototróficos oxigénicos. Se han considerado principalmente los tapetes microbianos por tratarse de zonas litorales frecuentemente expuestas a la contaminación por el crudo.

Para ello se ha analizado la diversidad y los perfiles de biomasa de las cianobacterias en diferentes tapetes microbianos de Europa sometidos a diferente grado de contaminación por petróleo. Se han hecho ensayos similares en sistemas artificiales como en los mesocosmos y finalmente se ha aislado y caracterizado un consorcio de microorganismos con capacidad para degradar petróleo, en este caso se ha ensayado especialmente el Maya, un petróleo rico en azufre y por lo tanto muy tóxico.

Estructura de la Tesis

La investigación realizada forma parte del proyecto europeo **MATBIOPOL** "Role of Microbial **Mat**s in **Bio**remediations of hydrocarbon **Pol**luted coastal zones". Todo ello queda reflejado en los capítulos de la tesis que a continuación se expone.

Capítulo I: En este capítulo se introducen de forma general las cianobacterias, considerando su importancia tanto evolutiva como ecofisiológica. Se hace énfasis en su papel colonizador de ambientes contaminados por petróleo y se centran los objetivos de la tesis.

Capítulo II: Se describe la metodología utilizada. Cuando se han requerido poner a punto métodos específicos no estandarizados, éstos se describen formando parte de los resultados, como es el caso del aislamiento de *Microcoleus* consorcio, descrito en el capítulo V.

Capítulo III: Entre los tapetes microbianos naturales no contaminados estudiados, los que presentan una estructura estratificada más estable son los del delta del Ebro y los de Salins-de-Giraud. En el primer caso, la diversidad y los cambios poblacionales de las cianobacterias mediante CLSM ya han sido previamente estudiados. En el presente trabajo se ha realizado el análisis de la diversidad, la abundancia relativa en profundidad de las cianobacterias y los perfiles de biomasa de *Microcoleus chthonoplastes* de los tapetes microbianos de Salins-de-Giraud. Este estudio se ha hecho extensivo a su distribución, en un ciclo día-noche y se han correlacionado los resultados con los obtenidos (por otros autores durante el mismo muestreo) para las bacterias fototróficas anoxigénicas.

Capítulo IV: Se identifican las cianobacterias de todos los ambientes estudiados tanto naturales como artificiales. Se evalúan los cambios en la diversidad y en los perfiles de biomasa que experimentan las poblaciones de dichos

microorganismos, cuando se encuentran expuestos a contaminación por petróleo.

Capítulo V: En el presente trabajo se ha aislado por primera vez un consorcio de *Microcoleus* con capacidad para degradar el petróleo.

En este apartado se describen las técnicas para su aislamiento y cultivo. También se identifican los microorganismos que forman el consorcio mediante técnicas microscópicas y moleculares.

Finalmente se exponen las conclusiones generales del trabajo a partir de los resultados expuestos en cada uno de los apartados.

CAPÍTULO II: MATERIAL Y MÉTODOS

2.1. Caracterización y Muestreo de Tapetes Microbianos Naturales y Artificiales

2.2. Cultivos Celulares *Microcoleus* consorcio

2.2.1. Cultivos de Enriquecimiento

2.2.2. Aislamiento de *Microcoleus* consorcio

2.2.3. Identificación

A. Técnicas Microscópicas

B. Técnicas Moleculares

C. Técnicas de Análisis Químicos

Material y Métodos:

En este apartado se describen las zonas de muestreo y los métodos utilizados para el procesamiento de las muestras obtenidas de los tapetes microbianos contaminados y no contaminados por petróleo.

2.1. Caracterización y Muestreo de Tapetes Microbianos Naturales y Artificiales

Las muestras de los ambientes naturales y artificiales se tomaron y procesaron de acuerdo a los métodos que se exponen a continuación.

2.1.1. Descripción de los ecosistemas naturales estudiados

La descripción de los tapetes microbianos y sus características ambientales se describen en los siguientes apartados:

La Camarga (Francia)

Se han realizado muestreos en dos tapetes microbianos de esta zona, Salins-de-Giraud, no contaminado por petróleo y Etang de Bêrre, contaminado por petróleo.

Los tapetes microbianos de Salins-de-Giraud (Figura 5A) están situados a la derecha del río Rhône. El lugar estudiado es una laguna hipersalina, donde la salinidad oscila entre 70 y 150‰. Las muestras fueron obtenidas en Mayo del 2000 y en Junio del 2001.

Etang de Bêrre (Figura 5B), es una laguna que se encuentra a la izquierda del río Rhône y cuya salinidad varía entre 15 y 20‰. Esta laguna recibe vertidos de una refinería y su sedimento contiene una cantidad muy elevada de hidrocarburos, por lo que presenta un alto grado de contaminación desde hace varios años. Los muestreos se realizaron en Mayo del 2000.

Tanto en Salins-de-Giraud como en Etang de Bêrre, la temperatura oscila entre 3 y 25ºC a lo largo del año y se suele registrar una precipitación anual de 750 a 1000 L/m^2. En la figura 1 se muestra la ubicación de ambos tapetes microbianos.

Delta del Ebro (Península de los Alfaques, Tarragona-España)

Los tapetes microbianos del delta del Ebro no presentan contaminación por petróleo. Localizados al NE de la península Ibérica (40º40'N, 0º4'E), su salinidad oscila entre 40 y 70‰ y la temperatura varía entre 3 y 27ºC estando expuestos a una precipitación anual de 500 L/m^2 (Figura 2 y 5C). Las muestras fueron obtenidas en Mayo del 2000 y en Julio del 2003.

Islas Orkney (Escocia)

Los tapetes microbianos de las islas Orkney se sitúan en el NE de la costa de Escocia (58º41' y 59º24'N/2º22' y 4º25'O). Las dos muestras analizadas corresponden a Waulkmill bay y Swanbister bay (Figura 3, 5D y 5E), ambos tapetes microbianos estuvieron muy contaminados por petróleo, aunque en la actualidad la contaminación es prácticamente inexistente.
La temperatura en estos ambientes naturales oscila entre 12 y 13ºC, la precipitación anual varía entre 750 y 950 L/m^2 y la salinidad es de 40‰.

Tanto las imágenes de los mapas como las fotos de los lugares de muestreo han sido obtenidas de la información publicada en la página web del Proyecto Europeo **MATBIOPOL** (http://www.univ-pau.fr/RECHERCHE/MATBIOPOL/index.htm).

Colònia de Sant Jordi:

Los tapetes microbianos de la Colònia de Sant Jordi no se encuentran contaminados por petróleo. Están localizados en el ángulo sur de Mallorca (2º39'E y a 39º34'N) (Figura 4 y 5F), y la temperatura oscila entre 17 y 22ºC, con una precipitación anual de 450 L/m^2. Las muestras analizadas se obtuvieron en Julio del 2001, éstas no formaban parte del proyecto anteriormente mencionado, pero aportan nuevos datos de ambientes no contaminados y por este motivo se han incluido en el presente trabajo.

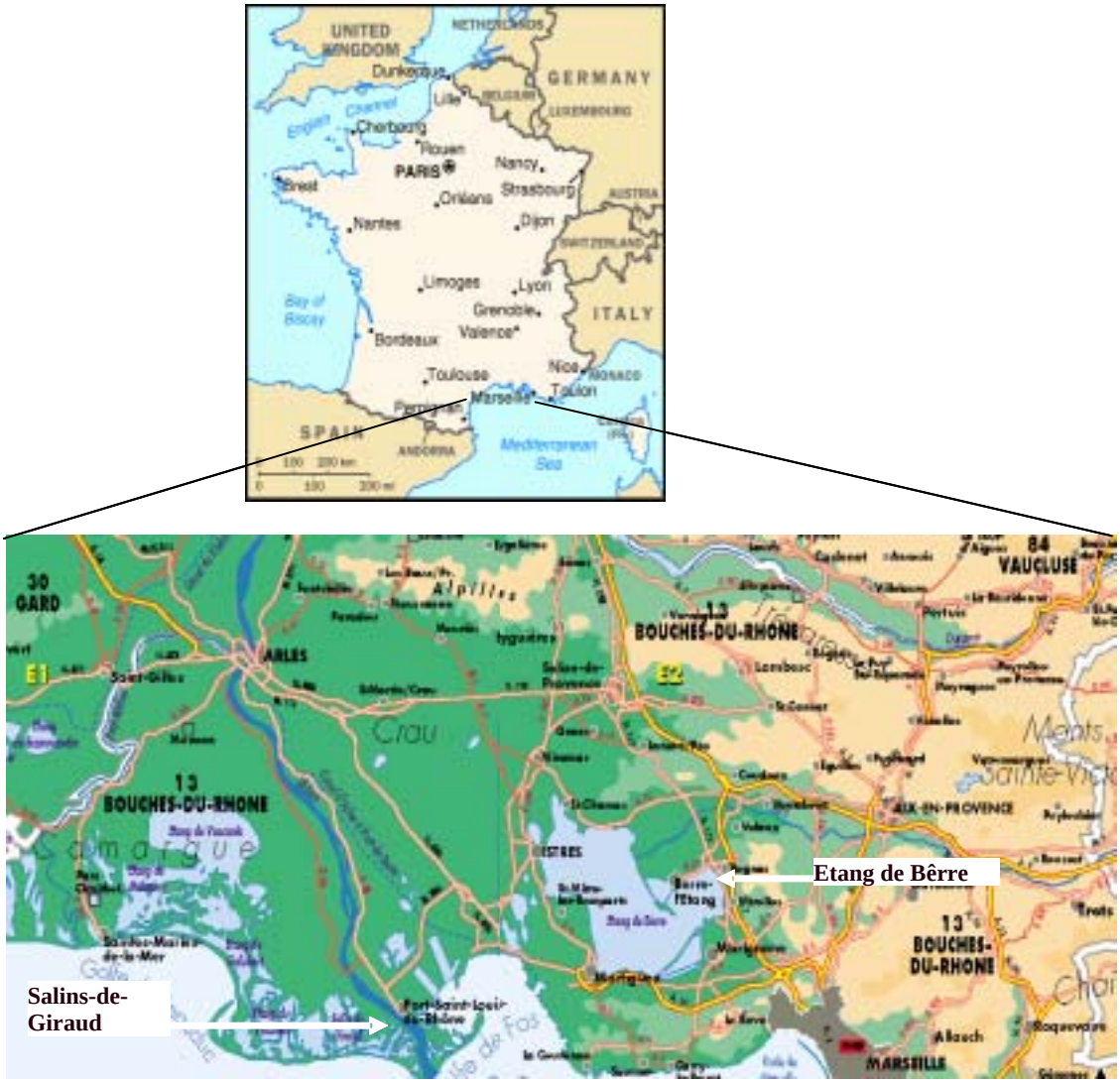

Figura 1. Mapa de la Camarga. Tapetes Microbianos de Salins-de-Giraud y Etang de Bêrre.

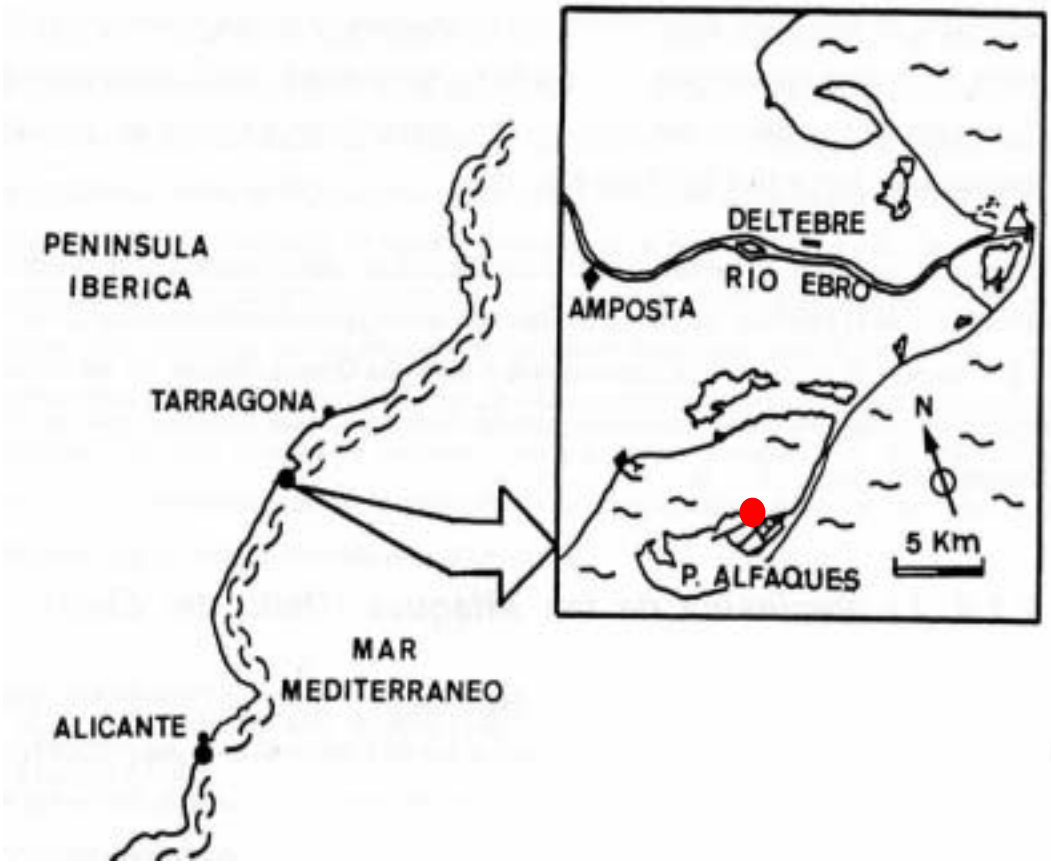

Figura 2. Mapa del delta del Ebro. Localización de los tapetes microbianos.

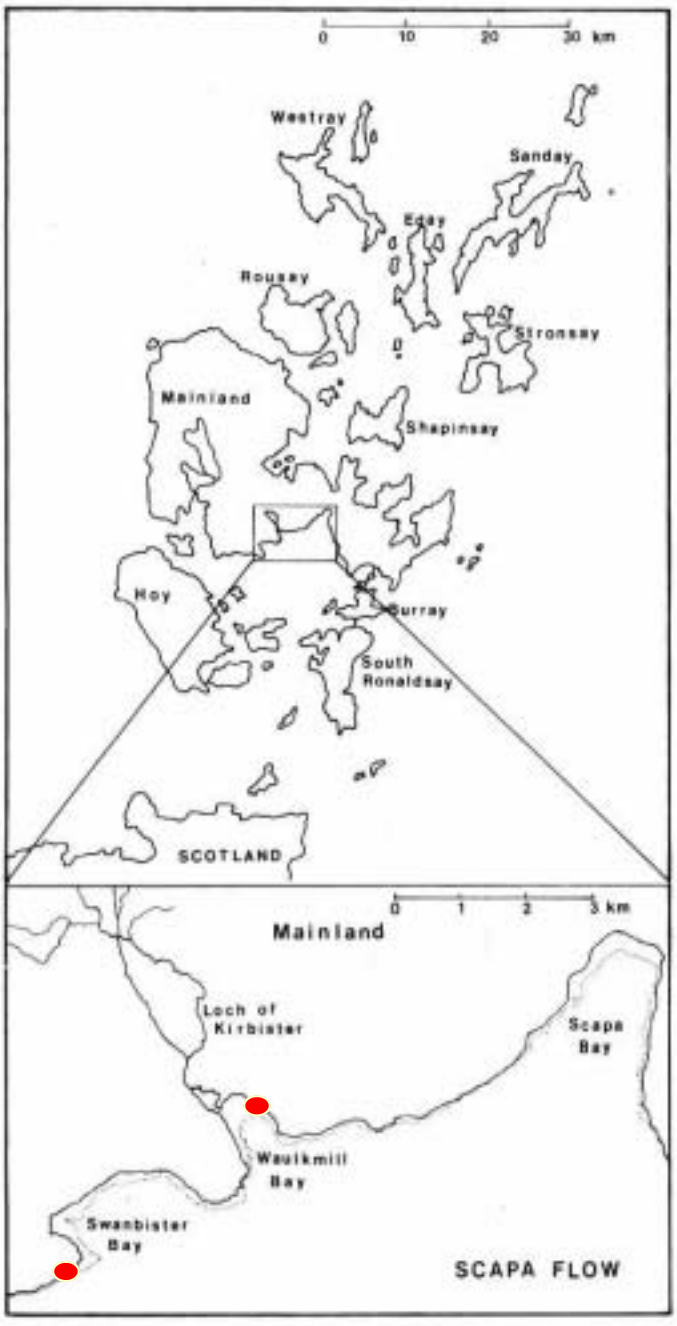

Figura 3. Mapa de las Islas Orkney. Tapetes Microbianos de Swanbister bay y de Waulkmill bay.

Figura 4. Localización de los tapetes microbianos de la Colònia de Sant Jordi.

Figura 5. Tapetes Microbianos

A. Salins-de-Giraud (La Camarga-Francia)
B. Etang de Bêrre (La Camarga-Francia)
C. delta del Ebro (Tarragona-España)
D. Swanbister Bay (Islas Orkney-Escocia)
E. Waulkmill Bay (Islas Orkney-Escocia)
F. Colònia de Sant Jordi (Mallorca- España)

2.1.2. Descripción de los ecosistemas artificiales

Estos ecosistemas se prepararon tanto a pequeña (microcosmos) como a gran escala (mesocosmos). La descripción de estos ambientes se detalla a continuación:

A. Microcosmos

Los microcosmos son sistemas experimentales de laboratorio en los que se simulan condiciones ambientales naturales. En el presente trabajo se han utilizado para el aislamiento de cianobacterias con capacidad para degradar petróleo.

El inóculo que se utilizó inicialmente en la preparación de los microcosmos procedía de los tapetes microbianos del delta del Ebro, en la zona de las Salinas de la Trinidad.

Se prepararon dos tipos de microcosmos: Uno de ellos era un microcosmo sin contaminar (control) y el otro contaminado por petróleo (Figura 6). Para su preparación un inóculo de 125 g de tapete microbiano se homogenizó con 100 ml de solución salina y 13.5 dm^3 de agua de mar (de la misma zona de muestreo). Los inóculos obtenidos se depositaron, para ambos casos, en cajas de polipropileno (33 x 41 x 25 cm) y se incubaron a 25ºC y a una intensidad de luz de 150µ$Em^{-2}s^{-1}$ (Llirós et al. 2003).

Del microcosmos contaminado se extrajeron muestras para la preparación de los cultivos de enriquecimiento de las cianobacterias.

Figura 6: Microcosmos. Cortesía Marc Llirós.

B. Mesocosmos

Los mesocosmos, son ambientes artificiales que simulan tapetes microbianos a gran escala. Se prepararon con tapetes microbianos del *Solar Lake,* Sinai-Egipto. Estos tapetes se trasladaron a estanques artificiales del Instituto Internacional de la Universidad de Eilat, donde se construyeron tres ecosistemas (Estanque I, II y III), en Febrero del 2001 (Figura 7). Los inóculos (tapetes microbianos) fueron mantenidos en las mismas condiciones que en el *Solar Lake* (80-90‰ de salinidad y entre 19-32ºC, con un pH de entre 7.8 a 8.2). Una vez estabilizados los mesocosmos, los estanques II y III se contaminaron por petróleo, mientras que el estanque I se dejó sin contaminar (experimento control). Las muestras que se analizaron corresponden al mes de Enero del 2002, ocho meses después de la contaminación con el petróleo Casablanca.

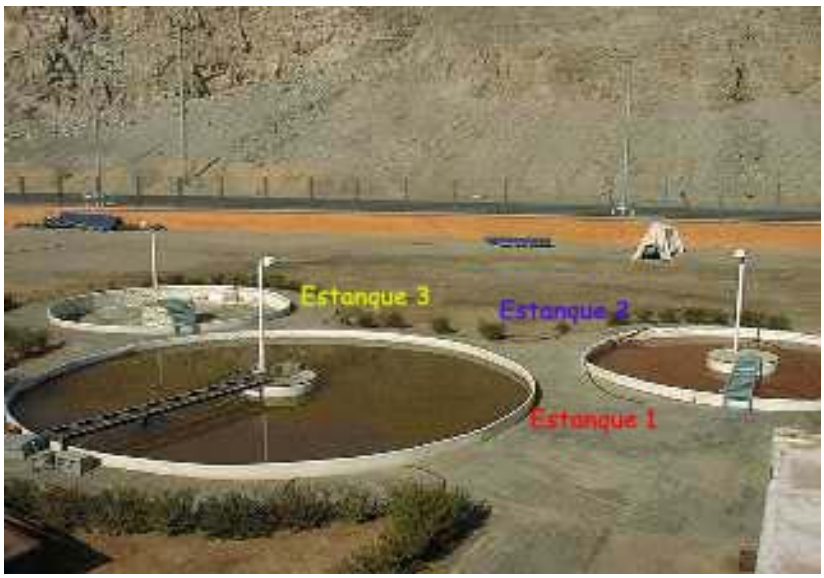

Figura 7: Mesocosmos de Eilat.

2.1.3. Procesamiento de las muestras

Con las muestras correspondientes a los estanques mencionados, se realizó el mismo tipo de estudio que en los ambientes naturales. No obstante, dado el tiempo de transporte, las muestras se fijaron con glutaraldheído al 2,5%. Posteriormente se lavaron repetidas veces con tampón fosfato, para eliminar los restos del fijador y se conservaron en nevera a 4ºC hasta su posterior procesamiento.

2.1.4. Microscopía Láser Confocal (CLSM)

El análisis de las muestras tanto para la identificación como para la determinación de la biomasa total se realizó por Microscopía Láser Confocal (Leica TCS 4d, Heildeberg,Alemania). Además la biomasa individual de cada cianobacteria se realizó en los ambientes contaminados por petróleo (Etang de Bêrre y Mesocosmos) basándose en la misma técnica microscópica. El CLSM (*Confocal Laser Scanning Microscopy*) se seleccionó ya que se trataba de una técnica microscópica que permitía la observación con escasa manipulación de la muestra. Así mismo permitió realizar series ópticas (*stacks*∗) de pocas micras de grosor de los tapetes microbianos, e identificar de manera nítida los diferentes géneros de cianobacterias basándose en la autofluorescencia que éstas emiten cuando se excitan a una determinada longitud de onda (Solé et al. 1998, 2001).

Caracterización e identificación de las cianobacterias

La caracterización e identificación de cianobacterias se realizó de acuerdo al Manual de Bergey's (Castenholz et al. 2001) considerando el diámetro, la septación y la presencia o no de vacuolas de gas y de la envuelta mucopolisacárida (EPS).

∗conjunto de imágenes o serie óptica formada a partir de sucesivas secciones ópticas tomadas en profundidad en un mismo punto de la muestra.

Determinación de la biomasa

Se ha trabajado en la continua optimización de un método, especialmente indicado, para determinar de manera rápida la biomasa de las cianobacterias en muestras de tapetes microbianos. En este trabajo experimental se han usado dos métodos cuya aplicación, separada en el tiempo, se ha basado en programas de análisis de imagen y en las mejoras aportadas por cada uno de ellos.

El primer programa informático utilizado fue el UTHSCSA *Image tool* 3.0, utilizando las proyecciones suma (imágenes bidimensionales) obtenidas por CLSM. Estas imágenes se transformaron en imágenes binarias (blanco/negro) usando el programa Adobe Photoshop 6.0 para Windows. De dichas imágenes se seleccionaron exclusivamente los contornos negros que correspondían a *Microcoleus chthonoplastes*, el resto de cianobacterias se eliminaron. Finalmente, a partir de datos de área y perímetro de cada contorno y de la aplicación de fórmulas descritas por Solé et al. (2001) se obtuvieron los resultados finales de biomasa expresados en mgC/cm^3 de sedimento.

El segundo método utilizado para la obtención de biomasa fue aplicando el programa *Image J* 1.33f. Este proceso utiliza *stacks* de imágenes que al igual que en el método anterior, se transformó todo el *stack* en imágenes binarias. Para obtener mejores resultados, en dicho programa se aplicó el *plugin Voxel Counter*. Esta aplicación específica permite la evaluación del porcentaje de píxeles entre el biovolumen de las cianobacterias y el volumen total de sedimento. Los resultados finales de biomasa también se expresaron en mgC/cm^3 de sedimento.

2.2. Cultivos Celulares. *Microcoleus* consorcio

2.2.1. Cultivo de enriquecimiento

Los cultivos de enriquecimiento se obtuvieron a partir de los microcosmos contaminados por petróleo 0.5 cm^2 de capa verde se inocularon en medio mineral Pfenning (van Gemerden y Beeftink, 1983) y se ensayaron diferentes condiciones de cultivo que se muestran en la tabla 1 del capítulo V.

En todos los casos, la incubación de los diferentes cultivos se realizó en condiciones aeróbicas y anaeróbicas a una intensidad de luz de 15$\mu Em^{-2}s^{-1}$ y a 27ºC.

2.2.2. Aislamiento de *Microcoleus* consorcio

El método descrito para el aislamiento de *Microcoleus* consorcio forma parte de los resultados del presente trabajo y por ello se describe en el capítulo V.

2.2.3. Identificación

A. Aplicación de técnicas microscópicas de alta resolución

Para la caracterización de los microorganismos se utilizaron las siguientes técnicas microscópicas:

Microscopía Láser Confocal (CLSM)

La microscopia láser confocal se utilizó para la caracterización e identificación de la cianobacteria filamentosa *Microcoleus chthonoplastes* en muestras de cultivo líquido.

Las muestras se depositaron en portaobjetos excavados y se observaron a 63X. Se obtuvieron secciones ópticas, proyecciones suma (2D) e imágenes estereoscópicas (3D).

Microscopía Electrónica de Transmisión (TEM)

Para determinar la caracterización ultraestructural de los microorganismos del consorcio, se realizaron secciones ultrafinas que se analizaron al microscopio electrónico de transmisión (TEM: *Transmision Electron Microscopy*).

Las muestras de los cultivos, procedentes tanto de medio líquido como sólido, se fijaron con glutaraldheído en tampón fosfato a una concentración final del 2,5% durante 2-3 horas a 4ºC (Esteve et al. 1990). Luego se realizaron varios lavados de las muestras, de una duración de 20 minutos cada una, para eliminar el exceso de fijador, utilizando para ello el mismo tampón. Posteriormente las muestras se fijaron con tetróxido de osmio (OsO_4) a 4ºC durante dos horas y se lavaron de nuevo con tampón fosfato.

A continuación, las muestras se centrifugaron a 5000xg durante 10 minutos y el *pellet* obtenido se incluyó en agar puro al 2%. Una vez solidificado el agar, se cortó en pequeños cubos que se deshidrataron en concentraciones crecientes de acetona (30, 50, 70 y 100%). Posteriormente, estas muestras se lavaron dos veces en óxido de propileno al 100%.

Finalmente las muestras fueron incluidas en resina Spur, utilizándose el piramidotomo (TM 60, C. Reichert AG. Wien, Austria) para piramidar las muestras y el ultramicrotomo (LKB 8800 Ultratome III. LKB-Produkter AB. Bromma, Suecia) para obtener las secciones ultrafinas. Los cortes ultrafinos se depositaron en rejillas de carbón y se tiñeron con citrato de plomo según el metodo descrito por Reynolds (1963).

Las muestras fueron observadas en el microscopio electrónico de transmisión HITACHI H-7000 (Hitachi Ltd. Japón).

Microscopía Electrónica de Barrido (SEM)

El SEM (*Scanning Electron Microscopy)* se utilizó para la caracterización de los microorganismos de *Microcoleus* consorcio.

Las muestras se fijaron durante 2 horas a 4ºC con glutaraldheído al 2,5%. El fijador se eliminó mediante repetidos lavados en tampón fosfato, de acuerdo con el método descrito por Miloning (1961). Posteriormente las muestras se filtraron en un filtro nucleopore, se deshidrataron en concentraciones crecientes de acetona (30, 50, 70 y 100%) y se procesaron de acuerdo al método aplicado por Nogués et al. (1994).

A continuación las muestras se desecaron al punto crítico, se montaron sobre unos soportes metálicos especiales y se metalizaron recubriéndose la superficie con una capa de 96 nm de oro.

Finalmente las muestras se observaron en el microscopio de barrido HITACHI S 570 (Hitachi Ltd., Japón).

B. Técnicas Moleculares

La identificación de los microorganismos heterotróficos del consorcio se realizó por las siguientes técnicas moleculares:

Extracción de DNA

La extracción de los ácidos nucleicos de los cultivos se realizó según el método descrito por Massana et al. (1997). A partir de las placas de agar Pfenning que contenían la muestra a analizar, se recogieron las colonias de *Microcoleus* consorcio y se resuspendieron en 2 ml de tampón de lisis (50 mM Tris-HCl, pH 8.3; 40mM EDTA, pH 8.0; 0.75 M sucrosa). Se agregaron a la muestra perlas de cristal estériles de 0,5 mm de diámetro y se agitaron en un vórtex para romper la vaina exopolisacárida de los filamentos de la cianobacteria. El DNA se extrajo

usando el método de lisis/fenol como se describe a continuación. La lisozima (1 $mg.ml^{-1}$) se añadió a las muestras, que posteriormente se incubaron a 37ºC y en agitación leve durante 45 minutos. A continuación, se agregaron: dodecil sulfato de sodio (concentración final del 1%) y proteinasa K (con una concentración final de 0.2 $mg.ml^{-1}$) a la muestra, incubándose la mezcla a 55ºC durante 60 minutos y con agitación. Los ácidos nucleicos se extrajeron con alcohol isoamílico fenolcloroformo (25:24:1, vol:vol:vol), realizándose este proceso dos veces. El fenol residual se eliminó con cloroformo-alcohol isoamílico (24:1, vol:vol). Los ácidos nucleicos se purificaron y concentraron con un Centricon-100 (millipore). La integridad del DNA se comprobó por electroforesis en gel de agarosa, y se cuantificó usando un marcador de DNA estándar (*Low DNA mass ladder*, *Invitrogen*). Se separaron muestras para el análisis por DGGE y para la librería genética.

PCR-DGGE (Reacción en Cadena de la Polimerasa-Electroforesis en Gel de Gradiente Desnaturalizante)

Los fragmentos del gen 16S rRNA para el análisis de DGGE se obtuvieron usando el cebador específico para bacterias 358F-GC y el cebador universal 907RM (Muyzer et al. 1998 y Schauer et al. 2000). La PCR se llevó a cabo con un termociclador Biometra usando el siguiente programa: desnaturalización inicial a 94°C (5 minutos); 10 ciclos de desnaturalización a 94°C (un minuto); anillamiento de 65 a 55°C (un minuto), disminuyendo un gradocentígrado en cada ciclo y una extensión a 72°C (3 minutos); 20 ciclos estándares a 55°C (1 minuto) y una extensión final a 72°C (5 minutos).

Los cebadores 344f-GC y 915r se utilizaron para la amplificación del 16S rRNA de arqueobacterias (Raskin et al. 1994 y Stahl et al. 1991). El protocolo de PCR incluyó un paso inicial de desnaturalización a 94ºC (5 minutos), seguido por 20 ciclos más de desnaturalización a 94ºC (un minuto), anillamiento de 71 a 61ºC (un minuto) disminuyendo un grado

centígrado cada ciclo, y una extensión a 72ºC (3 minutos). Se añadieron 15 ciclos adicionales a 61ºC.

Las mezclas de PCR llevaban: 1-10ng de DNA, con deoxinucleósido trifosfato a una concentración de 200 µM, 1.5 mM $MgCl_2$, los cebadores estaban a una concentración de 0.3 µM, 2.5 U de *Taq* polimerasa (Invitrogen) y tampón de PCR. Se agregó BSA (albúmina sérica bovina) a una concentración final de 600 $\mu g ml^{-1}$ para reducir al mínimo el efecto inhibitorio de sustancias húmicas (Harry et al. 1999). El volumen de reacción era de 50µl. Los productos de PCR se verificaron y cuantificaron por electroforesis en gel de agarosa con un marcador DNA estándar (*Low DNA mass ladder, Invitrogen*). El análisis por DGGE se realizó en un sistema de DCode (Bio-Rad) según Muyzer et al. (1998). Se preparó un gel de poliacrilamida al 6% en gradiente desnaturalizante mezclando soluciones al 0 y al 80% de agente desnaturalizante (urea 7M más 40% de formamida desionizada). 700 ng de producto de PCR se cargaron para cada muestra y el gel se hizo correr a 100V-60ºC durante 18h en tampón TAE 1x (40 mM Tris [pH 7.4], 20 mM acetato del sodio, 1M EDTA). El gel se tiñó con SybrGold (*Molecular Probes*) durante 45 minutos y se visualizó con luz UV en un Gel Doc (EQ -Bio-Rad).

Las bandas más prominentes se escindieron del gel y se resuspendieron en agua desionizada durante toda una noche. Las muestras se reamplificaron y purificaron con el *Kit* llamado *High Pure Product Purification* (Roche) para su secuenciación.

Librería Genética y Análisis del Polimorfismo de Restricción de la Longitud del Fragmento de DNA

Para la clonación, el gen 16S rRNA se amplificó entre las posiciones 27 y 1492 (numeración de la secuencia del gen 16S rRNA de *Escherichia coli*), con los cebadores 27F (5'-AGA GTT TGA TCM TGG CTC AG-3') y 1492R (5'-GGT TAC CTT GTT ACG ACT T-3'). Las mezclas de PCR contenían 10 ng del DNA estándar, cada deoxinucleósido trifosfato

estaba a una concentración de 200 µM, de 1.5 mM MgCl2, cada cebador a una concentración de 0.3 µM, 2.5 U de *Taq* polimerasa (Invitrogen) y tampón de PCR.

Las reacciones se realizaron en un termociclador automatizado (Biometra) con el siguiente ciclo: un paso inicial de desnaturalización a 94ºC (5 minutos), seguido por 30 ciclos a 94ºC (un minuto), a 55ºC (un minuto) y a 72ºC (2 minutos), y de un paso de extensión final a 72ºC (10 minutos). El producto de PCR se clonó con el *kit TOPO TA* (Invitrogen) según las instrucciones del fabricante. Las colonias positivas escogidas se transfirieron a una placa *multiwell* que contenía el medio de Luria-Bertani y glicerol al 7%, y se almacenaron a -80ºC. Los plásmidos recombinantes se extrajeron usando el kit *QIAprep spin miniprep* (QIAgen), siguiendo las instrucciones del fabricante. Los plásmidos purificados se digerieron a 37ºC con *Hae*III (Invitrogen) y el producto se procesó en gel de agarosa de bajo punto de fusión al 2.5%. Los patrones de bandas diferentes se eligieron para la secuenciación parcial. La cobertura de la biblioteca se calculó de acuerdo con la siguiente ecuación: $C=1-(n/N)$, donde n es el número de clones únicos y N es el número total de clones examinados (Ravenschlag et al. 1999).

La elección de los cebadores utilizados (358F cola GC y 907R para el análisis de DGGE, y 27F y 1492R para la biblioteca) se hizo deliberadamente porque no amplifican *Microcoleus* sp. De esta manera se eliminó la amplificación de esta cianobacteria sin interferir en los resultados finales.

Secuenciación del rRNA

Las reacciones de secuenciación lo realizó la empresa *Macrogen* (Corea) utilizando los cebadores 907R para las bandas bacterianas de DGGE (500 pb de longitud, aproximadamente), y 27F para los genes clonados del 16S rRNA. Se utilizó el *kit Big-dye Terminator* versión 3.1

para la secuenciación y las reacciones se efectuaron en un analizador automático ABI 3730XL – Analyzer con 96 capilares.

Las secuencias se analizaron con el programa informático *BLAST* (Altschul et al. 1997), para conseguir un primer indicio de la afiliación filogenética, y con el programa de *CHECK-CHIMERA* de RDP (Maidak et al. 2000), para determinar los artefactos quiméricos potenciales. Las secuencias se alinearon usando la herramienta de alineación automática del software ARB (http://www.mikro.biologie.tu-muenchen.de) (Ludwig et al. 1998). Las secuencias parciales se insertaron en el árbol optimizado derivado de datos completos de la secuencia utilizando *Quick add using parsimony tool*, que no afecta la topología inicial del árbol.

En la figura 6, se puede observar todo el procedimiento aplicado en la muestras analizadas.

Número de Acceso:

Cuarenta y cuatro secuencias del gen de 16S rRNA se enviaron al centro de datos de la EMBL (http://www.ebi.ac.uk/embl) y se recibieron los números de acceso siguientes: de AJ871043 a AJ871081 para la librería genética y de AJ870388 a AJ870392 para las bandas de DGGE (la asignación detallada para cada secuencia aparece en la figura 8 en el apartado de resultados).

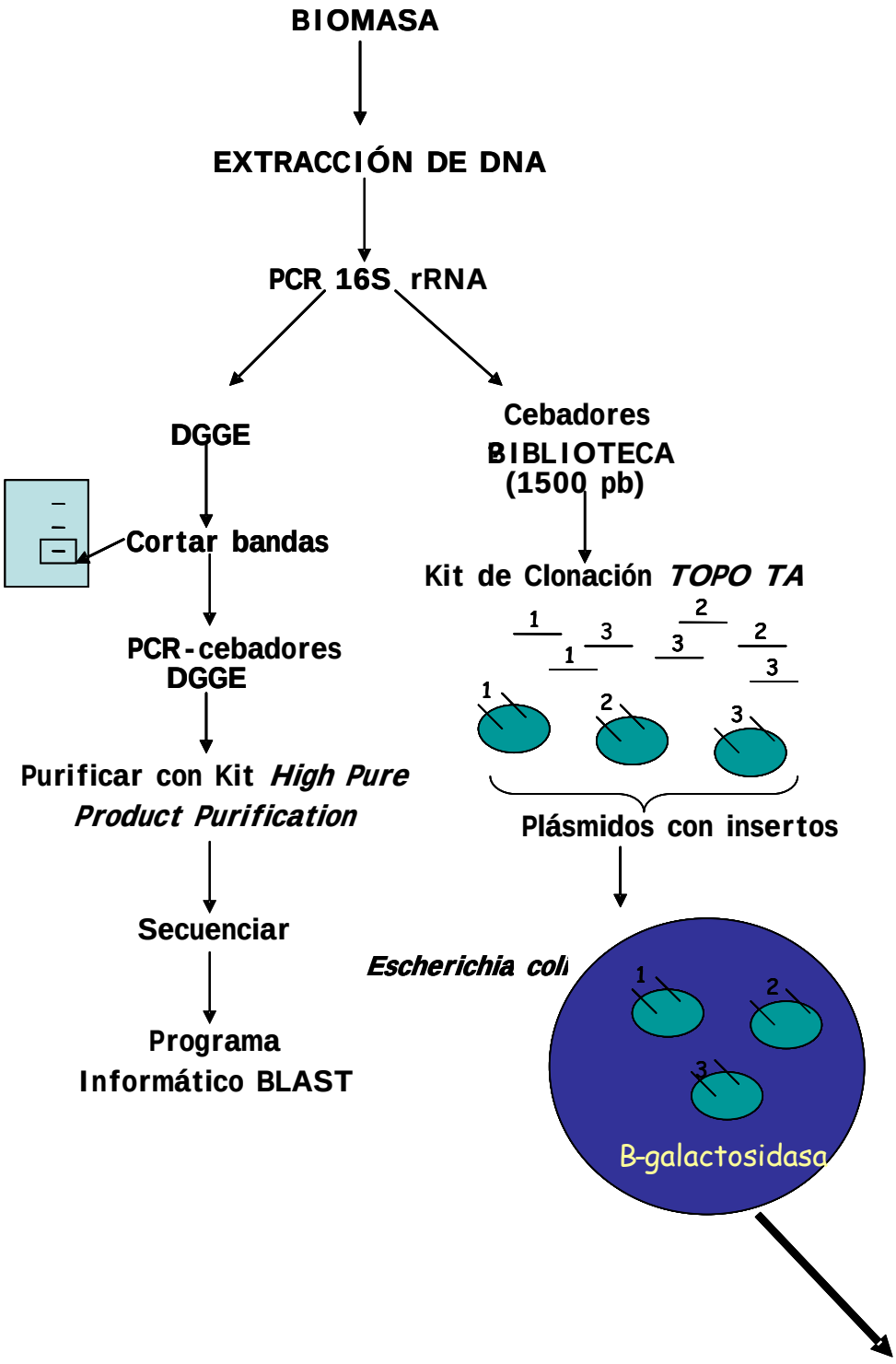
BIOMASA
EXTRACCIÓN DE DNA
PCR 16S rRNA
DGGE
Cebadores
BIBLIOTECA
(1500 pb)
Cortar bandas
Kit de Clonación TOPO TA
PCR-cebadores
DGGE
Purificar con Kit High Pure
Product Purification
Plásmidos con insertos
Secuenciar
Escherichia coli
Programa
Informático BLAST
B-galactosidasa

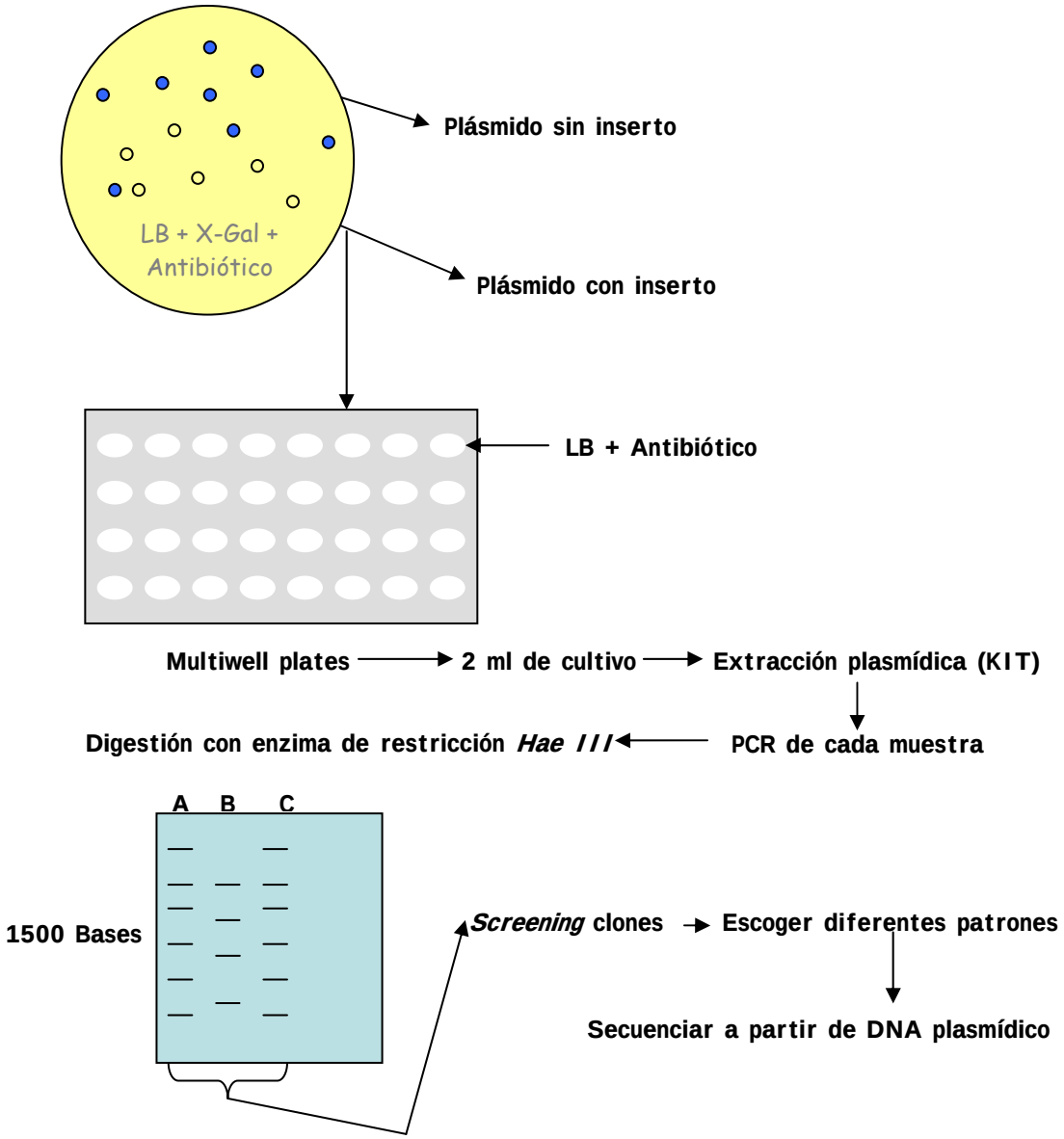

Figura 6: Técnicas moleculares aplicadas en la identificación de los microorganismos heterótrofos.

C. Técnicas de Análisis Químicos:

Las muestras, de los cultivos control y de los contaminados por petróleo del consorcio, se analizaron en el CSIC (Consell Superior d'Investigacions Científiques) por García de Oteyza et al. 2004.

El objetivo era determinar si el consorcio, toleraba o era capaz de degradar el petróleo Maya (seleccionado en este trabajo por ser muy tóxico). Para ello se realizó: separación por cromatografía de columna (CC), cromatografía de gases y cromatografía de gases acoplada a espectrometría de masas. Los resultados obtenidos de este estudio se comentan en el capítulo V en la discusión de los resultados.

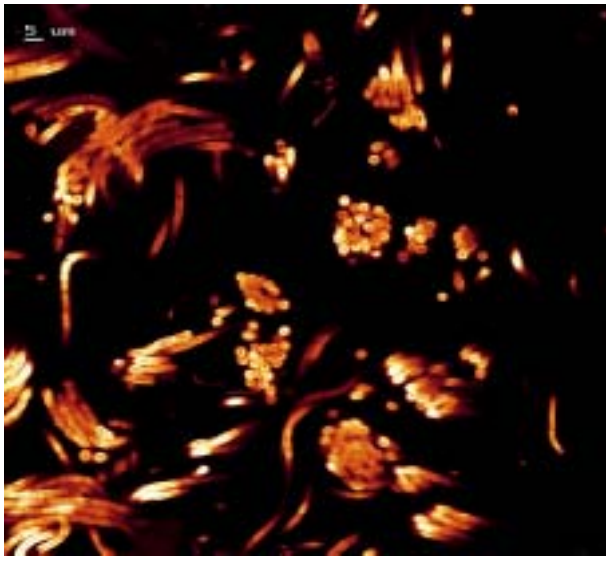

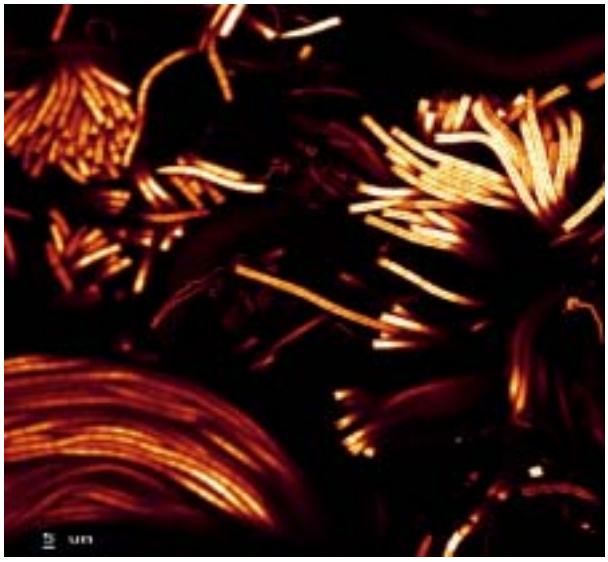

CAPÍTULO III: IDENTIFICACIÓN Y DISTRIBUCIÓN DE LAS CIANOBACTERIAS EN LOS TAPETES MICROBIANOS DE SALINS-DE-GIRAUD EN UN CICLO DÍA-NOCHE

Introducción

Resultados:

- Identificación y Distribución de las Cianobacterias en los Tapetes Microbianos de la Camarga
- Distribución de *Microcoleus chthonoplastes* durante un ciclo día-noche

Discusión

Introducción:

Como se ha indicado en el capítulo introductorio, los tapetes microbianos están compuestos por diferentes comunidades microbianas cuya distribución depende de los gradientes químicos generados por la actividad de éstas. Los microorganismos fototróficos oxigénicos y anoxigénicos se encuentran mayoritariamente en estos ecosistemas y son los que desempeñan el papel más importante como productores primarios. Las cianobacterias se encuentran en la capa superficial formando una compleja red y por lo tanto ayudando a la estabilización de estos ambientes. *Microcoleus chthonoplastes* es la cianobacteria más importante y dominante en los tapetes microbianos del delta del Ebro y Salins-de-Giraud, es por ello que a éstos se les denomina frecuentemente *Microcoleus mats*.

En las capas anóxicas más profundas de dichos tapetes, y en las que todavía incide la luz, las bacterias fototróficas del azufre participan en el flujo de energía, puesto que realizan simultáneamente la detoxificación de H_2S y la fotoasimilación de CO_2. Durante la noche, los gradientes químicos cambian drásticamente y exponen a las bacterias a diferentes condiciones ambientales. Como respuesta, los microorganismos efectúan movimientos migratorios, lo que les permite ubicarse a diferentes profundidades del tapete microbiano, este efecto se ha visto también en ambientes artificiales (Kühl & Fenchel 2000). Aunque las migraciones verticales se han descrito para diferentes microorganismos: bacterias oxidadoras del azufre (Nelson et al. 1986 a y b, Richardson L. 1996, Thar y Kühl 2001); bacterias sulfato reductoras (Krekeler et al. 1998, Teske et al. 1998) y cianobacterias (Whal y Walbsy 1984, Richardson et al. 1987, García-Pichel et al. 1994, Bebout y García-Pichel 1995), es difícil evaluar los parámetros que controlan la distribución vertical de las poblaciones, ya que interactúan entre ellos.

Esta es la causa de que muchas de las investigaciones se hayan centrado en los movimientos migratorios de un solo tipo de microorganismo como *Thioploca* spp. (Huettel et al. 1996) y *Synechococcus* sp. (Ramsing et al. 2000).

De los tapetes microbianos estudiados, los del delta del Ebro (Tarragona-España) y Salins-de-Giraud (La Camarga-Francia) son los más estabilizados y mantienen una típica estructura laminar. Puesto que la diversidad de las cianobacterias de los tapetes

del delta del Ebro, mediante el CLSM ha sido estudiada con anterioridad (Solé et al. 2003), en este capítulo se centra el estudio en Salins-de-Giraud, analizando la diversidad y la abundancia relativa en profundidad de las distintas cianobacterias identificadas. Así mismo se determinan los perfiles de biomasa de *Microcoleus chthonoplastes* y se estudia el movimiento migratorio de esta cianobacteria en un ciclo día-noche mediante CLSM.

Resultados:

El presente estudio se ha realizado en los tapetes microbianos de Salins-de-Giraud los días 11 y 12 de Junio del 2001, y a diferentes tiempos (9.40, 15.00, 18.00, 22.00, 4.00 y a las 7.30 horas). Las muestras se han procesado y analizado de acuerdo al método descrito en el apartado 2.1.3. de material y métodos.

Identificación y distribución de las cianobacterias en los tapetes microbianos de la Camarga:

En los tapetes microbianos de Salins-de-Giraud se han identificado mediante CLSM y de acuerdo con el Manual de Bergey's las siguientes cianobacterias filamentosas: *Microcoleus chthonoplastes*, *Halomicronema excentricum*, *Pseudanabaena* sp. y una picocianobacteria de 0.96 μm de diámetro. Entre las unicelulares *Gloeocapsa* sp. y miembros del grupo *Pleurocapsa*.

Las abundancias relativas de estas cianobacterias a diferentes profundidades del tapete se determinaron durante un ciclo día y noche (Figura 1). *M. chthonoplastes* (Figura 2) se encuentra uniformemente distribuido en el tapete y es la cianobacteria más abundante; distribuyéndose mayoritariamente en su superficie durante el día. *Halomicronema excentricum*, una cianobacteria típica de ambientes salinos, se distribuye a lo largo del tapete durante el día, mientras que por la noche se sitúa entre los 0 y 1.5 mm de profundidad. *Pseudanabaena* sp. se localiza a los 3.25 mm de profundidad y únicamente a las 9.40 h. Finalmente las picocianobacterias tienen su máxima abundancia entre los 2 y 4 mm. Entre las cianobacterias unicelulares mencionamos a *Gloeocapsa* sp. y que se encuentra a diferentes profundidades entre 0.5

y 2 mm a las 15.00h; a 0.25 mm a las 22.00h; y a 0.75 mm a las 4.00h; mientras que miembros del grupo *Pleurocapsa* tienen su máximo a las 4.00h a 2.25 mm.

Distribución de *Microcoleus chthonoplastes* durante un ciclo día y noche:

Los resultados obtenidos en el apartado anterior dan información sobre la abundancia relativa de cada cianobacteria por separado en profundidad. No obstante y puesto que *Microcoleus chthonoplastes* es la cianobacteria dominante se han estudiado los perfiles de biomasa de esta cianobacteria mediante CLSM, según el método descrito en el apartado anterior 2.1.4. de material y métodos.

En la figura 3, se aprecia que *Microcoleus chthonoplastes* a las 9.40h presentó valores altos de biomasa después de un periodo de oscuridad: a 1 mm (39.7 mgC/cm^3 de sedimento), a 1.75 mm (24.27 mgC/cm^3 de sedimento) y a 2.5 mm (29.53 mgC/cm^3 de sedimento).

A las 15.00 h, los filamentos se distribuyeron principalmente en la superficie del tapete con una concentración de 31.22 mgC/cm^3 de sedimento. A las 18.00h *Microcoleus chthonoplastes* alcanzó su máxima concentración (52.80 mgC/cm^3 de sedimento) a 0.5mm; mientras que las concentraciones más bajas se encontraron en las zonas más profundas del tapete.

Durante la noche (22.00h) esta cianobacteria filamentosa se localizó entre 0 y 1.5 mm de profundidad y no se detectó a partir de los 2.25 mm. A las 4.00h *M. chthonoplastes* se distribuyó homogéneamente a lo largo de los 3 mm del tapete estudiado.

Finalmente a las 7.30 h, la distribución de *Microcoleus chthonoplastes* era similar a la descrita a las 9.40 h. El máximo se dio entre 0.75 y 1 mm (35.25 mgC/cm^3 de sedimento – 33.25 mgC/cm^3 de sedimento). La concentración de biomasa de esta cianobacteria fue disminuyendo en profundidad, siendo de 25.88 mgC/cm^3 de sedimento a 1.75 mm y de 10.49 mgC/cm^3 de sedimento a 2.5 mm de profundidad.

Discusión:

Las cianobacterias en los tapetes microbianos de Salins-de-Giraud muestran movimientos verticales migratorios individuales durante el ciclo día y noche. *M. chthonoplastes*, una cianobacteria característica de los ambientes hipersalinos (Caumette et al.1994, Abed et al. 2002a) es la cianobacteria filamentosa más abundante y se ubica en diferentes capas del tapete a diferentes horas. Su distribución vertical es homogénea (de 4.00h a 7.30h) después de un periodo de oscuridad (de 6 a 9 horas) y es máxima cerca de la superficie (18.00h) después de casi 12 horas de un periodo de iluminación (Figura 3). Si esta distribución se compara además con los perfiles de oxígeno y de sulfhídrico del tapete, obtenidos por Wieland et al. 2005, se observa que los óptimos de crecimiento de *Microcoleus chthonoplastes* se dan en las capas óxicas (Epping et al. 1999, Wieland y Kühl 2000) y por tanto en ausencia de H_2S. No obstante también se observa que dicha cianobacteria puede crecer en presencia de H_2S, lo cual sugiere o bien una adaptación metabólica por parte de *M. chthonoplastes*, que en este caso podría realizar una fotosíntesis anoxigénica, puesto que en esta capa todavía incide la luz, o bien la presencia de dos poblaciones distintas de esta cianobacteria.

Por otra parte, en todos los perfiles la concentración de H_2S determinada siempre fue inferior a la descrita por de Witt y van Gemerden (1987) como inhibitoria para la fotosíntesis anoxigénica. Miller & Bebout (2004), también han estudiado el desarrollo de diferentes cianobacterias frente a las variaciones en la concentración de sulfhídrico del ambiente natural.

Las cianobacterias coexisten en los tapetes microbianos con las poblaciones de bacterias fototróficas anoxigénicas que se distribuyen en capas inferiores en las que todavía incide la luz y donde se encuentra el H_2S. Para estudiar el efecto que las propias poblaciones de bacterias fototróficas oxigénicas tiene sobre las anoxigénicas teniendo en cuenta los parámetros ambientales (descritos por Wieland et al. 2005), Fourçans et al. 2004 realizaron un análisis canónico de correspondencia entre los citados parámetros. Este análisis contempló los datos obtenidos en este apartado para la distribución vertical de las cianobacterias. El oxígeno, el pH y la biomasa de *Microcoleus chthonoplastes* se definieron como factores negativos para el desarrollo de las bacterias fototróficas anoxigénicas (PAB). *M. chthonoplastes* y otras cianobacterias podrían influenciar en la

distribución de las PAB, ya que ambos tipos de poblaciones pueden competir por determinados parámetros químicos (H_2S y O_2). La fotosíntesis oxigénica en la superficie del tapete durante el día produjo oxígeno con un incremento del pH a 9.4 a lo largo de los 1.5 milímetros desde la superficie del mismo (Wieland et al. 2005) generándose condiciones adversas para las PAB. Durante la noche, la concentración de oxígeno y el pH (6.8) fueron mucho más bajos, debido a la ausencia de fotosíntesis oxigénica y por tanto estas condiciones fueron más favorables para mantener a las PAB. Estudios semejantes se describieron con anterioridad para *Chromatium* sp. por van Gemerden y Beeftink (1981).

Los movimientos migratorios aquí descritos, para las cianobacterias y su relación con los microorganismos fototróficos anoxigénicos descritos por Fourçans et al. (enviado a *FEMS Microbial Ecology*), nos permite constatar la eficacia del CLSM y las técnicas moleculares en la distribución de los microorganismos. La distribución cuantitativa de *Microcoleus chthonoplastes* abre nuevas posibilidades a la distribución individualizada de cada tipo de cianobacteria en profundidad a escala micrométrica. Aunque a dicha escala, sí se poseía información sobre la distribución de parámetros ambientales (micro-electrodos) y también de distribución de la luz (fibra óptica) no era posible contabilizar las cianobacterias de forma tan precisa, como la que se obtiene por la aplicación de esta metodología. La distribución de *Microcoleus chthonoplastes* cuando es cuantitativa, nos aporta datos que correlacionados con los parámetros ambientales permite hipotetizar sobre el metabolismo que puede estar desarrollando esta cianobacteria directamente en el tapete, no solo en un ciclo día y noche, sino también en periodos de tiempos más largos.

La distribución precisa de las cianobacterias por esta técnica, ayuda a comprender la distribución de las PAB influida por los cambios en los parámetros físicos y químicos que producen las primeras con su metabolismo.

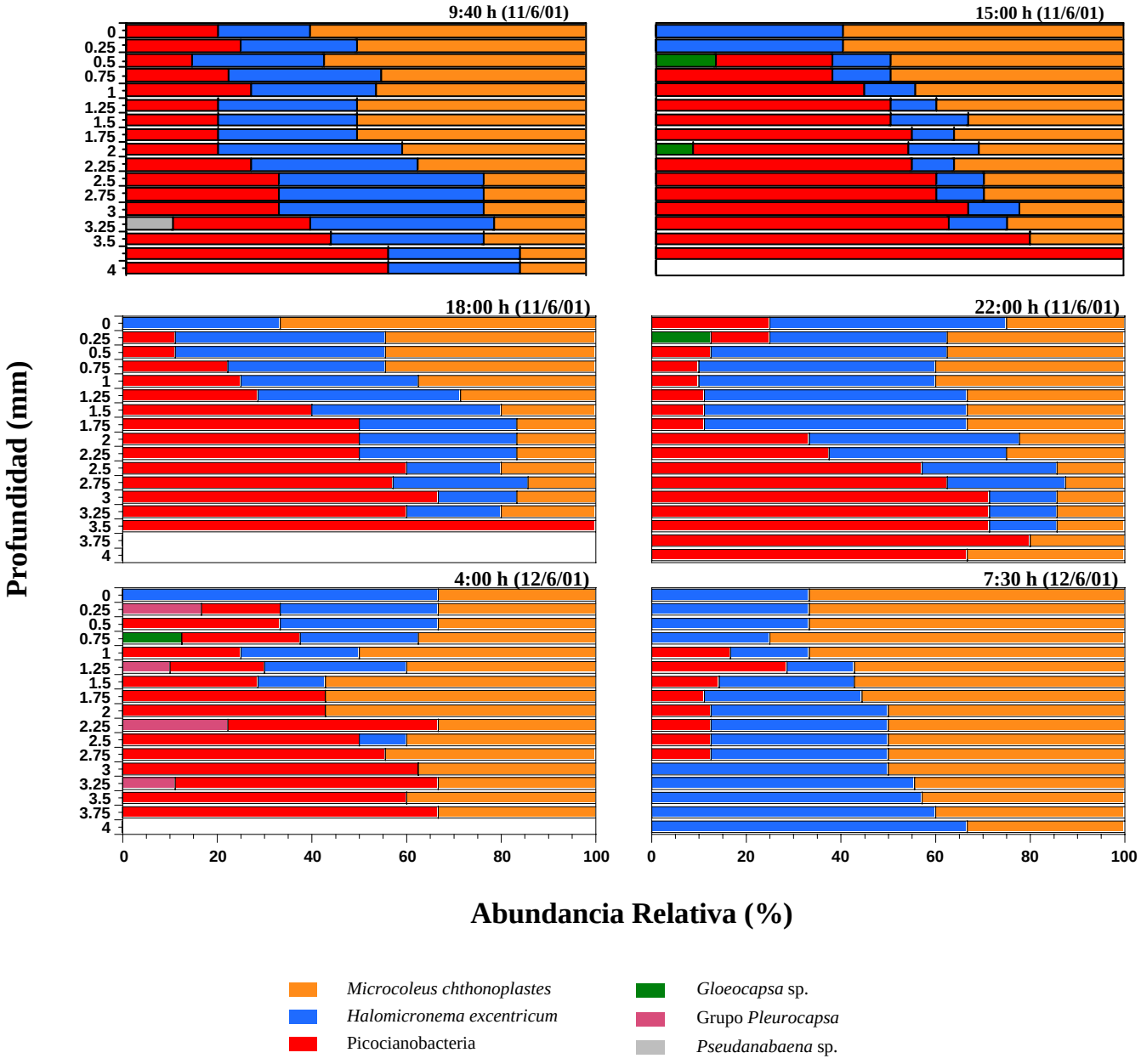

Figura 1: Abundancia relativa (%) en profundidad de las cianobacterias caracterizadas e identificadas por CLSM durante el ciclo día-noche en los tapetes microbianos de Salins-de-Giraud.

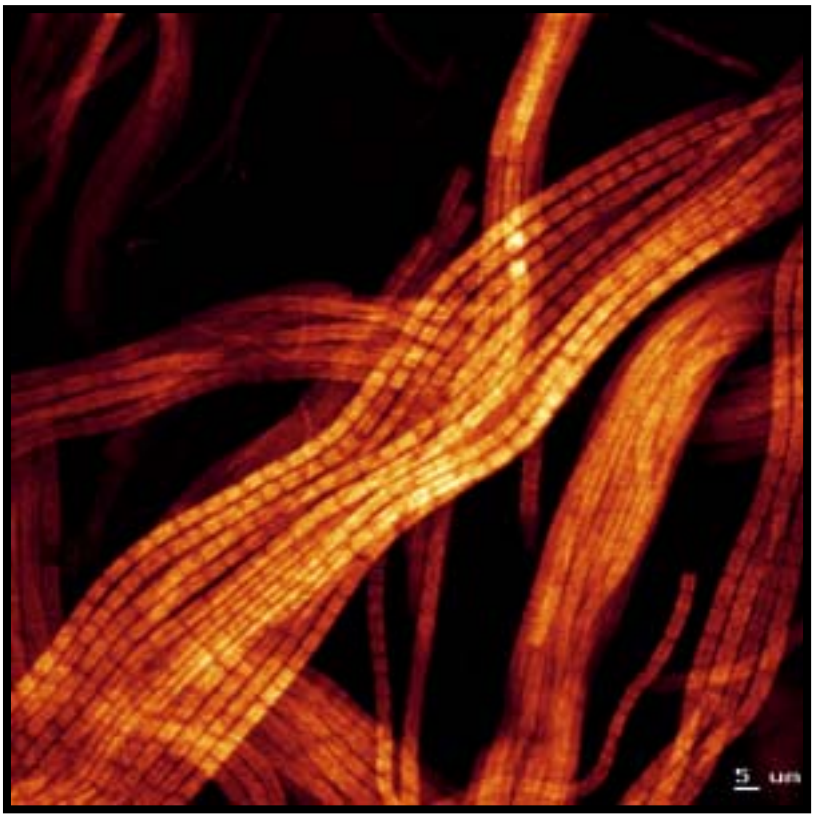

Figura 2: *Microcoleus chthonoplastes* formando haces de filamentos.

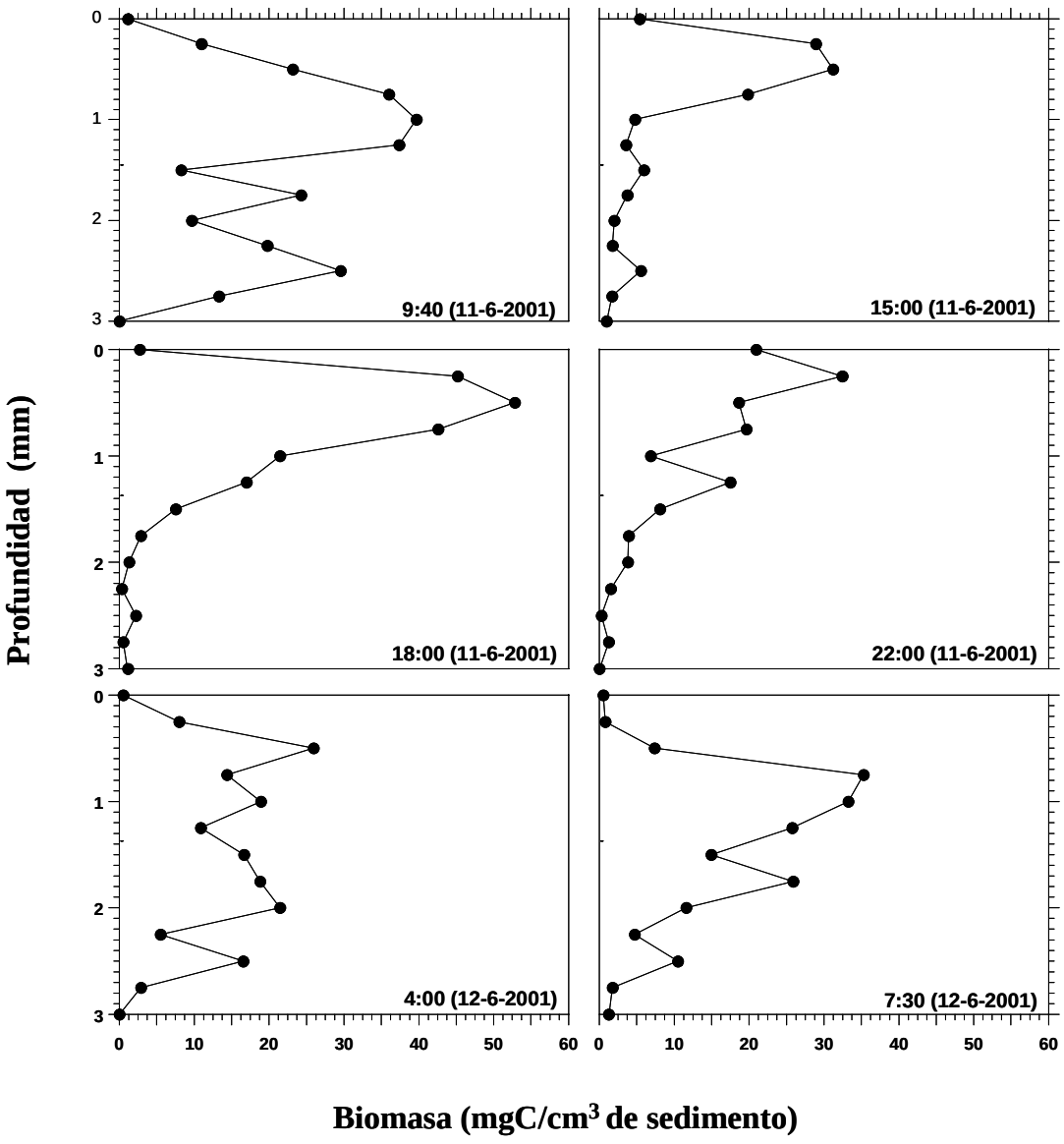

Figura 3: Perfiles de biomasa de *Microcoleus chthonoplastes* durante el ciclo día-noche.

CAPÍTULO IV: DIVERSIDAD DE LAS CIANOBACTERIAS EN AMBIENTES NATURALES Y ARTIFICALES CONTAMIANDOS POR PETRÓLEO. ANÁLISIS CUANTITATIVO

Introducción

Resultados y Discusión:

Análisis de la diversidad y determinación de la biomasa de las cianobacterias en tapetes microbianos de Europa con distinto grado de contaminación.

Análisis de la diversidad y determinación de la biomasa de las cianobacterias en Mesocosmos.

Introducción:

Los tapetes microbianos se han definido en el capítulo I del presente trabajo, como sedimentos estratificados bentónicos de pocos milímetros de grosor, estando estructurados en capas de diferentes coloraciones, que se corresponden con las poblaciones de microorganismos fotosintéticos. La ubicación de estos se ve influenciada por micro-gradientes de parámetros ambientales tanto químicos como físicos (Herbert R. A. 1985, Esteve et al. 1994, Wieland et al. 2003, Diestra et al. 2004, Fourçans et al. 2004). Estos parámetros, a su vez se ven afectados por la propia actividad de los microorganismos.

En general, existe un gran interés por determinar la diversidad microbiana en los ambientes naturales y en especial en los ambientes extremos para la vida, como son los tapetes microbianos. Diferentes estudios estiman que la diversidad conocida está tan solo entre el 0.1 y el 10% de la real, hecho probablemente debido a la dificultad para identificar a los microorganismos que actualmente no son cultivables. El desarrollo de las técnicas moleculares ha facilitado en parte la identificación de éstos (Fuhrman et al. 1993, Gray et al. 1996, Martin A. P. 2002).

No obstante, las estimas de la diversidad basadas en la de las distintas poblaciones de un ecosistema, tampoco encuentran solución en la aplicación de dichas técnicas ya que no son cuantitativas. Las cianobacterias de los tapetes microbianos no son una excepción a la problemática expuesta, aunque su mayor tamaño y la presencia de pigmentos, que emiten fluorescencia natural hacen más fácil, no solo su identificación sino también su cuantificación (Solé et al. 2003).

Las cianobacterias en general son ubicuas y toleran amplios márgenes de parámetros limitantes para la vida, como son; las elevadas temperaturas (Ferris et al. 1996) y la salinidad (Demergaso et al. 2003). Entre los parámetros químicos, el N_2 suele ser el factor más limitante y su fijación se ve regulada por el pH, la pO_2, el NH_4, el carbono orgánico disponible, el H_2S y la disponibilidad del agua (Steppe et al. 2001).

Estudios sobre la distribución espacial de los microorganismos demuestran que las mismas poblaciones pueden desarrollar diferentes características fisiológicas cuando se encuentran en distintos hábitats, tratándose no obstante de microorganismos que están

genéticamente relacionados, lo que todavía dificulta más su identificación (Moore et al. 1998).

En los últimos años, nuestro grupo de trabajo ha desarrollado una metodología utilizando el microscopio láser confocal, basada en la autofluorescencia natural emitida por las cianobacterias y en la obtención de secciones ópticas de alta resolución. Todo ello ha permitido la caracterización e identificación de estos microorganismos y además gracias a técnicas de análisis de imagen, la determinación de su biomasa.

Recientemente el análisis de imágenes por *stacks* y el uso del programa informático *Image J* ha hecho posible optimizar los cálculos de biomasa, al tratarse de un sistema fiable y rápido de obtención de datos precisos y que permite además analizar un gran número de muestras (Solé et al. enviado a *Journal Microscopy*).

En el presente capítulo, se analiza la diversidad de las cianobacterias en muestras procedentes de tapetes microbianos de diferentes puntos de Europa, con distinto grado de contaminación con petróleo. Además se valoran los cambios producidos en las poblaciones de cianobacterias en sistemas experimentales (mesocosmos) contaminados con petróleo Casablanca.

El objetivo principal es determinar, si los cambios en diversidad y biomasa total e individual de cada cianobacteria en profundidad, son atribuibles a la contaminación con petróleo, tanto en ambientes naturales como artificiales. Al mismo tiempo al comparar la diversidad de las cianobacterias en distintos tipos de tapetes microbianos, se obtiene información sobre la biogeografía de estas bacterias.

Resultados y Discusión:

En los últimos años, existe un creciente interés por el papel que las cianobacterias pueden desempeñar en las zonas costeras contaminadas con petróleo, de allí la importancia del estudio de su diversidad en ambientes contaminados y no contaminados. Es por ello que se han caracterizado e identificado dichos microorganismos, y se ha determinado los perfiles de biomasa total. De forma más precisa también se han analizado las variaciones cuantitativas en profundidad de cada tipo de cianobacterias encontradas en Etang de Bêrre y en Mesocosmos, ambos ambientes contaminados con petróleo.

A. Análisis de la diversidad y determinación de la biomasa de las cianobacterias en tapetes microbianos de Europa con distinto grado de contaminación.

Diversidad

Se han caracterizado mediante CLSM tapetes microbianos no contaminados con petróleo (delta del Ebro, Colònia de Sant Jordi, Salins-de-Giraud), poco contaminados (Islas Orkney) y muy contaminados (Etang de Bêrre).

La identificación de los distintos géneros de las cianobacterias se ha realizado según la caracterización propuesta por Castenholz et al. (2001). Ver tablas 1 y 2 y figura 1.

Las cianobacterias de tipo filamentoso como *Microcoleus chthonoplastes* dominaron en los tapetes microbianos del delta del Ebro, Salins-de-Giraud y de la Colònia de Sant Jordi. En estos dos últimos ambientes se detectaron también *Halomicronema excentricum,* cianobacteria que se caracteriza por desarrollarse en ambientes salinos y cuyo diámetro es de 0.96 μm; *Leptolyngbya* sp. y las cianobacterias todavía no identificadas de 1.25 μm de diámetro fueron dominantes en Salins-de-Giraud.

En Etang de Bêrre no se observaron ni *Microcoleus chthonoplastes* ni *Oscillatoria* sp., siendo las cianobacterias filamentosas *Lyngbya* sp. y *Phormidium* sp. las más abundantes. Se destaca la ausencia total de cianobacterias unicelulares, este hecho podría significar que el petróleo era

significativamente tóxico para estos microorganismos. Al-Hasan el. (1998) y Sorkhoh et al. (1995), proponen el efecto bioreparador que las cianobacterias filamentosas podrían desempeñar frente al petróleo; ya que existe un gran interés por el papel que puedan desempeñar las vainas de mucopolisacáridos de estos microorganismos ante esta sustancia tóxica.

En todos los ambientes no contaminados estudiados, se identificaron las cianobacterias unicelulares: *Synechocystis* sp. y *Chroococcus* sp., aunque también se detectó *Gloeocapsa* sp. en los tapetes del delta del Ebro y en la Colònia de Sant Jordi (Tabla 2). Las cianobacterias correspondientes al grupo *Pleurocapsa*, se observaron en los tapetes microbianos que presentan una baja contaminación, siendo éstas las mayoritarias en estos ecosistemas junto a *Borzia* sp., cianobacteria filamentosa que se caracteriza por presentar filamentos de 2 a 8 células.

Es interesante constatar la dominancia de cianobacterias filamentosas en los ambientes naturales que nunca estuvieron contaminados con petróleo. Por el contrario aquellos ambientes que presentaban una baja contaminación con petróleo como los tapetes microbianos de las Islas Orkney presentaban una mayor incidencia de cianobacterias unicelulares correspondientes a los dos tipos del grupo *Pleurocapsa* caracterizados.

Biomasa

Los tapetes microbianos estudiados tienen una textura distinta. Los del delta del Ebro, Salins-de-Giraud y Colònia de Sant Jordi son tapetes estratificados de textura consistente, favorecida por la presencia de la cianobacteria filamentosa *Microcoleus chthonoplastes*, que se encuentra a menudo formando redes de filamentos entrecruzados entre sí, ayudando de esta manera a la estabilización de estos ecosistemas (Mazor et al. 1996). Por otra parte los tapetes microbianos de las Islas Orkney son de tipo granuloso y muy poco estables, mientras que las muestras de Etang de Bêrre son densas y espesas, debido a la presencia continuada del crudo en este último ambiente. En los mesocosmos, las muestras son de textura mucilaginosa.

La estructura de las muestras ha motivado que tanto la diversidad como el cálculo de la biomasa se haya efectuado con mayor precisión en los tapetes de textura consistente.

Los perfiles de biomasa individual y total de las cianobacterias se determinó haciendo uso del programa informático *Image J* aplicado a los distintos *stacks* de imágenes obtenidas por CLSM a partir de los diferentes ecosistemas estudiados.

En los tapetes microbianos de la Colònia de Sant Jordi la concentración máxima de biomasa se encuentra entre 0,50 y 1 mm; en el delta del Ebro entre 0,50 y 1,75 mm y en Salins-de-Giraud entre 0,25 y 1,25 mm (Tabla 3). En estos dos últimos, los valores máximos de biomasa se corresponden con la zona fótica del tapete (Sole et al. 2003, Fourçans et al. 2004). Así mismo, cabe destacar que las cianobacterias en general no solo se encuentran en la capa óxica del tapete, sino que también se les puede encontrar en las capas anóxicas del mismo, lo que puede significar cierta versatilidad metabólica.

Fourçans et al. (2004) demostraron que en Salins-de-Giraud la capa anóxica se sitúa a partir del segundo milímetro, lo que justifica la baja concentración de biomasa de las cianobacterias a partir de dicha profundidad.

De los tapetes de las Islas Orkney, el de Waulkmill bay presentaba un mayor grado de estratificación que el de Swanbister bay. En el primer caso, la distribución de la biomasa total seguía un perfil parecido al de los ambientes anteriormente mencionados, con una concentración de 19,72 mgC/cm^3 de sedimento a 1.85 mm de profundidad. Esta distribución no se daba en el caso de Swanbister bay (Tabla 4).

En Etang de Bêrre, se observa una reducción de la biomasa total con 31,37 mgC/cm^3 de sedimento, en la superficie y 0,06 mgC/cm^3 de sedimento, a 3,6 mm de profundidad. No obstante el análisis de la diversidad muestra claras diferencias con respecto a los no contaminados. En este caso, las cianobacterias más abundantes son *Lyngbya* sp. y *Phormidium* sp. con una biomasa de 22,52 mgC/cm^3 de sedimento, y 8,85 mgC/cm^3 de sedimento, respectivamente (Tabla 5), mientras que no se detectaron *Microcoleus chthonoplastes* ni las cianobacterias unicelulares que se encontraban en los no contaminados.

B. Análisis de la diversidad y determinación de la biomasa de las cianobacterias en Mesocosmos.

En el apartado anterior se ha estudiado el efecto del petróleo en ambientes naturales. La dificultad de interpretar todas las posibles variables que pueden influir en el crecimiento de los microorganismos, además del petróleo, se intenta subsanar en este apartado mediante la utilización de mesocosmos.

Estos ambientes artificiales, en los que los parámetros ambientales están controlados de manera constante, permiten evaluar de manera más selectiva el efecto del petróleo sobre las cianobacterias, al comparar los resultados con los obtenidos en el mesocosmos control (sin contaminación).

En la tabla 6 se recogen los resultados obtenidos tanto en diversidad como en biomasa individual y total de las cianobacterias, en ambos tipos de mesocosmos; siendo la distribución la siguiente: en el primer milímetro, no se observan cambios de diversidad en ambos tipos de muestras. En el segundo milímetro, *Microcoleus chthonoplastes* es la cianobacteria dominante en el mesocosmos control (35,81 mgC/cm^3 de sedimento), siendo indetectables las otras cianobacterias. En cambio en presencia del crudo Casablanca, la concentración de biomasa de esta cianobacteria filamentosa disminuye (10,25 mgC/cm^3 de sedimento) mientras se detectan otras cianobacterias, aunque el perfil de biomasa total de estas últimas es mucho menor. En el tercer milímetro *Microcoleus chthonoplastes* se encuentra a una concentración de 16,83 mgC/cm^3 de sedimento en el experimento control y no experimenta grandes cambios en el mesocosmos contaminado (13,91 mgC/cm^3 de sedimento).

Podría concluirse que *Microcoleus chthonoplastes* no se ve afectado por la presencia del petróleo, y que los microorganismos restantes se encuentran a bajas concentraciones. Por otra parte la distribución de *Microcoleus chthonoplastes* en la muestra control es muy similar al de los ambientes naturales no contaminados estudiados. Los análisis de biomasa total refuerzan estos resultados.

Tabla 1: Diversidad de las cianobacterias filamentosas en los tapetes microbianos estudiados.

Microorganismo	**Diámetro (μm)**	**Septación**	**Vacuolas de gas**	**Vaina**	**Habitat (Abundancia)**
Microcoleus chthonoplastes	3.13 – 3.75	+	-	+	Ed (++++); Sg (+++); SJ (+++)
Oscillatoria sp.	9-14	+	-	+	Ed (+++);Wb (+++)
Lyngbya sp.	5.6 – 10.3	+	-	+	Eb(+++); Wb (+++); Ed (++)
Phormidium sp.	1.4 – 3.75	+ (células isodiamétricas)	-	+	Ed(++); Eb (++)
Pseudanabaena sp.	1.4 – 2.5	+ (células más largas que anchas)	+	+	Ed (++); Wb(+); Sg (+)
Spirulina sp.	1.9 – 3	-	-	+ (muy delgada)	Ed (+); SJ (++)
Leptolyngbya sp.	< 1	-	-	+	Sg (+++); Wb (++); Eb (+)
Limnothrix sp.	1.25	-	+	+	Sg (+++); Sb (+)
Borzia sp.	1.25 – 1.9	+	-	+(delgada)	Sb (+++); Eb (+)
Halomicronema excentricum	< 1.00	+	?	+	Sg (+++) SJ (++)
No identificado	0.96 (filamentos cortos)	+	-	+	Sg (+++); Eb (+)

Ed = delta del Ebro
Sg = Salins-de-Giraud
Eb = Etang de Bêrre
Sb = Swanbister bay
Wb = Waulkmill bay
SJ = Colònia de Sant Jordi

Tabla 2: Diversidad de las cianobacterias unicelulares en los tapetes microbianos estudiados.

Microorganismos	**Diámetro (μm)**	**División de las Células**	**Vaina**	**Habitat (Abundancia)**
Gloeocapsa sp.	4 × 14	2 ó 3 planos	+	Ed (+++); Wb (+++); SJ(++)
Chroococcus sp.	19 × 28	2 planos	+	Ed (++); SJ(+)
Synechocystis sp.	3.5 × 3.5	2 ó 3 planos	+ (delgada)	Ed(++); Sg (++)
Aphanothece sp.	5 × 7	Diferentes planos	+ (delgada)	Wb (++)
Myxosarcina sp.	6 × 8	Fisión binaria en 3 planes	+	Ed (+)
Microcystis sp.	1.9 × 1.9	Fisión binaria en diferentes planos	+	Sb (+++); Wb (++)
Stanieria	2 × 3	Fisión múltiple o en combinación con una limitada (1-3) fisión binaria	+	Sb (+)
Grupo *Pleurocapsa*	Diverso en tamaño y forma	Fisión binaria en muchos planos (pseudofilamentos)	-	Sb (+++); Wb (++)
Grupo *Pleurocapsa*	2 × 3	Fisión binaria en planos diferentes (agregados)	+	Wb (+++)

Ed = delta del Ebro
Sg = Salins-de-Giraud
Eb = Etang de Bêrre
Sb = Swanbister bay
Wb = Waulkmill bay
SJ = Colònia de Sant Jordi

Fig: 1A. *Oscillatoria* sp. (Ed), **1B.a.** *Chroococcus* sp. (Ed), **1B.b.** *Myxosarcina* sp. (Ed), **1C.** *Microcoleus chthonoplastes* (Sg), **1D.** *Leptolyngbya* sp. (Sg), **1E.** *Phormidium* sp. (Eb), **1F.** *Lyngbya* sp. (Eb), **Fig: 1G.** Grupo *Pleurocapsa* (pseudofilamentos) (Sb), **1H.a.** *Microcystis* sp. (Sb), **1H.b.** *Stanieria* sp. (Sb), **1I.a.** *Lyngbya* sp. (Wb), **1I.b.** *Microcystis* sp. (Wb) **1I.c.** *Oscillatoria* sp. (Wb), **1I.d.** *Gloeocapsa* sp. (Wb), **1J.a.** Grupo *Pleurocapsa* (agregados) (Wb), **1J.b.** *Gloeocapsa* sp. (Wb), **1J.c.** *Aphanothece* sp. (Wb), **1K.a.** *Gloeocapsa* sp., (SJ), **1K.b.** *Chroococcus* sp., (SJ), **1L.** *Halomicronema excentricum* (SJ).

Ed: delta del Ebro, Sg: Salins-de-Giraud, Eb: Etang de Bêrre, Sb: Swanbister Bay, Wb: Waulkmill Bay, SJ: Colònia Sant Jordi.

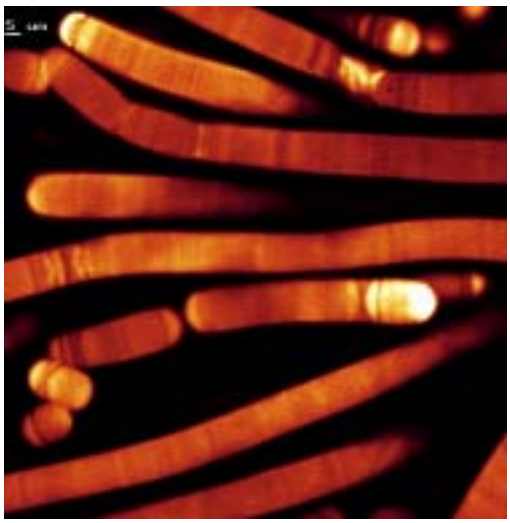

1A

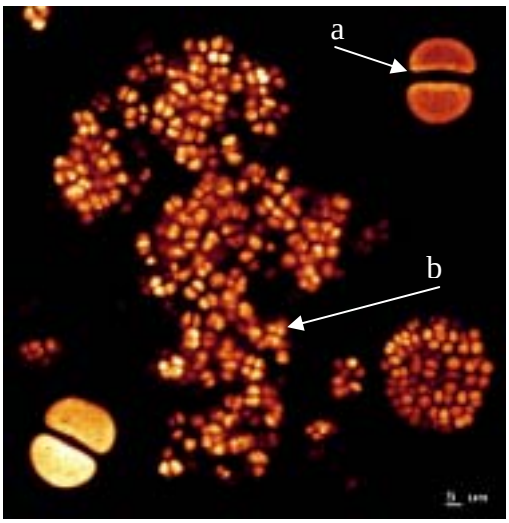

1B

1C

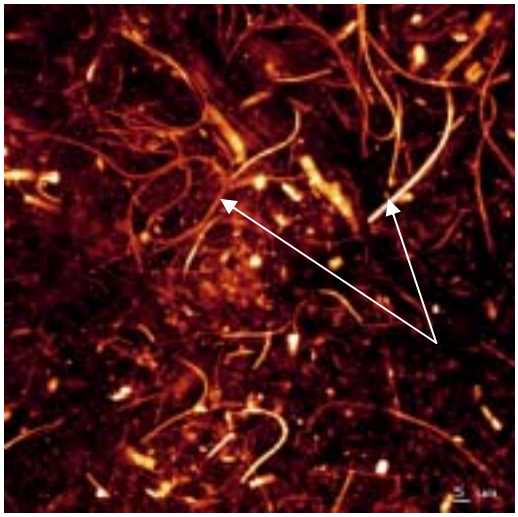

1D

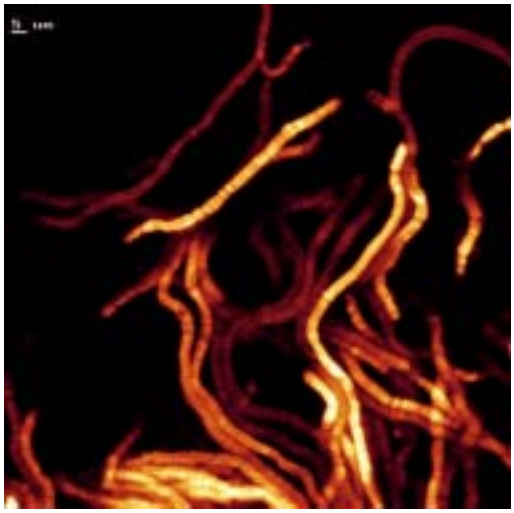

1E

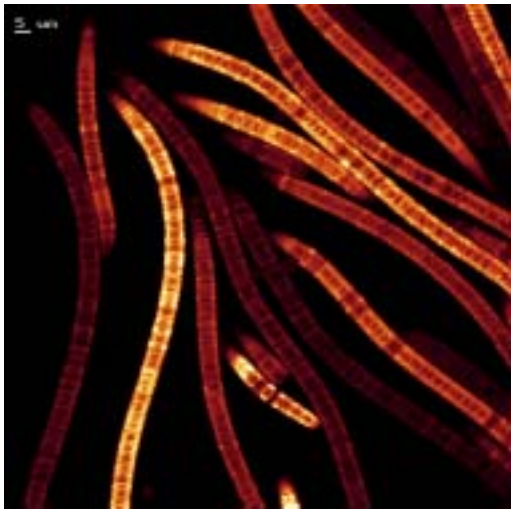

1F

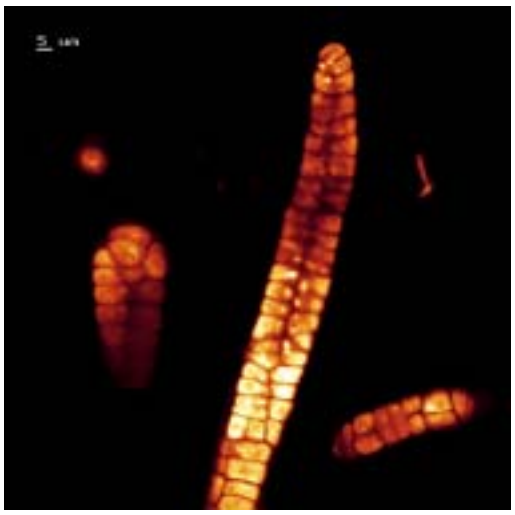

1G

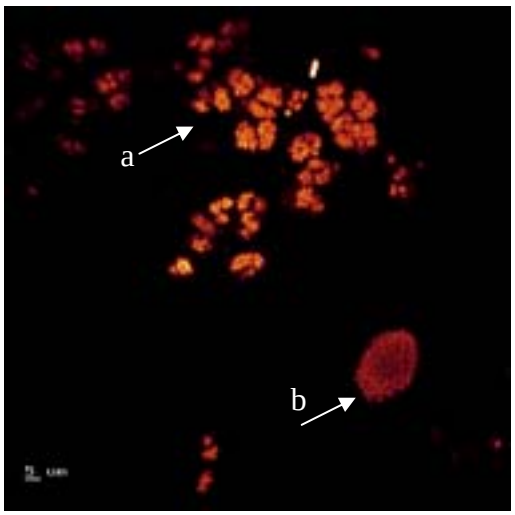

1H

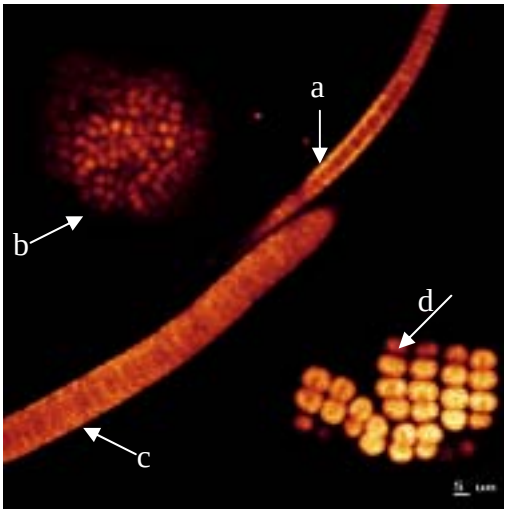

1I

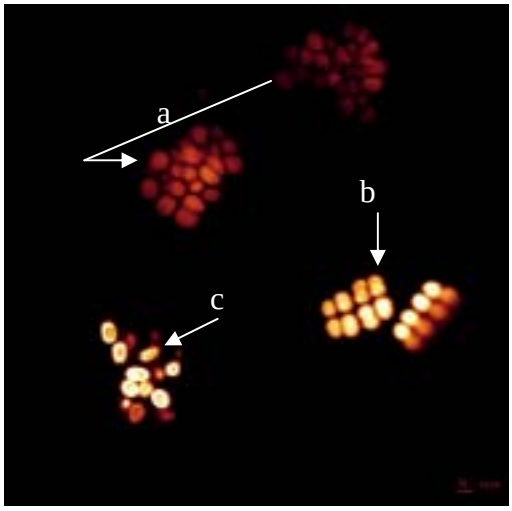

1J

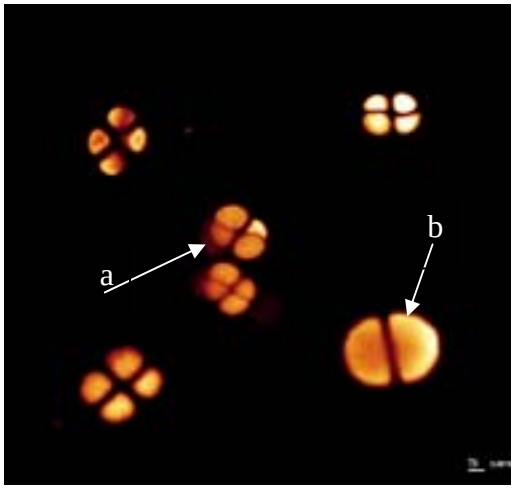

1K

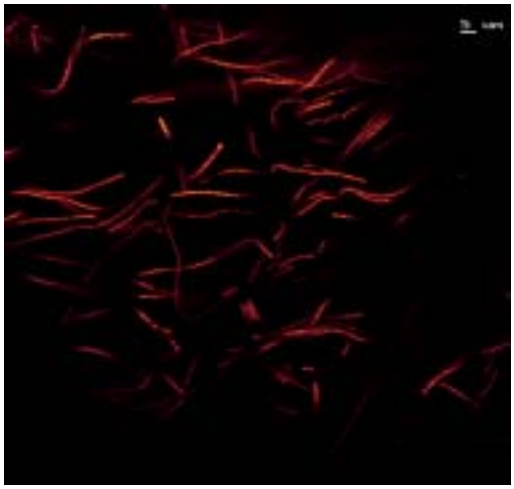

1L

Tabla 3: Biomasa total de los ambientes naturales no contaminados con petróleo.

BIOMASA TOTAL (mgC/cm^3 de sedimento)			
PROFUNDIDAD (mm)	**COLÒNIA DE SANT JORDI**	**DELTA DEL EBRO**	**SALINS-DE-GIRAUD**
0,00	5,04	7,49	4,43
0,25	5,71	14,57	21,42
0,50	10,61	37,23	26,14
0,75	9,67	43,11	23,17
1,00	10,08	58,76	16,42
1,25	7,95	43,62	11,89
1,50	8,12	46,63	4,85
1,75	5,86	25,21	2,06
2	4,19	12,42	1,74
2,25	3,74	12,56	0,28
2,50	5,47	10,53	2,15
2,75		11,03	1,46
3,00		2,36	1,04

Tabla 4: Biomasa total de los ambientes naturales ligeramente contaminados con petróleo.

BIOMASA TOTAL (mgC/cm^3 de sedimento)			
PROFUNDIDAD (mm)	**SWANBISTER BAY**	**PROFUNDIDAD (mm)**	**WAULKMILL BAY**
0	14,84	0	11,9
1,55	5,9	1,85	19,72
3,35	7,93	3,2	8,32
		5,1	6,63

Tabla 5: Diversidad, biomasa individual y total de las cianobacterias en Etang de Bêrre.

PROFUNDIDAD (mm)	MICROORGANISMOS	BIOMASA (mgC/cm^3 de sedimento)	BIOMASA TOTAL (mgC/cm^3 de sedimento)
0	*Lyngbya* sp.	22,52	31,37
	Phormidium sp.	8,85	
1,25	*Lyngbya* sp.	14,26	14,26
2,35	*Lyngbya* sp.	2,71	4,60
	filamentos no identificados	0,10	
	Borzia sp.	0,18	
	Otros	1,61	
3,6	*Borzia* sp.	0,06	0,06

Tabla 6: Diversidad, biomasa individual y total de las cianobacterias crecidas en mesocosmos sin contaminar y contaminados con petróleo Casablanca.

PROFUNDIDAD (mm)	MICROORGANISMOS	BIOMASA (mgC/cm^3 de sedimento)		BIOMASA TOTAL (mgC/cm^3 de sedimento)	
		CONTROL	CASABLANCA	CONTROL	CASABLANCA
1	*Microcoleus chthonoplastes*	3,75	10,00	8,77	13,79
	Spirulina sp.	0,67	0,44		
	Leptolyngbya sp.	1,22	0,29		
	Synechocystis sp.	0,14	0,78		
	Grupo *Pleurocapsa*	2,99	1,93		
	Gloeocapsa sp.	No detectado	0,35		
2	*Microcoleus chthonoplastes*	35,81	10,25	35,81	12,47
	Leptolyngbya sp.	No detectado	0,04		
	Gloeocapsa sp.	No detectado	0,55		
	Synechocystis sp.	No detectado	0,22		
	Grupo *Pleurocapsa*	No detectado	1,41		
3	*Microcoleus chthonoplastes*	16,83	13,91	16,83	16,20
	Grupo *Pleurocapsa*	No detectado	0,36		
	Synechocystis sp.	No detectado	0,23		
	Gloeocapsa sp.	No detectado	1,70		

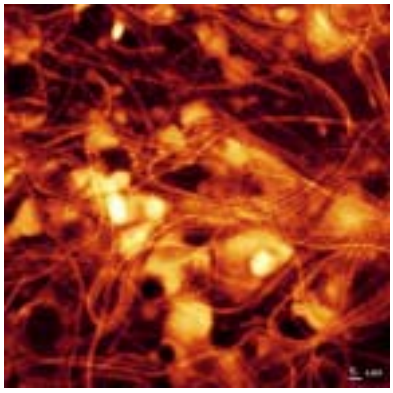

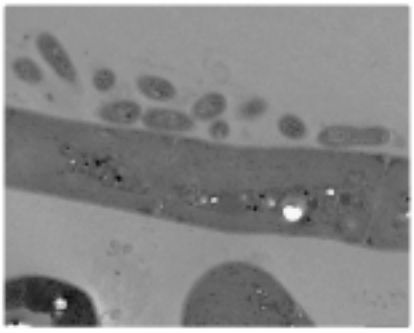

CAPÍTULO V: AISLAMIENTO Y CARACTERIZACIÓN DE UN CONSORCIO DE MICROORGANISMOS CON CAPACIDAD PARA DEGRADAR PETRÓLEO

Introducción

Resultados:

Aislamiento de un consorcio de microorganismos

Caracterización del consorcio mediante técnicas microscópicas

Determinación de las condiciones de cultivos que favorecen el crecimiento óptimo de *Microcoleus* consorcio

Identificación de los microorganismos que constituyen el consorcio por técnicas moleculares

Discusión

Introducción:

En ambientes extremos para la vida, las asociaciones entre microorganismos son muy frecuentes. Dichas asociaciones son taxonómicamente complejas y metabólicamente interactivas.

Diferentes autores han designado como consorcios este tipo de asociaciones, que a veces comprenden pocas especies de microorganismos, mientras que en otros casos abarcan poblaciones o se refieren a una comunidad microbiana completa (Paerl y Pinckney 1996, Abellá et al. 1998, Paerl et al. 2000). Este es el caso de los tapetes microbianos, en los que las asociaciones se favorecen a nivel de micro-escala con la finalidad de tamponar el efecto de diferentes parámetros extremos para la vida. Aún cuando los tapetes microbianos se han tomado como referencia para explicar la vida en condiciones limitantes, no todos los ambientes extremos son necesariamente el resultado de procesos naturales.

La agricultura, la urbanización de territorios, la industrialización, la conversión a gran escala de los ecosistemas naturales para la explotación humana, han dejado un gran impacto en el paisaje terrestre tanto estructural como funcionalmente (Vitousek et al. 1997). También las catástrofes naturales, como los vertidos de petróleo, pertenecen a este último apartado.

Los tapetes microbianos se han visto afectados en diferentes ocasiones por dichos vertidos, lo que somete a las poblaciones de bacterias de dichos ecosistemas a un efecto negativo añadido. Repetidas veces estos ambientes naturales han sufrido contaminación por diferentes sustancias tóxicas, siendo una de ellas el petróleo. El interés por estudiar los tapetes microbianos contaminados se inició después de la guerra del Golfo en 1991. Estudios en estos ecosistemas demostraron que existió una degradación de hidrocarburos, tanto aeróbica como anaeróbicamente (Al-Hasan et al. 1998). Abed et al. (2002b) demostraron que las cianobacterias tenían la capacidad de degradar compuestos de petróleo bajo condiciones aeróbicas, lo que implicaba que esta acción se realizaba en la capa superior de estos ecosistemas, la cual está formada básicamente por cianobacterias y bacterias heterotróficas.

Al-Hasan et al. (1998), demostraron que cultivos no axénicos de *Microcoleus chthonoplastes* y *Phormidium corium*, aislados a partir de tapetes microbianos

contaminados del Golfo de Arabia, eran capaces de degradar *n*-alcanos, además otros autores demostraron que diferentes cepas de estas bacterias fototróficas eran capaces de degradar también compuestos del petróleo (Radwan y Al-Hasan 2000, Raghukumar et al. 2001). Es importante mencionar que muchos de estos estudios remarcan la imposibilidad de obtener cultivos axénicos de las cianobacterias aisladas a partir de los tapetes microbianos contaminados, por lo que se han realizado diversas investigaciones donde las bacterias heterotróficas asociadas a las cianobacterias podrían ser las responsables de la biodegradación. Abed y Köster (2005), demostraron que las cianobacterias por sí mismas no son responsables de la degradación de los hidrocarburos, pero juegan un papel esencial en el desarrollo y actividad de los verdaderos degradadores, las bacterias heterotróficas. Aunque existen por tanto referencias puntuales al posible papel de las cianobacterias en la degradación de hidrocarburos, se sabe todavía muy poco sobre su efecto o utilización por parte de *Microcoleus chthonoplastes*, en general, la cianobacteria dominante en estos ecosistemas.

Microcoleus sp. es capaz en estos ambientes de producir importantes cantidades de EPS, que engloba haces de filamentos de dicha cianobacteria. Esta matriz orgánica semisólida, no solo estabiliza los sedimentos, sino que proporciona superficie y sustento para el crecimiento; ejerciendo además una actividad protectora frente los contaminantes, tales como, el petróleo, toxinas y diferentes metales pesados.

Algunos de los tapetes microbianos estudiados en el presente trabajo, están dominados por *Microcoleus* sp. y han sufrido contaminación por petróleo en distintas ocasiones. Es por ello que para estudiar el efecto del crudo, hemos desarrollado sistemas experimentales (microcosmos) en los que estudiar su efecto sobre las poblaciones de bacterias fotosintéticas oxigénicas (Llirós et al. 2003).

No obstante el objetivo de la investigación de este capítulo, era el aislamiento de *Microcoleus*, a partir de microcosmos contaminados y el estudio en cultivo axénico de su capacidad para degradar petróleo. Dado que desde las primeras observaciones se hizo patente que *Microcoleus* sp. se encontraba asociado a otros microorganismos, se denominó a los cultivos de dicha cianobacteria con el nombre de *Microcoleus* consorcio.

En este apartado se describe: el aislamiento y cultivo de dicho consorcio; la identificación de los microorganismos que lo componen mediante técnicas microscópicas de alta resolución y técnicas moleculares; y el tipo de simbiosis que se establece entre la cianobacteria y los microorganismos heterotróficos que constituyen el consorcio.

También se valoran las fracciones de petróleo Maya degradas por el consorcio y la posible implicación ecológica de dicho efecto.

Resultados:

Aislamiento de un consorcio de microorganismos con capacidad para el degradar petróleo:

Los cultivos del consorcio se obtuvieron a partir de las muestras tomadas de los microcosmos contaminados con petróleo (1A). En primer lugar, para obtener los cultivos de enriquecimiento, se inocularon fracciones de capa verde, procedente de los microcosmos, en botellas que contenían en todos los casos medio mineral Pfenning (van Gemerden y Beeftink, 1983) y diferentes condiciones de cultivo que se exponen a continuación:

a. **Cultivo Control:** Capa verde + Medio Pfenning sin carbonatos
b. **Cultivos con Petróleo:** Capa verde + Medio Pfenning + Petróleo Casablanca (alto contenido en hidrocarburos alifáticos) o Maya (hidrocarburos aromáticos y rico en compuestos azufrados).
c. **Cultivos sin Petróleo:** Capa verde + Medio Pfenning con carbonatos

En todos los casos los cultivos se incubaron en condiciones aeróbicas y anaeróbicas a una intensidad de luz de 15$\mu Em^{-2}s^{-1}$ y a 27ºC (Figura 1C).

Microcoleus consocio se obtuvo a partir de los cultivos de enriquecimiento correspondientes al cultivo tipo b (Figura 1B) y crecidos en condiciones anóxicas (Figuras 1D y 1E). A partir de estos cultivos se realizaron siembras en cultivo líquido y en placas, en anaerobiosis. Las placas contenían 150 µl de crudo Casablanca o Maya y se incubaron anaeróbicamente (jarras GasPak o bolsas anaeróbicas Anaerocult P de la casa Merck) y en las mismas condiciones de iluminación y temperatura utilizadas anteriormente.

Los cultivos líquidos se analizaron antes y después de la adición de los dos tipos de petróleo, indicados para determinar la capacidad del consorcio para degradar el crudo. El consorcio aislado (1F y 1G) degradó principalmente los compuestos azufrados heterocíclicos alifáticos tales como los alkyltiolanos y alkyltianos del petróleo Maya (García de Oteyza et al. 2004).

En la figura 2A, se observan masas densas del consorcio adheridas al crudo mediante la matriz polisacárida que excreta *Microcoleus* sp. Posteriormente, el consorcio se hizo crecer en medio sólido (Medio Mineral Pfenning + Agar), con la finalidad de obtener colonias aisladas. En la figura 2B se pueden distinguir dichas colonias y en la figura 3C, se aprecia un crecimiento confluente de *Microcoleus* consorcio sobre la placa de agar.

Caracterización del consorcio mediante técnicas microscópicas de alta resolución:

En este estudio aplicamos el CLSM, el TEM y el SEM para caracterizar los microorganismos del consorcio. El CLSM se utilizó para caracterizar e identificar a la cianobacteria que forma parte de este consorcio. En la figura 2D se puede observar la cianobacteria filamentosa entre gotas de petróleo. Los filamentos se caracterizan por presentar células más largas que anchas y con un diámetro de 3 μm, además muestran claras constricciones en su pared. Esta cianobacteria filamentosa, se ha identificado como *Microcoleus chthonoplastes* (Figura 2E) de acuerdo a la clasificación taxonómica propuesta por Castenholz et al. (2001). Las técnicas de microscópica electrónica como el SEM y el TEM se utilizaron para determinar si las colonias estaban formadas únicamente por *Microcoleus chthonoplastes* o si dicha cianobacteria se encontraba asociada a otros microorganismos. Las imágenes obtenidas por SEM indican la presencia de distintos bacilos unidos a la envoltura exopolisacárida (EPS) de la cianobacteria (Figura 3C). Las secciones ultrafinas de las mismas muestras, muestran las diferentes bacterias heterotróficas en el interior de la matriz de EPS y en asociación con *Microcoleus chthonoplastes* (Figura 3D). Este último fácilmente reconocible por la presencia de tilacoides, estructuras membranosas que contienen los pigmentos fotosintéticos (Figura 3A).

En la figura 3B, se pueden observar además unas inclusiones electrodensas. Aunque aún no se ha demostrado la naturaleza de estas inclusiones, algunos autores han descrito estructuras similares en otros microorganismos cuando crecen en presencia de petróleo (Singer y Finnerty, 1984).

En la imagen obtenida por SEM, se observan dos de los morfotipos de bacterias heterotróficas en contacto con la vaina polisacárida de *Microcoleus chthonoplastes*

(Figura 3C). La media de los diámetros de los tres tipos de bacterias obtenidas por TEM fueron: **tipo I** 0.30 μm con una desviación estándar de 0.033; **tipo II** 0.22 μm con una desviación estándar de 0.026 y el **tipo III** 0.50 μm con una desviación estándar de 0.060. La abundancia relativa fue de 76.5, 15.5 y 8% respectivamente.

Determinación de las condiciones de cultivo que favorecen el crecimiento óptimo de *Microcoleus* consorcio.

Una vez caracterizado el consorcio, se ensayaron diferentes condiciones de cultivo numeradas del 1 al 8 (Tabla 1), para determinar en primer lugar su dependencia a la luz y al O_2. Además se ensayaron como fuentes de carbono la presencia de carbonatos o el petróleo.

En dicha tabla se observa que *Microcoleus* consorcio presenta un crecimiento óptimo en presencia de luz, en anaerobiosis y con petróleo como única fuente de carbono (cultivo 1). Dado que en condiciones anaeróbicas y cuando el consorcio se incuba en ausencia de luz (cultivos 5 y 7), no existe crecimiento del consorcio, deducimos que los microorganismos heterotróficos son aeróbicos, por lo tanto dependen del oxígeno producido por *Microcoleus chthonoplastes*.

En ningún cultivo los microorganismos heterótrofos del consorcio crecieron en ausencia de luz, aunque estuvieran presentes en el medio mineral Pfenning los carbonatos (cultivos 6 y 7) o el petróleo (cultivos 5 y 8), lo que demuestra una total dependencia de éstos hacia la cianobacteria.

Identificación de los microorganismos que constituyen el consorcio por técnicas moleculares:

Aunque las técnicas microscópicas y en especial el TEM permitieron determinar los tipos morfológicos de las distintas bacterias heterotróficas que formaban el consorcio, se utilizó el RNA ribosómico 16S para su completa identificación.

El estudio se realizó a partir de los cultivos de *Microcoleus* consorcio crecidos en medio mineral Pfenning y de cultivos crecidos en presencia de petróleo.

La figura 4 muestra los resultados de la DGGE del cultivo control y del contaminado con el petróleo, donde se pueden observar diferencias entre ambas muestras.

Además, los resultados indican que los microorganismos heterotróficos identificados pertenecen a grupos con capacidad para fijar nitrógeno. Éstos además están repartidos en diferentes grupos filogenéticos, tales como las subclases Alfa, Beta y Gamma del grupo Proteobacteria y del grupo CBF (Figura 5). El consorcio utilizado como control estaba en cambio dominado por un microorganismo (88% de los clones) muy afín a *Pseudoxanthomonas mexicana* (con una similitud del 99.8%) (Tabla 2).

Discusión:

El CLSM, se ha utilizado en muchas ocasiones para caracterizar e identificar a las cianobacterias en ambientes naturales y artificiales bentónicos, con un alto grado de resolución. También en el presente trabajo se ha utilizado para identificar la cianobacteria del consorcio como *Microcoleus chthonoplastes* (Solé et al. 2003, Diestra et al. 2005). Por otro lado, el SEM y el TEM (particularmente este último) han permitido la determinación de la abundancia relativa de cada uno de los microorganismos heterotróficos del consorcio y la caracterización ultraestructural del mismo.

El uso de estas técnicas microscópicas de alta resolución, no solo han permitido la caracterización de los microorganismos que conforman el consorcio, sino también determinar la ubicación de los microorganismos heterótrofos, dentro del mucílago que rodea a *Microcoleus chthonoplastes*.

No obstante para la identificación de las bacterias heterotróficas se utilizaron además técnicas moleculares (Sánchez et al. 2005). Los resultados demuestran que las bacterias asociadas a *Microcoleus chthonoplastes*, desarrolladas en presencia de petróleo, pertenecen a las siguientes familias: Rhizobiaceae (*Rhizobium* sp., *Agrobacterium tumefaciens*, 26,6%), Rhodobacteraceae (*Thioclava pacifica*, *Roseobacter* sp., 28, 7%), Phyllobacterisceae (*Parvibaculum lavamentivoran*s, 13,9%) y Xhantomonadaceae (*Pseudoxanthomonas japonensis*, 11,7%).

En los cultivos que crecieron en ausencia de petróleo, la bacteria heterotrófica *Pseudoxanthomonas mexicana* era la más abundante 87,7% y pertenece a la familia Xhantomonadaceae.

En el presente trabajo se demuestra que varias secuencias de los genes 16S rRNA recuperadas de las bibliotecas genéticas corresponden a microorganismos fijadores de nitrógeno (Tabla 3).

Secuencias de *Rhizobium* sp. y *Agrobacterium* sp. se detectaron en los cultivos desarrollados en presencia de petróleo. *Pseudomonas stutzeri* ha sido detectado tanto en cultivos controles como en cultivos contaminados con el crudo. Este microorganismo fija el nitrógeno en condiciones de microaerofilia y en estado libre (Desnoues et al. 2003). Se especula mucho sobre el papel de estos microorganismos como abastecedores de nitrógeno para el desarrollo de *Microcoleus* sp. bajo ciertas condiciones. Además se ha demostrado que *Rhizobium* sp. y *Agrobacterium* sp. son bacterias degradadoras de petróleo (Lebkowska et al. 1995, Frassineti et al. 1998). Estos estudios están de acuerdo con los de otros autores que demuestran la tendencia de las cianobacterias a formar consorcios (Paerl y Pinckney 1996) y a los realizados por Steppe (2001) que demuestran la existencia de bacterias epifitas fijadoras de nitrógeno asociadas a *Microcoleus* sp.

Los resultados sugieren que los microorganismos asociados a *Microcoleus chthonoplastes*, podrían realizar la fijación del nitrógeno y la degradación de los hidrocarburos, mientras que *Microcoleus chthonoplastes* proporcionaría un hábitat y oxígeno a las bacterias heterotróficas.

Por otra parte se ha demostrado que el consorcio está implicado en la degradación de los compuestos heterocíclicos alifáticos del petróleo Maya (García de Oteyza et al. 2004). Así mismo ni este último ni el petróleo Casablanca tienen ningún efecto tóxico sobre *Microcoleus* consorcio, siendo el primero el que potencia el crecimiento de dicho consorcio.

Por otra parte se ha demostrado que aunque el consorcio se desarrolle tanto en presencia de petróleo Casablanca como en el Maya, degrada especialmente los compuestos heterocíclicos alifáticos como los alquiltiolanos y los alquiltianos (compuestos azufrados) del petróleo Maya. Estos resultados son importantes desde el punto de vista ambiental, ya que este crudo es muy tóxico.

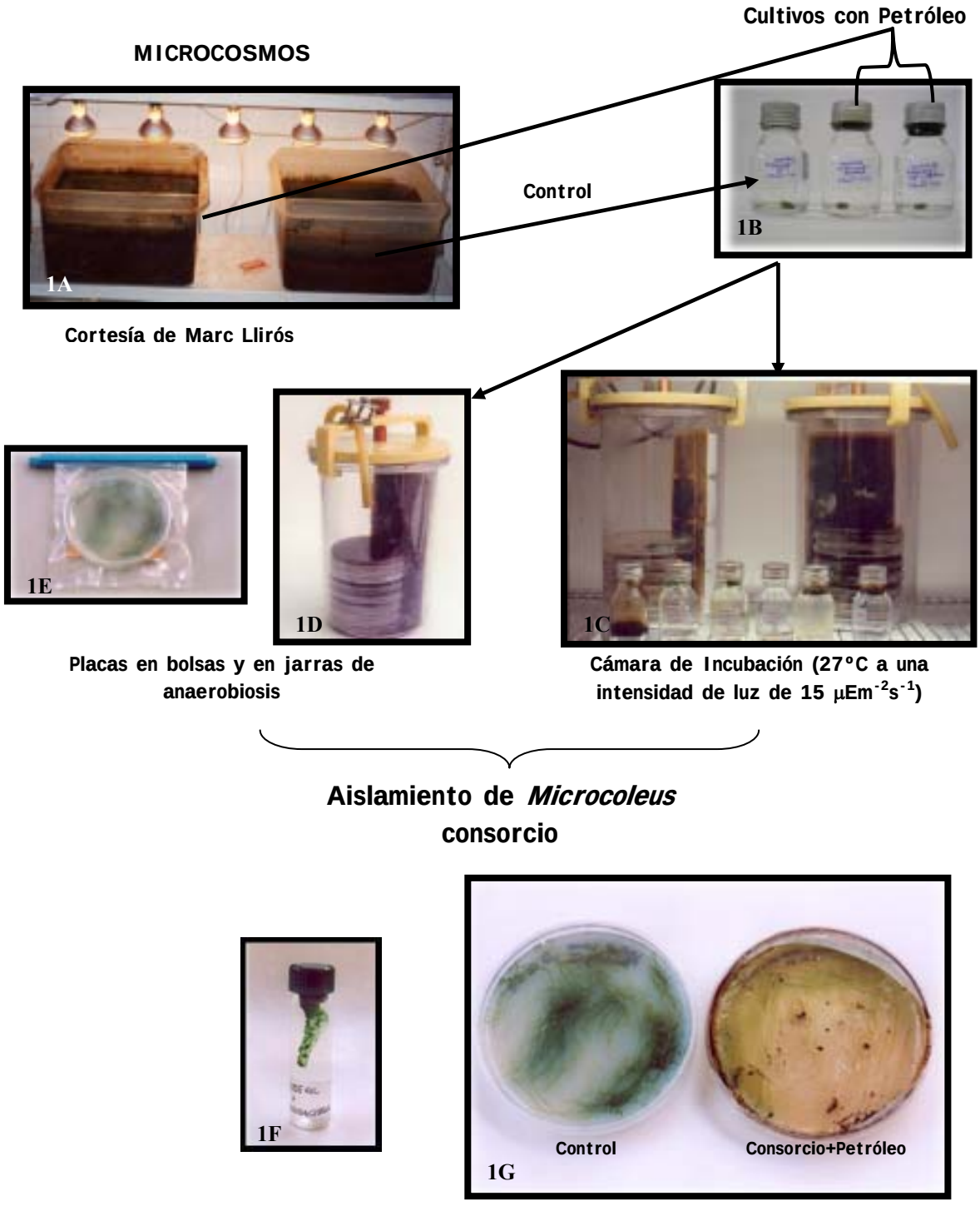

Figura 1: Aislamiento de *Microcoleus* consorcio.

Fig. 2A

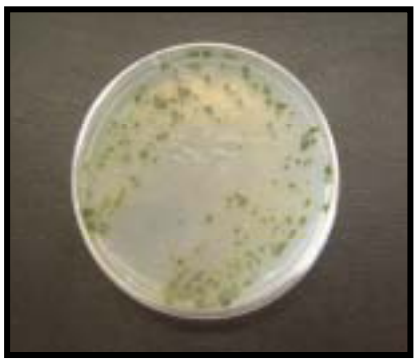

Fig. 2B

Fig. 2C

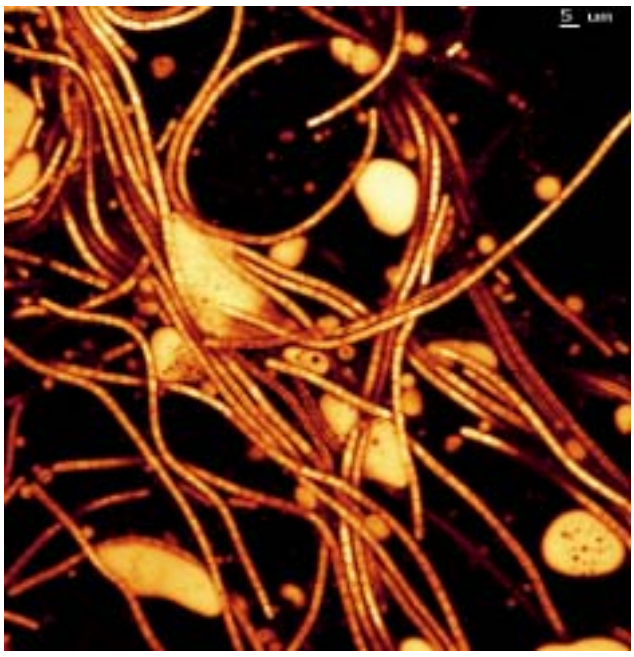

Fig. 2D

Fig. 2E

Figura 2: 2A. *Microcoleus* consorcio adherido al petróleo Maya. 2B. *Microcoleus* consorcio en colonias aisladas en cultivo control. 2C. *Microcoleus* consorcio, creciendo en presencia del crudo. 2D. Filamentos de *Microcoleus chthonoplastes* entre gotas de petróleo. 2E. Filamentos de *Microcoleus chthonoplastes*.

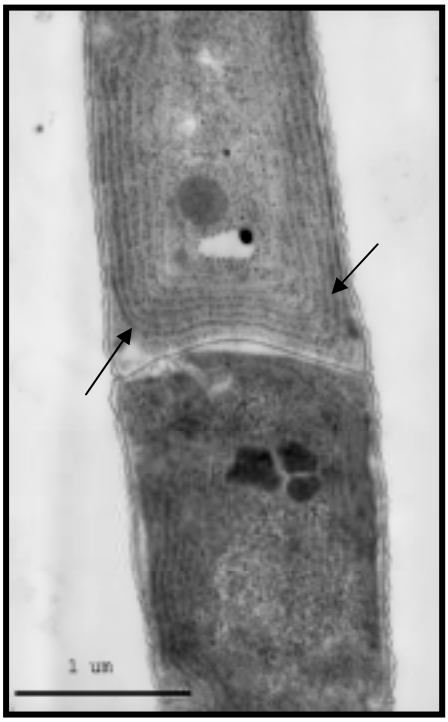

Fig. 3A

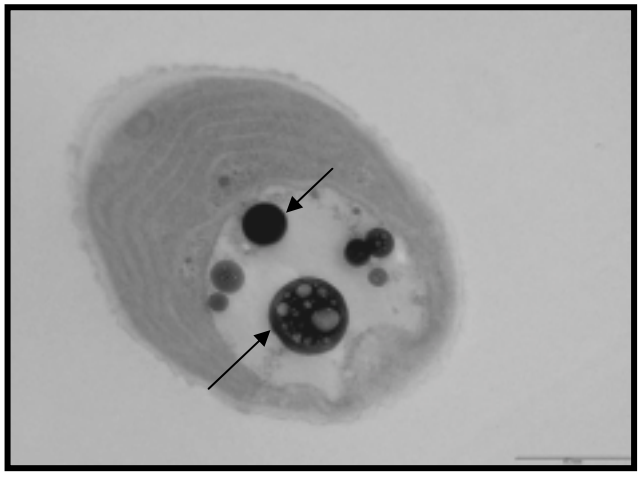

Fig. 3B

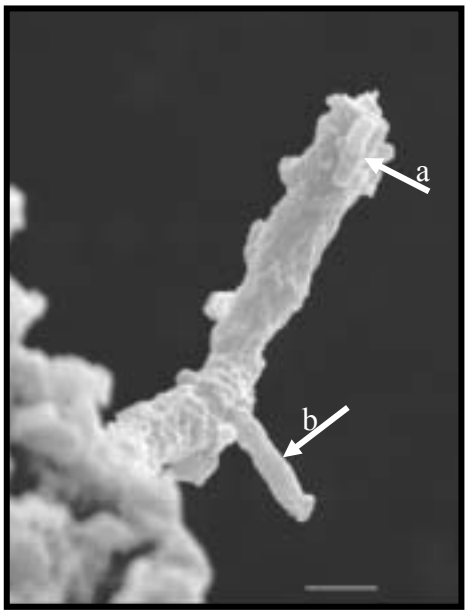

Fig. 3C

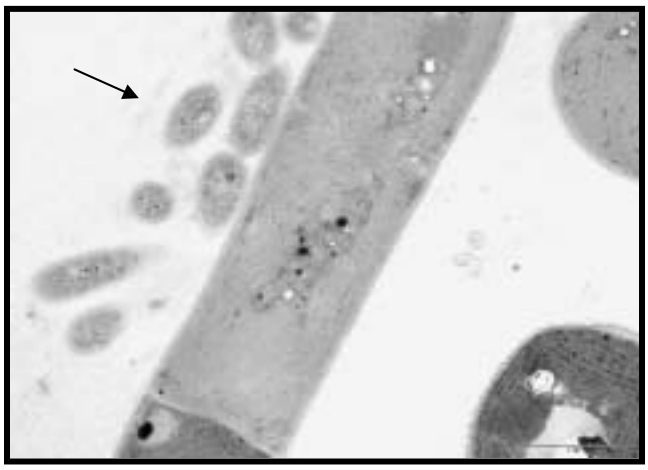

Fig. 3D

Figura 3: 3A. Sección ultrafina de *Microcoleus chthonoplastes*, las flechas señalan los tilacoides (1μm). 3B. Sección ultrafina de *Microcoleus chthonoplastes* de cultivos contaminados con petróleo. Las flechas indican la presencia de las inclusiones electrodensas (500μm). 3C. (a y b) Microorganismos heterotróficos adheridos a la vaina exopolisacárida de *Microcoleus chthonoplastes* (1μm). 3D. Microorganismos heterótrofos dentro de la vaina exopolisacárida de *Microcoleus chthonoplastes* (1μm).

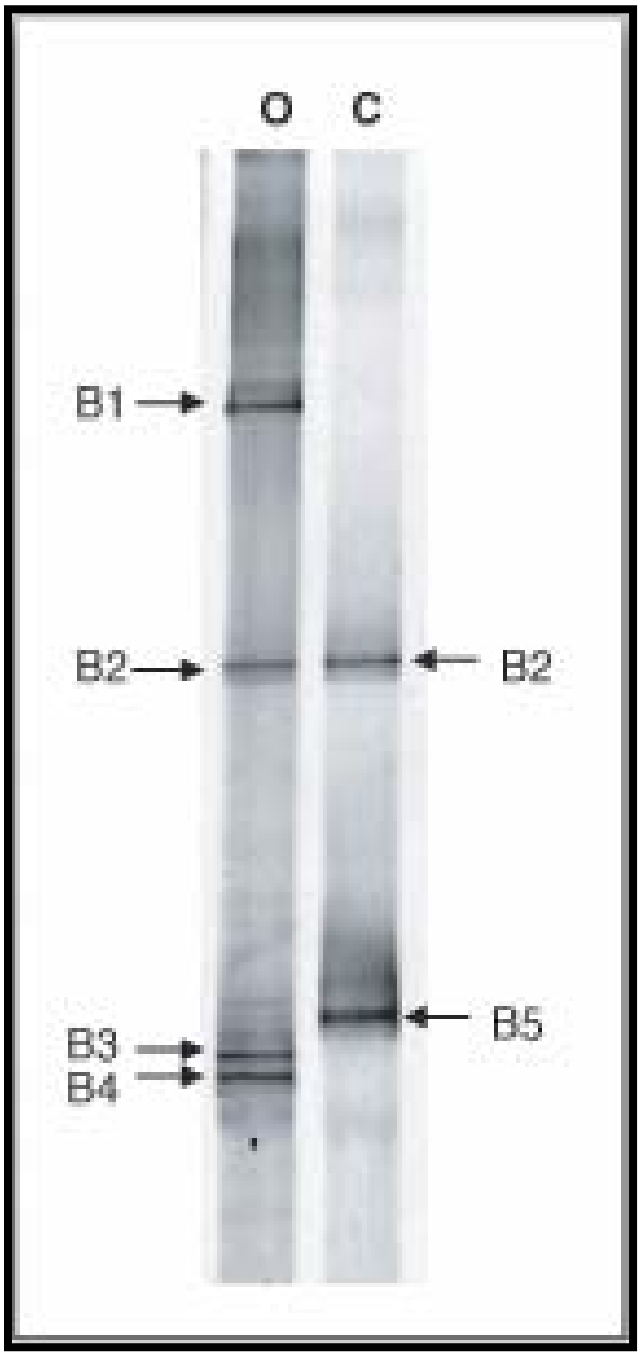

Figura 4: Imagen del gel de DGGE amplificado con cebadores bacterianos (O: consorcio con petróleo, C: Control).

Figura 5: Árbol filogenético, incluyendo las secuencias de dos librerías genéticas (O: consorcio con petróleo, C: control). La barra indica el 10% de similitud de la secuencia. Las secuencias que aparecen en el gel de DGGE y las librerías genéticas se marcan en rectángulos grises.

Tabla 1: Cultivos de *Microcoleus* consorcio bajo diferentes condiciones de crecimiento.

Cultivo	Luz	O_2	Fuente de Carbono		Crecimiento
			CO_3^-	Petróleo	
1	+	-	-	+	++++
2	+	+	-	+	++
3	+	-	-	-	+
4	+	+	+	-	+
5	-	-	-	+	-
6	-	+	+	-	-
7	-	-	+	-	-
8	-	+	-	+	-

Tabla 2 Afiliación filogenética de las secuencias de los clones recuperados (O: consorcio con petróleo, C: control).

GRUPO	CORRESPONDENCIA CON (Número de Acceso)	SIMILITUD %	CORRESPONDENCIA CON CULTIVO MÁS CERCANO (Número de Acceso)	SIMILITUD %	% clones	
					O	C
α **Proteobacteria**	*Rhizobium* sp. (AF364858)	98,1			25,5	-
	Agrobacterium tumefaciens (AF508094)	97,2			1,1	-
	Thioclava pacifica (AY656719)	97,7			25,5	-
	α proteobacterium (AY162070)	97,7	*Roseobacter* sp. (AY332661)	97,7	3,2	-
	Roseomonas sp. (AF533359)	94,1			1,1	-
	Roseomonas gilardii (AY150051)	94,4			-	0,5
	Hyphomonas polymorpha (AJ227813)	99,2			-	1,1
	Bacteria no cultivable (AF143824)	97,8	*Parvibaculum lavamentivorans* (AY387398)	97,1	1,1	-
	Parvibaculum lavamentivorans (AY387398)	99,6			12,8	1,6
β **Proteobacteria**	Bacteria no cultivable (AB186829)	98,9	*Hydrogenophaga* sp. (AB166889)	98,5	2,1	-
	Bacteria no cultivable (AY625151)	99,4	*Hydrogenophaga taeniospiralis* (AF078768)	99,2	3,2	-
δ **Proteobacteria**	*Pseudomonas stutzeri* (U26414)	99,9			8,5	0,5
	Pseudomonas stutzeri (AJ006103)	99,7			-	6,4
	Pseudoxanthomonas mexicana (AF273082)	99,8			-	87,7
	No cultivable δ proteobacterium (AJ619035)	99,9	*Pseudoxanthomonas japonensis* (AB008507)	99,6	11,7	-
	No cultivable δ proteobacterium (AF445725)	98,4	*Aquamonas vora* (AY544768)	94,7	1,1	-
	No cultivable δ proteobacterium (AF445726)	96,7	*Pseudoxanthomonas daejeonensis* (AY550264)	93,7	1,1	-
CFB	Bacteria no cultivable (AF502210)	95,5	*Cytophaga* sp. (AF250407)	96,7	1,1	2,1
	Bacteria Antártica (AJ441001)	94,5	*Cytophaga* sp. (X85210)	94,1	1,1	-

Tabla 3 Secuencias similares a las bandas bacterianas que aparecen en la figura 4.

Banda	Correspondencia con:	% similitud (nº bases)[a]	Grupo Taxonómico	Nº Acceso
B1	Bacteroides no cultivados	95,8 (525)	CFB	AJ534682
B2	Bacteria no cultivada	98,7 (532)	CFB	AF502212
B3	*Rhizobium* sp.	98,9 (528)	α-Proteobacteria	AY500261
B4	*Thioclava pacifica*	98,5 (530)	α -Proteobacteria	AY656719
B5	*Pseudoxanthomonas mexicana*	99,6 (560)	δ-Proteobacteria	AF873082

[a] Los números que están entre paréntesis son el número de bases usados para calcular los niveles de similitud.

Conclusiones:

1. El CLSM es la técnica microscópica que mejores resultados ha dado en la caracterización e identificación de las cianobacterias de los tapetes microbianos. Este tipo de microscopía que utiliza una fuente de luz láser, permite realizar secciones ópticas de pocos milímetros de grosor en sedimentos compactados, como son los tapetes microbianos, a la vez que detecta la autofluorescencia producida por las cianobacterias "in vivo" y con escasa manipulación de la muestra. Así mismo, a partir de las imágenes obtenidas por el CLSM, se ha podido determinar los perfiles de biomasa de las cianobacterias, aplicando técnicas de análisis de imagen, donde el programa *Image J* 1.33f es el que ofrece mayor precisión e información.

Los tapetes microbianos estudiados responden a diferentes grados de contaminación por petróleo, lo que ha permitido hacer un estudio comparativo de la influencia de éste en la selección de las poblaciones de cianobacterias.

2. En los ambientes no contaminados por petróleo (delta del Ebro, Salins-de-Giraud y Colònia de Sant Jordi) se han identificado tanto cianobacterias filamentosas (*Microcoleus chthonoplastes*, *Oscillatoria* sp. *Lyngbya* sp., *Limnothrix* sp.) como unicelulares (*Gloeocapsa* sp., *Chroococcus* sp, *Synechocystis* sp.). Los valores más altos de biomasa total se encontraron en la capa óxica.

3. En los tapetes microbianos de las Islas Orkney (Swanbister y Waulkmill bay) poco contaminados por petróleo, se identificaron principalmente cianobacterias unicelulares correspondientes al grupo *Pleurocapsa*. La concentración máxima de biomasa total de cianobacterias, en el caso de Swanbister bay, se localizó entre 0 y 1.55 mm (14,84 mgC/cm^3 de sedimento), y en el caso de Waulkmill bay, entre 1.85 y 3.2 mm (19,72 mgC/cm^3 de sedimento).

4. En Etang de Bêrre, tapete microbiano permanentemente contaminado por petróleo, se caracterizaron e identificaron exclusivamente cianobacterias de tipo filamentoso, y se observó una disminución de biomasa total a lo largo del tapete. *Lyngbya* sp. fue la cianobacteria más abundante, con una biomasa individual de 22, 52 mgC/cm^3 de sedimento entre 0 y 1.25 mm.

5. En los ecosistemas artificiales de Eilat (Mesocosmos), se observó que la cianobacteria dominante fue *Microcoleus chthonoplastes* tanto en las muestras control como en las contaminadas por el petróleo Casablanca. Además se pudo observar, que las cianobacterias unicelulares se detectaron solo en los tapetes contaminados, aunque en muy baja concentración.

6. *Microcoleus chthonoplastes* es la cianobacteria dominante en la mayoría de los tapetes microbianos estudiados. Se trata de una cianobacteria ubicua que tolera altos niveles de contaminación por petróleo. En ambientes no contaminados, como los tapetes de Salins-de-Giraud se encuentra tanto en las capas óxicas (31.22 mgC/cm^3 de sedimento) como anóxicas (28.91 mgC/cm^3 de sedimento) y en presencia de H_2S, lo que indica además la versatilidad metabólica de dicha cianobacteria.

7. Se ha aislado *Microcoleus* consorcio, una agrupación estable de microorganismos, que presenta unas condiciones óptimas de crecimiento cuando se cultiva en medio Pfenning en presencia de petróleo y en anaerobiosis, a 27ºC y con una intensidad de luz de 15 $\mu Em^{-2}s^{-1}$.

8. La caracterización del consorcio por técnicas microscópicas de alta resolución revelan que *Microcoleus* consorcio está formado por una cianobacteria *Microcoleus chthonoplastes* y diferentes bacterias heterotróficas que se encuentran en el interior de la envuelta exopolisacárida de la cianobacteria.

9. Se ha visto que los microorganismos heterotróficos identificados mediante las técnicas moleculares fueron en su mayoría fijadoras de nitrógeno y que pertenecen a varios grupos filogenéticos como a las α, β y γ, subclases de Proteobacteria, y al grupo CFB.

10. Los resultados del apartado anterior junto con los obtenidos del crecimiento del consorcio en diferentes condiciones de cultivo (presencia y ausencia de luz, oxígeno y fuente de carbono) demuestran que *Microcoleus chthonoplastes* proporciona probablemente oxígeno a las bacterias heterotróficas y que éstas fijan el nitrógeno, que suministran a la cianobacteria, a la vez que degradan el petróleo.

11. De las conclusiones anteriores se podría deducir, que en los ambientes naturales y también en los artificiales las cianobacterias en general toleran la presencia del petróleo, aún cuando se producen cambios en las poblaciones y en su biomasa por el efecto del crudo.

En el caso de *Microcoleus chthonoplastes*, la cianobacteria dominante, se ha demostrado que ésta además degrada las fracciones más tóxicas del petróleo Maya, por su acción conjunta con microorganismos heterotróficos, con los que forma un consorcio.

Referencias Bibliográficas:

1. **Abed R. M., García-Pichel F. & Hernández-Mariné M.** (2002a) Polyphasic characterization of benthic, moderately halophilic, moderately thermophilic cyanobacteria with very thin trichomes and the proposal of *Halomicronema excentricum* gen. nov., sp. nov. Arch. Microbiol. 177: 361-370.
2. **Abed R. M. M., Safi N. M. D., Köster J., de Beer D., El-Nahhal Y., Rullköter J. & García-Pichel F.** (2002b) Microbial diversity of a heavily polluted microbial mats and its community changes following degradation of petroleum compounds. *Appl Environ Microbiol*. 68: 1674-1683.
3. **Abed R. M. M. & Köster J.** (2005) The direct role of aerobic heterotrophic bacteria associated with cyanobacteria in the degradation of oil compounds. *Int Biodeterior Biodegrad*. 55: 29-37.
4. **Abellá C. A., Cristine X. P., Martínez A., Pibernat I. & Vila, X.** (1998) Two new motile phototrophic consortia: "*Chlorochromatium lunatum"* and "*Pelochromatium selenoides"*. *Arch Microbiol.* 169: 452-459.
5. **Al-Hasan R. H., Sorkhoh N. A., Al-Bader D. & Radwan, S.S.** (1994) Utilization of hydrocarbons by cyanobacteria from microbial mats on oily coasts of the Gulf. *Appl Microbiol Biotechnol.* 41: 615-619.
6. **Al-Hasan, R.H., Al-Bader, D., Sorkhoh, N.A. & Radwan, S.S.** (1998) Evidence for *n*-alkane consumption and oxidation by filamentous cyanobacteria from oil-contaminated coasts of the Arabian Gulf. *Mar Biol.* 130, 521-527.
7. **Al-Hasan, R.H.,Khanafer M., Eliyas M. & Radwan, S.S.** (2001) Hydrocarbon accumulation by picocianobacteria from the Arabian Gulf. *J Appl Microbiol.* 91: 531-540.
8. **Altschul S. F., Madden T. L., Shäfer A. A., Zhang J, Zhang Z., Miller W. & Lipman D. J.** (1997) Gapped BLAST and PSI-BLAST: a new generation of protein database search programs. *Nucleic Acids Res*. 25: 3389-3402.
9. **Bebout, M. & García-Pichel, F. (**1995) UV-B. Induced vertical migrations of cyanobacteria in microbial mats. *Appl. Environ. Microbiol.* 61: 4215-4222.

10. **Benlloch S., López-López A., Casamayor E. O., Ovreas L., Goddard V., Daae, F. L., Smerdon G., Massana R., Joint I., Thingstad F., Pedros-Alio C. & Rodriguez-Valera, F.** (2002) Prokaryotic genetic diversity throughout the salinity gradient of a coastal solar saltern. *Environ. Microbiol.* 4: 349-360.
11. **Bergman B., Gallon J. R., Rai A. N. & Stal, L.J. (**1997) N_2 fixation by non–heterocystous cyanobacteria. FEMS *Microbiol. Ecol.* 19: 139-18.
12. **Brock T. D.** (1978) The habitats. Thermophilic microorganisms and life at high temperatures, Springer-Verlag. New York.
13. **Campbell S. E.** (1979) Soil stabilization by a prokaryotic desert crust: implications for Precambrian land biota. *Orig. Life* 9: 335-348.
14. **Canfield D. E. & Des Marais D. J.** (1991) Aerobic sulfate reduction in microbial mats. *Science* 251:1471-1473.
15. **Casamayor E. O., Massana R., Benlloch S., Ovreas L., Diez B., Goddard V. J., Gasol J. M., Joint I., Rodríguez-Valera F. & Pedrós-Alió C.** (2002) Changes in archaeal, bacterial and eukaryal assemblages along a salinity gradient by comparison of genetic fingerprinting methods in a multipond solar saltern. *Appl Environ Microbiol.* 4: 338-348.
16. **Castenholz R. W.** (2001) Phylum BX. Cyanobacteria. Oxygenic photosynthetic bacteria. In: Boone DR, Castenholz RW (Eds.) Bergey's Manual of Systematic Bacteriology. The Archea and the Deeply Branching and Phototrophic Bacteria, vol 1. Springer, Berlin, pp 473–599.
17. **Caumette P., Matheron R., Raymond N. & Relexans J. C.** (1994) Microbial mats in the hypersaline ponds of Mediterranean salterns (Salins-de-Giraud, France). *FEMS Microbiol Ecol*. 13: 273-286.
18. **Cohen, Y. & Rosenberg E. (**1989) Photosynthesis in cyanobacterial mats and its relation to the sulfur cycle. pp. 22-36. In: Microbial mats, physiological ecology of benthic microbial communities. A model for microbial sulfur interactions. *Am. Soc. Microb*. Washington, D. C.
19. **Cohen Y.** (2002) Bioremediation of oil by marine microbial mat. *Int Microbiol.* 5(4): 189-193.

20. d'Amelio E. D., Cohen Y. & Des Marais, D. J. (1987) Association of a new type of gliding, filamentous, purple phototrophic bacterium inside bundles of *Microcoleus chthonoplastes* in hypersaline cyanobacterial mats. *Arch Microbiol.* 147: 213-220**.**

21. de Philippis R., Margheri M. C., Materassi R. & Vincenzini M. (1998) Potential of unicellular cyanobacteria from saline environments as exopolysaccharide producers. *Appl. Environ. Microbiol.* 64: 1130-1132.

22. de Wit R. & van Gemerden H. (1987) Oxidation of sulfide to thiosulfate by *Microcoleus chthonoplastes*. *FEMS Microbiol Lett.* 45: 7-13.

23. Decho, A.W. (1990) Microbial exopolymer secretions in ocean environments: their role(s) in food webs and marine process. *Oceanogr Mar Bio. Ann. Rev.* 28: 73-153.

24. Demergasso C., Chong G., Galleguillos P., Escudero L., Esteve I. & Martínez-Alonso M. (2003) Tapetes microbianos del Salar de Llamará, Norte de Chile. *Revista Chilena de Historia Natural*. 76: 485-499.

25. Desnoues N., Lin M., Guo X., Ma L., Carreno-López R. & Elmerich C. (2003) Nitrogen fixation genetics and regulation in a *Pseudomonas stutzeri* strain associated with rice. *Microbiology*. 149: 2251-2262.

26. Diestra E., Solé A. & Esteve I. (2004). A comparative study of cyanobacterial diversity in polluted and unpolluted microbial mats by jeans CLSM. *Ophelia* 58 (3): 151-156.

27. Diestra E., Solé A., Martí M., García de Oteyza T., Grimal J. O. & Esteve I. (2005) Characterization of an oil-degrading *Microcoleus* consortium by means of confocal laser scanning microscopy, scanning electron microscopy and transmission electron microscopy. *Scanning*. 27: 176-180.

28. Epping E. H. G., Khalili A. & Thar R. (1999) Photosynthesis and the dynamics of oxygen consumption in a microbial mat as calculated from transient oxygen microprofiles. *Limnol Oceanogr.* 44:1936–1948.

29. Esteve I., Montesinos E., Mitchell J. G. & Guerrero R. (1990) A quantitative ultrastructural study of *Chromatium minus* in the bacterial layer of Lake Cisó (Spain). *Arch Microbiol*. 153: 316-323.

30. **Esteve I., Martínez M., Mir J. & Guerrero, R.** (1992) Typology and structure of microbial mats communities in Spain: A preliminary study. *Limnetica* 8: 185-195.
31. **Esteve I., Cevallos D., Martínez-Alonso M., Gaju N. & Guerrero, R.** (1994) Development of versicolored microbial mats: Succession environmental significance. *NATO ASI Series.* G-35: 415-420.
32. **Ferris M. J., Muyzer G. & Ward D. M.** (1996) Denaturing gradient gel electrophoresis profiles 16s rRNA-defined populations inhabiting a hot spring microbial mat community. *Appl Environ Microbiol*. 62: 340-346.
33. **Fourçans A., García de Oteyza T., Wieland A., Solé A., Diestra E., van Bleijswijk J., Grimalt J. O., Kühl M., Esteve I., Muyzer G., Caumette P. & Durán, R.** (2004). Characterization of functional bacterial groups in a hypersaline microbial mat community (Saline-de-Giraud, Camargue, France). *FEMS Microbial Ecol.* 51: 55-70.
34. **Fourçans A., Solé A., Diestra E., Ranchau-Peyruse A., Esteve I., Caumette P. & Durán, R.** Vertical migrations of phototrophic bacterial populations in a hypersaline microbial mat from Saline-de-Giraud (Camargue, France).Submitted to *FEMS Microbial Ecol.*
35. **Frassinetti S., Setti L., Corti A., Farrinelli P., Montevechi P. & Vallini G.** (1998) Biodegradation of dibenzothiophene by a nodulating isolate of *Rhizobium melilote*. *Can J Microbiol.* 44 (3): 289-297.
36. **Fuhrman J. A., McCallen K. & Davis A. A.** (1993) Phylogenetic diversity of substrate marine microbial communities from the Atlantic and Pacific oceans. *Appl Environ Microbiol.* 59: 1294-1302.
37. **García de Oteyza Tirso.** (2003) Procesos de fotooxidación y biodegradación por tapices microbianos en petróleos. Departamento de Química Ambiental. Instituto de Investigaciones Químicas y Ambientales de Barcelona. Tesina-Proyecto de Tesis.
38. **García de Oteyza T., Grimalt J. O., Diestra E., Solé. A. & Esteve I.** (2004) Changes in the composition of polar and apolar crude oil fractions Ander the action of *Microcoleus* consortia. *Appl Microbiol Biotechnol*. 66: 226-232.

39. **García-Pichel F. & Castenholz R. W.** (1991) Characterization and biological implication of scytonemina a cyanobacterial sheath pigment. *J Phycol.* 27: 395-409.
40. **García-Pichel F., Mechling M. & Castenholz R. W.** (1994) Diel migrations of microorganims within a benthic, hypersaline mat community. *Appl. Environ. Microbiol.* 60: 1500-1511.
41. **García-Pichel F., Prufert-Bebout L. & Muyzer, G.** (1996) Phenotypic and cosmopolitan cyanobacterium. A*ppl. Environ. Microbiol*. 62: 3284-3291.
42. **García-Pichel F., López- Cortés A. & Nübel U.** (2001) Phylogenetic morphological diversity of cyanobacteria in soil desert crusts from the Colorado Plateau. *Appl. Environ. Microbiol.* 67: 1902-1910.
43. **Giani D., Seeler J., Giani L. & Krumbein, W. E.** (1989) Microbial mats and physicochemistry in a saltern in the Bretagne (France) and in a laboratory scale saltern model. *FEMS Microbiol. Ecol.* 62: 151-162.
44. **Gray J. P. & Herwing R. P.** (1996) Phylogenetic analysis of the bactrrial communities in marine sediments. *Appl Environ Microbiol.* 62: 4049-4059.
45. **Groetzinger J. P. & Knoll A. H.** (1999) Stromatolites in Precrambian carbonates: evolutionary milepost or environmental dipsticks? *Ann Earth Planet Sci.* 27: 313-358.
46. **Harry M., Gambier B., Bourezgui Y & Garnier-Sillam E.** (1999) Evaluation of purification procedures for DNA extracted from organic samples: interferences with humic substances. *Analysis* 27: 439-442.
47. **Herbert R. A** (1985) Development of mass blooms of photo-synthetic bacteria on sheltered beaches in Scapa Flow, Orkney Islands. *Proc Roy Soc Edinburgh* 87B:15-25.
48. **Huettel M., Forster S., Klöser S. & Fossing H, (1996)** Vertical migration in the sediment-dwelling sulphur bacteria *Thioploca* spp. In overcoming diffusion limitations. *Appl Environ Microbiol* 1863-1872.
49. **Johnson I.** (1999) Fluorescent probes for living cells. *Histochemical Journal.* 30: 123-140.

50. Krekeler D., Teske A. & Cypionka H. (1998). Strategies of sulphate-reducing bacteria to escape oxygen stress in a cyanobacterial mat. *FEMS Microbiol Ecol.* 25: 89-96.

51. Kühl M & Fenchel T. (2000) Bio-optical characteristics and vertical distribution of photosynthetic pigments and photosynthesis in an artificial cyanobacterial mat. *Microb Ecol*. 40:85-93

52. Lebkowska M., Kawowska E & Miaskiewicz E. (1995) Isolation and identification of bacteria from petroleum derivatives contaminated soil. *Act Microbiol Pol.* 44 (3-4): 297-303.

53. Llirós M., Munill X., Solé A., Martínez-Alonso M., Diestra E. & Esteve, I. (2003). Analysis of cyanobacteria biodiversity in pristine and non polluted microbial mats in microcosms by confocal laser scanning microscopy (CLSM). In: *Science, Technology and Education of Microscopy*: an Overview, p. 483-48**9.** *In* A. Mendez-Vilas (ed.) FORMATEX Microscopy Book Series. Vol 1.

54. López-Cortés A., García-Pichel F., Nübel U. & Vázquez-Juárez R. (2001) Cyanobacterial diversity in extremal environments in Baja California, México: A polyphasic study. *Int. Microbiol.* 4: 227-236.

55. Ludwig W., Strunk O., Klugbauer S., Klugbauer N., Weinzenegger M., Neumaier J., Bachleitner M. & Schleifer K. H (1998) Bacterial phylogeny based on comparative sequences análisis. *Electrophoresis.* 19: 554-568.

56. Maidak B. L., Cole J. R., Lilburnt T. G., Parker C. T. Jr., Sarman P. R., Stredwick J. M., Garrity G. M., Li B., Olsen G. S., Pramarik S., Schmidt J. M. & Tiedje J. M. (2000). The RDP (Ribosomal Data Project) continues. *Nucleic Acids Res.*28: 73-174.

57. Margulis L., López Baluja L., Awramik S. M.& Sagan D. (1986) Community living long befote man: Fósil and living microbial mats and earthy life. *Sci Total Environ*. 56: 379-397.

58. Martin A. P. (2002) Phylogenetic approaches communities. *Appl Environ Microbiol.* 68: 3673-3682.

59. **Massana R., Murray A. E., Preston M. & DeLong E. F.** (1997) Vertical distribution and phylogenetic characterization of marine planktonic Archea in the Santa Barabara Chanel. *Appl Environ Microbiol.* 63: 50-56.
60. **Mazor G., Kidron, G. J., Vonshak A. & Abeliovich, A.** (1996) The role of cyanobacterial exoploysaccharides in structuring desert microbial crusts. *FEMS Microbiol. Ecol*. 21: 121-130.
61. **Medina S. A., Huerta Ochoa S. & Gutierrez-Rojas M.** (2005) Hydrocarbon biodegradation in oxygen-limited sequential batch reactors by consortium from weathered oil-contamined soil. *Can J Microbiol./ Rev Can Micorbiol*. 51 (3): 231-239.
62. **Mejharaj M., Singleton I., McClure N. C. & Naidu R.** (2000) Influence of petroleum hydrocarbon contamination on micro algae and microbial activities in a long-term contaminated soil. *Arch. Environ. Contam. Toxicol*. 38: 439-445.
63. **Menezes S. A., de Oliveira Camargo F. A., Okeke B. C. & Frankenberger W. T. Jr.** (2005) Diversty of biosurfactant producing microoganisms isolated from soil contaminated with diesel oil. *Microbiol Res.* 160 (3): 249-255.
64. **Miller S. R. & Bebout B. M.** (2004) Variation in Sulfide Tolerance of Photosystem II in Phylogenetically Diverse Cyanobacteria from Sulfidric Habitats. *Appl. Environ. Microbiol.* 70: 736-744.
65. **Miloning G.** (1961) Advantages of phosphate buffer OsO_4 solutions in fixation. *J Appl Phys.* 32: 1637.
66. **Mir J., Martínez-Alonso M., Esteve I. & Guerrero, R.** (1991) Vertical stratification and microbial assemblage of a microbial mat in the Ebro Delta (Spain). *FEMS Microbiol. Ecol.* 86: 59-68.
67. **Mir J. & Esteve I.** (1992) The SEM in microbial ecology. *Microsc Anal*. 29: 31-33.
68. **Moezelaar R., Bijvank S. M. & Stal, L.** (1996) Fermentation and sulfur reduction in the mat-building cyanobacterium *Microcoleus chthonoplastes*. *Appl. Environ. Microbiol.* 62: 1752-1758.
69. **Moore L. R., Rocap G. & Chisholm S. W.** (1998). Physiology and molecular phylogrny of coexisting. *Prochlorococcus* ecotypes. *Nature*. 393: 464-467.

70. **Muyzer G., Brinkhoff T., Nübel U., Santegoeds C., Schäfer H. & Wawer C.** (1998) Denaturing gradient gel electroforesis (DGGE) in microbial ecology. In: Akkermans A. D.L, van Elsas J. D., Breeijn F. J. (eds.). Molecular microbial ecology manual. Kluver Academic Publishers, Dordrecht. The Netherlands, pp. 3.4.4/ 1-27.
71. **Nelson D. C., Revsbech N. P.& Jørgensen B. B.** (1986a) Microoxic-anoxic niche of *Beggiatoa* spp.: microelectrode survey of marine and freshwater strains. *Appl Environ Microbiol.* 52: 161-168.
72. **Nelson D. C., Jørgensen B. B. & Revsbech N. P.** (1986b) Growth pattern and yield of a chemoautotrophic *Beggiatoa* sp. In oxygen-sulfide microgradients. *Appl Environ Microbiol.* 52: 225-233.
73. **Nogués C., Martí M., Boada M. & Ponsà M.** (1994). A simple method for processing individual oocytes and embryos for electron microscopy. *J. Microsc.* 174: 51-54.
74. **Oren A. & Shilo M.** (1979) Anaerobic heterotrophic dark metabolism in the cyanobacterium *Oscillatoria limnetica* and lactate fermentation. *Arch Microbiol.* 122: 77-84.
75. **Paerl H. W & Pinckney J. L.** (1996) Microbial consortia: Their roles in aquatic production and biogeochemical cycling. *Microb Ecol.* 31: 225-247.
76. **Paerl H. W., Pinckney J. L. & Steppe T. F.** (2000) Cyanobacterial-bacterial mat consortia: examining the functional unit of microbial survival and growth in extreme environments. *Environ Microbiol.* 2 (1): 11-26.
77. **Radwan S. S. & Al-Hasan R. H.** (2000) Oil pollution and cyanobacteria, p. 307-319. In: Whitton B. A: & Potts M. (ed.). The ecology of cyanobacteria. *Kluwer Academic Oublishers*, Dordretch, The Netherlands.
78. **Raghukumar C., Vipparty V., David J. J. & Chandramohan D.** (2001) Degradation of crude oil by marine cyanobacteria. *Appl Microbiol Biotechnol.* 57 (3): 433-436.
79. **Ramsing N. B., Ferris M. J. & Ward D. M.** (2000) Highly ordered vertical of *Synechococcus* population within the one-millimeter-thick photic zone of a hot spring cyanopbacterial mat. *Appl Environ Microbiol.* 66 (3): 1038-1049.

80. Raskin L., **Stromley J. M., Rittman B. E. & Stahl D. A.** (1994) Group-specific 16S rRNA hybridization probes to describe natural communities of methanogens. *Appl Environ Microbiol.* 60: 1232-1240.

81. Ravenschlag K., Sahm K., Pernthaler J & Amann R. (1999) High bacterial diversity in permanently cold marine sediments. *Appl Environ Microbiol.* 65: 3982-3989.

82. Reynolds E. S. (1963). The use of lead citrate at high pH as an electron-opaque stain in electron microscopy. *J. Cell Biol.* 17: 208-212.

83. Richardson L. L. & Castenholz R. W. (1987) Diel vertical movements of the cyanobacterium *Oscillatoria terebriformis* in a sulfide-rich microbial mat. *Appl. Environ. Microbiol.* 53: 2142-2150.

84. Richardson, L. L. (1996) Horizontal and vertical migration patterns of *Phormidium corallyticum* and *Beggiatoa* spp. associated with black-band disease of corals. *Microb. Ecol.* 32: 323-335.

85. Sánchez O., Diestra E., Esteve I. & Mas J. (2005) Molecular characterization o fan oil-degradin cyanobacterial consortium. *Microbiol Ecol.* 000-000.

86. Schauer M., Massana R. & Pedrós-Alió C. (2000) Spatial differences in bacterioplankton composition along the catalan coast (NW Mediterranean) assessed by molecular fingerprinting. *FEMS Microbial Ecol.* 33: 51-59.

87. Schopf J. W. (2000) Solution to Darwin´s dilemma: discovery of the missing Precrambian record of life. *Proc Acad Sci* USA. 97 (13): 6947-6953.

88. Singer M. E. & Finerty N. R. (1984) Microbial metabolism of straight-chain and branched alkanes. In: Petroleum Microbiology (Ed. Atlas R. M.) Mac Millan Oublishing Co., New York. 1: 1-53

89. Solé A., Gaju, N., Guerrero R. & Esteve I. (1998) Confocal laser scanning microscopy of Ebro Delta microbial mats. *Microsc. Anal.* 29: 13-15.

90. Solé A., Gaju N., Mendez-Álvarez S. & Esteve, I. (2001) Confocal laser scanning microscopy as a tool to determine cyanobacteria biomass in microbial mats. *J. Microscopy*. 204: 258-262.

91. Solé A., Gaju N. & Esteve I. (2003) The biomass dynamics of cyanobacteria in an annual cycle determined by confocal laser scanning microscopy. *Scanning*. 25: 1-7.

92. **Solé A., Mas J. & Esteve I.** Computerised image análisis for measuring cyanobacterial biomasa by confocal laser scanning microscopy. Submitted to *J Microscopy*.

93. **Sorkhoh N. A., Al-Hasan R. H: Khanafer M. & Radwan S. S:** (1995) Establishment of oil-degrading bacteria associated with cyanobacteria in oil-polluted soil.*J Appl. Bacteriol.* 78 (2): 194-199.

94. **Stahl D. A. & Amann R. I.** (1991) Development and application of nucleic acid probes.IN: Stackebrandt E., Goodfellow M (eds.) Nucleic acid techniques in bacterial systematics, Wiley, New York. N. Y. pp. 205-248.

95. **Stal L. J.** (1994) Microbial mats in coastal environments. In *Microbial Mats*. Stal, L.J., and Caumette, P. (eds). Berlin Heidelberg: Springer-Verlag, pp. 21-32.

96. **Stal L. J & Moezellar R.** (1997) Fermetation in cyanobacteria. *FEMS Microbial Rev.* 21: 179-211.

97. **Steppe T. F., Pincknry J. L., Dybe J. & Paerl H. W.** (2001) Diazotrophy in modern marine bahamian stromatolites. *Microbial Ecol.* 42: 36-44.

98. **Thar, R. & Kühl M.** (2001) Motility of *Marinochromatium gracile* in response to light, oxygen, and sullfide. *Appl Environ Microbiol*. 67: 5410-5419.

99. **Teske A., Ramsing N. B., Habicht K., Fukui M., Kuver J., Jørgensen B. B. & Cohen Y.** (1998) Sulfate-reducing bacteria and their activities in cyanobacterial mats of solar lake (Sinai, Egypt). *Appl Environ Microbiol.* 64: 2943-2951.

100. **van Gemerden H.& Beeftink H. H.** (1981) Coexistence of *Chlorobium* and *Chromatium* in a sulphide-limited continuous culture. *Arch Microbiol.* 129: 32-34.

101. **van Gemerden H.& Beeftink H. H.** (1983) Ecology of hotrophic bacteria, In: Studies in Microbiology (Ed. Ormerod J. G.) *Blackwell Scientific Publications*, Cambridge. 146-185.

102. **Villbrandt M. & Stal L. J.** (1996) The effect of sulfide on nitrogen fixation in heterocystous and non-heterocystous cyanobacterial mat communities. *Algol Stud*. 83: 549-563.

103. **Vitousek P. M., Mooney H. A., Lubchenko J. & Melillo J. M.** (1997) Human domination of earth's ecosystems. *Science*. 277: 494-499.

104. **Whale G. F. & Walsby A. E.** (1984) Motility of the cyanobacterium *Microcoleus chthonoplastes* in mud. *Phycol. J.* 19: 117-123.

105. Wieland A. & Kühl M. (2000) Irradiance and temperature regulation of oxygenic photosynthesis and O2 consumption in a hypersaline cyanobacterial mat (Solar Lake, Egypt). *Mar Biol*. 137:71–85.

106. Wieland A., Kühl M., McGowan L., Fourçans A., Duran R., Caumette P., García de Oteyza T., Grimalt J. O., Solé A., Diestra E., Esteve I. & Herbert, R. A. (2003). Microbial Mats on the Orkney Islands Revisited: Microenvironment and Microbial Community Composition. *Microb Ecol.* 46: 371-390.

107. Wieland A., Zopfi J., Benthien M. & Kühl, M. (2005) Biogeochemistry of an iron-rich hypersaline microbial mat (Camargue, France). *Microb Ecol.* 49: 34-49.

108. Woese C. R. (1987) Bacterial Evolution. *Microbiol Rev* 51: 221-271.

Agradecimientos

Es una tarea difícil el agradecer a todas las personas que han contribuido en la realización de este trabajo, la verdad es que no existen palabras para poder demostrar y expresar todo mi agradecimiento.

En primer lugar, agradezco a mi directora de tesis, la Dra. Isabel Esteve, ya que gracias a ella he tenido la oportunidad de realizar esta tesis doctoral, jamás terminaré de agradecerle todo el apoyo y cariño brindado. He de mencionar a Toni, que también es director de esta tesis, muchas gracias por el apoyo y por haberme enseñado el uso de mi herramienta de trabajo el "CLSM", en general gracias por todo!!!

Agradezco también al Servei de Microscòpia, especialmente a Mercé y Onofre, ya que han sido ellos quienes me han orientado y enseñado durante estos años. Así mismo, agradezco al Dr. Jordi Mas y a la Dra. Olga Sánchez por la colaboración y ayuda prestada en cada momento, muchas gracias.

No podía dejar de agradecer a mi mami, que es por ella que he llegado hasta aquí, su empeño y lucha han permitido y permite que mis hermanos y yo salgamos adelante. He de agradecer a mi papi por apoyarme siempre, y a mis niños Cesarín, Karito y Mariana espero que de alguna manera u otra se puedan sentir orgullosos de mí. Esta tesis está dedicada a ustedes, mi verdadera inspiración. Los amo y mil gracias familia por estar siempre conmigo!!!

Espero que a partir de ahora no me olvide de agradecer a nadie, si lo hago porfi perdonarme, es la parte final y me emociono de solo saber que ya falta casi nada para poder encuadernar la tesis…

No podía dejar de mencionar a mis amigos del alma, a quienes quiero con locura, Eva y Leo, la verdad es que tendría que escribir páginas y páginas para decir gracias, gracias, gracias…, pero comprenderán es una tesis doctoral y no un libro de agradecimientos, ES BROMA (típico en mí, no?). Les deseo lo mejor del mundo y siempre, siempre los voy a llevar dentro de mi "bobo".

A mis amigas, churris y compañeras de laboratorio: Almu y Miris. Almu, cariño, espero que en estas breves líneas queden plasmadas la gracias que he de darte, pero mejor serán apuchorrones, no? Gracias por saber escucharme y sobre todo por realizar las siembras de mis bebes (*Microcoleus* consorcio) durante este último año. Te quiero corazón!!! Miris, mi ÑIÑA, piensa que eres un ser maravilloso y que te mereces lo

mejor, eres única e irremplazable. Sigue luchando por lo que quieres y sabes que cuando necesites de alguien cuentas conmigo. Te quiero bixo.
Eli, gracias por ayudarme cuando lo necesité, te he llegado a coger un cariño enorme. Gracias por todo bombón, como diría nuestra locumbeta.
Lidia, CUCHI, no me podía olvidar de ti. Con lo bien que nos lo pasábamos tomando "coffe" con Marc y Toni. A veces echo tanto de menos aquellos momentos, gracias por brindarme tu amistad.
Maira, gracias por haberme dedicado siempre un tiempito espero y deseo de corazón que las cosas te salgan de maravilla.
Marc, fuiste la primera persona con quien empecé a trabajar en el "labo", gracias por haber sido tan amable conmigo, espero y deseo de corazón que te vaya bien por Gerona.

Quisiera mencionar también a todos mis amigos, incluidos los que están en Perú, que a pesar de estar a más de 6000 Km. se que están conmigo. Maggy, Johi, Ruby, Ceci, Carlos, Maribel, Raquel, Raúl, María, Carla, Sole…a todos mil gracias.

Todas las personas que he mencionado son especiales y cada una de ellas tienen un lugar en mi corazón, pero me gustaría agradecer a esa personita que es tan especial para mí, le agradezco que se haya preocupado por mí a lo largo de todo este tiempo. Te adoro con toda mi alma, y mil gracias por haberme aconsejado y por haber estado allí siempre, necesitaría más de cuatro líneas para agradecerte, en fin gracias!

Artículos publicados correspondientes al trabajo experimental realizado.

MOLECULAR CHARACTERIZATION OF AN OIL-DEGRADING CYANOBACTERIAL CONSORTIUM

Olga Sánchez*, Elia Diestra, Isabel Esteve, and Jordi Mas

Departament de Genètica i Microbiologia, Universitat Autònoma de Barcelona, 08193 Bellaterra, Spain

An article submitted to: Microbial Ecology (13/6/05)

Running title: Oil-degrading *Microcoleus chthonoplastes* consortium

***Correspondence to**: O. Sánchez, Departament de Genètica i Microbiologia, Facultat de Ciències, Universitat Autònoma de Barcelona, 08193 Bellaterra, Spain. Phone: 34-935813011. Fax: 34-935812387. E-mail: **olga.sanchez@uab.es**

Abstract

Recent studies have shown that the cyanobacterium *Microcoleus chthonoplastes* forms a consortium with heterotrophic bacteria present within the cyanobacterial sheath. These studies also show that this consortium is able to grow in the presence of crude oil, degrading aliphatic heterocyclic organo-sulphur compounds as well as alkylated monocyclic and polycyclic aromatic hydrocarbons. In this work we characterize this oil-degrading consortium through the analysis of the 16S rRNA gene sequences. We carried out the study in cultures of *Microcoleus* grown in mineral medium and in cultures of the cyanobacterium grown in mineral medium supplemented with crude oil. The results indicate that most of the clones found in the polluted culture correspond to well-known oil-degrading and nitrogen-fixing microorganisms, and belong to different phylogenetic groups, such as the Alpha, Beta and Gamma subclasses of Proteobacteria, and the CFB group. The control is dominated by one predominant organism (88% of the clones) closely affiliated to *Pseudoxanthomonas mexicana* (similarity of 99.8%). The presence of organisms closely related to well-known nitrogen fixers like *Rhizobium* and *Agrobacterium* suggests that at least some of the cyanobacteria-associated heterotrophic bacteria are responsible of nitrogen fixation and degradation of hydrocarbon compounds inside the polysaccharidic sheath, while *Microcoleus* would provide a habitat and a source of oxygen and organic matter.

Keywords: *Microcoleus*, consortium, crude oil, biodegradation

Introduction

Studies carried out by several authors [5, 17] attribute to cyanobacteria an important role in the biodegradation of organic pollutants. In fact, there is evidence that microbial communities dominated by cyanobacteria can be actively involved in oil degradation [2]. Observations made after oil spills in the Arabian Gulf showed that cyanobacteria grew forming heavy thick mats on the top of the sediments [4, 39]. Other studies have focused on the capacity of cyanobacteria isolates to degrade hydrocarbons. Cerniglia et al [9, 10] observed the degradation of naphthalene, a major component of the water-soluble fraction of crude oil, and biphenyl, by the same strain of *Oscillatoria*. It has also been reported that phenanthrene can be metabolized by the unicellular marine cyanobacterium *Agmenellum quadruplicatum* [27]. Also, *Oscillatoria salina*, *Plectonema tenebrans* and *Aphanocapsa* sp. degraded crude oil when grown in artificial medium and natural seawater [32].

However, it is by no means clear whether oil degradation is carried out by cyanobacteria alone or by heterotrophic bacteria associated to cyanobacteria. Some studies point to heterotrophic bacteria associated to cyanobacteria as co-responsible of hydrocarbon degradation. Al-Hasan et al [5] demonstrated that non-axenic cyanobacterial samples containing *Microcoleus chthonoplastes* and *Phormidium corium* consumed and oxidized *n*-alkanes. They found that cyanobacterial growth steadily declined with progressive axenity, and they identified four genera and species of associated heterotrophic bacteria able to oxidize *n*-alkanes, such as *Rhodococcus rhodochrous*, *Arthrobacter nicotianae*, *Pseudomonas* sp. and *Bacillus* sp., although cyanobacteria contributed directly to hydrocarbon uptake and oxidation. On the other hand, Al-Hasan et al [6] demonstrated that picocyanobacteria from the Arabian Gulf accumulated hydrocarbons from the water body, but did not utilize these compounds, and the authors assumed that associated bacteria may be carrying out the degradation of these contaminants. Furthermore, Abed and Köster [1] confirmed that *Oscillatoria*-associated aerobic heterotrophic bacteria were responsible for the biodegradation of *n*-alkanes.

Recent studies have shown that *Microcoleus chthonoplastes* developed forming a consortium with heterotrophic bacteria capable of biodegrading crude oil [16].

This consortium was able to grow in the presence of sulphur-rich petroleum, although the changes in crude oil composition were small, involving essentially degradation of aliphatic heterocyclic organo-sulphur compounds such as alkylthiolanes and alkylthianes. Also other group of compounds, such as the alkylated monocyclic and polycyclic aromatic hydrocarbons underwent some degree of transformation. Ultrathin sections of this cyanobacterium revealed the presence of different bacterial morphotypes inside the polysaccharidic *Microcoleus* sheath [13].

In this work we used molecular techniques, such as Denaturing Gradient Gel Electrophoresis (DGGE) and clone libraries, in order to characterize the components of this consortium.

Methods

Microorganism and culture conditions

Microcoleus chthonoplastes was isolated from microcosms of Ebro Delta microbial mats (Tarragona, Spain) polluted with Maya crude oil by means of serial transfers in agar plates containing the mineral medium described by Van Gemerden and Beeftink [42] as previously described by Diestra et al [13]. The cultures were grown in anoxic conditions under a continuous light regime (15 $\mu E.m^{-2}.s^{-1}$) at 27ºC. Initially, our aim was the isolation of pure cultures of *Microcoleus,* but microscopic observations by TEM (Transmission Electron Microscopy) and SEM (Scanning Electron Microscopy) indicated the existence of other bacteria growing in intimate contact with *Microcoleus* filaments. With TEM, we observed heterotrophic bacteria growing within the polysaccharidic sheath, while SEM allowed the visualization of bacteria adhered to *Microcoleus* filaments [13].

The consortium was grown on agar plates both with mineral medium containing carbonate as the only carbon source and with the same medium lacking carbonate and supplemented with 150 µl of Maya crude oil spread on top of the plate.

DNA extraction

Nucleic acid extraction of cultures was performed as described by Massana et al [24]. Samples of cyanobacterial biomass collected from the surface of the plates were suspended in 2 ml of lysis buffer (50 mM Tris-HCl, pH 8.3; 40 mM EDTA, pH 8.0; 0.75 M sucrose). 0,5-mm-diameter sterile glass beads were added to the cultures, and vortexed in order to disrupt the filaments. DNA was extracted using the lysis/phenol extraction method as described below. Lysozyme (1 $mg \cdot ml^{-1}$ final concentration) was added and samples were incubated at 37ºC for 45 min in slight movement. Then, sodium dodecyl sulphate (1% final concentration) and proteinase K (0.2 $mg \cdot ml^{-1}$ final concentration) were added and samples were incubated at 55ºC for 60 min in slight movement. Nucleic acids were extracted twice with phenol-chloroform-isoamyl alcohol (25:24:1, vol:vol:vol), and the residual phenol was removed once with choloroform-isoamyl alcohol (24:1, vol:vol). Nucleic acids were purified, desalted and concentrated with a Centricon-100 concentrator (Millipore). DNA integrity was checked by agarose gel electrophoresis, and quantified using a low DNA mass ladder as a standard (Invitrogen). The same extract of the two samples was splitted for analysis by DGGE and clone library.

PCR-DGGE fingerprinting

Fragments of the 16S rRNA gene suitable for DGGE analysis were obtained by using the bacterial specific primer 358F with a 40 bp GC-clamp, and the universal primer 907RM [26, 35]. PCR was carried out with a Biometra thermal cycler using the following program: initial denaturation at 94°C for 5 min; 10 touchdown cycles of denaturation (at 94°C for 1 min), annealing (at 65–55°C for 1 min, decreasing 1°C each cycle) and extension (at 72°C for 3 min); 20 standard cycles (annealing at 55°C, 1 min) and a final extension at 72°C for 5 min.

Primers 344f-GC and 915r were used for archaeal 16S rRNA amplification [33, 37]. The PCR protocol included an initial denaturation step at 94 ºC for 5 min, followed by 20 touchdown cycles of denaturation (at 94 ºC for 1 min), annealing (at 71 to 61 ºC for 1 min, decreasing 1 ºC each cycle), and extension at 72 ºC for 3 min. This procedure was followed by 15 additional cycles at an annealing

temperature of 61 ºC. During the last cycle of the program, the length of the extension step was 10 min [8].

PCR mixtures contained 1-10 ng of template DNA, each deoxynucleoside triphosphate at a concentration of 200 µM, 1.5 mM $MgCl_2$, each primer at a concentration of 0.3 µM, 2.5 U *Taq* DNA polymerase (Invitrogen) and PCR buffer supplied by the manufacturer. BSA (Bovine Serum Albumin) at a final concentration of 600 $\mu g \cdot ml^{-1}$ was added to minimize the inhibitory effect of humic substances [18]. The volume of reactions was 50 µl. PCR products were verified and quantified by agarose gel electrophoresis with a low DNA mass ladder standard (Invitrogen).

The DGGE was run in a DCode system (Bio-Rad) as described by Muyzer et al [26]. A 6% polyacrylamide gel with a gradient of DNA-denaturant agent was cast by mixing solutions of 0% and 80% denaturant agent (100% denaturant agent is 7 M urea and 40% deionized formamide). Seven hundred ng of PCR product were loaded for each sample and the gel was run at 100 V for 18 h at 60°C in 1xTAE buffer (40 mM Tris [pH 7.4], 20 mM sodium acetate, 1 mM EDTA). The gel was stained with SybrGold (Molecular Probes) for 45 min, rinsed with 1xTAE buffer, removed from the glass plate to a UV-transparent gel scoop, and visualized with UV in a Gel Doc EQ (Bio-Rad).

Prominent bands were excised from the gels, resuspended in milli-q water overnight, reamplified and purified using a High Pure PCR Product Purification Kit (Roche) for its sequencing.

Clone library and RFLP analysis

For cloning, bacterial 16S rRNA gene was amplified between positions 27 and 1492 (*Escherichia coli* 16S rRNA gene sequence numbering), using the primers 27F (5'-AGA GTT TGA TCM TGG CTC AG-3') and 1492R (5'-GGT TAC CTT GTT ACG ACT T-3'). PCR mixtures contained 10 ng of template DNA, each deoxynucleoside triphosphate at a concentration of 200 µM, 1.5 mM $MgCl_2$, each primer at a concentration of 0.3 µM, 2.5 U *Taq* DNA polymerase (Invitrogen) and PCR buffer supplied by the manufacturer. Reactions were carried out in an automated thermocycler (Biometra) with the following cycle: an initial denaturation step at 94ºC for 5 min, followed by 30 cycles of 1 min at

94ºC, 1 min at 55ºC and 2 min at 72ºC, and a final extension step of 10 min at 72ºC.

The PCR product was cloned with the TOPO TA cloning kit (Invitrogen) according to manufacturer's instructions. Putative positive colonies were picked, transferred to a multi-well plate containing Luria-Bertani medium and 7% glycerol, and stored at –80ºC. Recombinant plasmids were extracted using the QIAprep spin miniprep kit (QIAgen), following manufacturer's instructions. Purified plasmids were digested at 37ºC overnight with *Hae*III (Invitrogen) and the product was run in 2.5% low melting point agarose gel. The different band patterns were chosen for partial sequencing. The coverage of the clone library was calculated according to the following equation: C=1-(*n*/*N*), where *n* is the number of unique clones and *N* is the total number of clones examined [34].

Our choice of these primers (358F with a GC clamp and 907R for DGGE analysis, and 27F and 1492R for clone libraries) was deliberate because they do not amplify Microcoleus. We checked this using the match probe tool of the ARB program package applying as target strings the primer sequences and also with cultures of Microcoleus. This allowed us to eliminate the high background of this dominant microorganism, since it could have interfered in the final results.

rRNA sequencing

Sequencing reactions were performed by Macrogen (Korea) with the primers 907R for bacterial DGGE bands (approximately 500 bp in length), and 27F for cloned 16S rRNA genes. They utilized the Big-dye Terminator version 3.1 sequencing kit and reactions were run in an automatic ABI 3730XL Analyzer – 96 capillary type.

Sequences were subjected to a BLAST search [7] to get a first indication of the phylogenetic affiliation, and to the CHECK-CHIMERA program from RDP [22] to determine potential chimeric artifacts. Sequences were aligned by using the automatic alignment tool of the ARB program package (http://www.mikro.biologie.tu-muenchen.de) [20]. Then partial sequences were inserted into the optimized tree derived from complete sequence data by the *Quick add using parsimony tool*, which does not affect the initial tree topology.

The resulting tree was pruned to save space and only the closest relatives were retained.

Accession numbers

Forty-four 16S rRNA gene sequences were sent to the EMBL database (http://www.ebi.ac.uk/embl) and received the following accession numbers: from AJ871043 to AJ871081 for the clone library and from AJ870388 to AJ870392 for the DGGE bands (the detailed assignation for each sequence appears in Fig. 2).

Results

Microcoleus chthonoplastes was grown both on agar plates containing mineral medium with carbonate as the only carbon source, and on agar plates with the same medium composition, except for carbonate, which had been omitted and replaced by a small amount of crude oil. Cyanobacterial biomass was collected from the surface of the plates and after DNA extraction, the diversity of the 16S rRNA genes present in the samples was characterized by DGGE analyses and also by sequencing the clone libraries built from each, the control (C) and the oil-polluted (O) culture.

DGGE analysis of the consortium

DGGE analysis of the control and the oil polluted culture using the general bacterial primers 344F-GC and 907R showed the existence of substantial differences between samples (Fig. 1). Comparison of the two cultures demonstrated that in both cases, the number of bands observed in the DGGE gel was low (two bands in the control and four bands in the oil polluted culture), indicating low diversity of microorganisms associated to *Microcoleus*.

Prominent bands were sequenced, and the closest matches (and percentages of similarity) for the sequences retrieved were determined by a BLAST search (Table 1). The number of bases used to calculate each similarity value is also shown in Table 1 as an indication of the quality of the sequence. One of the

bands (B2), present in both samples, was related to an uncultured Bacteroidetes microorganism. In the oil polluted sample (O), one of the most intense bands (band B3) corresponded to a microorganism closely related to *Rhizobium* sp. Another two bands appeared in this lane; they were related to an uncultured Bacteroidetes microorganism (band B1) and to *Thioclava pacifica* (Rhodobacteraceae, band B4). The control had also one prominent band (band B5) closely related to *Pseudoxanthomonas mexicana* (Xanthomonadaceae).

Clone library construction and rRNA sequencing

DGGE is a fingerprinting technique that allows easy and fast comparison of related microbial profiles, but sequences obtained from excised DGGE bands are short and of variable quality, sufficient to determine broad phylogenetic affiliations but inadequate to carry out a precise phylogenetic analysis. Thus, we investigated the phylogenetic composition of the two samples (O and C) by building two independent clone libraries. We obtained 94 and 187 clones for samples O and C, which resulted in different RFLP patterns respectively. A representative clone of each OTU (Operational Taxonomic Unit) was partially sequenced. Their frequency in the library, the similarity values and their closest relatives are listed in Table 2. The coverage of the libraries were 87,2 and 95,7% for samples O and C respectively. Members of the α and γ subclasses of Proteobacteria were the main components of the two samples.

In general, groups of bacteria that could only be detected in the oil contaminated sample included members of the Rhizobiaceae (*Rhizobium* and *Agrobacterium tumefaciens*, 26%), members of the Rhodobacteraceae (*Thioclava pacifica* and *Roseobacter*, 29%), as well as ß- Proteobacteria closely related to *Hydrogenophaga* (5%). Only one species of α-Proteobacteria identified as *Hyphomonas polymorpha* was unique to the control sample (1.1%). The remaining sequences were found both in the control and in the polluted sample although with different frequencies, and included members of the families Pseudomonadaceae, Xanthomonadaceae, Phyllobacteriaceae and the CFB group. It is remarkable that 88% of the clones in the control sample (C) corresponded to *Pseudoxanthomonas mexicana*. In general, there was agreement between the DGGE and the gene library data. Inclusion of all the sequences in a phylogenetic tree indicates that all the DGGE band sequences

corresponded to several of the most abundant clones recovered from the library (see Fig. 2). However, a relatively large number of clones, some of them quite abundant, were not represented in the DGGE gel.

Discussion

Basically, our results demonstrate that bacteria associated to *Microcoleus chthonoplastes* grown in the presence of crude oil belong to the following four families: Rhizobiaceae (*Rhizobium* sp., *Agrobacterium tumefaciens*, 26.6%). Rhodobacteraceae (*Thioclava pacifica*, *Roseobacter* sp., 28.7%), Phyllobacteriaceae (*Parvibaculum lavamentivorans*, 13.9%) and Xanthomonadaceae (*Pseudoxanthomonas japonensis*, 11.7%). In the control culture grown in the absence of crude oil, the most abundant organism (*Pseudoxanthomonas mexicana*, 87.7% of the clones) belongs to the family Xanthomonadaceae.

Growth of heterotrophic bacteria associated to *Microcoleus* or other cyanobacteria has been reported before [29]. Steppe et al [38] demonstrated the existence of epiphytic nitrogen-fixing bacteria forming a diazotrophic consortium with *Microcoleus* spp. This observation is particularly interesting because *Microcoleus*, which does not have the capacity to fix nitrogen, is the major constituent of marine microbial mats, well known for their ability to proliferate in nitrogen deficient environments.

In a separate study, Olson et al [28] described a similar phenomenon in cyanobacteria-dominated microbial aggregates embedded in the permanent ice cover of Lake Bonney (Antartica) and in cyanobacterial mats found in soils adajacent to the ice edge. Their microscopic observations revealed the presence of heterotrophic bacteria associated to cyanobacteria and also growing in their mucilaginous sheath. Based on the presence of nifH sequences typical of heterotrophic organisms, the authors suggested that they were probably contributing to nitrogen fixation.

In our case, several of the 16S rRNA sequences recovered from the gene libraries correspond to nitrogen-fixing microorganisms. Two of these organisms (*Rhizobium* and *Agrobacterium*) were only detected in the cultures of

Microcoleus which had been grown in the presence of oil. The third organism, *Pseudomonas stutzeri*, found in the culture incubated with oil and also in the control, fixes nitrogen under microaerophilic conditions in the free-living state [12]. It is tempting to speculate about a possible role of these organisms as nitrogen providers for growth of *Microcoleus* under the conditions tested.

There is evidence that some of the nitrogen-fixing species found (*Rhizobium* and *Agrobacterium*) can also develop in oil-contaminated soils [3, 19, 31, 41]. These publications pointed at the potential use of nodule-forming symbiotic bacteria for oil bioremediation.

On the other hand, when the consortium was grown in the presence of oil, we identified several clones closely related to *Pseudomonas stutzeri*. It was also detected in the control, although at a lower percentage (7%). The genus *Pseudomonas* has been associated extensively with the degradation of petroleum compounds [23, 43]. Members of this group are able to degrade S- and N-heterocyclic [15], alkanes and other polyaromatic hydrocarbons [26]. An algal-bacterial consortium formed by *Chlorella sorokiana* and a *Pseudomonas migulae* strain was able to degrade phenanthrene [25] in two-phase partitioning bioreactors. *Pseudomonas* can also grow associated with cyanobacteria [5]. Furthermore, *Pseudomonas stutzeri* was isolated from fuel-contaminated Antarctic soils [14]; the authors pointed to a possible selection of diazotrophs, since fuel-contaminated soils have adequate carbon but present nitrogen-limited conditions.

Several species of purple nonsulfur bacteria metabolize aromatic compounds during phototrophic growth, including in particular the species *Rhodopseudomonas palustris*, but also *Rhodomicrobium vannieli*, *Rhodocyclus purpureus*, *Phaeospirillum fulvum* and *Rhodobacter capsulatus* [21]. We could detect some members of the family Rhodobacteraceae in samples O and C, although they seemed more abundant in the oil-polluted sample.

In addition, we could identify other minor groups capable of degrading hydrocarbon compounds. Some clones shared a high similarity (99%) with *Parvibaculum lavamentivorans*, a heterotroph that grow with octane and is able to initiate catabolism of linear alkylbenzenesulfonate [36].

It has also been described that the ß-Proteobacterium *Hydrogenophaga* sp., which was detected in our oil-degrading consortium, can metabolize 4-aminobenzenesulfonate when growing in a mixed culture with *Agrobacterium* [11].

Pseudoxanthomonas mexicana was first described by Thierry et al [35]. Until now, little is known about the physiology of this organism, beyond the fact that it has a stricty respiratory metabolism and that it can reduce nitrite to N_2O. Exploration of the metabolic capabilities of this microorganism would be essential in order to understand its ecological function in the consortium, particularly the ability to degrade organic compounds.

In a recent study, Abed and Köster [1] evaluated the role of cyanobacteria and their associated aerobic heterotrophic bacteria in biodegradation of petroleum compounds. They found that five different cyanobacteria (*Aphanothece halophyletica*, *Dactyolococcopsis salina*, *Halothece* strain EPUS, *Oscillatoria* strain OSC, and *Synechocystis* strain UNIGA) were able to degrade *n*-alkanes, while three isolates (*Aphanothece halophyletica*, *Oscillatoria* strain OSC and *Synechocystis* strain UNIGA) degraded aromatic compounds. The authors demonstrate that the heterotrophic bacteria associated with *Oscillatoria* strain OSC are responsible for the observed biodegradation. The molecular analysis of cultures of *Oscillatoria* grown on different petroleum model compounds shows the presence of associated heterotrophic bacteria belonging to the γ subclass of Proteobacteria. The control experiment (Oscillatoria culture without model compounds) reveals the presence of a bacterial sequence from the Cytophaga/Flavobacteria/Bacteroides group.

The metabolic capacities displayed by the organisms found in association with *Microcoleus* in our study are in agreement with the type of degradation previously reported for this consortium by Garcia de Oteyza et al [16]. Summarizing, our findings suggest that the microorganisms associated with the cyanobacterium *Microcoleus chthonoplastes* could be carrying out most of the nitrogen fixation and degradation of hydrocarbon compounds inside the polysaccharidic sheath. As discussed by other authors, degradation of petroleum compounds is unlikely to be characteristic for cyanobacteria,

although they play an indirect role in mixed populations like microbial mats by supporting the growth and activity of the actual degraders [1, 2].

In general, as stated by Paerl and Pinckney [29], many prokaryotes develop microbial consortial associations with other prokaryotes and eukaryotes depending on their nutrient necessities. In our consortium *Microcoleus* would provide a habitat and a readily available source of oxygen and organic matter produced by excretion of photosynthates, cell lysis and decomposition, while the accompanying bacteria would contribute to the consortium by fixing nitrogen. Furthermore, the complete degradation of petroleum compounds to CO_2 can be used by cyanobacteria for photosynthesis.

Acknowledgments

This work was supported by grants BOS2000-0139, REN2000-0332-P4 and DPI2003-0860-C03-02 from the Ministerio de Ciencia y Tecnología to J Mas.

References

1. Abed RMM, Köster J (2005) The direct role of aerobic heterotrophic bacteria associated with cyanobacteria in the degradation of oil compounds. Int Biodeter Biodegr 55: 29-37

2. Abed RMM, Safi NMD, Köster J, de Beer D, El-Nahhal Y, Rullkötter J, Garcia-Pichel F (2002) Microbial diversity of a heavily polluted microbial mat and its community changes following degradation of petroleum compounds. Appl Environ Microbiol 68: 1674-1683

3. Aitken MD, Stringfellow WT, Nagel RD, Kazunga C, Chen SH (1998) Characteristics of phenanthrene-degrading bacteria isolated from soils contaminated with polycyclic aromatic hydrocarbons. Can J Microbiol 44: 743-752

4. Al-Hasan RH, Sorkhoh NA, Al-Bader DA, Radwan SS (1994) Utilization of hydrocarbon by cyanobacteria from microbial mats on oily coasts of the Gulf. Appl Microbiol Biotechnol 41: 615-619

5. Al-Hasan RH, Al-Bader DA, Sorkhoh NA, Radwan SS (1998) Evidence for *n*-alkane consumption and oxidation by filamentous cyanobacteria from oil-contaminated coasts of the Arabian Gulf. Mar Biol 130: 521-527

6. Al-Hasan RH, Khanafer M, Eliyas M, Radwan SS (2001) Hydrocarbon accumulation by picocyanobacteria from the Arabian Gulf. J Appl Microbiol 91: 533-540

7. Altschul SF, Madden TL, Schäffer AA, Zhang J, Zhang Z, Miller W, Lipman DJ (1997) Gapped BLAST and PSI-BLAST: a new generation of protein database search programs. Nucleic Acids Res 25: 3389-3402

8. Casamayor EO, Schäfer H, Bañeras Ll, Pedrós-Alió C, Muyzer G (2000) Identification of and spatio-temporal differences between microbial assemblages from two neighboring sulphurous lakes. Comparison by microscopy and denaturing gel electrophoresis. Appl Environ Microbiol 66: 499-508

9. Cerniglia CE, Van Baalen C, Gibson DT (1980) Metabolism of naphthalene by the cyanobacterium *Oscillatoria* sp., strain JCM. J Gen Microbiol 116: 485-494

10. Cerniglia CE, Van Baalen C, Gibson DT (1980) Oxidation of byphenyl by the cyanobacterium *Oscillatoria* sp, strain JCM. Arch Microbiol 125:203-207

11. Dangmann E, Stolz A, Kuhm AE, Hammer A, Feigel B, Noisommit-Rizzi N, Rizzi M, Reuss M, Knackmamss HJ (1996) Degradation of 4-aminobenzenesulfonate by a two-species baxcterial coculture. Physiological interactions between *Hydrogenphaga palleronii* S1 and *Agrobacterium radiobacter* S2. Biodegradation **7**: 223-229

12. Desnoues N, Lin M, Guo X, Ma L, Carreño-López R, Elmerich C (2003) Nitrogen fixation genetics and regulation in a *Pseudomonas stutzeri* strain associated with rice. Microbiology 149: 2251-2262

13. Diestra E, Solé A, Martí M, Garcia de Oteyza T, Grimalt JO, Esteve I (2005) Characterization of an oil-degrading *Microcoleus* consortium by means of CLSM, SEM and TEM. Scanning 27 (in press)

14. Eckford R, Cook FD, Saul D, Aislabie J, Foght J (2002) Free-living heterotrophic nitrogen-fixing bacteria isolated from fuel-contaminated Antarctic soils. Appl Environ Microbiol 68: 5181-5185

15. Foght JM, Westlake WS (1998) Degradation of polycyclic aromatic hydrocarbons and aromatic heterocycles by a *Pseudomonas* species. Can J Microbiol 34: 1135-1141

16. Garcia De Oteyza T, Grimalt JO, Diestra E, Solé T, Esteve I (2004) Changes in the composition of the polar and apolar crude oil fractions under the action of *Microcoleus* consortia. Appl Microbiol Biotechnol 66: 226-232

17. Grötzschel S., Köster J, Abed RMM, de Beer D (2002) Degradation of petroleum model compounds immobilized on clay by a hypersaline microbial mat. Biodegradation 13: 273-283

18. Harry M, Gambier B, Bourezgui Y, Garnier-Sillam E (1999) Evaluation of purification procedures for DNA extracted from organic samples: interferences with humic substances. Analysis 27: 439-442

19. Lebkowska M, Karwowska E, Miaskiewicz E (1995) Isolation and identification of bacteria from petroleum derivatives contaminated soil. Acta Microbiol Pol 44: 297-303

20. Ludwig W, Strunk O, Klugbauer S, Klugbauer N, Weizenegger M, Neumaier J, Bachleitner M, Schleifer KH (1998) Bacterial phylogeny based on comparative sequence analysis. Electrophoresis 19: 554-568

21. Madigan MT, Jung DO, Resnick SM (2001). Growth of the purple bacterium *Rhodobacter capsulatus* on the aromatic compound hippurate. Arch Microbiol 175: 462-465

22. Maidak BL, Cole JR, Lilburn TG, Parker CTJr., Saxman PR, Stredwick JM, Garrity GM, Li B, Olsen GJ, Pramanik S, Schmidt TM, Tiedje JM (2000). The RDP (Ribosomal Database project) continues. Nucleic Acids Res 28: 73-174

23. Margesin R., Labbé D., Schinner F., Greer CW, Whyte LG (2003) Characterization of hydrocarbon-degrading microbial populations in contaminated and pristine alpine soils. Appl Environ Microbiol 69: 3085-3092

24. Massana, R., Murray AE, Preston M, DeLong EF (1997) Vertical distribution and phylogenetic characterization of marine planktonic Archaea in the Santa Barbara Channel. Appl Environ Microbiol 63: 50-56

25. Muñoz R, Guieysse B, Mattiasson B (2003) Phenanthrene biodegradation by an algal-bacteria consortium in two-phase partitioning bioreactors. Appl Microbiol Biotechnol 61: 261-267

26. Muyzer G, Brinkhoff T, Nübel U, Santegoeds C, Schäfer H, Wawer C. (1998) Denaturing gradient gel electrophoresis (DGGE) in microbial ecology. In: Akkermans ADL, van Elsas JD, Bruijn FJ (eds) Molecular microbial ecology manual, Kluwer Academic Publishers, Dordrecht, The Netherlans, pp. 3.4.4./1-27

27. Narro ML, Cerniglia CE, Van Baalen C, Gibson DT (1992) Metabolism of phenanthrene by the marine cyanobacterium *Agmenellum quadruplicatum* PR-6. Appl Environ Microbiol 58: 1351-1359

28. Olson JB, Steppe TF, Litaker RW, Paerl HW (1998) N_2-fixing microbial consortia associated with the Ice Cover of Lake Bonney, Antarctica. Microb Ecol 36: 231-238

29. Paerl HW, Pinckney JL (1996) A mini-review of microbial consortia: their roles in aquatic production and biogeochemical cycling. Microb Ecol 31: 225-247

30. Palleroni N (1993) *Pseudomonas* classification. Antonie Van Leeuwenhoek 64: 231-251

31. Prantera MT, Drozdowicz A, Gomes-Leite S, Soares-Rosado A (2002) Degradation of gasoline aromatic hydrocarbons by two N_2-fixing soil bacteria. Biotechnol Lett 24: 85-89

32. Raghukumar C, Vipparty V, David JJ, Chandramohan D (2001) Degradation of crude oil by cyanobacteria. Appl Microbiol Biotechnol 57: 433-436

33. Raskin L, Stromley JM, Rittmann BE, Stahl DA (1994) Group-specific 16S rRNA hybridization probes to describe natural communities of methanogens. Appl Environ Microbiol 60: 1232-1240

34. Ravenschlag K, Sahm K, Pernthaler J, Amann R (1999) High bacterial diversity in permanently cold marine sediments. Appl Environ Microbiol 65: 3982-3989

35. Schauer M, Massana R, Pedrós-Alió C (2000) Spatial differences in bacterioplankton composition along the Catalan coast (NW Mediterranean) assessed by molecular fingerprinting. FEMS Microl Ecol 33: 51-59

36. Schleheck D, Tindall BJ, Rossello-Mora R, Cook AM (2004) *Parvivaculum lavamentivorans* gen. nov., sp. nov., a novel heterotroph that initiates catabolism of linear alkylbenzenesulfonate. Int J Syst Evol Microbiol 54: 1489-1497

37. Stahl DA, Amann RI (1991) Development and application of nucleic acid probes. In: Stackebrandt E., Goodfellow M. (eds) Nucleic acid techniques in bacterial systematics, Wiley, New York, NY, pp 205-248

38. Steppe TF, Olson JB, Paerl HW, Litaker RW, Belnap J (1996) Consortial N_2 fixation: a strategy for meeting nitrogen requirements of marine and terrestrial cyanobacterial mats. FEMS Microbiol Ecol 21: 149-156

39. Sorkhoh NA, Al-Hasan R, Radwan S, Hopner T (1992) Self-cleaning of the Gulf. Nature 359:109

40. Suominen L, Jussila MM, Mäkeläinen K, Romantschuk M, Lindström K (2000) Evaluation of the *Galega-Rhizobium galegae* system for the bioremediation of oil-contaminated soil. Environ Pollut 107: 239-244

41. Thierry S, Macarie H, Iizuka T, Geissdorfer W, Assih EA, Spanevello M, Verhe F, Thomas P, Fudou R, Monroy O, Labat M, Ouattara AS (2004) *Pseudoxanthomonas mexicana* sp. nov, and *Pseudoxanthomonas japonensis* sp. nov., isolated from diverse environments, and emended descriptions of the genus *Pseudoxanthomonas* Finkmann et al. 2000 and of its type species. Int J Syst Evol Microbiol 54: 2245-2255

42. Van Gemerden H, Beeftink HH (1983) Ecology of phototrophic bacteria. In: Ormerod JG (ed) The phototrophic bacteria: anaerobic life in the light, Blackwell Scientific Publications, Oxford, pp 146-185

43. Zhang H, Kallimanis A, Koukhou AI, Drainas C (2004) Isolation and characterization of novel bacteria degrading polycyclic aromatic hydrocarbons from polluted Greek soils. Appl Microbiol Biotechnol 65: 124-131

Table 1. Sequence similarities of excised bacterial bands that appear in Fig. 1
[a] The numbers in parentheses are the numbers of bases used to calculate the levels of sequence similarity

Band	Closest match	% similarity (nº bases)[a]	Taxonomic group	Accession nº
B1	Uncultured Bacteroidetes	95,8 (525)	CFB	AJ534682
B2	Uncultured bacterium	98,7 (532)	CFB	AF502212
B3	*Rhizobium* sp.	98,9 (528)	α-Proteobacteria	AY500261
B4	*Thioclava pacifica*	98,5 (530)	α-Proteobacteria	AY656719
B5	*Pseudoxanthomonas mexicana*	99,6 (560)	γ-Proteobacteria	AF1973082

Table 2. Phylogenetic affiliation of clone sequences retrieved (O: culture with oil; C: control without oil)

GROUP	CLOSEST MATCH (Acc. Number)	SIMILARITY %	CULTURED CLOSEST MATCH (Acc. Number)	SIMILARITY %	% clones O	% clones C
α - Proteobacteria	*Rhizobium* sp. (AF364858)	98,1			**25,5**	-
	Agrobacterium tumefaciens (AF508094)	97,2			1,1	-
	Thioclava pacifica (AY656719)	97,7			**25,5**	-
	α proteobacterium (AY162070)	97,7	*Roseobacter* sp. (AY332661)	97,7	3,2	-
	Roseomonas sp. (AF533359)	94,1			1,1	-
	Roseomonas gilardii (AY150051)	94,4			-	0,5
	Hyphomonas polymorpha (AJ227813)	99,2			-	1,1
	Uncultured bacterium (AF143824)	97,8	*Parvibaculum lavamentivorans* (AY387398)	97,1	1,1	-
	Parvibaculum lavamentivorans (AY387398)	99,6			**12,8**	1,6
β - Proteobacteria	Uncultured bacterium (AB186829)	98,9	*Hydrogenophaga* sp. (AB166889)	98,5	2,1	-
	Uncultured bacterium (AY625151)	99,4	*Hydrogenophaga taeniospiralis* (AF078768)	99,2	3,2	-
γ - Proteobacteria	*Pseudomonas stutzeri* (U26414)	99,9			8,5	0,5
	Pseudomonas stutzeri (AJ006103)	99,7			-	6,4
	Pseudoxanthomonas mexicana (AF273082)	99,8			-	**87,7**
	Uncultured γ proteobacterium (AJ619035)	99,9	*Pseudoxanthomonas japonensis* (AB008507)	99,6	**11,7**	-
	Uncultured γ proteobacterium (AF445725)	98,4	*Aquamonas vora* (AY544768)	94,7	1,1	-
	Uncultured γ proteobacterium (AF445726)	96,7	*Pseudoxanthomonas daejeonensis* (AY550264)	93,7	1,1	-
CFB	Uncultured bacterium (AF502210)	95,5	*Cytophaga* sp. (AF250407)	96,7	1,1	2,1
	Antarctic bacterium (AJ441001)	94,5	*Cytophaga* sp. (X85210)	94,1	1,1	-

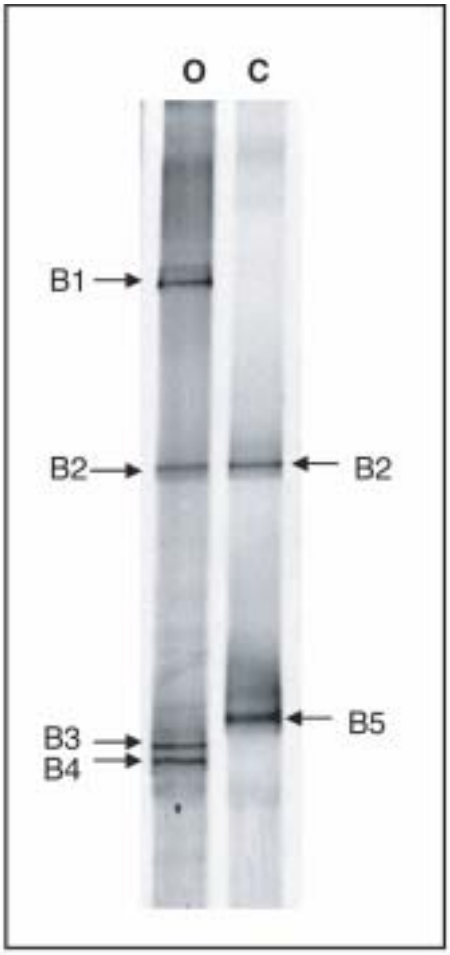

Figure 1. Negative image of DGGE gel with PCR products amplified with bacterial primer sets (O: consortium with oil, C: consortium without oil).

OPHELIA 58 (3): 151-156 (December 2004)

A COMPARATIVE STUDY OF CYANOBACTERIAL DIVERSITY IN POLLUTED AND UNPOLLUTED MICROBIAL MATS BY MEANS CLSM

Elia Diestra, Antonio Solé and Isabel Esteve*

Department of Genetics and Microbiology. Autonomous University of Barcelona. Bellaterra. 08193 Barcelona, Spain.

*Corresponding author: Elia Diestra Villanueva, phone: +34-93-5813255, fax: +34-93-5812387
E-mail: elia.diestra@uab.es

ABSTRACT

This paper is a summary of the results obtained from a study of the diversity of cyanobacteria in oil polluted and unpolluted natural environments.

Our work group identified the different genera of cyanobacteria by means of CLSM, as this technique is specifically appropriate for studying the diversity of these microorganisms in stratified benthonic environments (microbial mats).

The cyanobacteria identified in pristine ecosystems show that the most abundant cyanobacteria correspond to the genera: *Microcoleus chthonoplastes*, *Oscillatoria* sp., *Lyngbya* sp., *Leptolyngbya* sp., and *Limnothrix* sp. *Phormidium* sp.and *Pseudanabaena* sp. were also identified, although they were less abundant. On the other hand, in the ecosystems heavily polluted with oil (Etang de Bèrre) neither *Microcoleus chthonoplastes* nor *Oscillatoria* sp. were detected, although the other genera mentioned were. With respect to coccoid cyanobacteria, the most abundant groups in the Ebro delta were *Gloeocapsa* sp. and *Synechocystis* sp. and also the genus *Chroococcus* sp. with *Synechocystis* sp. dominating the mats from Saline de Giraud. The microbial mats from Orkney Islands showed a different composition from those above (*Pleurocapsa*-group and *Microcystis* sp., *Aphanothece* sp. and *Merismopedia* sp.)

Keywords: Cyanobacteria, microbial mats, confocal laser scanning microscopy, crude oil pollution.

INTRODUCTION

Microbial mats are widely distributed throughout the world. The microorganisms that compose them have aroused scientific due to their high tolerance of extreme conditions (Cohen and Rosenberg, 1989). Along with the fact that microbial mats are understood to be living replicas of stromatolites which has also generated an extraordinary interest from the evolutionary point of view (Bergman et al. 1997, Fay 1992, Chapman and Margulis 1998).

Although many populations of both phototrophic and autotrophic microorganisms colonise these environments, cyanobacteria (phototrophic oxygenic bacteria) are the most important primary producers in these ecosystems. Their ability to live in extreme environments (López-Cortés et al. 2001) and to produce exopolysaccharides (Mazor et al. 1996, De Philippis et al. 1998) is also very well-known.

Our work group has studied microbial mats situated along the eastern Spanish Mediterranean coast, identifying the different types of microbial mats and the dominant populations in each case, (Esteve et al. 1992). In particular, we have centred our study on Ebro Delta (Tarragona) microbial mats in which, as well as identifying the populations of phototrophic microorganisms, we have studied the spatial and temporal dynamic of these populations (Esteve et al. 1994).

In the past two years we have applied the Confocal Laser Scanning Microscopy (CLSM) to study phototrophic populations, as one of the most important characteristics of cyanobacteria is that they emit natural fluorescence. CLSM, not only enables the identification of cyanobacteria (Solé et al. 1998, Solé et al. 2001, Wieland et al. 2003), but also allowed us to quantify each of the different genera separately and to calculate each group's biomass and its space-time dynamic (Solé et al. 2003).

Recent studies suggest that these microorganisms may play a role in hydrocarbon breakdown in polluted environments (Mejharaj et al. 2000, Zheng et al. 2001).

Here we present a comparative study of cyanobacterial diversity from different polluted and unpolluted microbial mats from all over Europe. The aim of this work was to study both types of microbial mats to determine which phototrophic microorganisms might have the most important role in the breakdown of hydrocarbons.

MATERIAL AND METHODS

The sampling and treatment of the sediment cores, taken from the different microbial mats until confocal analysis has been described in Wieland et al. (2003).

The samples were analyzed with a compound microscope (Olympus BH2, Japan) and a laser confocal microscope (Leica TC54d, Germany). Different fluorescence confocal images (590 nm) summa projections and stereoscopic images were obtained when the samples were excited with an excitation beam of 568 nm.

After screening the different cyanobacteria present in all the confocal images from the sampling sites, each type of cyanobacterium was identified according to morphological criteria outlined to Castenholz et al. (2001).

RESULTS AND DISCUSSION

In this study, a comparison of cyanobacteria diversity was made in different microbial mats: pristine (Ebro delta and Saline de Giraud), low polluted (Swanbister bay, Waulkmill bay and St. Peter's bay) and high polluted (Etang de Bêrre).

The cyanobacteria identified in these ecosystems are shown in Tables 1 and 2. The cyanobacteria *Borzia* sp, was only detected in microbial mats from the Orkney Islands (Fig 1). This genus *Borzia* sp. is characterised by very short trichomes of 2 – 8 cells, with conspicuous constrictions at the crosswalls of various diameters, with little or no motility, and with cells that are usually shorter than they are wide (Castenholz et al. 2001). This cyanobacterium have also been described in microbial mats with high concentrations of salt, like those at Salines de Palmer (Mallorca-Spain), (data non shown). On the other hand, in the ecosystems heavily polluted with oil (Etang de Bêrre) neither *Microcoleus chthonoplastes* nor *Oscillatoria* sp.

Table 1: Filamentous cyanobacteria

Microorganism	Diameter(μm)	Septation	Gas vacuoles	Sheath	Habitat/Abundance
Microcoleus chthonoplastes	3.13 – 3.75	+	-	+	Ed (++++); Sg (++)
Oscillatoria sp.	9-14	+	-	+	Ed (+++);Wb (+++)
Lyngbya sp.	5.6 – 10.3	+	-	+	Eb(+++); Wb (+++); Ed (++); Pb (+)
Phormidium sp.	1.4 – 3.75	+ (isodiametric cells)	-	+	Ed(++); Eb (++)
Pseudanabaena sp.	1.4 – 2.5	+ (cells longer than wide)	+	+	Ed (++); Wb(+)
Spirulina sp.	1.9 – 3	-	-	+	Ed (+); Pb (+)
Leptolyngbya sp.	< 1 (large filaments)	-	-	+	Sg (+++); Wb (++); Eb (+)
Limnothrix sp.	13.25	-	+	+	Sg (+++); Eb (+); Sb (+)
Borzia sp.	1.25 – 1.9 (short filaments)	+	-	+ (thin)	Pb (++); Sb (+++)
Unidentified	< 1.25 (short filaments	+	-	+	Sg (+++); Eb (+)
Unidentified	1.56	-	-	+	Pb (+++)

Ed = Ebro delta
Sg = Salin de Giraud
Eb = Etang de Berre
Sb = Swanbister bay
Wb = Waulkmill bay
Pb = St. Peter's bay

were detected, although the other genera mentioned were.

The most abundant unicellular cyanobacteria in the Ebro delta and Saline de Giraud were: *Synechocystis* sp. and *Chroococcus* sp. *Gloeocapsa* sp. (table 2) was also in the Ebro delta. The microbial mats from the Orkney Islands showed a different composition from those above. In this case, the *Pleurocapsa*-group was very abundant, along with the genera *Microcystis* sp., *Aphanothece* sp. and *Merismopedia* sp (Fig 1).

It is also important to mention the total absence of unicellular cyanobacteria in Etang de Bêrre (natural ecosystem polluted with oil).

The differences in the diversity of cyanobacteria in the different mats could be attributed to the different environmental parameters pertinent to each of them, as well as oil pollution itself. However, it must be borne in mind that in the mats that suffered oil pollution at some time during their formation (Orkney Islands) or in those heavily contaminated (Etang de Bêrre) some filamentous cyanobacteria like *Microcoleus chthonoplastes* were practically undetectable. This fact has also been proven by various typological studies in the Ebro Delta, in which it was shown that these cyanobacteria appear only in well developed microbial mats (Guerrero et al. 1993, Bebout et al. 1995, García-Pichel et al. 1996).

The confocal microscope has allowed us to determine the biodiversity of the different samples with a degree of clarity greater than any other microscopic technique used and it can be particularly recommended for use in the study of microbial mats.

ACKNOWLEDGEMENTS

This work was supported by the Spanish grant CICYT BOS 2001-2035 to I. E, and the financial support by the EC (MATBIOPOL project, grant EVK3-CT-1999-00010). We are grateful to the staff of the Servei de Microscòpia of the Autonomous University of Barcelona, specially to Mercè Martí for their help with confocal techniques and applications.

REFERENCES

Bebout, M. and García-Pichel, F. 1995. UV-B. Induced vertical migrations of cyanobacteria in microbial mats. Appl. Environ. Microbiol., 61: 4215-4222.

Bergman, B., Gallon, J. R., Rai, A.N. and Stal, L.J. 1997. N2 fixation by non – heterocystous cyanobacteria. FEMS Microbiol. Ecol., 19: 139-18

Castenholz, R.W.2001. Phylum BX Cyanobacteria. Oxygenic Photosynthetic Bacteria. pp. 473-599. In:

Table 2: Unicellular cyanobacteria

Microorganism	Diameter(μm)	Cell division planes	Sheath	Habitat/Abundance
*Gloeocapsa*group	4 × 14	2 or 3 planes	+	Ed (+++); Wb (+++)
Chroococcus sp.	19 × 28	2 planes	+	Ed (++)
*Synechocystis*group	3.5 × 3.5	2 or 3 planes	+	(thin) Ed(++); Sg (++)
*Synechocystis*group	5 × 6	2 or 3 planes	+	Pb(++)
Merismopedia sp.	4.4 × 6	2 planes	+	Pb (+++)
Aphanothece sp.	5 × 7	Many different planes	+ (thin)	Wb (++); Pb (++)
Myxosarcina sp.	6 × 8	Binary fission in 3 planes	+	Ed (+)
Microcystis sp.	1.9 × 1.9	Binary fission in different planes	+	Sb (+++); Pb (+++); Wb (++)
*Pleurocapsa*group *Stanieria*	2 × 3	Multiple fissions or in combination with limited (1-3) binary fissions	+	Sb (+)
*Pleurocapsa*group	Diverse in size and form	Binary fissions in several planes (pseudofilaments)	-	Sb (+++); Pb (++), Wb (++)
*Pleurocapsa*group	2 × 3	Binary fissions in many different planes	+	Wb (+++)
Unidentified	1.25 × 2	2 planes	+	Pb (+)
Unidentified	1.5 × 1.5	Binary fissions in many different planes	+	Pb (+)

Ed = Ebro delta
Sg = Salin de Giraud
Eb = Etang de Berre
Sb = Swanbister bay
Wb = Waulkmill bay
Pb = St. Peter's bay

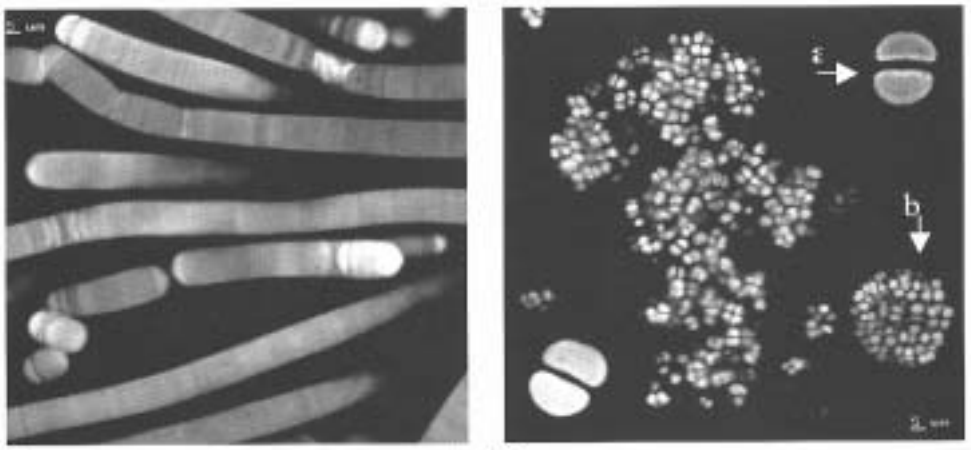

1A 1B

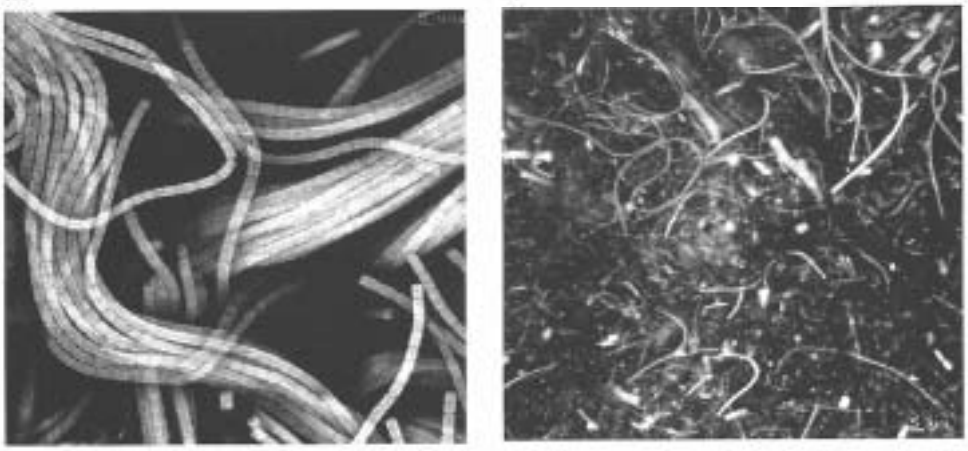

1C 1D

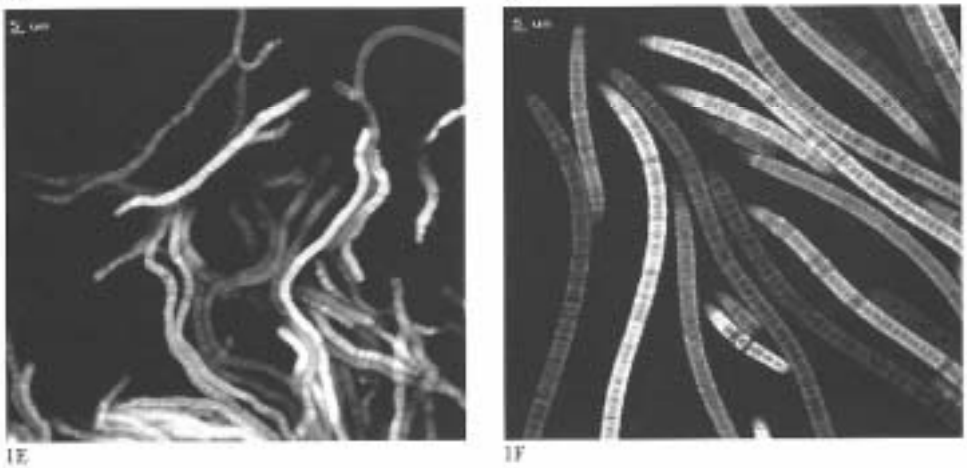

1E 1F

Fig: 1A. *Oscillatoria* sp. (Ed), 1B.a. *Chroococcus* sp. (Ed), 1B.b. *Myxosarcina* sp. (Ed), 1C. *Microcoleus chthonoplastes* (Sg), 1D. *Leptolyngbya* sp. (Sg), 1E. *Phormidium* sp. (Eb), 1F. *Lyngbya* sp. (Eb).

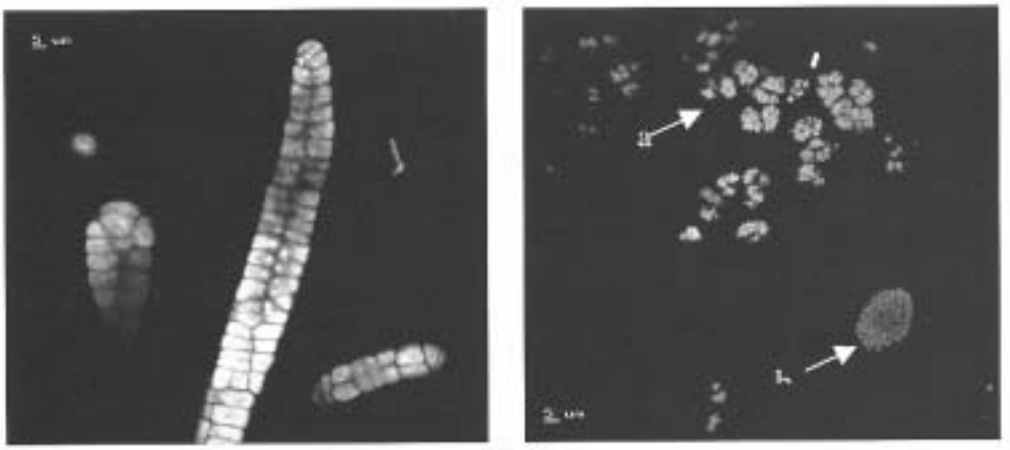

1G 1H

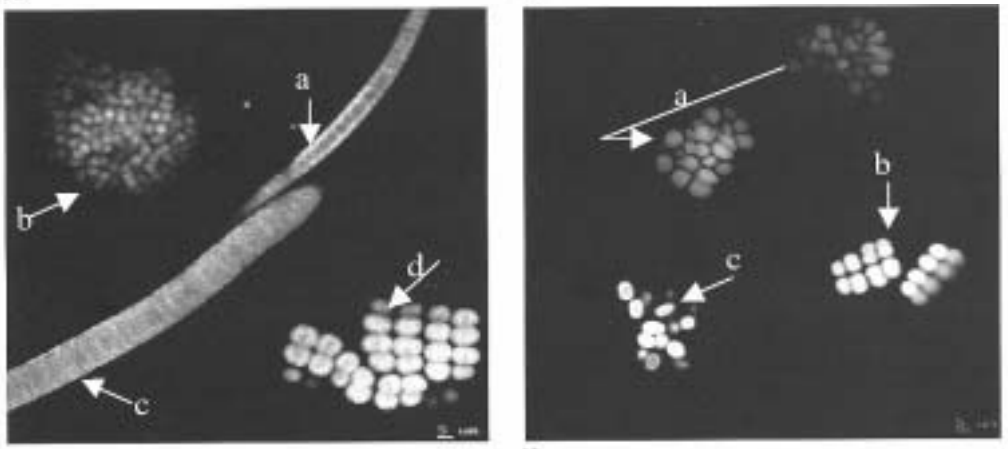

1I 1J

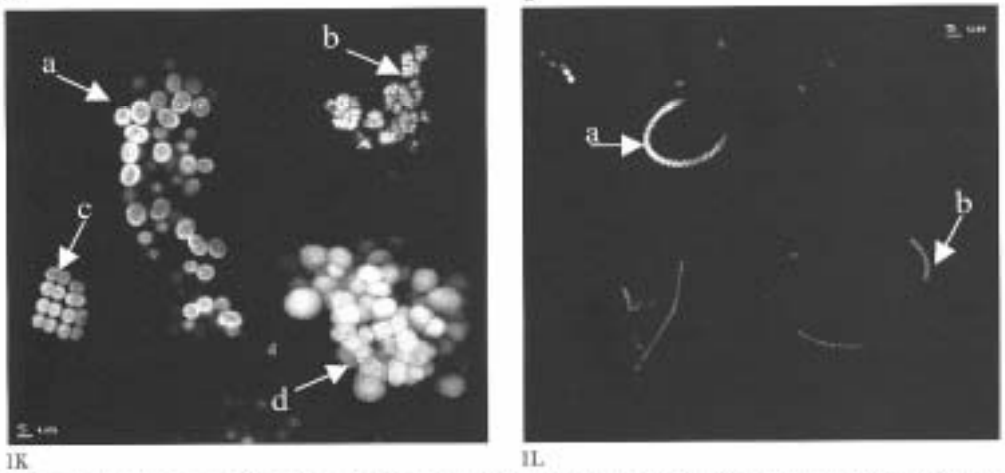

1K 1L

Fig: 1G. *Pleurocapsa*-group (Sb), 1H.a. *Microcystis* sp. (Sb), 1H.b. *Stanieria* sp. (Sb), 1I.a. *Lyngbya* sp. (Wb), 1I.b. *Microcystis* sp. (Wb) 1I.c. *Oscillatoria* sp. (Wb), 1I.d. *Gloeocapsa* sp. (Wb), 1J.a. *Pleurocapsa*-group (Wb), 1J.b. *Gloeocapsa* sp. (Wb), 1J.c. *Aphanothece* sp. (Wb), 1K.a. *Aphanothece* sp. (Pb), 1K.b. *Microcystis* sp., (Pb), 1K.c. *Synechocystis*-group (Pb), 1K.d. *Pleurocapsa*-group (Pb), 1L.a. *Spirulina* sp. (Pb), 1L.b. *Borzia* sp. (Pb).
Ed: Ebro delta, Sg: Saline de Giraud, Eb: Etang de Bêrre, Sb: Swanbister Bay, Wb: Waulkmill Bay, Pb: St. Peter's Bay.

Bergey's Manual Systematic Bacteriology. Vol 1. The Archea and deeply branching and phototrophic bacteria. Boone, D.R., Castenholz, R.W. and Garrity, G.M.(eds).Springer-Verlag. New York.

Cohen, Y. and Rosenberg E. 1989. Photosynthesis in cyanobacterial mats and its relation to the sulfur cycle. pp. 22-36. In: Microbial mats, physiological ecology of benthic microbial communities. A model for microbial sulfur interactions. Am. Soc. Microb. Washington, D. C.

Cohen, Y. 2002. Bioremediation of oil by marine microbial mats. Inter. Microbiol., 5: 189-193.

Chapman, M.J. and Margulis, L. 1998. Morphogenesis by symbiogenesis. Internat. Microbiol., 1: 319-373.

De Philippis, R., Margheri, M. C., Materassi, R. and Vincenzini, M. 1998. Potential of unicellular cyanobacteria from saline environments as exopolysaccharide producers. Appl. Environ. Microbiol., 64: 1130-1132.

Esteve, I., Martínez-Alonso, M., Mir, J. and Guerrero, R. 1992. Typology and structure of microbial mat communities in Spain: A preliminary study. Limnetica 8: 185-195.

Esteve, I., Cevallos, D., Martínez-Alonso, M., Gaju, N. and Guerrero, R. 1994. Development of versicolored microbial mats: Succession environmental significance. NATO ASI Series. G-35: 415-420.

Fay, P. 1992. Oxygenic relations of nitrogen fixation in cyanobacteria. J. Microbiol., 56: 340-373.

García-Pichel, F., Prufert-Bebout L. and Muyzer, G. 1996. Phenotypic and cosmopolitan cyanobacterium. Appl. Environ. Microbiol., 62: 3284-3291.

Guerrero, R., Urmeneta J. and Rampone, G. 1993. Distribution of types of microbial mats at the Ebro Delta, Spain. Biosystems. 31: 135-144.

López-Cortés, A., García-Pichel, F., Nübel, U. and Vázquez-Juárez, R. 2001. Cyanobacterial diversity in extremal environments in Baja California, México: a polyphasic study. Int. Microbiol., 4: 227-236.

Mazor, G., Kidron, G.J. Vonshak, A. and Abeliovich, A. 1996. The role of cyanobacterial exopolysaccharides in structuring desert microbial crusts. FEMS Microbiol. Ecol., 21: 121-130.

Mejharaj, M., Singleton, I., McClure, N.C. and Naidu, R. 2000. Influence of petroleum hydrocarbon contamination on micro algae and microbial activities in a long-term contaminated soil. Arch. Environ. Contam. Toxicol., 38: 439-445.

Solé, A., Gaju, N., Guerrero, R. and Esteve, I. 1998. Confocal laser scanning microscopy of Ebro Delta microbial mats. Microscopy and Analysis (Europ. Ed).29: 13-15.

Solé, A., Gaju, N., Mendez-Álvarez, S. and Esteve, I. 2001. Confocal laser scanning microscopy as a tool to determine cyanobacteria biomass in microbial mats. J. Microscopy, 204: 258-262.

Solé, A., Gaju, N. and Esteve, I. 2003. The biomass dynamics of cyanobacteria in an annual cycle determined by confocal laser scanning microscopy. Scanning 25: 1-7.

Wieland, A., Kühl, M., Mcgowan, L., Fourçans, A., Duran, R, Caumette, P., García de Oteyza, T., Grimalt, J. O., Solé, A., Diestra, E., Esteve, I. and Herbert, R. A. 2003. Microbial Mats on the Orkney Islands Revisited: Microenvironment and Microbial Community Composition. Microbial. Ecol. 000-000.

Zheng, Z., Breedveld, G. and Agaard, P. 2001. Biodegradation of soluble aromatic compounds of jet fuel under anaerobic conditions: laboratory batch experiments. Appl. Microbiol. Biotechnol., 57: 572-578.

Appl Microbiol Biotechnol (2004) 66: 226–232
DOI 10.1007/s00253-004-1694-3

ENVIRONMENTAL BIOTECHNOLOGY

Tirso Garcia De Oteyza · Joan O. Grimalt · Elia Diestra · Antonio Solé · Isabel Esteve

Changes in the composition of polar and apolar crude oil fractions under the action of *Microcoleus* consortia

Received: 1 April 2004 / Revised: 8 June 2004 / Accepted: 11 June 2004 / Published online: 5 August 2004

Abstract Cultures of *Microcoleus* consortia polluted with two different types of crude oil, one with high content in aliphatic hydrocarbons (Casablanca) and the other rich in sulphur and aromatic compounds (Maya), were grown for 50 days and studied for changes in oil composition. No toxic effects from these oils were observed on *Microcoleus* consortia growth. In fact, the interface layer between the oils and the water culture medium proved to be the ideal site for consortia development, leading to a wrapping effect of the oil layers by these organisms. Despite this affinity of cyanobacteria for the oil substrate, the changes in oil composition were small. *Microcoleus* consortia did not induce transformation in the aliphatic-rich oil, and the modifications in the sulphur and aromatic-rich oil were small. The latter essentially involved degradation of aliphatic heterocyclic organo-sulphur compounds such as alkylthiolanes and alkylthianes. Other groups of compounds, such as the alkylated monocyclic and polycyclic aromatic hydrocarbons, carbazoles, benzothiophenes and dibenzothiophenes, also underwent some degree of transformation, involving only the more volatile and less alkylated homologues.

Introduction

Highly productive photosynthetic microbial mats develop at the water-sediment interface in shallow environments such as estuaries, lagoons or sheltered sandy beaches. Most of these mats form horizontally stratified layers in which organisms are distributed along microgradients of oxygen, sulphide, light and temperature, among others. A typical microbial mat structure of marine coastal areas involves cyanobacteria on top, followed by purple sulphur photosynthetic bacteria, green sulphur photosynthetic bacteria, and sulphate-reducing bacteria at the bottom (Cohen and Rosenberg 1989). These microbial systems have been observed to play a role in the remediation of oil-polluted coastal areas in marine and hypersaline waters. Microbial mats have been observed to rapidly cover entire areas of oil-polluted sediment, e.g. within a few months, being considered a first step towards natural bioremediation (Sorkhoh et al. 1992). In contrast, other reports indicate that growth of cyanobacterial building mats results in preservation of the oil residues (Barth 2003). Both approaches provide evidence that cyanobacteria are the main and most abundant primary prokaryotic producers in microbial mats, requiring that the effect of these organisms on crude oil degradation be addressed. Evidence supporting the biodegradation capacity of cyanobacteria for the elimination of crude oil residues is still very limited, and is focussed on specific oil constituents such as *n*-alkanes (Al-Hasan et al. 1994, 1998; Raghukumar et al. 2001). In other cases, degradation experiments with model compounds such as aromatic hydrocarbons have been reported (Cerniglia 1984; Cerniglia et al. 1980; Raghukumar et al. 2001). To the best of our knowledge no results on cyanobacterial degradation of either polar or apolar oil fractions have been described to date. *Microcoleus* sp. is the dominant cyanobacterium in microbial mats in the Ebro Delta. *Microcoleus* is a filamentous oxygenic phototrophic bacterium that forms bundles of trichomes enclosed by a polysaccharide sheath. This cyanobacterium has been shown to play an important role in stabilising delta sediments. Morphological characteristics and annual space-time variations of this cyanobacterium biomass have been reported elsewhere (Solé et al. 2003). The ability of *Microcoleus* sp. to tolerate petroleum has been demonstrated as it grows in polluted microbial mats such as the Etang de Bêrre and in artificial laboratory systems (microcosms) polluted with

T. G. De Oteyza · J. O. Grimalt (✉)
Department of Environmental Chemistry (IIQAB-CSIC),
Jordi Girona, 18,
08034 Barcelona, Catalonia, Spain
e-mail: jgoqam@cid.csic.es
Tel.: +34-93-4006122
Fax: +34-93-2045904

E. Diestra · A. Solé · I. Esteve
Department of Genetics and Microbiology, Faculty of Sciences,
Autonomous University of Barcelona,
08193 Bellaterra, Catalonia, Spain

petroleum (Llirós et al. 2003). However, its role in the biodegradation of petroleum has not yet been established. Cultures of this cyanobacterium from polluted microbial mats growing in microcosms have been obtained recently. Ultrastructural analysis of *Microcoleus* colonies grown on Petri dishes reveals the existence of *Microcoleus* consortia formed by *Microcoleus* and heterotrophic bacteria included in the polysaccharide sheaths of *Microcoleus* sp. filaments. The present study describes the crude oil transformations upon degradation with *Microcoleus* consortia. Two crude oils, Casablanca and Maya, were selected as reference materials for this purpose. Casablanca crude contains mainly aliphatic hydrocarbons (59.5%) and, to a lesser extent, aromatic hydrocarbons (27%) (Table 1). Asphaltenes and polar compounds are present only in minor amounts. This oil is similar to many oils from the Arabian Gulf such as Arabian light or Kuwait. Maya oil is heavy and sulphur-rich, containing more than 2% sulphur. Aromatic hydrocarbons (43%) are more abundant than aliphatic hydrocarbons (29.5%) (Table 1). Asphaltenes and resins in the maltene fraction are present in relatively high amounts. In principle, this latter crude oil is potentially more harmful to marine ecosystems than Casablanca-type oils due to its higher viscosity and higher content of heterocyclic compounds (thiophenes, phenols, quinolines or acridines), which are often toxic and water-soluble (Barron et al. 1999). The changes in composition of aliphatic and aromatic hydrocarbons, and nitrogen and sulphur-containing compounds from these two oils are described.

Materials and methods

Microcoleus consortia isolated from polluted microbial mats were grown in mineral Pfenning medium (according to van Gemerden and Beeftink 1983). A 300 µl sample of Casablanca or Maya oils was added on top of separate culture bottles (see Fig. 1). Control experiments were performed in parallel keeping the oils in the same mineral medium but without *Microcoleus* consortia inoculum. Both controls and cultures were illuminated at 15 $\mu Em^{-2}s^{-1}$ and kept at 27°C. Structural examination of *Microcoleus* consortia was performed by confocal laser scanning microscopy using a Leica True Confocal Scanner TSC 4D. The samples were observed with a 63×1.4 numerical aperture and a Plan Apochromat oil immersion objective lens under 590 nm fluorescence excitation. Control oils and oil samples (±100–150 µl crude oil) from the cultures at the beginning and at the end of the experiments (50 days) were analysed. Samples were dissolved in *n*-hexane in order to precipitate the asphaltenes. The compounds soluble in *n*-hexane—the maltene fraction—were fractionated by column chromatography in a 34×0.9 cm^2 i.d. column filled with 8 g each of 5% water-deactivated alumina (top) and silica (bottom). The adsorbents in these columns, neutral silica gel (70–230 mesh, Merck) and alumina (70–230 mesh, Merck), were extracted with dichloromethane-methanol (2:1, v/v) in a Soxhlet apparatus for 24 h. After solvent evaporation, the silica and alumina were heated at 120°C and 350°C, respectively, for 12 h. These adsorbents were then deactivated by addition of 5% Milli-Q-grade water. Six fractions were separated by elution with 20 ml *n*-hexane (F1), 20 ml 10% dichloromethane in *n*-hexane (F2), 40 ml 20% dichloromethane in *n*-hexane (F3), 40 ml 25% *n*-hexane in dichloromethane (F4), 20 ml 5% methanol in dichloromethane (F5) and 40 ml 10% methanol in dichloromethane (F6). The hydrocarbon fractions (F1–F3) were evaporated to dryness and re-dissolved in *iso*-octane. The polar fractions (F4–F6) were re-dissolved in dichloromethane and derivatised with diazomethane. Gas chromatography (GC) was performed with a Varian Model Star 3400 equipped with a flame ionisation detector and a Varian 8200 CX septum programmable injector (SPI). A DB-5 capillary column (30 m×0.25 mm i.d.; film thickness 0.25 µm) was used. Hydrogen was the carrier gas (50 cm/s). The oven temperature program was 70–140°C at 10°C/min, 140–310°C at 4°C/min (holding time 20 min). The injector temperature program was from 100°C to 300°C at 200°C/min. The detector temperature was 330°C. Nitrogen was used as make-up gas (30 ml/min). Detector gas flows were hydrogen (30 ml/min) and air (300 ml/min). The samples were also analysed by GC coupled to a mass spectrometer (GC-MS) using a Fisons MD-800 instrument. Spectra were obtained in the electron impact mode (70 eV) scanning from *m*/*z* 50 to 550 every second. A HP-5 capillary column (30 m ×0.25 mm i.d.; film thickness 0.25 µm) was used. Helium was the carrier gas (1 ml/min). The oven temperature program was 70–140°C at 10°C/min, 140–310°C at 4°C/min (holding time 20 min). Injector, transfer line and ion source temperatures were 300, 280 and 200°C, respectively. Injection was in the splitless mode (*iso*-octane, hot needle technique) keeping the split valve closed for 48 s.

Table 1 Relative proportion of the crude oil column chromatography fractions (%)

	Casablanca		Maya	
	Original	After degradation	Original	After degradation
F1 Aliphatic hydrocarbons	59.5	n.d.[a]	29.5	39
F2 Aromatic hydrocarbons (monocyclic)	12	n.d.	10	12
F3 Aromatic hydrocarbons (polycyclic)	15	n.d.	33	26
F4 Polar compounds	5.7	n.d.	10	7.8
F5 Polar compounds	0.8	n.d.	1.6	1.6
F6 Polar compounds	6.8	n.d.	15.5	13

[a]Not degraded

Results

A few days after oil addition to the cultures, *Microcoleus* consortia started to grow towards the crude oil, nearly wrapping it. Figure 1 compares the growth of the consortia in an initial culture and in a culture obtained after 6 days of incubation under the conditions described in Materials and methods. A confocal laser scanning microscopy image of *Microcoleus* sp. filaments attached to oil drops is shown in Fig. 2. Ultrathin section of this cyanobacterium revealed the presence of three different heterotrophic bacteria inside the *Microcoleus* sheath. The diameter of these heterotrophic bacteria are 0.30 μm (type I), 0.22 μm (type II) and 0.40 μm (type III). Various experiments were carried out with these consortia grown in the presence and absence of light, as well as with and without a source of carbon, and with and without oxygen. The results revealed that optimum growth is obtained in anaerobiosis, in the presence of light, and with crude oil, which indicates that degradation is carried out by the heterotrophic bacteria using the oxygen supplied to them by *Microcoleus* sp., which carries out oxygenic photosynthesis (Diestra et al. 2004). The wrapping effect was observed for both crude oils used in the experiment. Nonetheless, the cultures with Maya oil developed to a greater extent. As observed in these experiments, all fractions of Maya oil except F1 underwent some degree of transformation; in contrast, no changes were observed in Casablanca oil (Table 1).

Aliphatic hydrocarbons

Consistent with the results reported in Table 1, no changes were observed among GC-amenable aliphatic hydrocarbons, such as *n*-alkanes, branched alkanes, cyclic-alkanes, isoprenoids, sesquiterpenoids, tricyclic triterpanes, hopanes and steranes, either in Casablanca or in Maya oil (Fig. 3). These results are somewhat contradictory with other results from the literature reporting *n*-alkane degradation upon cyanobacterial growth (Al-Hasan et al. 1994). However, as indicated in some reports (e.g. Al-Hasan et al. 1994), *n*-alkane degradation was observed in non-axenic cyanobacterial cultures whereas aliphatic hydrocarbon degradation was not produced with pure organotrophic bacterial cultures. *n*-Alkanes are currently the first hydrocarbons eliminated in crude oil microbial degradation (Peters and Moldowan 1993). In the experiments presented here, these compounds were not altered upon exposure to *Microcoleus* consortia. Not even short-chain homologues like *n*-undecane were depleted and the C_{17}/pristane and C_{18}/phytane ratios remained unchanged. Thus, the observed mixtures correspond to very early stages of crude oil biodegradation.

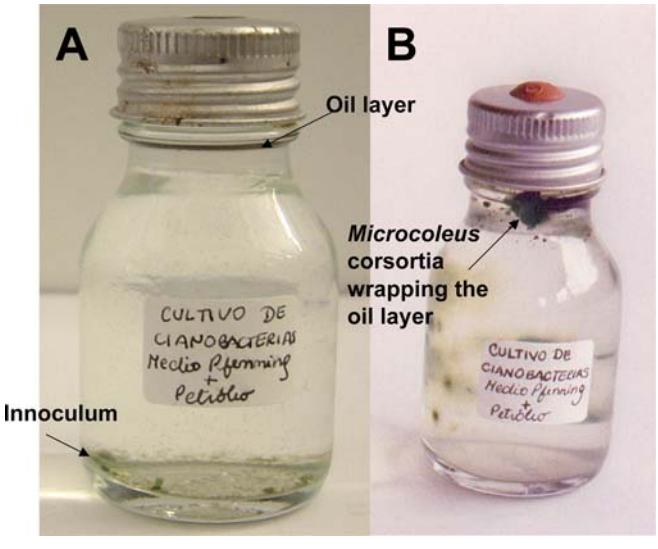

Fig. 1 **a** Initial culture and **b** culture obtained after 6 days of incubation of *Microcoleus* consortia with crude oil. Note the *green spots* attached to the crude oil indicating the affinity of the consortium for this hydrocarbon mixture

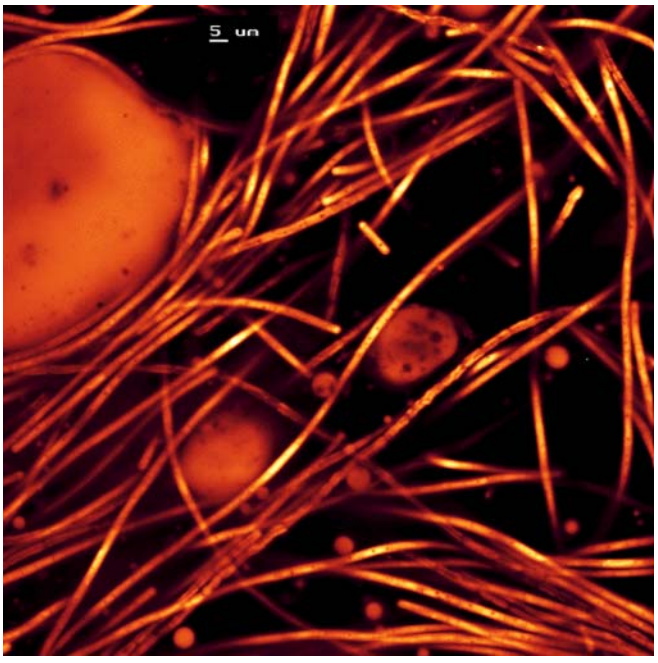

Fig. 2 Confocal laser scanning microscopy image showing filaments of *Microcoleus* consortia attached to oil drops

Aromatic hydrocarbons

These compounds encompass two fractions, F2 and F3, involving monocyclic and polycyclic hydrocarbons, respectively. The former group is composed mostly of alkylbenzenes and the latter of alkylnaphthalenes together with some alkylfluorenes, alkylbenzothiophenes, alkyldibenzothiophenes and alkylphenanthrenes. The alkylbenzenes encompass a benzene ring substituted by an aliphatic long chain and sometimes one or two additional methyl groups. They have been identified by examination of the characteristic mass ions of alkylated benzenes (*m*/*z*=91), toluenes (*m*/*z*=105) and xylenes (*m*/*z*=119). The alkylated naphthalenes, fluorenes, phenanthrenes, benzothiophenes and dibenzothiophenes form a series with

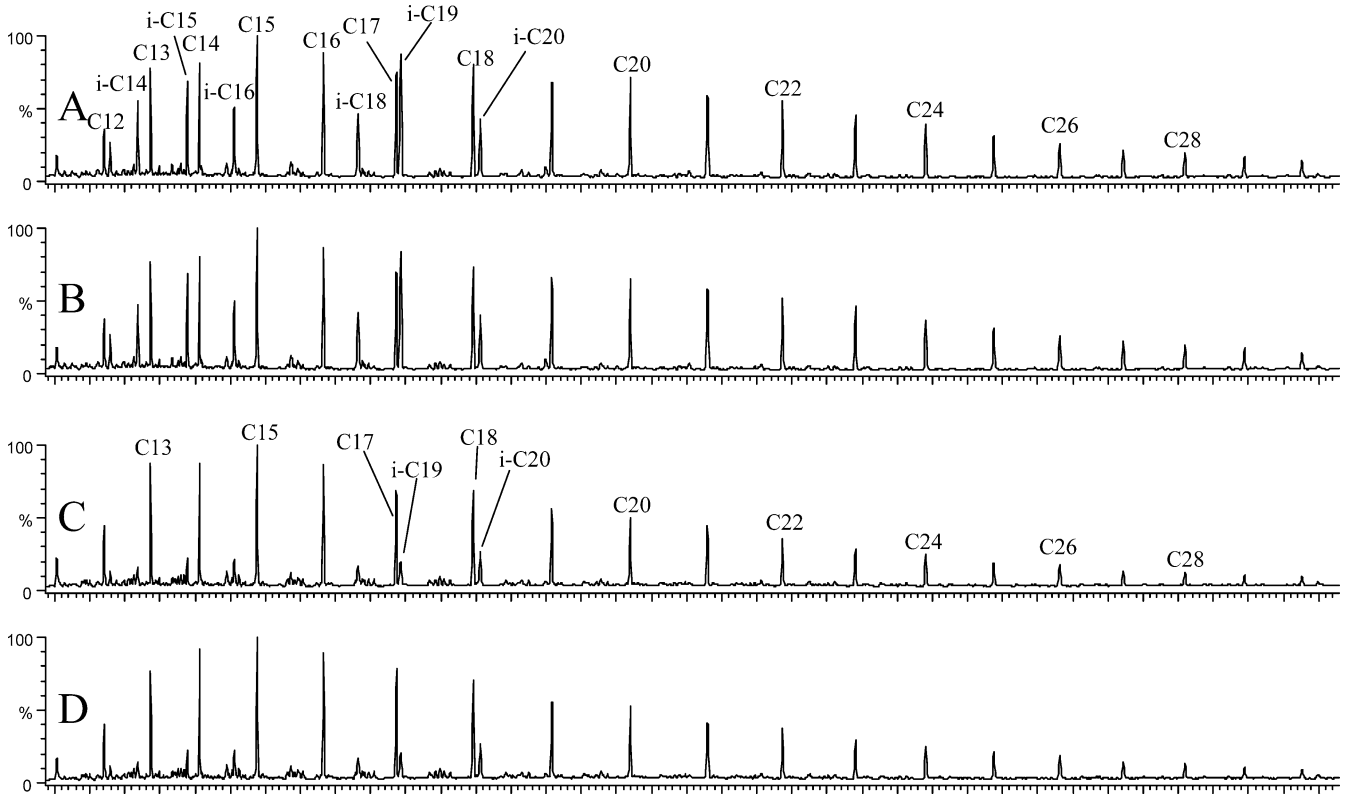

Fig. 3 Aliphatic hydrocarbon fraction of the original (**a**, **c**) and biodegraded (**b**, **d**) Casablanca (**a**, **b**) and Maya (**c**, **d**) crude oils

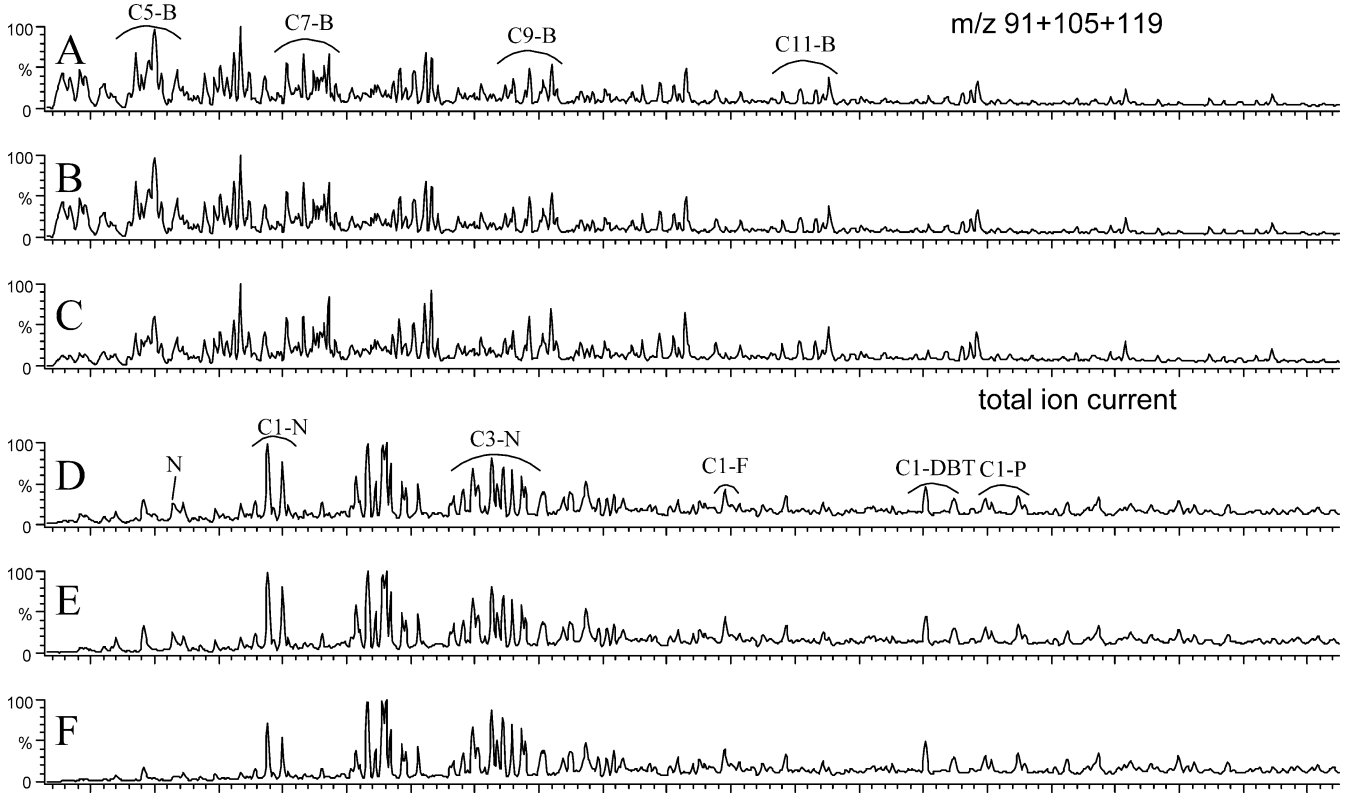

Fig. 4 Original (**a**, **d**), control (**b**, **e**) and biodegraded (**c**, **f**) aromatic monocyclic (**a**–**c**)and polycyclic (**d**–**f**) hydrocarbons of Maya crude oil. *CX-B* Alkylbenzenes, *N* naphthalene, *CX-N* alkylnaphthalenes, *CX-F* alkylfluorenes, *CX-DBT* alkydilbenzothiophenes, *CX-P* alkylphenanthrenes

the parent compound and homologues with increasing degrees of methyl substitution at different positions. They have been identified by examination of the mass fragments of the molecular ions of the parent compounds and C_1, C_2 and C_3 substitution, e.g. *m/z* 128, 142, 156 and 170 for the alkylnaphthalenes, *m/z* for 166, 180, 194 and 208 for the alkylfluorenes, *m/z* 178, 192, 206 and 220 for the alkylphenanthrenes, *m/z* 162, 176, 190 and 204 for the alkylbenzothiophenes and *m/z* 184, 198, 212 and 226 for the alkyldibenzothiophenes. Degradation of the lower molecular weight compounds was observed in both fractions of Maya oil (Fig. 4). Among alkylbenzenes, the biodegraded oil contained no C_4 homologues, about 50% of the initial C_5 homologue content was eliminated, some C_6 homologues were degraded to about 20%, and relative decreases were observed in the C_7 and C_8 homologues. In the polycyclic aromatic fraction, naphthalene was eliminated and the methylnaphthalenes were depleted to around 50%. Homologues with higher degrees of alkylation were not degraded. The loss of the more volatile hydrocarbons in these two aromatic fractions is not due to abiotic processes, e.g. volatilisation or photooxidation, since these compounds were preserved in the control oils. Casablanca oil contains the same series of monocyclic and polycyclic aromatic compounds as Maya oil. However, no transformation in the composition of these hydrocarbons was observed upon consortia growth. The main difference between the two oils is the relatively high proportion of aliphatic hydrocarbons in the former. As indicated above, these hydrocarbons are refractory to consortia action in both cases. Perhaps the preservation of the aromatic compounds in Casablanca oil can be explained by a hindering effect due to the higher proportion of aliphatic hydrocarbons in this oil than in Maya, which prevents effective contact between the consortium and compounds that may by metabolised by it. Alternatively, it could also be that aromatic compounds are susceptible to degradation only in the presence of other polar oil compounds that are more labile to consortia metabolism such as the sulphur-containing compounds described below. These compounds could provide molecular moieties that are needed to initiate transformation of aromatic hydrocarbons by consortia metabolism.

Sulphur-containing hydrocarbons

The GC-amenable compounds of Maya oil encompass series of cis and trans mid-chain alkylthiolanes (*m/z* 87; Fig. 5), 2-alkylthianes (*m/z* 101; Fig. 5), alkylbenzothiophenes (Fig. 6) and alkyldibenzothiophenes (Fig. 6). Both alkylthiolanes and alkylthianes were identified according to mass spectral and retention time data reported elsewhere (Schmid et al. 1987; Sinninghe Damsté et al. 1989). Alkylbenzothiophenes were identified by comparison with the mass spectral and retention time data reported for Rozel Point oil (Sinninghe Damsté et al. 1987). The proportions of the methyldibenzothiophenes, namely the

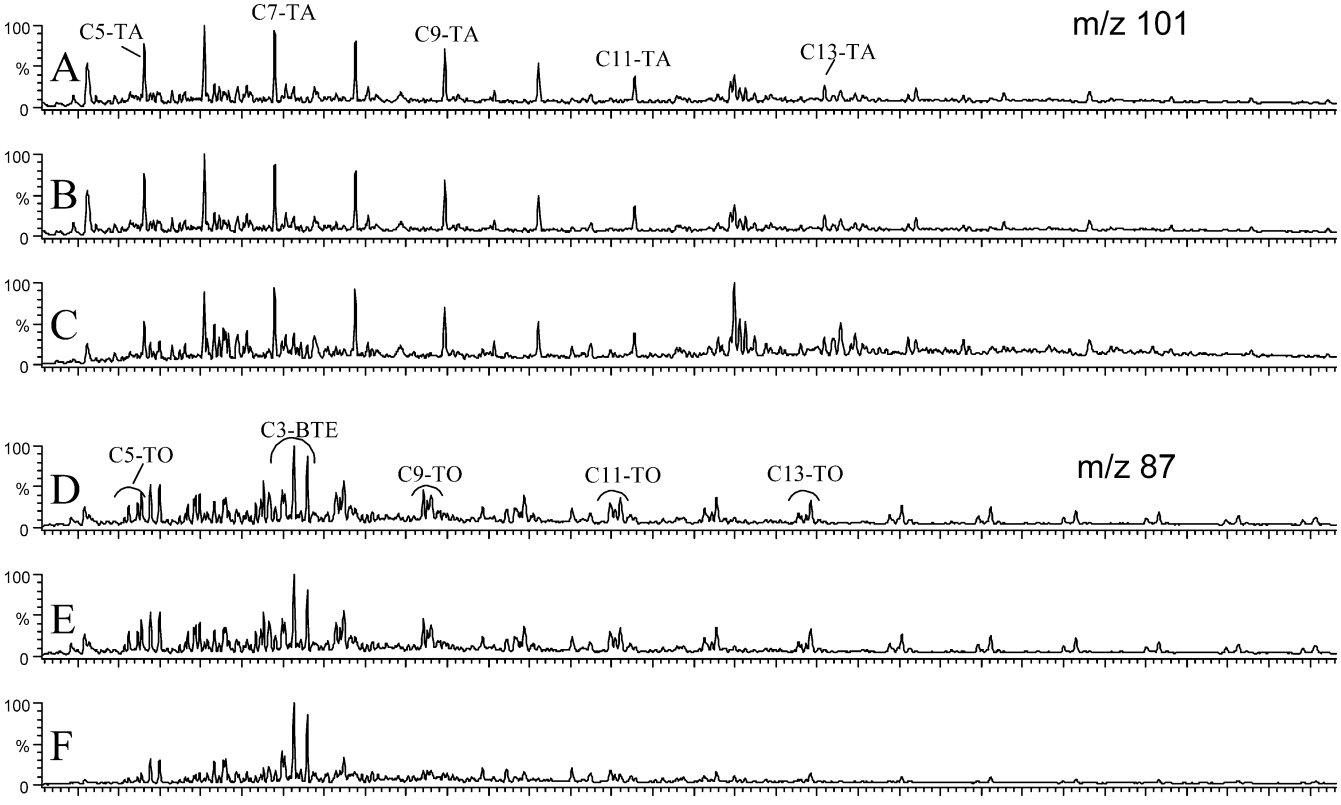

Fig. 5 Original (**a**, **d**), control (**b**, **e**) and biodegraded (**c**, **f**) alkylthianes (**a**–**c**) and alkylthiolanes (**d**–**f**) of Maya crude oil. *CX-TA* Alkylthianes, *CX-TO* alkylthiolanes, *CX-BTE* alkylbenzothiophenes

ratio between 1-methyldibenzothiophene and 3+2-methyldibenzothiophenes, is similar to the composition encountered in oils from evaporitic environments such as Amposta (Albaiges et al. 1986) Analysis of the crude oil mixtures after this period of growth revealed that most alkylthiolanes and alkylthianes had been eliminated (Fig. 5). Again, removal of these compounds is not due to abiotic processes, e.g. volatilisation or photooxidation, since they remain in the oil controls (Fig. 5). In contrast, the distribution of alkylbenzothiophenes and alkyldibenzothiophenes underwent a lower degree of transformation (Fig. 6). C_2-benzothiophenes were depleted by about 30% and dibenzothiophene by about 10% whereas the dibenzothiophenes of higher degree of alkylation were not degraded. Casablanca crude does not have thianes or thiolanes, and only a small quantity of benzothiophenes and dibenzothiophenes. No degradation was observed for these compounds in this oil. The elimination of organosulphur compounds observed in these experiments occurs similarly to previously described cases involving other organisms. Thus, aerobic microbial strains, e.g. *Pseudomonas* sp., isolated from sites chronically polluted with oil residues have also led to the elimination of alkylthiolanes and alkylthianes and a decrease in some alkylbenzothiophenes and alkyldibenzothiophenes in sulphur-rich crude oils such as Amposta oil (Grimalt et al. 1991). In this latter case, oil biodegradation also involved a strong depletion of *n*-alkanes, which were entirely eliminated. Alkylthiolanes and alkylthianes are therefore more labile to biodegradation than alkylbenzothiophenes and alkyldibenzothiophenes. These different properties reflect the stability of the sulphur-containing aromatic rings due to δ-electron delocalisation in fused aromatic ring systems.

Nitrogen-containing hydrocarbons

Alkylcarbazoles are found in both Casablanca and Maya oils. *Microcoleus* consortia action involves no transformation of the former but depletion of carbazol and methylcarbazoles in the latter, to about 60% and 40%, respectively (Fig. 6). Again, the lack of degradation in Casablanca oil could be due to the hindering effect of the large proportion of aliphatic hydrocarbons, or to the requirement of the presence of other compounds more labile to consortia transformation, such as the sulphur-containing compounds, to initiate the transformation.

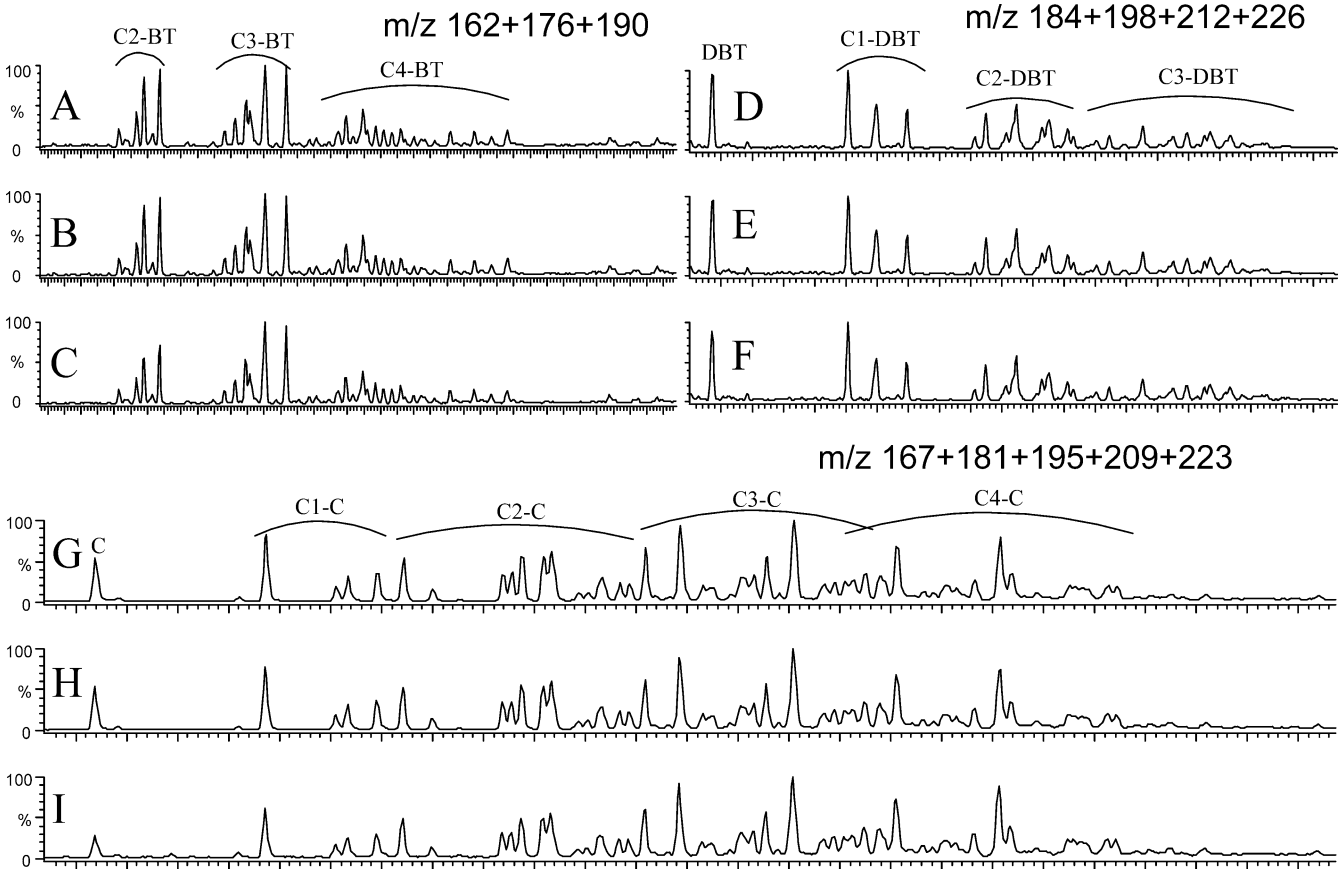

Fig. 6 Original (**a**, **d**, **g**), control (**b**, **e**, **h**) and biodegraded (**c**, **f**, **I**) alkylbenzothiophenes (**a**–**c**), alkyldibenzothiophenes (**d**–**f**) and alkylcarbazoles (**g**–**I**) of Maya crude oil. *CX-BT* Alkylbenzothiophenes, *CX-DBT* alkyldibenzothiophenes, *C* carbazole, *CX-C* alkylcarbazoles

Discussion

Microcoleus sp. can likely degrade crude oil due to consortia containing the above-mentioned three different heterotrophic organisms. Crude oil degradation was not observed in control experiments. Neither aliphatic nor aromatic sulphur-rich oils have any toxic effects on the *Microcoleus* consortia. Conversely, the interface layer between the oil and water culture media seems to be an ideal site for consortia growth. This observation is consistent with field reports from oil-polluted coastal areas indicating the rapid growth of cyanobacteria in sites occupied by microbial mats (Sorkhoh et al. 1992). The affinity of *Microcoleus* consortia for oil is observed irrespective of oil composition. Thus, Casablanca and Maya oils represent end-member cases of oils extracted for commercial purposes. In fact, Maya oil contains materials that enhance *Microcoleus* consortia growth even more than Casablanca oil. This result is interesting from an environmental standpoint. Whereas Maya oil is more viscous, less volatile, and contains more deleterious compounds (such as the stinking sulphur-containing molecules) Casablanca oil essentially comprises aliphatic hydrocarbons and is less viscous and more volatile. The latter is currently eliminated more easily from the environment both by abiotic processes and bacterial degradation. Aliphatic hydrocarbons are refractory to *Microcoleus* consortia attack. In contrast, aromatic hydrocarbons, both monocyclic and polycyclic, sulphur-containing compounds such as thiolanes and thianes, and nitrogen-containing compounds such as carbazoles, are degraded. In the case of both aromatic hydrocarbons and carbazoles, the compounds undergoing higher transformation are those with a lower degree of alkylation, which is again consistent with the observed resistance of aliphatic hydrocarbons to *Microcoleus* consortia metabolism. Thiolanes and thianes are degraded irrespective of the degree of alkyl substitution, indicating that thioether bonds are easily accessible to transformation by *Microcoleus* consortia. However, when sulphur atoms are integrated into aromatic polycyclic molecules, the compounds are much more resistant to degradation. Similar results were observed in a previous study involving microbial biodegradation of sulphur-rich crude oils with aerobic bacteria such as *Pseudomonas* sp. (Grimalt et al. 1991). Both results indicate that oil compounds containing saturated sulphur-containing rings are more labile to degradation than molecules with aromatic sulphur-containing rings. Overall, *Microcoleus* consortia appear to be organisms with the ability to biodegrade crude oil but to a lesser extent than several heterotrophic eubacteria, which are the organisms currently identified to be responsible for crude oil degradation in chronically polluted coastal sites. Thus, despite the fact that these organisms tend to grow attached to oil residues, and therefore reduce the contact between spilled oil and marine ecosystems, they metabolise only a minor part of the oil constituents.

Acknowledgement Financial contribution from the European Union MATBIOPOL project EVK3-CT-1999-00010 is acknowledged.

References

Albaiges J, Algaba J, Clavell E, Grimalt JO (1986) Petroleum geochemistry of the Tarragona Basin (Spanish Mediterranean off-shore). Org Geochem 8:293–297

Al-Hasan R, Sorkhoh NA, Al-Bader DA, Radwan SS (1994) Utilization of hydrocarbon by cyanobacteria from microbial mats on oily coasts of the Gulf. Appl Microbiol Biotechnol 41:615–619

Al-Hasan R, Al-Bader DA, Sorkhoh NA, Radwan SS (1998) Evidence for *n*-alkane consumption and oxidation by filamentous cyanobacteria from oil-contaminated coasts of the Arabian Gulf. Mar Biol 130:521–527

Barron MG, Podrabsky T, Ogle S, Ricker RW (1999) Are aromatic hydrocarbons the primary determinant of petroleum toxicity to aquatic organisms? Aquat Toxicol 46:253–268

Barth HJ (2003) The influence of cyanobacteria on oil polluted intertidal soils at the Saudi Arabian Gulf shores. Mar Pollut Bull 46:1245–1252

Cerniglia CE (1984) Microbial metabolism of polycyclic aromatic hydrocarbons. Adv Appl Microbiol 30:31–71

Cerniglia CE, Van Baalen C, Gibson DT (1980) Metabolism of naphthalene by the cyanobacterium *Osillatoria* sp., strain JCM. J Gen Microbiol 116:485–494

Cohen Y, Rosenberg E (1989) Microbial mats. Physiological ecology of benthic microbial communities. ASM, Washington

Diestra E, Solé A, Martí M, García De Oteyza T, Grimalt JO, Esteve I (2004) Characterization of *Microcoleus* consortia with capacity to degrade crude oil by means of CLSM, SEM and TEM. Res Microbiol (in press)

Gemerden H van, Beeftink HH (1983) Ecology of phototrophic bacteria. In: Ormerod JG (ed) The phototrophic bacteria: anaerobic life in the light. Studies in Microbiology, vol 4. Blackwell, Oxford, pp 146–185

Grimalt JO, Grifoll M, Solanas AM, Albaiges J (1991) Microbial degradation of marine evaporitic crude oils. Geochim Cosmochim Acta 55:1903–1913

Llirós M, Munill X, Solé A, Martínez-Alonso M, Diestra E, Esteve I (2003) Analysis of cyanobacteria biodiversity in pristine and polluted microbial mats in microcosmos by confocal laser scanning microscopy (CLSM). In: Mendez-Vilas (ed) Science, technology and education of microscopy: an overview. 288 FORMATEX Microscopy Book Series, vol 1, pp 483–489

Peters KE, Moldowan JM (1993) The biomarker guide. Interpreting molecular fossils in petroleum and ancient sediments. Prentice Hall, Englewood Cliffs

Raghukumar C, Vipparty V, David JJ, Chandramohan D (2001) Degradation of crude oil by marine cyanobacteria. Appl Microbiol Biotechnol 57:433–436

Schmid JC, Connan J, Albrecht P (1987) Occurrence and geochemical significance of long-chain dialkylthiacyclopentanes. Nature 329:54–56

Sinninghe Damsté JS, de Leeuw JW, Kok-van Dalen AC, de Leeuw MA, de Lange F, Rijpstra WIC, Schenck PA (1987) The occurrence and identification of series of organic sulphur compounds in oils and sediment extracts. I. A study of Rozel Point Oil (USA). Geochim Cosmochim Acta 51:2369–2391

Sinninghe Damsté JS, Rijpstra WIC, de Leeuw JW, Schenck PA (1989) The occurrence and identification of series of organic sulphur compounds in oils and sediment extracts: II. Their presence in samples from hypersaline and non-hypersaline palaeoenvironments and possible application as source, palaeoenvironmental and maturity indicators. Geochim Cosmochim Acta 53:1323–1341

Solé A, Gaju N, Esteve I (2003) The biomass dynamics of cyanobacteria in an annual cycle determined by confocal laser scanning microscopy. Scanning 25:1–7

Sorkhoh N, Al-Hasan R, Radwan S, Hoepner T (1992) Self-cleaning of the Gulf. Nature 359:109

ELSEVIER

FEMS Microbiology Ecology 51 (2004) 55–70

FEMS MICROBIOLOGY Ecology

www.fems-microbiology.org

Characterization of functional bacterial groups in a hypersaline microbial mat community (Salins-de-Giraud, Camargue, France)

Aude Fourçans [a], Tirso García de Oteyza [b], Andrea Wieland [c], Antoni Solé [d], Elia Diestra [d], Judith van Bleijswijk [e], Joan O. Grimalt [b], Michael Kühl [c], Isabel Esteve [d], Gerard Muyzer [f], Pierre Caumette [a], Robert Duran [a,*]

[a] *Laboratoire d'Ecologie Moléculaire EA 3525, Université de Pau et des Pays de l'Adour, avenue de l'Université, BP 1155, F-64013 Pau Cedex, France*
[b] *Department of Environmental Chemistry (ICER-CSIC), E-08034 Barcelona, Spain*
[c] *Marine Biological Laboratory, Institute of Biology, University of Copenhagen, DK-3000 Helsingør, Denmark*
[d] *Department of Genetics and Microbiology, Autonomous University of Barcelona, E-08193 Bellaterra, Spain*
[e] *Royal Netherlands Institute of Sea Research, Texel, The Netherlands*
[f] *Department of Biotechnology, Delft University of Technology, NL-2628 BC Delft, The Netherlands*

Received 20 October 2003; received in revised form 19 April 2004; accepted 13 July 2004

First published online 20 August 2004

Abstract

A photosynthetic microbial mat was investigated in a large pond of a Mediterranean saltern (Salins-de-Giraud, Camargue, France) having water salinity from 70‰ to 150‰ (w/v). Analysis of characteristic biomarkers (e.g., major microbial fatty acids, hydrocarbons, alcohols and alkenones) revealed that cyanobacteria were the major component of the pond, in addition to diatoms and other algae. Functional bacterial groups involved in the sulfur cycle could be correlated to these biomarkers, i.e. sulfate-reducing, sulfur-oxidizing and anoxygenic phototrophic bacteria. In the first 0.5 mm of the mat, a high rate of photosynthesis showed the activity of oxygenic phototrophs in the surface layer. Ten different cyanobacterial populations were detected with confocal laser scanning microscopy: six filamentous species, with *Microcoleus chthonoplastes* and *Halomicronema excentricum* as dominant (73% of total counts); and four unicellular types affiliated to *Microcystis*, *Chroococcus*, *Gloeocapsa*, and *Synechocystis* (27% of total counts). Denaturing gradient gel electrophoresis of PCR-amplified 16S rRNA gene fragments confirmed the presence of *Microcoleus*, *Oscillatoria*, and *Leptolyngbya* strains (*Halomicronema* was not detected here) and revealed additional presence of *Phormidium*, *Pleurocapsa* and *Calotrix* types. Spectral scalar irradiance measurements did not reveal a particular zonation of cyanobacteria, purple or green bacteria in the first millimeter of the mat. Terminal-restriction fragment length polymorphism analysis of PCR-amplified 16S rRNA gene fragments of bacteria depicted the community composition and a fine-scale depth-distribution of at least five different populations of anoxygenic phototrophs and at least three types of sulfate-reducing bacteria along the microgradients of oxygen and light inside the microbial mat.

Keywords: Bacterial community composition; Biomarkers; Confocal microscopy; Microbial mat; Microsensors; Bacterial diversity

1. Introduction

Photosynthetic microbial mats develop at the water–sediment interface in shallow environments such as

* Corresponding author. Tel.: +33 5 5940 7468; fax: +33 5 5940 7494.
E-mail address: robert.duran@univ-pau.fr (R. Duran).

0168-6496/$22.00
doi:10.1016/j.femsec.2004.07.012

estuaries [1,2], sheltered sandy beaches [3,4], or hypersaline salterns [5,6]. Most of these microbial mats are formed of horizontally stratified, multicolored and cohesive thin layers of several functional groups of microorganisms, such as cyanobacteria, colorless sulfur bacteria, purple sulfur bacteria and sulfate-reducing bacteria, distributed along vertical microgradients of oxygen, sulfide and light [7,8].

Hypersaline mats from salterns represent interesting ecosystems adapted to fluctuating salinity conditions. Microbial mats existing in the most hypersaline ponds of the salterns of Salins-de-Giraud (Camargue, French Mediterranean coast) have been described in ecological and microbiological, and recently molecular studies over the last 10 years [5,9–11]. These saline ponds with water salinity between 150‰ and 300‰ (w/v) contain microbial mats similar to those previously described in other hypersaline habitats [6,12]. They are formed of an upper layer of cyanobacteria belonging to the genus *Phormidium*, covering a purple layer of phototrophic bacteria mainly composed of members of the genera *Halochromatium* [13] and *Halothiocapsa* [14], well adapted to such high salinities. Molecular studies [9] showed that the bacterial composition of these mats was more diverse than expected both in Bacterial and in Archaeal groups.

In the present study, we investigated another mat from the same salterns growing in ponds with lower salinity (70–150‰ (w/v)). This mat developed over several decades in large areas used by the Saltern Company as water reservoirs for salt production. The aim of this analysis was to characterize the composition of the functional bacterial groups developing in the Camargue microbial mat. The simultaneous use of different methods for analysis of bacterial composition and microenvironment, allowed a precise in situ analysis of the Camargue mat. In the mat, the major bacterial groups were investigated by characteristic biomarkers, confocal laser scanning microscopy (CLSM), denaturing gradient gel electrophoresis (DGGE) and terminal-restriction fragment length polymorphism (T-RFLP) analysis of PCR amplified 16S rRNA genes or functional gene fragments. In order to understand the bacterial occurrence and distribution at the microscale level, all the microbiological results were related to microenvironmental gradients determined by in situ microsensor measurements.

2. Materials and methods

2.1. Sampling site description

The sampling site was in a very large shallow pond at the saltern of Salins-de-Giraud, close to the sand barrier and the sea coast (43°27′35″ N, 04°41′28″ E, Camargue, France). This pond was used for the storage of pre-concentrated seawater. In this pond of about 10 km^2 area, the water column never exceeded 20 cm depth and its salinity ranged from 70‰ to 150‰ (w/v). The photosynthetic microbial mat covered a large proportion of this pond and also of other adjacent ponds, and was constituted of thin laminated cohesive layers. Due to its development over several decades, the mat was about 5–10 cm thick. The underlying sediment was mostly composed of a mixture of sand and clay.

2.2. Sampling procedure

All mat samples analyzed were collected in May 2000, by mean of plexiglass cores. For biomarker analysis, mat cores of 26 mm inner diamater were immediately frozen until further analysis. For confocal laser scanning microscopy, two cores (18 mm i.d.) were transferred into small plastic tubes containing 2.5% (v/v) glutaraldehyde in phosphate buffer (0.2 M, pH 7.4, adjusted to the appropriate salinity with NaCl), and stored at 4 °C until further processing. For DGGE and T-RFLP, the upper 10 mm of the mat cores (35 mm i.d.) were sliced off aseptically, transferred to sterile Petri dishes, frozen in liquid nitrogen, and then stored at −80 °C.

2.3. Microsensor measurements of O_2 and oxygenic photosynthesis profiles

Depth profiles of O_2 and gross oxygenic photosynthesis were measured in May 2000. Microsensor measurements were done in situ from a small measuring platform placed above the mat. A Clark-type O_2 microsensor [15] connected to a picoammeter (UniSense A/S, Aarhus, Denmark) was manually operated with a micromanipulator (Märzhäuser, Wetzlar, Germany) mounted on a heavy solid stand. Microsensor signals were recorded with a strip battery-operated chart recorder (Servogor, Leeds, UK) operated via batteries. The O_2 microsensor had a tip diameter of 6 μm, a stirring sensitivity of ∼2% and a response time, t_{90}, of 0.2 s. The O_2 microsensor was linearly calibrated on site from readings of microsensor current in the overlying water and in the anoxic part of the mat (2% O_2). Dissolved O_2 concentrations in the overlying water were determined by Winkler titration [16]. Experimental light–dark shifts for in situ measurements of oxygenic gross photosynthesis [17] were performed with a custom-made, light-impermeable box, which was deployed by avoiding physical contact with the sensor and thus disturbance of microsensor readings.

2.4. Spectral scalar irradiance measurements with fiber-optic microprobes

Mat samples were collected in February 2001 for spectral scalar irradiance measurements under controlled conditions in a laboratory. Due to the time difference

between the sampling times (May 2000 for all other analyses), some seasonal changes in the small-scale vertical location of the different photosynthetic microorganisms in the mat cannot be excluded, despite a similar macroscopic appearance of the mat at both times. For spectral light measurements, a fiber-optic scalar irradiance microprobe [18], was connected to a sensitive fiber-optic diode array spectrometer with a spectral range of 250–950 nm (PMA-11, Hamamatsu Photonics, Toyooku, Japan). Profiles of spectral scalar irradiance were measured in the mat by stepwise inserting the microprobe with a motor-driven micromanipulator (Märzhäuser, Eugene, USA) at a zenith angle of 140° relative to the incident light beam. The downwelling spectral scalar irradiance at the mat surface was measured by positioning the scalar irradiance microprobe over a black light trap at the same position relative to the incident light as the mat surface. Scalar irradiance spectra in the mat were normalized to the downwelling spectral scalar irradiance at the mat surface. Attenuation spectra of scalar irradiance were calculated over discrete depth intervals from the scalar irradiance profiles according to Kühl and Fenchel [19].

2.5. Analysis of fatty acids, hydrocarbons, alcohols and alkenones

The microbial mat samples were extracted after homogenization with methanol, dichloromethane and *n*-hexane. Fatty acids were separated from the extracts after saponification. Afterwards the neutral lipids were fractionated by column chromatography with silica and alumina into different compound classes. Hydrocarbons and polar fractions were analyzed by gas chromatography (GC) and gas chromatography mass spectrometry (GC-MS) after derivatisation. The methodology was described in detail recently by Wieland et al. [4].

2.6. Confocal laser scanning microscopy

The mat samples were analyzed with a microscope (Olympus BH2, Tokyo, Japan) and a confocal laser-scanning microscope (Leica TCS 4d, Heidelberg, Germany) equipped with an argon–krypton laser. For confocal analysis, slices of defined dimensions were placed on cavity slides, sealed with cover slips and observed under an excitation beam of 568 nm. Pigment fluorescence emission was detected with a 590 nm long pass filter. Different 512×512 pixel confocal images in two (optical sections) and three-dimensions (sum of projections and stereoscopic images) were obtained from these samples. The cyanobacteria were identified using different morphological criteria according to Castenholz [20], i.e. diameter (μm), cell division patterns, and the presence or absence of a sheath for unicellular morphotypes. Presence of septation and gas vacuoles was also considered for filamentous cyanobacteria. In addition, the abundance of each cyanobacterial genera was determined by counting the different morphotypes obtained from CLSM images. A total of 663 filamentous and 237 unicellular cyanobacteria were analyzed.

2.7. DGGE analysis

Genomic DNA was extracted from the mat samples using the UltraClean Soil DNA Isolation Kit (Mobio Laboratories, Carlsbad, USA) according to manufacturer's instructions. Serial dilutions of genomic DNA (up to 10^{-4}) were made in sterile water and stored at −20 °C. To specifically amplify the 16S rRNA gene fragments of oxygenic phototrophs, 1 or 2 μl of the DNA dilutions were used as templates in 50 or 100 μl PCR reactions using primer pair CYA359F + GC/CYA781R and PCR conditions as described by Nübel et al. [21]. The two different reverse primers CYA781RA and CYA781RC were added in separate PCR reactions. DGGE was performed according to Schäfer and Muyzer [22] with conditions optimized for the oxygenic phototroph specific PCR fragments [21], on 1 mm thick 6% acrylamide/bisacrylamide gels with urea-formamide (UF) gradient of 20–80%. On top of the gradient gel, an acrylamide gel without UF was cast to obtain loading slots. Gels were run in TAE (40 mM Tris-acetate pH 8.5, 1 mM EDTA) buffer for 3.5 h at 200 V and at a constant temperature of 60 °C. Subsequently, the gels were stained in an ethidium bromide solution (0.5 $\mu g\,ml^{-1}$) and inspected under UV illumination using a Fluor-S Multi Imager (Bio-Rad, Hercules, USA). Contrast and brightness of the photographs were optimized using Adobe PhotoShop software (Adobe, San Jose, USA). DNA fragments separated by DGGE were excised from the gel [23], re-amplified, purified using the Qiaquick gel extraction kit (Qiagen, Hilden, Germany), and then sequenced. Purified bands were sequenced in two directions using the BigDye Terminator cycle sequencing kit (Applied Biosystem, Foster City, USA) on an ABI PRISM 310 genetic analyzer (Applied Biosystem). Close relatives to consensus sequences were searched in the GenBank Database maintained by the NCBI using BLAST search [24]. Subsequently, new sequences and their closest relatives were added to the ARB database [25] and aligned using the automatic alignment tool. Alignments were then checked and corrected manually taking the alignments of oxygenic phototrophs that were already in the ARB database as templates. Phylogenetic analysis was performed in ARB using several different algorithms (e.g., maximum parsimony, neighbour-joining, maximum likelihood) to check the consistency of the tree structure. All three methods gave similar topology. Neighbour joining was used to draw the phylogenetic tree. The GenBank accession numbers of each

partial 16S rRNA gene clone (SdG1 to SdG7) are AY393850 to AY393856.

2.8. T-RFLP analysis

The upper 2 mm of the mat cores were sliced into 200 μm sections with a cryomicrotome (MICROM GmbH, Walldorf, Germany), and from the third mm into 500 μm section for vertical depth resolution. The mat slices were ground together with liquid nitrogen in a mortar with a pestle and genomic DNA was extracted using the UltraClean Soil DNA isolation kit (MoBio Laboratories, Carlsbad, USA) according to the manufacturer. All extracted genomic DNA samples were stored at −20 °C until further processing. T-RFLP analysis was performed with different primer sets, 8f–926r [26,27], 8f–SRB385 [28], and pb557f–pb750r [29], according to the experimental conditions described in Wieland et al. [4]. Respectively, these primer sets targeted the whole bacterial community, the sulfate-reducing bacteria (SRB), and the phototrophic anoxygenic bacteria (PAB). Restriction enzymes used in T-RFLP analysis were *Hae*III and *Rsa*I (New England Biolabs, Beverly, UK), for analysis of the entire bacterial diversity, and *Hae*III and *Hin6*I for the SRB and PAB. Triplicates for each layer were analyzed to avoid analytical artifacts and assure the reproducibility of the method. Dominant terminal restriction fragments (T-RFs) over 100 fluorescent units in intensity and present in each replicate sample were selected. The size of each T-RF was determined according to molecular weight standard TAMRA 500 (Applied Biosystem) with an acceptable error of ±1 bp. From T-RF values, genus or species identification were made by predicted digestions using the TAP-TRFLP program of the RDP (Ribosomal Database Project) web site (http://rdp.cme.msu.edu/) [30]. T-RFLP profiles were normalized by calculating relative abundances of each T-RFs from height fluorescence intensity. Combining data from each restriction enzyme, we compared normalized T-RFLP profiles by correspondence factorial analysis (CFA).

2.9. Correspondence factorial analysis

CFA is an ordination method by similarity matrix that reduces in two or three dimensions the dispersion diagram of samples compared (in this case T-RFLP profiles). Axes correspond to synthetic variables (T-RFs) and their influence (percent relative abundance) in the distribution of samples analyzed [31]. Using CFA, two-dimensional plots were prepared, showing variance within data sets on a series of axes. To clearly present the results two graphs were constructed using MVSP v3.12d software (Kovach Computing Service, Anglesey, Wales) [32]. One graph was constructed for T-RFs (or OTUs, operational taxonomic units) and the other for layers using the same axis.

The fact that some samples do not appear in the CFA graph is due to insufficient DNA yield for some analyses.

3. Results

3.1. Description and environmental conditions of the microbial mat

3.1.1. Structure of the microbial mat

The microbial mat was composed of three distinct colored layers. An upper, approximately 2 mm thick, brown–green colored layer was composed of filamentous cyanobacteria morphologically related to the genus *Microcoleus*, and of unicellular cyanobacteria similar to the form genus *Synechocystis*. Under this dense cyanobacterial layer, an ∼1 mm thick purple layer was composed of purple non-sulfur bacteria morphologically resembling members of Rhodospirillaceae and Chromatiaceae families (R. Guyoneaud, personal communication). Beneath these two layers a black zone of more than 1 cm occurred with iron sulfide precipitates, indicating intense sulfate-reduction activity. The physical and chemical parameters measured in the sampling site (Table 1) were generally constant.

Table 1
Comparison of physical and chemical parameters in the water column of the sampling site measured at 15 h each day of sampling

Dates	Temperature (°C)	O_2 (μmol l^{-1})	Redox (mV)	pH	Salinity (‰)
23.05.00	20	17.0 ± 0.1	+3[a] ± 1 −4[b] ± 1	8.39 ± 0.02	103 ± 1
25.05.00	23	ND	+90[a] ± 1 ND[b]	8.50 ± 0.02	75 ± 1

ND, not determined.
[a] Surface.
[b] 10 mm depth.

3.1.2. Depth profiles of O_2, gross photosynthesis, and spectral scalar irradiance

High O_2 consumption in the mat led to a low O_2 concentration and O_2 penetration in situ during the night (5:32 h, 17 °C, 94‰ (v/w)), confining the oxic zone to the top 0.2 mm of the mat (Fig. 1). In the afternoon (15:50 h, 30 °C, 100‰ (v/w)), high rates of oxygenic photosynthesis led to a strong increase in O_2 concentration both in the overlying water and within the mat. The O_2 penetration depth in the mat increased to 2 mm. Gross oxygenic photosynthesis was measurable in the top 0.6 mm of the mat with a peak in photosynthetic activity at 0.3–0.6 mm depth. An important photosynthetic activity at 0.3–0.6 mm depth indicated the presence and/or activities of oxygenic phototrophs in the upper mat layers.

From measured spectral scalar irradiance profiles, distinct spectral regions of pronounced absorption could be ascribed to the presence of different pigments (Fig. 2, upper graph). The presence of cyanobacteria led to pronounced scalar irradiance minima at around 630 and 680 nm, corresponding to phycocyanin and chlorophyll *a* (Chl *a*) absorption, respectively. The scalar irradiance minima in the region between 800 and 900 nm corresponds to bacteriochlorophyll *a* (Bchl *a*) absorption, indicating the presence of purple bacteria. A shoulder at 740–750 nm indicated some absorption by Bchl *c* present in green photosynthetic bacteria. In the spectral region of 400–550 nm, scalar irradiance was strongly attenuated due to Chl *a* and carotenoid absorption.

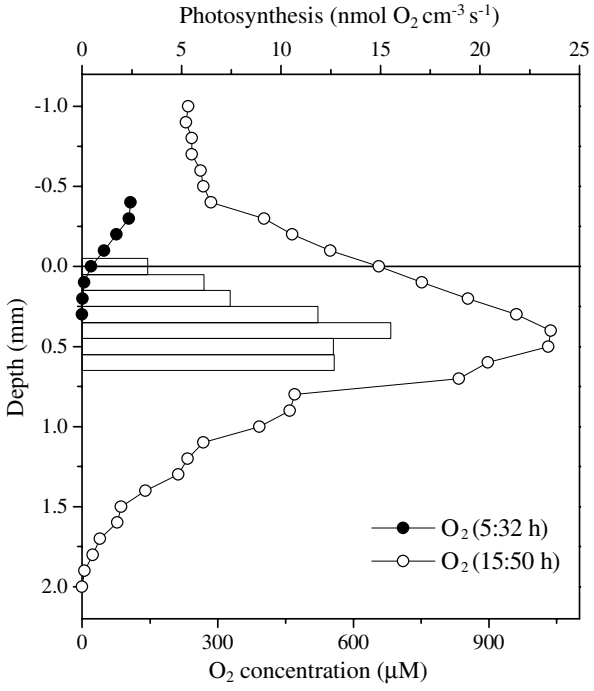

Fig. 1. In situ depth profiles of O_2 and gross photosynthesis (bars) measured during the afternoon (15:50 h) and night (5:32 h) in mats from a pre-concentration pond of the Salins-de-Giraud saltern.

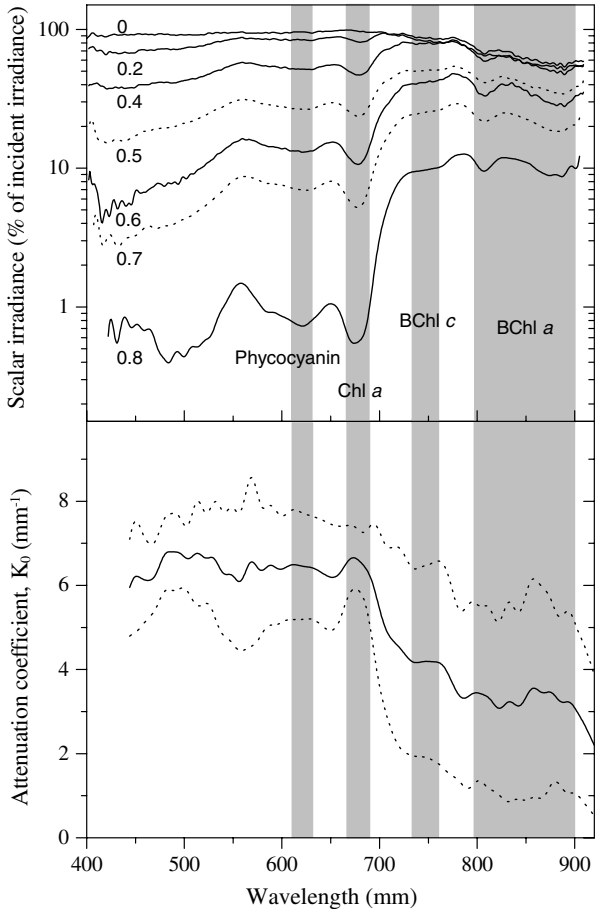

Fig. 2. Depth profiles of spectral scalar irradiance in the Camargue mat normalized to the downwelling spectral scalar irradiance at the mat surface (upper graph). Numbers indicate depth (mm). Average attenuation spectrum of scalar irradiance over the depth interval of 0–0.8 mm (lower graph), calculated from the profile shown in the upper graph. Broken lines indicate the standard deviations of the attenuation coefficients, K_0.

Absorption by Chl *a*, phycocyanin, Bchl *a*, and Bchl *c* occurred in all mat layers within the top 0.8 mm of the mat, indicating a homogeneous distribution of these photosynthetic groups. However, the spectral scalar irradiance in the wavelength regions of Chl *a*, phycocyanin and carotenoid absorption were more strongly attenuated than wavelengths corresponding to Bchl *a* and Bchl *c* absorption (Fig. 2, lower graph), indicating as expected a dominance of cyanobacteria in the surface layer of the mat.

3.2. Bacterial community composition in the top active layers of the microbial mat

3.2.1. Bacterial community composition estimated by biomarkers

Fatty acids were the major lipid compounds found in the microbial mat. Their distribution essentially encompassed C_{14}–C_{22} homologues, namely *n*-hexadec-9(Z)-enoic, *n*-hexadecanoic, *n*-octadec-9(Z)-enoic,

n-octadec-11(Z)-enoic, *iso*-pentadecanoic and *anteiso*-pentadecanoic acids (Fig. 3(a)), typically representative of algal and bacterial communities [33,34].

Cyclopropylnonadecanoic acid was also a major compound in the distribution of fatty acids. This compound is abundant in purple phototrophic bacteria such

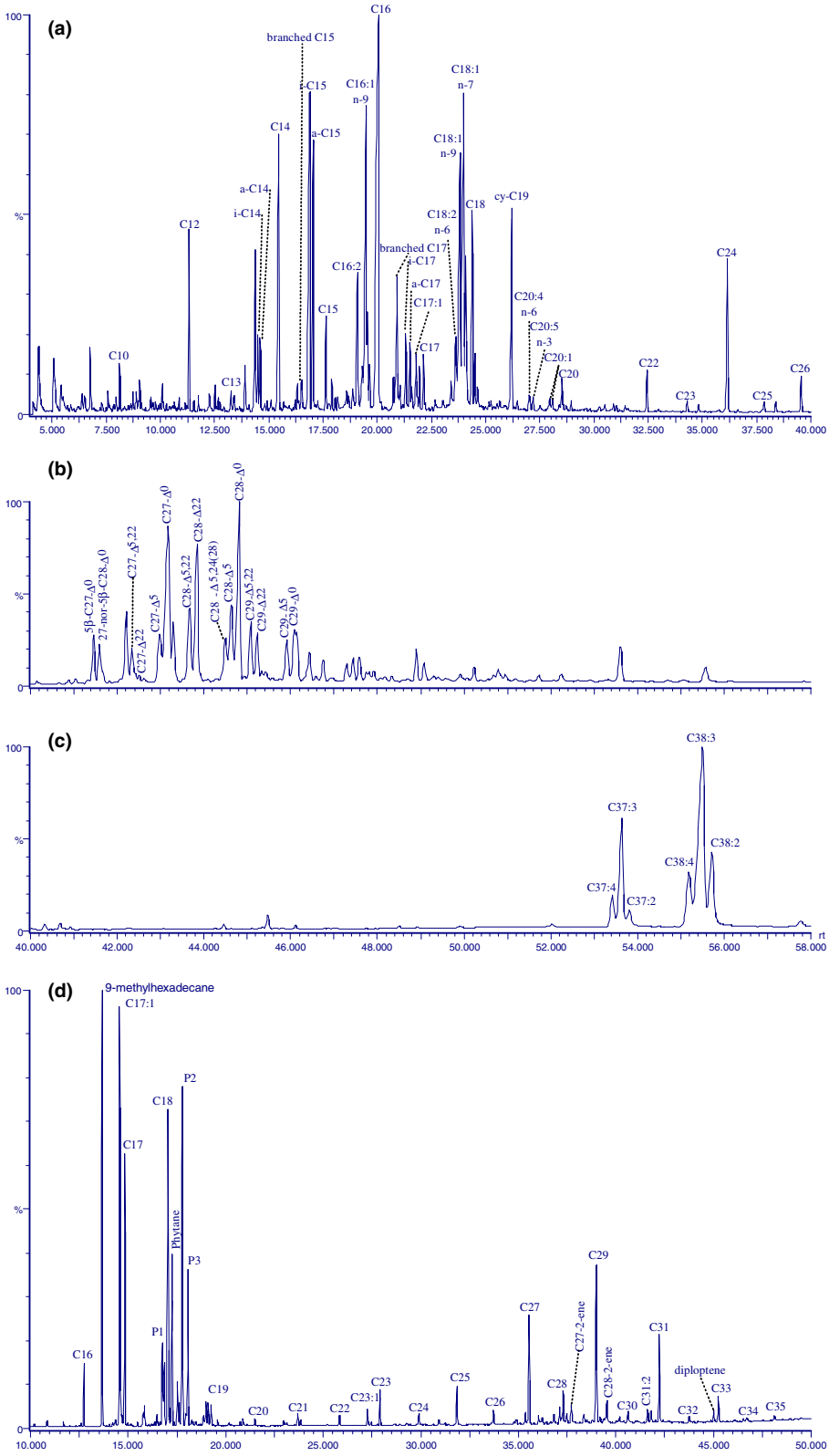

Fig. 3. Gas chromatographic profiles showing the major (a) fatty acids, (b) alcohol and (c) alkenone fractions, (d) hydrocarbons (P1, P2, P3 phytenes) from Salins-de-Giraud microbial mat.

as *Rhodobacter* and *Ectothiorhodospira* where it occurs together with significant amounts of *n*-octadec-11(Z)-enoic acid [35]. *Iso*- and *anteiso*-pentadecanoic acids are abundant in SRB and sulfur-oxidizing bacteria such as *Thiomicrospira* [35]. The high abundance of *iso*- and *anteiso*-pentadecanoic acids, as well as of cyclopropyl-nonadecanoic and *n*-octadec-11(Z)-enoic acids likely reflects the dominance of two different populations exchanging hydrogen sulfide, which could be sulfate-reducing and purple phototrophic bacteria, respectively.

n-Heptadecane and *n*-heptadecenes were the main hydrocarbons (Fig. 3(c)). These compounds are generally found in cyanobacteria [36,37] or in phototrophic eukaryota [38]. Other hydrocarbons specific of cyanobacterial inputs, such as 9-methylhexadecane, were also found in major proportions, indicating the dominance of cyanobacteria in this mat.

The sterol distribution of this mat showed minor proportions of sterols having the unsaturated positions at Δ^5, Δ^{22} and $\Delta^{5,22}$ (Fig. 3(b)), which could originate from cyanobacteria [37,39,40], Chlorophyta [41,42], or diatoms [42–44]. However, the common diatom marker 24-methylcholesta-5,24(28)-dien-3β-ol [42–44] was only found in minor proportion.

Phyt-1-ene, which occurred together with other phytene homologues, also constituted one of the major hydrocarbon groups (Fig. 3(d)). These hydrocarbons are characteristic for methanogenic bacteria [45].

3.2.2. Diversity of oxygenic phototrophs

Confocal laser scanning microscopy and molecular techniques were used to identify the cyanobacteria of the Camargue microbial mat. Using CLSM, both filamentous and unicellular cyanobacteria were found in the mat (Table 2 and Fig. 4). Filamentous types were the most abundant, accounting for 73.6% of the total cyanobacteria present (Table 2). *Microcoleus chthonoplastes* (Fig. 4(b)) dominated the filamentous cyanobacterial community, as typically found in hypersaline mats [1,46,47]. *Halomicronema excentricum*, characterized by thin filaments and cylindrical shape (less than 1 μm wide trichomes) (Fig. 4(c)) [48], and another filamentous cyanobacterium (Fig. 4(c)) with thin filaments and short trichomes that could not be identified, were the second most frequent filamentous cyanobacteria. *Leptolyngbya* sp., *Limnothrix* sp. and *Pseudanabaena* sp. filaments detected in this study at abundances of 9.9% and 6.6%, respectively, have also been found in other mats as well, e.g. from the Ebro delta [1,46,47] and the Orkney Islands [4]. Unicellular cyanobacteria *Chroococcus* sp., *Microcystis* sp. and members of *Synechocystis* (Fig. 4(d)) and *Gloeocaspsa* groups represented 26.4% of the total cyanobacteria in the Camargue mat (Table 2).

In addition to CLSM analysis, a molecular approach was used to describe the oxygenic phototroph community composition. PCR amplified 16S rRNA gene products specific for cyanobacteria, were separated by DGGE. Fifteen different bands were counted, and the major bands were excised from the gel (bands 1–7 in Fig. 5(a)) and retrieved for DNA sequencing. In combination with CLSM, phylogenetic analysis of these sequences (SdG1 to SdG7 in Fig. 5(b)) showed that the pristine hypersaline Camargue mat was dominated by the filamentous cyanobacteria: genera *Microcoleus* (SdG5 and SdG6), *Oscillatoria* (SdG3) and *Leptolyngbya* (SdG7 in Fig. 5(b)). Other cyanobacteria composing this mat were related to the unicellular *Pleurocapsa* sp. (SdG1), *Calotrix* sp. (SdG4), and *Phormidium* sp. (SdG2).

3.2.3. Bacterial community structure at a microscale level

The organization and composition of the bacterial community in the mat was investigated by T-RFLP

Table 2
Morphological identification of cyanobacteria in microbial mats of Salins-de-Giraud by CLSM according to Castenholz [20], and their relative abundances

Microorganisms	Diameter (μm)	Septation	Gas vacuole	Sheath	Cell division	Abundance (%)
Filamentous cyanobacteria						
Microcoleus chthonoplastes	3.13–3.75	+	–	+	Perpendicular division	20.8
Halomicronema excentricum	0.96	+	–	+	Perpendicular division	13.2
Unidentified	<1.25 (short filaments)	+	–	+	Perpendicular division	13.2
Leptolyngbya sp.	<1 (large filaments)	+	–	+	Perpendicular division	9.9
Limnothrix sp.	1.25	+	–	+	Perpendicular division	9.9
Pseudanabaena sp.	2.5	+	+	+	Perpendicular division	6.6
Unicellular cyanobacteria						
Synechocystis-group (marine cluster)	3.5 × 3.5	–	–	+ (thin)	2 or 3 planes	6.6
Gloeocapsa-group	4 × 14	–	–	+	2 or 3 planes	6.6
Chroococcus sp.	19 × 28	–	–	+	2 planes	6.6
Microcystis sp.	1.9 × 1.9	–	–	+	Binary fission in different planes	6.6

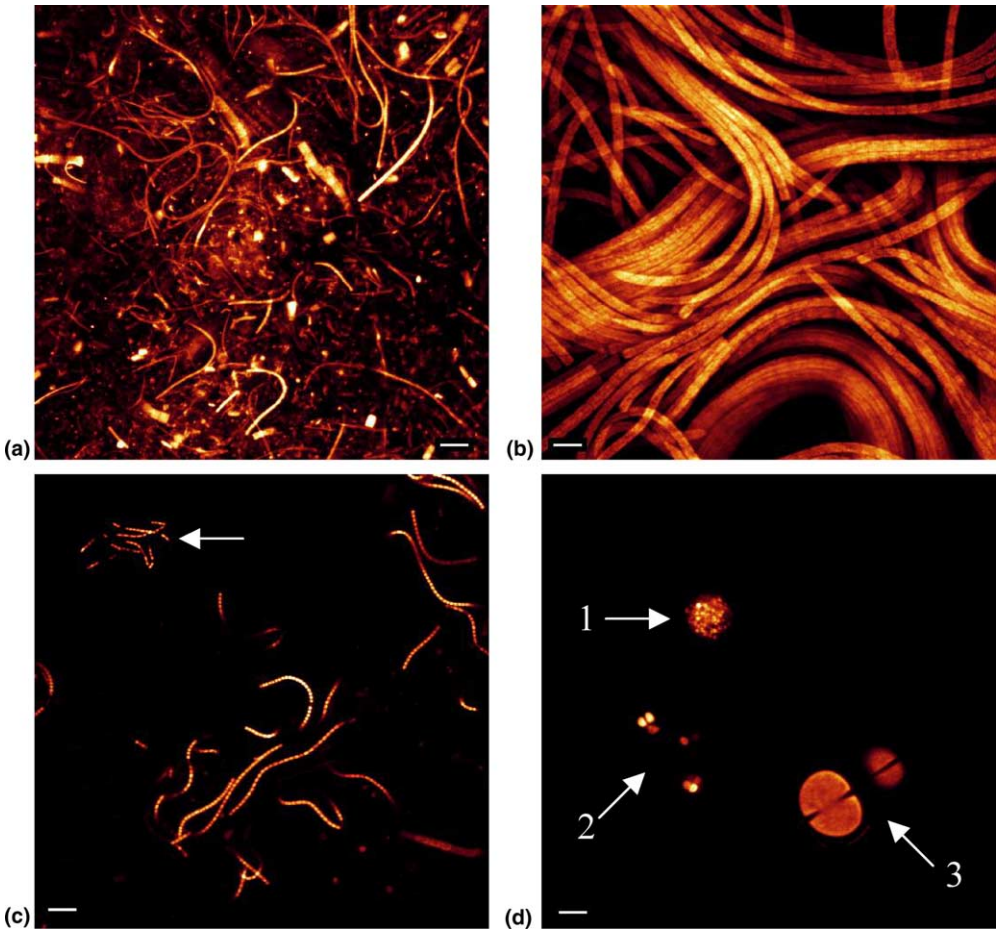

Fig. 4. CLSM images in Salins-de-Giraud microbial mat. (a) *Leptolyngbya* sp., (b) *Microcoleus chthonoplastes,* (c) *Halomicronema excentricum* and the unidentified filaments (indicated by arrow), (d) 1. *Microcystis* sp., 2. *Synechocystis*-group., 3. *Chroococcus* sp. (c) and (d) images are photographic compositions. Scale bar = 10 μm.

using the eubacterial primer set 8f-926r [26,27], targeting a partial sequence of the 16S rRNA gene. For each microlayer within the top 3 mm of the mat, and of the underlying layer, characteristic T-RFLP profiles (approximately 35 T-RFs with *Hae*III digestion) were obtained (data not shown). A CFA combining the data from *Hae*III and *Rsa*I T-RFLP profiles revealed a particular distribution in three zones: a surface layer (0–0.2 mm), a large mid layer (0.2–3 mm), and a deeper region (underlying layer) (Fig. 6(a)). This distribution was mostly explained by the first axis (27.8%) particularly for the deep third millimeter. Plots of T-RFs in Fig. 6(b) showed that T-RF 58 bp (*Rsa*I), presumably *Desulfomicrobium baculatum,* and T-RFs 205 and 244 pb (*Hae*III), presumably members of the genera *Desulfobulbus* and *Streptomyces* respectively, were dominant in this deeper zone. In contrast, the structure of the surface mat (0–0.2 mm) was explained by the second axis (11.8%, Fig. 6(a)), which was influenced by T-RFs of 125 bp (*Rsa*I digest), 200 and 297 bp (*Hae*III digest) (Fig. 6(b)). These T-RFs that match members of the *Neisseria, Chloroflexus* and*Mycoplasma* genera were particularly present in this surface layer.

SRB were accessed by T-RFLP using the specific primer pair 8f–385r [28], and two restriction enzymes *Hae*III and *Hin*6I. The CFA of this data set also showed a specific distribution of the SRB. Particularly, two distinct SRB communities were characteristic of the deeper layer (2.5–3 mm) and of the layer at 1.4–1.6 mm (Fig. 7(a)). This later layer seemed to be independent, since the first axis (40.7%) alone explained the distinct structure of the mid layer. Fig. 7(b) shows that this mid layer was characterized by many T-RFs. Among them, T-RFs of 200 and 270 bp (*Hae*III) that could be related to genera *Desulfovibrio* and *Desulfobacter*, respectively, were dominant. The composition of the third millimeter of the mat was essentially explained by the second axis (14.8%, Fig. 7(a)), which was influenced by many T-RFs (Fig. 7(b)). Among them, T-RFs of 72 and 197 bp (*Hae*III) and of 55 bp (*Hin*6I) were dominant. The

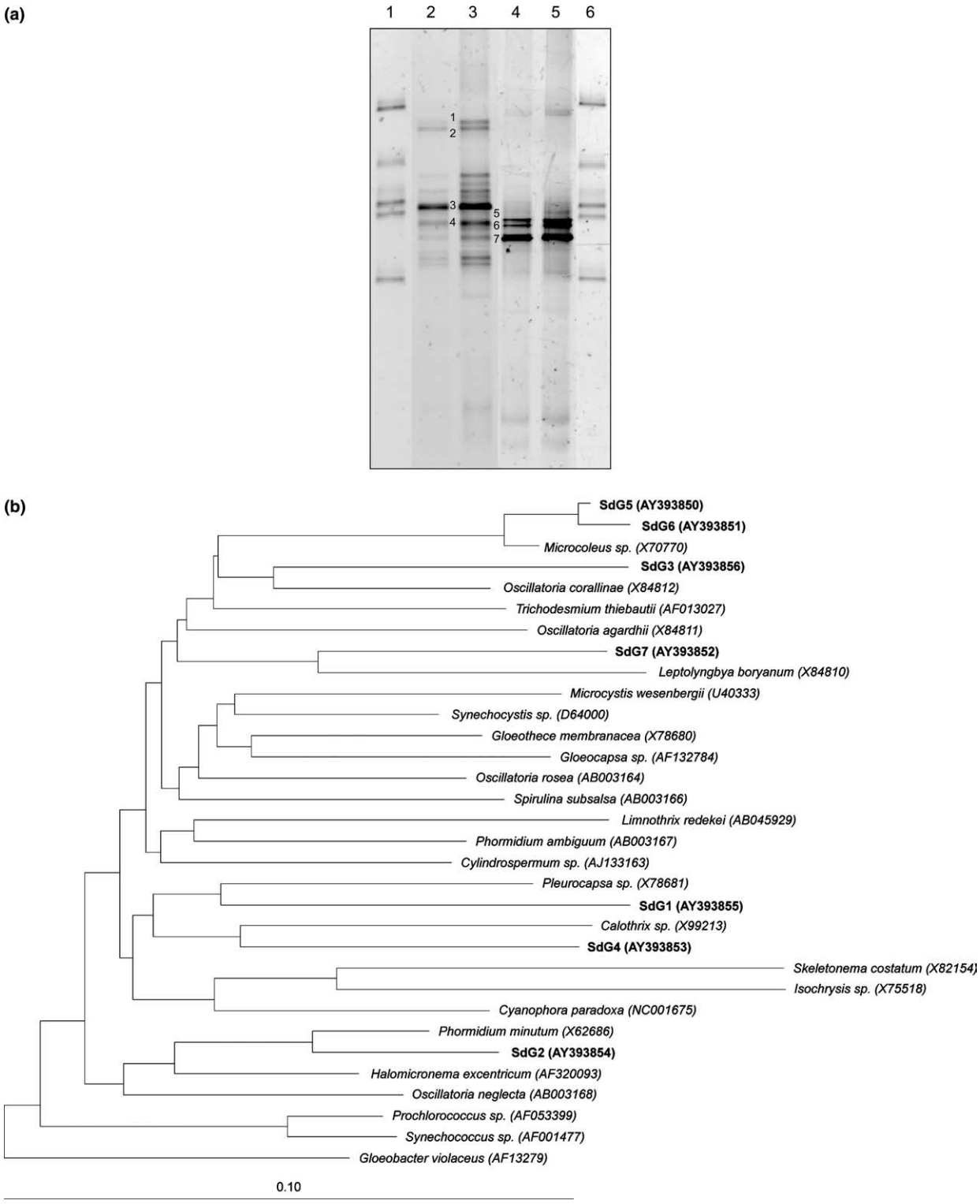

Fig. 5. (a) DGGE analysis of 16S rRNA gene fragments of oxygenic phototrophs. The PCR products were obtained with two different primer sets and genomic DNA from the microbial mat of Salins-de-Giraud (SdG). Lanes 1 and 6, marker fragments; lanes 2 and 3, PCR products obtained with primers CYA359F and GC/CYA781Rb; lanes 4 and 5 PCR products obtained with primers CYA359F + GC/CYA781Ra. 300 ng PCR product was loaded in each lane. The numbers in figures refer to bands that were excised from the gel, sequenced and used for phylogenetic analysis. (b) Neighbour-joining phylogenetic tree based on 16S rRNA gene sequence data showing the affiliation of predominant oxygenic phototrophs (i.e., cyanobacteria and diatoms) in the microbial mat of Salins-de-Giraud. Sequences determined in this study are shown in bold. The consistency of the tree structure was checked using several different algorithms. The sequences of *Thermus aquaticus* and *Chloroflexus aurantiacus* were used as the outgroup, but were pruned from the tree. The scale bar represents 10% estimated sequence divergence.

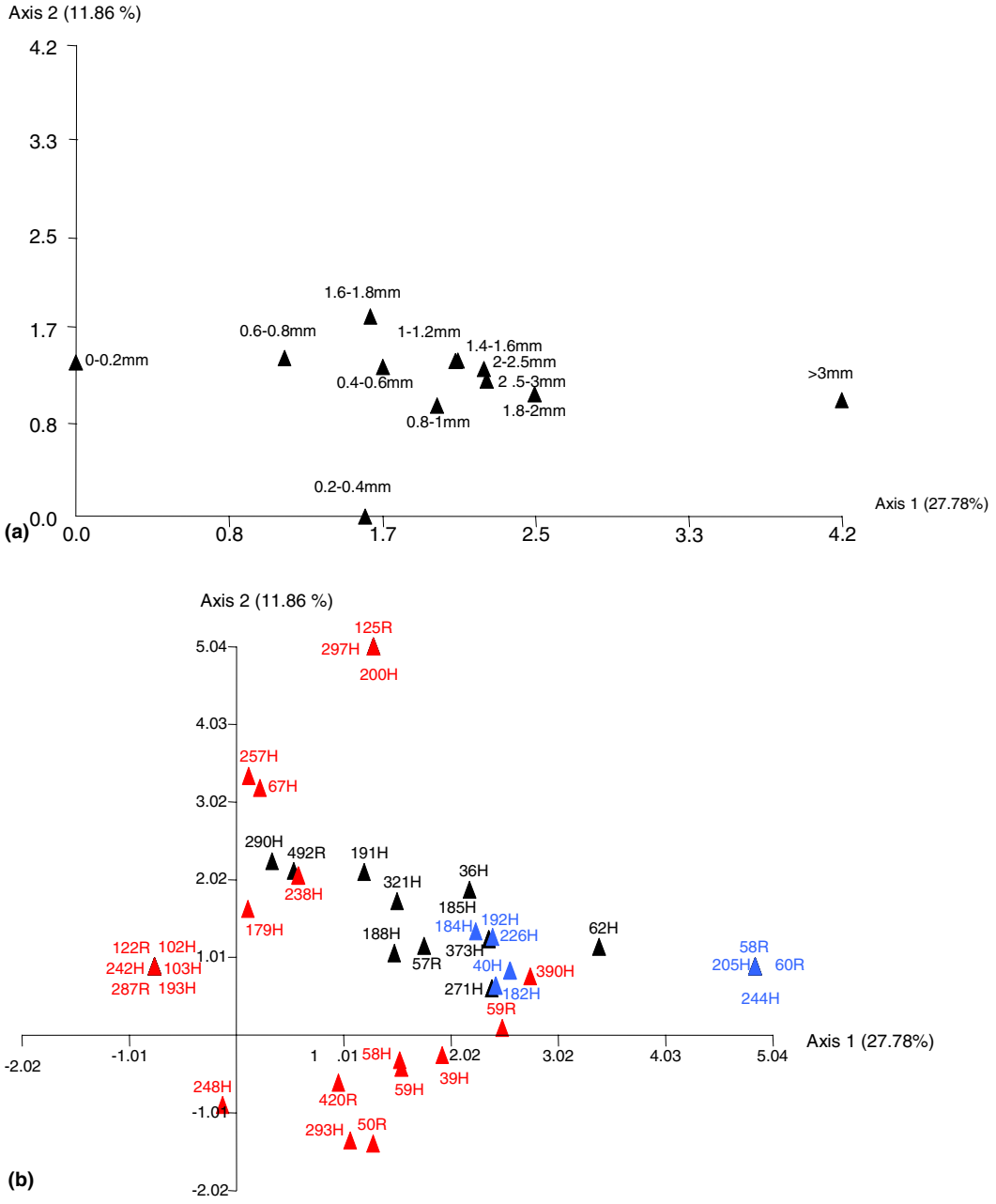

Fig. 6. CFA of the whole bacterial communities. (a) CFA of each layer of the 3 mm of Salins-de-Giraud microbial mat. Each black triangle was represented by a 5′ end T-RFLP pattern corresponding to the combined digests *Hae*III and *Rsa*I of the 16s rRNA genes. (b) CFA of variables, i.e., T-RFs derived from the CFA in panel (a). Each number corresponds to the T-RF length in base pairs. Letters H and R, after this number, correspond to *Hae*III and *Rsa*I T-RFs, respectively. Red and blue triangles correspond to T-RFs specific from the oxic (<2 mm) and anoxic zone (>2 mm) of the mat, respectively. Black triangles correspond to T-RFs non-specific from the mat zonation.

T-RF of 72 bp may possibly represent some *Desulfovibrio* communities.

In addition to SRB communities, the PAB were also investigated in the same layers. Their presence in the mat was detected with the primer pair pb557f–pb750r [29], targeting the *pufM* gene, which encodes a subunit of the photosynthetic center of purple sulfur and non-sulfur bacteria. CFA on T-RFLP patterns of these PAB communities revealed their organization in five layers through the top 3 mm of the mat (Fig. 8(a)). The distribution of the layers from 0.2 to 0.4 mm and from 0.4 to 1.8 mm was explained by the first axis (38.4%) corresponding to T-RF (199 pb, *Hae*III) possibly related to *Halochromatium salexigens* (Fig. 8(b)). The three other layers, from 0 to 0.2 mm, from 1.8 to 2 mm, and from 2.5 to 3 mm, were mostly influenced by the second axis

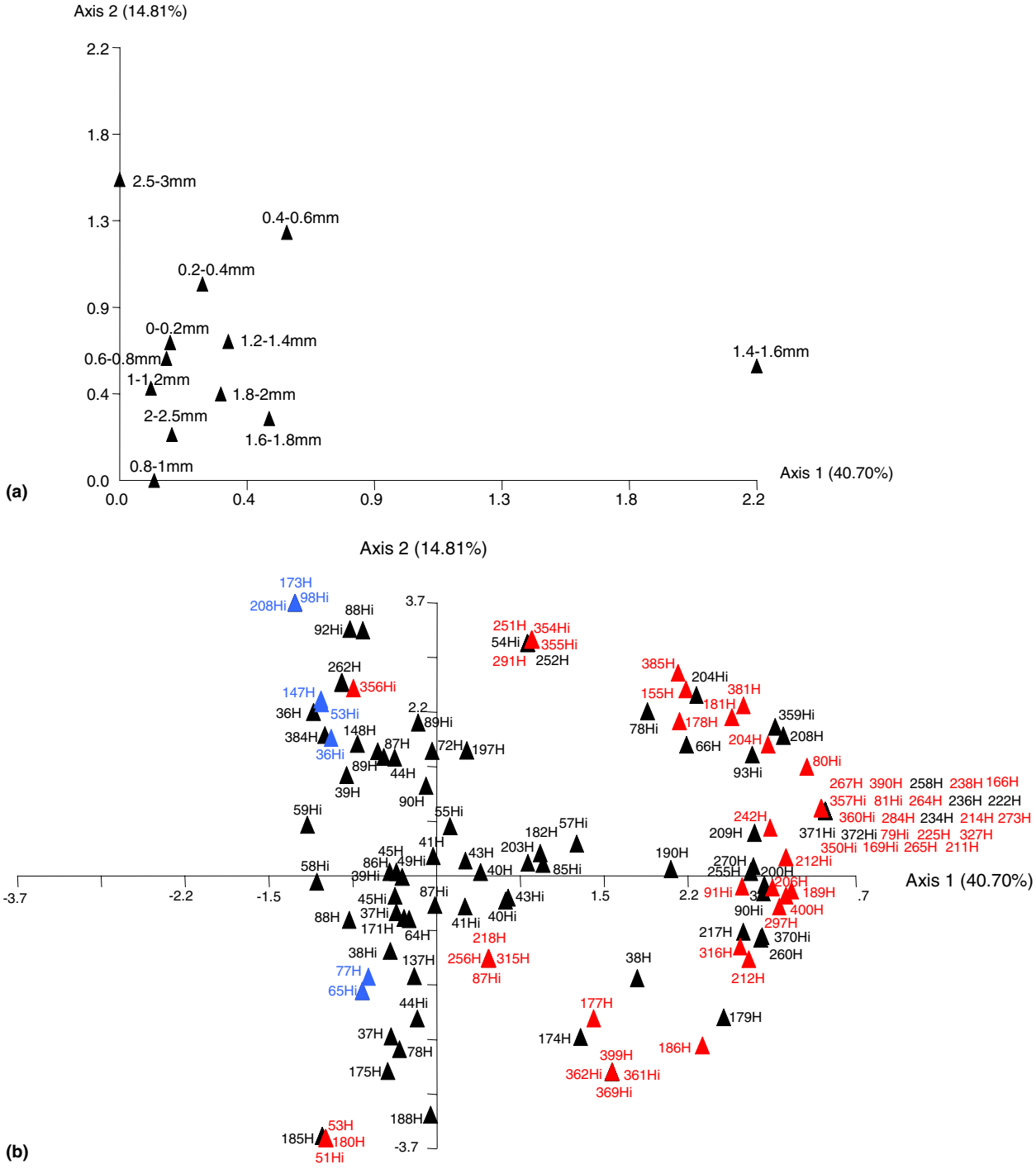

Fig. 7. CFA of the sulfate-reducing communities. (a) CFA of each layer of the 3 mm of Salins-de-Giraud microbial mat. Each black triangle was represented by a 5′ end T-RFLP pattern corresponding to the combined digests *Hae*III and *Hin*6I of the 16s rRNA genes. (b) CFA of variables, i.e., T-RFs derived from the CFA in panel (a). Each number corresponds to the T-RF length in base pairs. Letters H and Hi, after this number, correspond to *Hae*III and *Hin*6I T-RFs, respectively. Red and blue triangles correspond to T-RFs specific from the oxic (<2 mm) and anoxic zone (>2 mm) of the mat, respectively. Black triangles correspond to T-RFs non-specific from the mat zonation.

(12%). The CFA plots (Fig. 8(b)) showed that this second axis was explained mainly by the presence of the major T-RF of 137 bp (*Hin*6I) potentially corresponding to *Roseospira marina*.

4. Discussion

The investigated photosynthetic microbial mat showed a spatial distribution of different functional

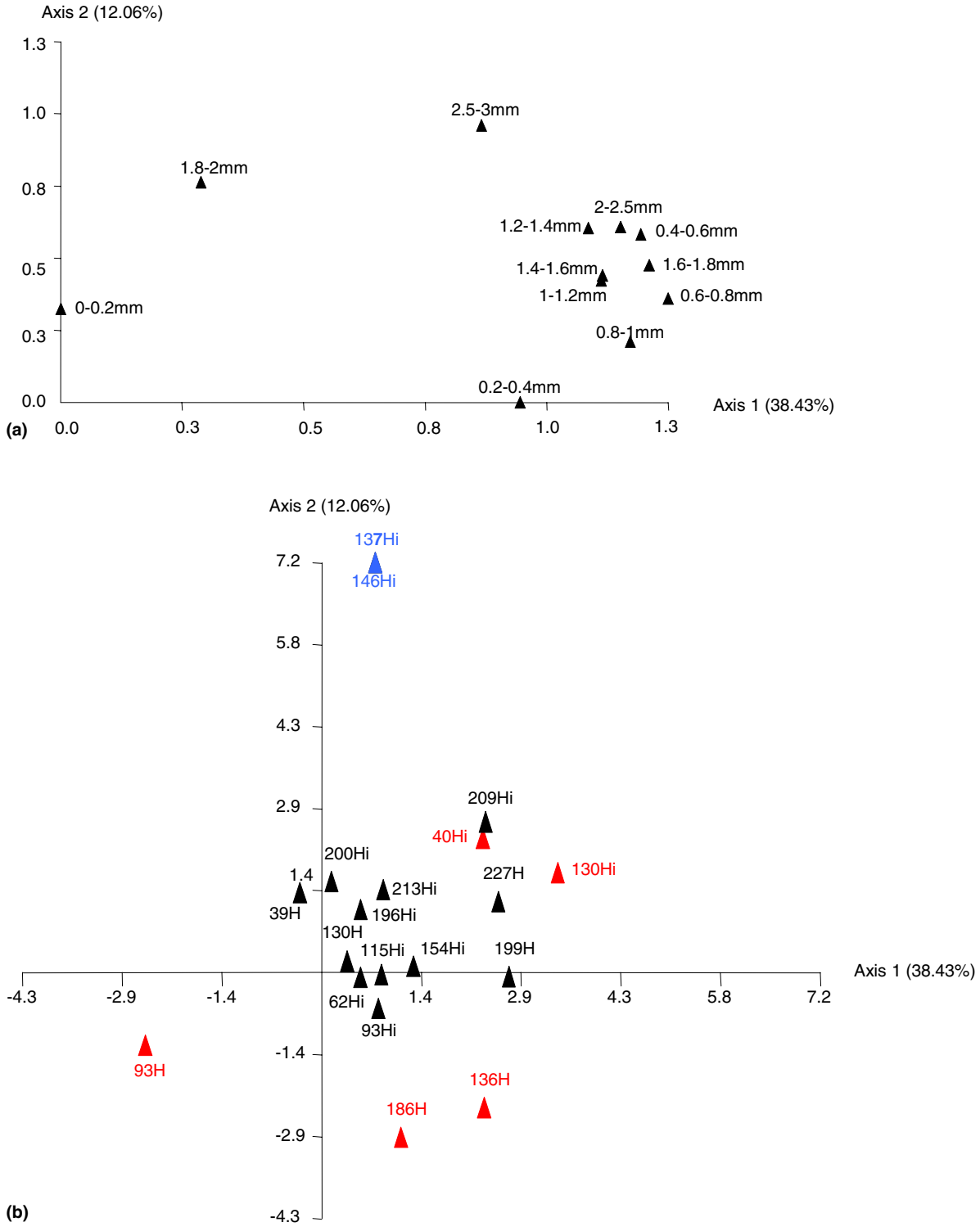

Fig. 8. CFA of the phototrophic anoxygenic communities. (a) CFA of each layer of the 3 mm of Salins de Giraud microbial mat. Each black triangle was represented by a 5′ end T-RFLP pattern corresponding to the combined digests *Hae*III and *Hin*6I of the PufM encoding gene. (b) CFA of variables, i.e., T-RFs derived from the CFA in panel (a). Each number corresponds to the T-RF length in base pairs. Letters H and Hi, after this number, correspond to *Hae*III and *Hin*6I T-RFs, respectively. Red and blue triangles correspond to T-RFs specific from the oxic (<2 mm) and anoxic zone (>2 mm) of the mat, respectively. Black triangles correspond to T-RFs non-specific from the mat zonation.

groups at the microscale level. As revealed by spectral scalar irradiance (Fig. 2), by CLSM (Table 2), and by DGGE (Fig. 5), the cyanobacteria were dominant and rather diverse photosynthetic microorganisms active in the first millimeter of the mat. Analyses of biomarkers (Fig. 3) corroborated these observations of a dominance

of oxygenic phototrophs, since major fatty acids (*n*-octadec-9(Z)-enoic acid), alcohols (5α(H)-stanols), and hydrocarbons (*n*-heptadecane, *n*-heptadecenes, and 9-methylhexadecane) found in this mat corresponded to cyanobacteria [49].

Identification of oxygenic phototrophs down to the genus or even species level was done by confocal laser scanning microscopy and sequencing analysis (PCR-DGGE-sequencing). Two dominant filamentous cyanobacteria *Microcoleus* sp. and *Leptolyngbya* sp. were identified by both techniques. Other oxygenic phototrophs were either identified by CLSM (*Halomicronema*, *Limnothrix*, *Pseudanabaena*, *Synechocystis* – group, *Gloeocapsa* – group, *Chroococcus*, and *Microcystis*) or by sequencing analysis (*Phormidium*, *Calotrix*, *Pleurocapsa*, *Oscillatoria*). Thus, the combination of both CLSM and DGGE was useful to fully describe the oxygenic phototrophic communities.

As described previously, bacterial biodiversity depends on gradient salinity, with a decreasing bacterial diversity when salinity increases [50–52]. However, in this investigated halophilic microbial mat, the diversity of oxygenic phototrophs is moderate in comparison to those previously described [53] with the dominance of *M. chthonoplastes* a typical inhabitant of halophilic microbial mat [54–56]. At higher salinities, other cyanobacterial morphotypes, like *Phormidium,* could be dominant [5].

Within the mat, analysis of biomarkers revealed the presence of purple bacteria like *Rhodobacter* and *Ectothiorhodospira*, and also of SRB. *Iso*- and *anteiso*-pentadecanoic acids are abundant in SRB and sulfur-oxidizing bacteria such as *Thiomicrospira* [35]. Cyclopropylnonadecanoic acid was also a major compound in the distribution of fatty acids. This compound is abundant in purple phototrophic bacteria such as *Rhodobacter* and *Ectothiorhodospira* where it occurs together with significant amounts of *n*-octadec-11(Z)-enoic acid [35]. The ratio between these two acids (0.5) could be related to the growth status of the microbial mat, with a high relative proportion of the cyclopropyl acid being indicative of stationary growth [57]. The high abundance of *iso*- and *anteiso*-pentadecanoic acids, as well as of cyclopropylnonadecanoic and *n*-octadec-11(Z)-enoic acids likely reflects the dominance of two different populations exchanging hydrogen sulfide, which could be sulfate-reducing and purple phototrophic bacteria, respectively. By the use of specific primer sets, T-RFLP allowed us to distinguish photosynthetic anoxygenic bacteria (PAB) and SRB organized in five and three distinct bacterial groups among the first 3 mm of this mat, respectively (Figs. 7 and 8).

Measurements of the spectral scalar irradiance revealed the presence of purple bacteria in the surface layer of the mat, especially in the zone at 0.5–0.8 mm depth (Fig. 2). This confirms the observation with T-RFLP, showing the presence of distinct populations at 0.4–1.8 mm. In contrast, only few PAB were observed in the upper layer (0–0.4 mm) (Fig. 8(a)). Therefore, the PAB developing at greater depths in the mat could be adapted to lower light intensities, as compared to the PAB community of the surface layer, since light is strongly attenuated in the mat (Fig. 2). Moreover, oxygen could also play a role in the stratification of the PAB, discriminating populations of different tolerance to the presence of oxygen, especially in the surface layer of the mat with high oxygen concentrations (Fig. 1).

We could demonstrate the presence of *Desulfobacter*-like and *Desulfovibrio*-like SRB, in the mid layer of the mat, corresponding to the fluctuating oxic and anoxic zone during the diel cycle (Fig. 1). Many *Desulfovibrio* species were isolated from the oxic zone of microbial mats, and were found to be able to tolerate and consume oxygen [58,59]. An oxygen tolerant SRB community that could not be correlated by T-RFLP to any known SRB inhabited the 1.6 mm top layer that is completely oxic during the day. Previous molecular studies have described the presence of *Desulfonema*-like species in the oxic surface layer of several microbial mats [60,61]. They were found to be metabolically versatile with a high affinity to oxygen. In the deeper 3 mm layer, our study showed that one SRB population was specific to the anoxic layer, indicating probably a high sensitivity to oxygen. Thus, T-RFLP analysis illustrated a vertical stratification of the SRB within the top 3 mm layers of the mat, that could be explained by their behavioral responses to oxygen including aggregation, migration to anoxic zones, and aerotaxis [58].

The microscale zonation of these populations is partly controlled by the microgradients of oxygen, sulfide and light. In the investigated mat, no free sulfide was measurable with microsensors (Fig. 2), but iron sulfide precipitates, and measurements of sulfate reduction rates (SRR) (Rod Herbert, unpublished results) indicated high bacterial sulfate reduction activity and subsequent precipitation of the produced sulfide by iron. Investigation of the biogeochemistry of the mat in year 2001 confirmed that this Camargue mat is characterized by high sulfate reduction rates and a high iron and FeS content [62]. Additionally, in this mat *Chloroflexus*-like bacteria, detected by T-RFLP, were found as important members in the surface layer community (Fig. 6). Their presence was also indicated by the BChl *c* absorption detected in the top layer of the mat (Fig. 2). These microorganisms could play an important role in hypersaline and iron-rich microbial mats [63].

Biomarkers also evidenced organic matter contributions to these microbial mats from other origins. Thus, C_{37}–C_{38} di-, tri- and tetra-unsaturated alkenones (Fig. 3(b)) are specific of Hapthophyceae [64,65]. However, their occurrence cannot be attributed to species typically

found in pelagic environments and are probably related to unknown species. Moreover, a distribution of C_{23}–C_{35} *n*-alkanes predominated by the odd carbon numbered homologues, namely C_{29}, C_{31} and C_{33}, was found. This distribution is representative of inputs from higher plants [66] and is currently found in microbial sediments from coastal environments [67]. The allochthonous origin of these *n*-alkanes is clear based on their biosynthetic origin. The absence of higher plants nearby hypersaline systems suggest that their presence in microbial mat systems such as the one in Camargue may reflect the influence of wind transported remains from nearby higher plants, as already observed in other hypersaline areas [67]. Further evidence of the external origin of these C_{23}–C_{35} *n*-alkanes has been obtained in other coastal Mediterranean systems from comparison of the δ^{13} C isotopic composition of these *n*-alkanes and in situ generated microbial mat lipids. Whereas the former exhibit the typical values of higher plant compounds, e.g. $<-20‰$, the latter reflect the intense use of CO_2 as consequence of the high productivity and therefore the δ^{13} C isotopic values are much heavier, $>-20‰$ [68].

5. Conclusions

The results presented here demonstrated a clear stratification of the main photosynthetic and sulfur bacterial populations in distinct and specific vertical microlayers according to their physiological characteristics. The first active millimeter of this photosynthetic microbial mat was dominated by filamentous cyanobacteria such as *M. chtonoplastes*. Beneath this cyanobacterial layer, sulfur oxidizing bacteria like *Thiomicrospira* were present. Although diverse anoxygenic phototrophic bacteria such as *Rhodobacter* and *Ectothiorhodospira* inhabited this mat, *H. salexigens* and *R. marina* were dominant in surface and deep zones, respectively. Sulfate reducing bacteria responsible of high sulfate reduction rates were distributed within the depth profile. *Desulfonema* dominated the oxic surface, *Desulfobacter* and *Desulfovibrio* the mid oxic–anoxic layer while oxygen sensitive SRB were located in the deeper zone. Others organisms such as algae and diatoms contributed to the microbial mat structure and development.

In man-made artificial salterns, where such a type of mat develops, environmental conditions can change dramatically on a short term [62]. The structures of bacterial communities in microbial mats have mainly been described globally at the macroscale level. In contrast, this study of the hypersaline Camargue microbial mat represents the first exhaustive investigation, which clearly shows the structure and the distribution of the main bacterial communities at the microscale level according to the microgradients of oxygen and light.

Acknowledgements

We acknowledge the financial support by the EC (MATBIOPOL project, grant EVK3-CT-1999-00010). The authors are grateful to the company of Salins-dumidi at Salins-de-Giraud for facilitating access to the salterns, sampling and field experiments. A.F. is partly supported by a doctoral grant from the general council of Atlantic Pyrenees. M.K. was supported by the Danish Natural Science Research Council (contract no. 9700549). Anni Glud is gratefully acknowledged for microsensor construction and assistance during the field experiment.

References

[1] Esteve, I., Martínez, M., Mir, J. and Guerrero, R. (1992) Typology and structure of microbial mats communities in Spain: A preliminary study. Limnetica 8, 185–195.
[2] Mir, J., Martínez-Alonso, M., Esteve, I. and Guerrero, R. (1991) Vertical stratification and microbial assemblage of a microbial mat in the Ebro Delta (Spain). FEMS Microbiol. Ecol. 86, 59–68.
[3] van Gemerden, H., Tughan, C.S., de Wit, R. and Herbert, R.A. (1989) Laminated microbial ecosystems on sheltered beaches in Scapa Flow, Orkney Islands. FEMS Microbiol. Lett. 62, 87–101.
[4] Wieland, A., Kühl, M., McGowan, L., Fourçans, A., Duran, R., Caumette, P., Garcia De Oteyza, T., Grimalt, J.O., Solé, A., Diestra, E., Esteve, I. and Herbert, R.A. (2003) Microbial mats on the Orkney islands revisited: microenvironment and microbial community composition. Microbial Ecol. 46, 371–390.
[5] Caumette, P., Matheron, R., Raymond, N. and Relexans, J.C. (1994) Microbial mats in the hypersaline ponds of Mediterranean salterns (Salins-de-Giraud, France). FEMS Microbiol. Ecol. 13, 273–286.
[6] Giani, D., Seeler, J., Giani, L. and Krumbein, W.E. (1989) Microbial mats and physicochemistry in a saltern in the Bretagne (France) and in a laboratory scale saltern model. FEMS Microbiol. Ecol. 62, 151–162.
[7] van Gemerden, H. (1993) Microbial mats: A joint venture. Marine Geol. 113, 3–25.
[8] Revsbech, N.P., Jørgensen, B.B., Blackburn, T.H. and Cohen, Y. (1983) Microelectrode studies of the photosynthesis and O_2, H_2S and pH profiles of a microbial mat. Limnol. Oceanogr. 28, 1062–1074.
[9] Mouné, S., Caumette, P., Matheron, R. and Willison, J.C. (2003) Molecular sequence analysis of prokaryotic diversity in the anoxic sediments underlying cyanobacterial mats of two hypersaline ponds in Mediterranean salterns. FEMS Microbiol. Ecol. 44, 117–130.
[10] Mouné, S., Eatock, C., Matheron, R., Willison, J.C., Hirschler, A., Herbert, R. and Caumette, P. (2000) *Orenia salinaria* sp. nov., a fermentative bacterium isolated from anaerobic sediments of Mediterranean salterns. Int. J. Syst. Evol. Microbiol. 50 (Pt 2), 721–729.
[11] Mouné, S., Manac'h, N., Hirschler, A., Caumette, P., Willison, J.C. and Matheron, R. (1999) *Haloanaerobacter salinarius* sp. nov., a novel halophilic fermentative bacterium that reduces glycine-betaine to trimethylamine with hydrogen or serine as electron donors; emendation of the genus *Haloanaerobacter*. Int. J. Syst. Bacteriol. 49 (Pt 1), 103–112.

[12] Jørgensen, B.B. and Des Marais, D.J. (1988) Optical properties of benthic photosynthetic communities: Fiber-optic studies of cyanobacterial mats. Limnol. Oceanogr. 33, 99–113.
[13] Caumette, P., Baulaigue, R. and Matheron, R. (1988) Characterization of *Chromatium salexigens* sp. nov., a halophilic Chromatiaceae isolated from Mediterranean salinas. Syst. Appl. Microbiol. 10, 284–292.
[14] Caumette, P., Baulaigue, R. and Matheron, R. (1991) *Thiocapsa halophila* sp. nov., a new halophilic phototrophic purple sulfur bacterium. Arch. Microbiol. 155, 170–176.
[15] Revsbech, N.P. (1989) An oxygen microelectrode with a guard cathode. Limnol. Oceanogr. 34, 474–478.
[16] Grasshoff, K., Ehrhardt, M. and Kremling, K. (1983) Methods of seawater analysis, Weinheim.
[17] Revsbech, N.P. and Jørgensen, B.B. (1983) Photosynthesis of benthic microflora measured with high spatial resolution by the oxygen microprofile method: Capabilities and limitations of the method. Limnol. Oceanogr. 28, 749–756.
[18] Lassen, C., Ploug, H. and Jørgensen, B.B. (1992) A fibre-optic scalar irradiance microsensor: application for spectral light measurements in sediments. FEMS Microbiol. Ecol. 86, 247–254.
[19] Kühl, M. and Fenchel, T. (2000) Bio-optical characteristics and the vertical distribution of photosynthetic pigments and photosynthesis in an artificial cyanobacterial mat. Microbial Ecol. 40, 94–103.
[20] Castenholz, R.W. (2001) Phylum Bx. Cyanobacteria. Oxygenic Photosynthetic Bacteria, 2nd ed., New York, pp. 473–599.
[21] Nübel, U., Garcia-Pichel, F. and Muyzer, G. (1997) PCR primers to amplify 16S rRNA genes from cyanobacteria. Appl. Environ. Microbiol. 63, 3327–3332.
[22] Schäfer, H. and Muyzer, G. (2001) Denaturing Gradient Gel Electrophoresis in Marine Microbial Ecology. pp. 425–468.
[23] Muyzer, G., Brinkhoff, T., Nübel, U., Santegoeds, C., Schäfer, H. and Wawer, C. (1998) Denaturing gradient gel electrophoresis (DGGE) in microbial ecology. Kluwer, Dordrecht, 1–27.
[24] Wheeler, D.L., Church, D.M., Federhen, S., Lash, A.E., Madden, T.L., Pontius, J.U., Schuler, G.D., Schriml, L.M., Sequeira, E., Tatusova, T.A. and Wagner, L. (2003) Database resources of the National Center for Biotechnology. Nucl. Acids Res. 31, 28–33.
[25] Ludwig, W., Strunk, O., Westram, R., Richter, L., Meier, H., Yadhukumar, A., Buchner, A., Lai, T., Steppi, S., Jobb, G., Forster, W., Brettske, I., Gerber, S., Ginhart, A.W., Gross, O., Grumann, S., Hermann, S., Jost, R., Konig, A., Liss, T., Lussmann, R., May, M., Nonhoff, B., Reichel, B., Strehlow, R., Stamatakis, A., Stuckmann, N., Vilbig, A., Lenke, M., Ludwig, T., Bode, A. and Schleifer, K.-H. (2004) ARB: a software environment for sequence data. Nucl. Acids. Res. 32, 1363–1371.
[26] Lane, D.J. (1991) rRNA Sequencing. pp. 115–175.
[27] Weisburg, W.G., Barns, S.M., Pelletier, D.A. and Lane, D.J. (1991) 16S ribosomal DNA amplification for phylogenetic study. J. Bacteriol. 173, 697–703.
[28] Amann, R., Binder, B., Olson, R., Chisholm, S., Devereux, R. and Stahl, D. (1990) Combination of 16S rRNA-targeted oligonucleotide probes with flow cytometry for analyzing mixed microbial populations. Appl. Environ. Microbiol. 56, 1919–1925.
[29] Achenbach, L.A., Carey, J. and Madigan, M.T. (2001) Photosynthetic and phylogenetic primers for detection of anoxygenic phototrophs in natural environments. Appl. Environ. Microbiol. 67, 2922–2926.
[30] Maidak, B.L., Cole, J.R., Lilburn, T.G., Parker Jr., C.T., Saxman, P.R., Farris, R.J., Garrity, G.M., Olsen, G.J., Schmidt, T.M. and Tiedje, J.M. (2001) The RDP-II (Ribosomal Database Project). Nucl. Acids Res. 29, 173–174.
[31] Gauch, J.H.G. (1982) Multivariate Analysis in Community Ecology, New York, p. 298.
[32] Kovach, W.L. (1999) MVSP – a Multivariate Statistical Package for Windows, ver. 3.1., Wales UK.
[33] Grimalt, J.O. and Albaiges, J. (1990) Characterization of the depositional environments of the Ebro Delta (western Mediterranean) by the study of sedimentary lipid markers. Marine Geol. 95, 207–224.
[34] Volkman, J.K., Johns, R.B., Guillan, F.T., Perry, G.J. and Bavor, H.J. (1980) Microbial lipids of an intertidal sediment-I. Fatty acids and hydrocarbons. Geochim. Cosmochim. Acta 44, 1133–1143.
[35] Grimalt, J.O., de Witt, R., Teixidor, P. and Albaiges, J. (1992) Lipid biogeochemistry of *Phormidium* and *Microcoleus* mats. Org. Geochem. 19, 509–530.
[36] Han, J., McCarthy, E.D., Calvin, M. and Benn, M.H. (1968) Hydrocarbon constituents of the blue-green algae *Nostoc muscorum*, *Anacystis nudulans*, *Phormidium luridum* and *Chlorogloea fritschii*. J. Chem. Soc., 2785–2791.
[37] Paoletti, C., Pushparaj, B., Florenzano, G., Capella, P. and Lercker, G. (1976) Unsaponifiable matter of green and blue-green algal lipids as a factor of biochemical differentiation of their biomasses: II. Terpenic alcohol and sterol fractions. Lipids 11, 266–271.
[38] Blumer, M., Guillard, R.R.L. and Chase, T. (1971) Hydrocarbons of marine phytoplankton. Marine Biol. 8, 183–189.
[39] Nes, W.R. and McKean, M.L. (1977). Biogeochemistry of Steroids and Other Isoprenoids, Baltimore, MD.
[40] Nishimura, M. (1977) Origin of stanols in young lacustrine sediments. Nature 270, 711–712.
[41] Patterson, G.W. (1974) Sterols of some green algae. Comp. Biochem. Physiol. B 47, 453–457.
[42] Ballantine, J.A., Lavis, A. and Morris, R.J. (1979) Sterols of the phytoplankton – effects of illumination and growth stage. Phytochemistry 18, 1459–1466.
[43] Orcutt, D.M. and Paterson, G.W. (1975) Sterol, fatty acid and elemental composition of diatoms grown in chemically defined media. Comp. Biochem. Physiol. B 50, 579–583.
[44] Kates, M., Tremblay, P., Anderson, R. and Volcani, B.E. (1978) Identification of the free and conjugated sterol in a non-photosynthetic diatom, *Nitzschia alba* as 24-methylene cholesterol. Lipids 13, 34–41.
[45] Tornabene, T.G., Langworthy, T.A., Holzer, G. and Oro, J. (1979) Squalenes, phytanes and other isoprenoids as major neutral lipids of methanogenic and thermoacidophilic "archaebacteria". J. Mol. Evolut. 13, 73–83.
[46] Solé, A., Gaju, N. and Esteve, I. (2003) The biomass dynamics of cyanobacteria in an annual cycle determined by confocal laser scanning microscopy. Scanning 25, 1–7.
[47] Solé, A., Gaju, N., Guerrero, R. and Esteve, I. (1998) Confocal laser scanning microscopy of Ebro Delta microbial mats. Microsc. Anal. (Europ. Ed) 29, 13–15.
[48] Abed, R.M., Garcia-Pichel, F. and Hernández-Mariné, M. (2002) Polyphasic characterization of benthic, moderately halophilic, moderately thermophilic cyanobacteria with very thin trichomes and the proposal of *Halomicronema excentricum* gen. nov., sp. nov. Arch. Microbiol. 177, 361–370.
[49] Chuecas, L. and Riley, J.P. (1969) Component fatty acids of the total lipids of some marine phytoplankton. J. Marine Biol. Assoc. UK 49, 97–116.
[50] Benlloch, S., López-López, A., Casamayor, E.O., Ovreas, L., Goddard, V., Daae, F.L., Smerdon, G., Massana, R., Joint, I., Thingstad, F., Pedros-Alio, C. and Rodriguez-Valera, F. (2002) Prokaryotic genetic diversity throughout the salinity gradient of a coastal solar saltern. Environ. Microbiol. 4, 349–360.
[51] Casamayor, E.O., Massana, R., Benlloch, S., Ovreas, L., Diez, B., Goddard, V.J., Gasol, J.M., Joint, I., Rodríguez-Valera, F. and Pedrós-Alió, C. (2002) Changes in archaeal, bacterial and eukaryal assemblages along a salinity gradient by comparison of genetic fingerprinting methods in a multipond solar saltern. Environ. Microbiol. 4, 338–348.

[52] Nübel, U., García-Pichel, F. and Muyzer, G. (2000) The halotolerance and phylogeny of cyanobacteria with tightly coiled trichomes (*Spirulina* Turpin) and the description of *Halospirulina tapeticola* gen. nov., sp. nov. Int. J. Syst. Evol. Microbiol. 50, 1265–1277.

[53] Nübel, U., García-Pichel, F. and Muyzer, G. (1997) PCR primers to amplify 16S rRNA genes from cyanobacteria. Appl. Environ. Microbiol. 63, 3327–3332.

[54] Karsten, U. (1996) Growth and organic osmolytes of geographically different isolates of *Microcoleus chthonoplastes* (cyanobacteria). from benthic microbial mats: Response to salinity change. J. Phycol. 32, 501–506.

[55] Guerrero, R., Urmeneta, J. and Rampone, G. (1993) Distribution of types of microbial mats at the Ebro Delta, Spain. Biosystems 31, 135–144.

[56] Jonkers, H.M., Ludwig, R., DeWit, R., Pringault, O., Muyzer, G., Niemann, H., Finke, N. and De Beer, D. (2003) Structural and functional analysis of a microbial mat ecosystem from a unique permanent hypersaline inland lake: 'La Salada de Chiprana' (NE Spain). FEMS Microbiol. Ecol. 44, 175–189.

[57] Navarrete, A., Urmeneta, J. and Guerrero, R. (2001) Physiological status and community composition of microbial mats by signature lipid biomarkers. pp. 111–116.

[58] Cypionka, H. (2000) Oxygen respiration by *Desulfovibrio* species. Ann. Rev. Microbiol. 54, 827–848.

[59] Cypionka, H., Widdel, F. and Pfennig, N. (1985) Survival of sulfate-reducing bacteria after oxygen stress, and growth in sulfate-free oxygen-sulfide gradients. FEMS Microbiol. Lett. 31, 39–45.

[60] Minz, D., Fishbain, S., Green, S.J., Muyzer, G., Cohen, Y., Rittmann, B.E. and Stahl, D.A. (1999) Unexpected population distribution in a microbial mat community: sulfate-reducing bacteria localized to the highly oxic chemocline in contrast to a eukaryotic preference for anoxia. Appl. Environ. Microbiol. 65, 4659–4665.

[61] Minz, D., Flax, J.L., Green, S.J., Muyzer, G., Cohen, Y., Wagner, M., Rittmann, B.E. and Stahl, D.A. (1999) Diversity of sulfate-reducing bacteria in oxic and anoxic regions of a microbial mat characterized by comparative analysis of dissimilatory sulfite reductase genes. Appl. Environ. Microbiol. 65, 4666–4671.

[62] Wieland, A., Zopfi, J., Benthien, M. and Kühl, M. (2004) Biogeochemistry of an iron-rich hypersaline microbial mat (Camargue, France). Microbial Ecology, in press.

[63] Pierson, B.K. and Parenteau, M.N. (2000) Phototrophs in high iron microbial mats: microstructure of mats in iron-depositing hot springs. FEMS Microbiol. Ecol. 32, 181–196.

[64] Volkman, J.K., Guillan, F.T., Johns, R.B. and Eglinton, G. (1981) Sources of neutral lipids in a temperate intertidal sediment. Geochim. Cosmochim. Acta 45, 1817–1828.

[65] Marlowe, I.T., Brassell, S.C., Eglinton, G. and Green, J.C. (1984) Long chain unsaturated ketones and esters in living algae and marine sediments. Org. Geochem. 6, 135–141.

[66] Eglinton, G. and Hamilton, R.J. (1967) Leaf epicuticular waxes. Science 156, 1322.

[67] Barbe, A., Grimalt, J.O., Pueyo, J.J. and Albaigés, J. (1990) Characterization of model evaporitic environments through the study of lipid components. Org. Geochem. 16, 815–828.

[68] Schouten, S., Hartgers, W.A., Lòpez, J.F., Grimalt, J.O. and SinninghеDamsté, J.S. (2001) A molecular isotopic study of 13C-enriched organic matter in evaporitic deposits: recognition of CO_2-limited ecosystems. Org. Geochem. 32, 277–286.

MICROBIAL ECOLOGY

Microb Ecol (2003) 46:371–390
DOI: 10.1007/s00248-002-0108-2

Microbial Mats on the Orkney Islands Revisited: Microenvironment and Microbial Community Composition

A. Wieland,[1] M. Kühl,[1] L. McGowan,[2] A. Fourçans,[3] R. Duran,[3] P. Caumette,[3] T. García de Oteyza,[4] J.O. Grimalt,[4] A. Solé,[5] E. Diestra,[5] I. Esteve,[5] R.A. Herbert[2]

[1] Marine Biological Laboratory, University of Copenhagen, Strandpromenaden 5, DK-3000 Helsingør, Denmark
[2] Division of Environmental and Applied Biology, School of Life Sciences, University of Dundee, Dundee DD1 4HN, UK
[3] Laboratoire d'Ecologie Moléculaire-Microbiologie, Université de Pau et des Pays de l'Adour, Avenue de l'Université, IBEAS, F-64000 Pau, France
[4] Department of Environmental Chemistry (ICER-CSIC), Jordi Girona 18, E-08034 Barcelona, Spain
[5] Department of Genetics and Microbiology, Autonomous University of Barcelona, E-08193 Bellaterra, Spain

Received: 7 November 2002; Accepted: 4 March 2003; Online publication: 14 August 2003

Abstract

The microenvironment and community composition of microbial mats developing on beaches in Scapa Flow (Orkney Islands) were investigated. Analysis of characteristic biomarkers (major fatty acids, hydrocarbons, alcohols, and alkenones) revealed the presence of different groups of bacteria and microalgae in mats from Waulkmill and Swanbister beach, including diatoms, Haptophyceae, cyanobacteria, and sulfate-reducing bacteria. These analyses also indicated the presence of methanogens, especially in Swanbister beach mats, and therefore a possible role of methanogenesis for the carbon cycle of these sediments. High amounts of algal lipids and slightly higher numbers (genera, abundances) of cyanobacteria were found in Waulkmill Bay mats. However, overall only a few genera and low numbers of unicellular and filamentous cyanobacteria were present in mats from Waulkmill and Swanbister beach, as deduced from CLSM (confocal laser scanning microscopy) analysis. Spectral scalar irradiance measurements with fiber-optic microprobes indicated a pronounced heterogeneity concerning zonation and density of mainly anoxygenic phototrophs in Swanbister Bay mats. By microsensor and T-RFLP (terminal restriction fragment length polymorphism) analysis in Swanbister beach mats, the depth distribution of different populations of purple and sulfate-reducing bacteria could be related to the microenvironmental conditions. Oxygen, but also sulfide and other (inorganic and organic) sulfur compounds, seems to play an important role in the stratification and diversity of these two major bacterial groups involved in sulfur cycling in Swanbister beach mats.

Correspondence to: A. Wieland; E-mail: awieland@zi.ku.dk

Introduction

Laminated microbial communities frequently develop in the upper intertidal zone of sandy beaches and tidal flats (e.g., [79, 16, 87, 49]). After initial colonization and succession of cyanobacteria [79], the mature states of these stratified phototrophic communities develop into microbial mats, consisting of a thin top layer of sand and/or diatoms covering a dense layer of filamentous cyanobacteria. Below the cyanobacteria, a distinct layer of purple sulfur bacteria is often present with a reduced black layer of precipitated iron sulfides underneath due to intensive sulfate reduction [84]. Sulfate-reducing bacteria are also present at high numbers in the upper millimeters of the mats [88, 98]. Because of the macroscopically visible lamination such coastal microbial mats were named colored sands or "Farbstreifensandwatt" [33]. Both cyanobacteria and anoxygenic phototrophs contribute to sediment binding and stabilization of the sediment [28]. The dominant cyanobacterium is generally *Microcoleus chthonoplastes* [79, 16, 84, 89], whereas the immotile *Thiocapsa roseopersicina* is often the dominant purple sulfur bacterium [16, 87, 84].

Mass blooms of purple sulfur bacteria, mainly *T. roseopersicina*, have been observed during summer in the intertidal zone of sheltered sandy beaches in Scapa Flow on the Orkney Islands [31, 85, 86]. Three different laminated microbial mats were described [86], distinguished by the position of the cyanobacterial layer above or beneath the purple sulfur bacterial layer, or by its complete absence and therefore exclusive development of purple sulfur bacteria in the top layer of the sediment. Mats with a typical lamination pattern (see above) were most common [86]. However, cyanobacteria were only present at relatively low population densities, and *M. chthonoplastes* was absent in all investigated mats [86].

The beaches of Scapa Flow are locally enriched in nitrogen-containing organic matter due to decomposition of accumulated macroalgal debris [31, 86]. In Scapa Bay, additional organic matter was supplied by discharges from local whiskey distilleries [86]. The high organic carbon content of the sediments leads to availability of low molecular weight organic substrates for sulfate-reducing bacteria, and the produced sulfide serves as an electron donor for anoxygenic photosynthesis by purple sulfur bacteria [31]. Distinct microcolonies formed by the purple sulfur bacteria (mainly *T. roseopersicina*) can effectively bind sediment grains. This aggregation leads to a reduction of erosion and, therefore, to a stabilization of the sediment [85]. Although these aggregates may not be as effective as the cohesive structures of cyanobacterial mats in stabilizing sandy sediments and preventing erosion, purple sulfur bacteria and mainly *T. roseopersicina* were capable of rapidly recolonizing eroded sites on beaches in Scapa Flow [85].

Further characteristics of these sediment ecosystems dominated by purple sulfur bacteria are the absence of chemolithotrophic sulfur bacteria, normally present in marine microbial mats [88], and the almost permanent exposure of purple sulfur bacteria to O_2 at the sediment surface [85, 86].

In this study, the composition of the microbial community and the microenvironmental conditions in microbial mats from Orkney Islands beaches was investigated. This included determination of phototrophic populations with confocal laser scanning microscopy (CLSM) and fiber-optic microprobe-based spectrometry in microbial mats from Waulkmill and Swanbister beaches. Dominant groups of mat-inhabiting microorganisms were determined by their characteristic biomarkers. Furthermore, the stratification of major bacterial groups in relation to microenvironmental gradients was investigated in Swanbister beach mats. For this, O_2 and sulfur cycling was quantified by controlled microsensor experiments in the laboratory and by sulfate reduction rate measurements. The depth-zonation and diversity of the entire microbial community and of the major bacterial groups involved in sulfur cycling in Swanbister beach mats were analyzed with terminal restriction fragment length polymorphism (T-RFLP).

Materials and Methods

Sampling

Sediment samples were taken in July 2000 at low tide with Plexiglas core tubes (53 mm i.d.) on beaches of Waulkmill and Swanbister Bay located in Scapa Flow, Orkney Islands (a map with locations can be found in [86]). *In situ* temperature and salinity of remaining stagnant seawater were 12–13°C and 40‰ at the time of sampling. Downwelling irradiance around noon on clear and sunny days was >1100 μmol photons $m^{-2}s^{-1}$. Sampled sediment cores were transported to the laboratory of the Orkney County Council Marine Unit on Orkney Island (Mainland), where microsensor measurements were performed under controlled conditions.

Microsensor Measurements

Clark-type O_2 [72] and H_2S [36, 50] microsensors connected to a picoammeter (Unisense A/S, Denmark), and glass pH microelectrodes [74] connected to a high-impedance mV-meter (WPI Inc., USA) were used for fine-scale measurements of O_2 and sulfide distribution in Swanbister beach mats. Oxygenic gross photosynthesis was quantified with the light–dark shift method [73]. The O_2 microsensor had a tip diameter of 10 μm, a stirring sensitivity of ~1%, and a response time, t_{90}, of ~0.4 s. The H_2S microsensor had a tip diameter of 40 μm and was coated with a black enamel paint to avoid light interference [50]. The length and the tip diameter of the pH-sensitive glass of the pH microelectrode were 250 and 10 μm, respectively.

The O_2 microsensor was linearly calibrated in the experimental setup (see below) by a two-point calibration using readings of microsensor current in the air saturated overlying water (100% air saturation) and in the anoxic part of the mats (0% O_2). Dissolved O_2 concentrations of air saturated seawater at experimental temperatures and salinities were calculated according to García and Gordon [27]. The pH microelectrode was calibrated in standard buffer solutions (Radiometer, Denmark). The pH of the overlying water in the experimental setup was determined with a commercial pH meter calibrated in standard buffer solutions (Radiometer, Denmark). The readings of the pH microelectrode in the overlying water were adjusted to the measured pH of the seawater. The H_2S microsensor was calibrated in anoxic buffer solutions (0.2 M phosphate buffer, pH 7.5) of increasing sulfide concentrations. A sample of each sulfide buffer solution was fixed in zinc acetate (5% w/v) for subsequent spectrophotometric analysis of sulfide concentration after Fonselius [23] with modifications, i.e., acidification of the samples to pH <1 with 6 M HCl and determination of the absorption of the formed complex at the second peak (750 nm) in the spectrum (C. Steuckart, unpublished). Calculation of H_2S and total sulfide (S_{tot}) concentration profiles from H_2S and pH microsensor data was as described in Wieland and Kühl [97], using pK_1 values calculated from experimental temperatures according to Hershey et al. [32].

Experimental Microsensor Setup

Sediment cores were mounted in a flow chamber modified for insertion of whole sediment cores [21]. A constant flow over the mat surface of aerated seawater from the sampling site was generated with a submersible water pump (Aqua Clear, Germany) connected to the flow chamber. Measurements were performed at room temperature (21°C ± 1°C). The mat was illuminated with a fiber-optic halogen light source (KL 2500, Schott, Germany) and the downwelling irradiance at the mat surface was quantified with an underwater quantum irradiance meter (QSL-101, Biospherical Instruments, USA). The microsensors were fixed together with the measuring tips in the same horizontal plane within an area of ca. 0.5–1 cm^2 of the mat surface in a motor-driven micromanipulator (Märzhäuser, Germany; Oriel, USA) mounted on a heavy solid stand. Microsensor signals were recorded with strip chart recorders (Servogor, UK; Kipp & Zonen, The Netherlands) and with a computer data acquisition system (LabView, National Instruments, USA) that also controlled the micromanipulator. Gross photosynthesis measurements in steps of 100- or 200-μm vertical depth intervals were performed as described in Wieland and Kühl [97].

Spectral Scalar Irradiance Measurements with Fiber-Optic Microprobes

A fiber-optic scalar irradiance microprobe [52] was connected to a sensitive fiber-optic diode array spectrometer with a spectral range of 250–950 nm (PMA-11, Hamamatsu Photonics, Japan). Profiles of spectral scalar irradiance in the mats were measured by stepwise inserting the microprobe with a motor-driven micromanipulator (Märzhäuser, Germany; MICOS GmbH, Germany; Jenny Electronics AG, Switzerland) at a zenith angle of 135° relative to the incident light beam. The mats were illuminated vertically with a fiber-optic halogen light source (KL 2500, Schott, Germany). Measurements were performed at vertical depth intervals of 200 μm. The downwelling spectral scalar irradiance at the mat surface was measured by positioning the scalar irradiance microprobe over a black light trap at the same position relative to the light field as the mat surface. Scalar irradiance spectra at various depths in the mats were normalized to the downwelling scalar irradiance at the mat surface. Attenuation spectra of scalar irradiance were calculated over discrete depth intervals from the depth profiles of spectral scalar irradiance by

$$K_0 = \ln(E_1/E_2)/(z_2 - z_1) \quad (1)$$

where K_0 is the vertical spectral attenuation coefficient for scalar irradiance, and E_1 and E_2 are the spectral scalar irradiance measured at depths z_1 and z_2 in the mat, where $z_2 > z_1$ [48].

Calculations

Diffusive O_2 fluxes across the mat-water interface were calculated from O_2 profiles using Fick's first law of diffusion as described in Wieland and Kühl [96]. Areal rates of O_2 consumption in the aphotic zone, R_{aphot}, were calculated as the downward O_2 flux, J_s, at the lower boundary of the photic zone:

$$J_s = -\phi D_s \, dC/dz \quad (2)$$

where dC/dz is the linear concentration gradient, ϕ is the sediment porosity, and D_s is the sediment diffusion coefficient, which was calculated from the porosity and D_0 according to Ullman and Aller [83]. The D_0 of O_2 was taken from Broecker and Peng [8] and corrected for experimental temperatures and salinities [53]. Fluxes of H_2S were calculated according to Eq. 2 from the linear part of the profiles. The diffusion coefficient of H_2S was estimated as $D_0(H_2S)=0.7573\ D_0(O_2)$ (Tables for seawater and gases, Unisense A/S, Denmark).

Determination of Sediment Porosity

Sediment porosity (mL water cm^{-3}) was determined ($n = 5$) on samples collected from Swanbister Bay in July 2001 using a 2.5-cm diameter stainless steel corer. The cores were sectioned using a sediment slicer to give the following four consecutive depth horizons: 0–5 mm, 5–10 mm, 10–20 mm, and 20–30 mm. Porosity was measured as weight loss after drying at 110°C for 24 h.

Determination of Sulfate Reduction Rates

Triplicate sediment cores (13 mm i.d.) were collected from Swanbister Bay in truncated 5-mL disposable syringes and sealed with Suba seals (W. Freeman Ltd., UK). Carrier-free $^{35}SO_4^{2-}$ (10 μL; Amersham Pharmacia Biotech, UK) was injected through the Suba seal using a microliter syringe into each sediment core, giving an average activity of 50 kBq cm^{-3}. To ensure even distribution of the isotope throughout the cores the isotope was added progressively as the syringe needle was withdrawn. At the end of the 12-h incubation period at ambient temperature (16°C) in the dark, the cores were sectioned to give the following depth horizons: 0–10 mm, 10–20 mm, and 20–30 mm. Each sediment section was transferred to plastic bottles containing 5 mL of a 20% w/v zinc acetate solution to stop biological activity and preserve sulfide. The samples were then frozen and stored until they were required for analysis. Production of $H_2^{35}S$ was determined using the one-step distillation method of Fossing and Jørgensen [24]. Sulfate reduction rates were calculated according to the method of Isaksen and Finster [35]. Porewater sulfate was determined according to the method of Tabatabai [80].

Confocal Laser Scanning Microscopy

Sediment cores (18 mm i.d.) were taken from Waulkmill and Swanbister Bay using truncated 20-mL disposable syringes. The samples were transferred into small plastic containers containing 2.5% glutaraldehyde in a phosphate buffer (0.2 M) adjusted to the appropriate salinity with NaCl. The samples were fixed for 3 h and then washed 2–3 times with phosphate buffer. The samples were stored at 4°C until further analysis.

The samples were investigated with a compound microscope (Olympus BH2, Japan) and a laser confocal microscope (Leica TCS 4d, Germany) equipped with an argon–krypton laser. For confocal analysis, subsamples (slices) of defined dimension were placed in cavity slides, covered and sealed with coverslips, and observed under an excitation beam of 568 nm. Pigment fluorescence emission was detected with a 590 nm long-pass filter. Optical sections (every focal plane), optical series (all focal planes from each imaged area), summa images (all optical series projected to one image), and stereoscopic images (one image in three dimensions from every optical series) were obtained from these analyses. A volume data set was generated by combining all optical sections.

After screening of the different cyanobacteria present in all images from each sampling site, each type of cyanobacterium was identified after morphological criteria according to Castenholz [10].

Analysis of Fatty Acids, Hydrocarbons, Alcohols, and Alkenones

Sediment cores (26 mm i.d.) were collected on Waulkmill and Swanbister beach and stored frozen until further analysis. The upper 4 cm of the mat samples (approximately 10 g) were homogenized with a mortar and extracted three times with methanol, dichloromethane, and *n*-hexane. Extracts were saponified with 30 mL of KOH (6% w/v) in methanol and the neutral components were recovered by extraction with 3 × 30 mL of *n*-hexane. The alkaline mixture was then acidified to pH 2 with 5 mL of HCl, and the acidic compounds were recovered by extraction with 3 × 30 mL of *n*-hexane. The neutral compounds were fractionated in a column filled with silica (8 g, bottom) and alumina (8 g, top). These packings were prepared previously by heating at 120°C and 350°C for 12 h, respectively. Milli-Q water was added to both adsorbents for deactivation (5%). Six fractions were obtained by successive elution with 20 mL of *n*-hexane, 20 mL of *n*-hexane/dichloromethane (9:1), 40 mL of *n*-hexane/dichloromethane (8:2), 40 mL of *n*-hexane/dichloromethane 75% (1:3), 20 mL of dichloromethane/methanol (95:5), and 40 mL of dichloromethane/methanol (9:1). The two most polar fractions were silylated after redissolution in 100 μL of dichloromethane and addition of 100 μL bis(trimethylsilyl)trifluoroacetamide (heating 1 h at 60°C). The fatty acid fractions were methylated before instrumental analysis using diazomethane, which was synthesized as described elsewhere [91]. These fractions were dissolved in 100 μL of *n*-hexane and diazomethane was added until the yellowish color remained.

Samples were analyzed by gas chromatography and flame ionization detection in a Varian Star 3400 (Varian Inc., USA). A 30 m capillary column (0.25 mm i.d.) coated with DB-5 (25 μm film thickness) was used with hydrogen as carrier gas. The oven was kept at 70°C for 1 min, heated to 140°C at 10°C/min, then to 310°C at 4°C/min, and finally held at 310°C for 30 min. The temperature of the detector was 330°C. Analyses by gas chromatography and mass spectrometric detection were performed with a Fisons MD-800 quadrupole mass analyzer (Thermo Instruments, UK). Samples were injected in splitless mode at 300°C into a 30 m capillary column (0.25 mm i.d.) coated with DB-5 (25 μm film thickness). Helium was used as carrier gas and the temperature program was as described above. Mass spectra were recorded in electron impact mode at 70 eV by scanning between m/z 50–650 every second. Ion source and transfer line were kept at 300°C.

T-RFLP Analysis

Sediment cores (35 mm i.d.) were taken with Falcon tubes from Swanbister Bay. The upper 10 mm of the sediment core was sliced off aseptically, transferred to sterile petri dishes, frozen in liquid nitrogen, transported on dry ice, and finally stored at −80°C until further analysis. The upper 2 mm of the mat cores

Table 1. Phylogenetic and photosynthetic primers used in T-RFLP analysis[a]

Primer	Sequence (5′ → 3′)	Target gene	Target group	Reference
8F	AGA GTT TGA TCC TGG CTC AG	*ssu 16S rDNA*	Eubacteria	[54]
926R	CCG TTC AAT TCC TTT RAG TTT	*ssu 16S rDNA*	Eubacteria	[54]
BSR 385R	CGG CGT CGC TGC GTC AGG	*ssu 16S rDNA*	SRB	[2]
PB 557F	CGCACCTGGACTGGAC	*PufM*	PAB	[1]
PB 750R	CCCATGGTCCAGCGCCAGAA	*PufM*	PAB	[1]

[a] Amplimer sizes for the different primer sets: *16S rDNA* eubacteria, 918 bp; *16S rDNA* sulfate-reducing bacteria, 377 bp; *pufM*, 229 bp. All 16S rDNA primer names are based on *E. coli* numbering. SRB denotes sulfate-reducing bacteria and PAB purple anoxygenic bacteria

was sliced with a cryomicrotome (MICROM GmbH, Germany) at around 200 μm, and the third millimeter at around 500 μm vertical depth resolution. From these mat slices, DNA was extracted with the UltraClean Soil DNA Isolation Kit using the alternative lysis method (MoBio Laboratories Inc., USA). All extracted genomic DNA samples were stored at −20°C until further processing.

The different primers used for T-RFLP analysis to assess the bacterial community structure are listed in Table 1. For T-RFLP analysis, forward (f) and reverse (r) primers were fluorescently labeled with TET and HEX (E.S.G.S. Cybergene group, France), respectively. The PCR amplification mixture contained 12.5 μL hot start *Taq* polymerase mix (Qiagen, Netherlands), 0.5 μL of each primer (20 μM), and 1 μL of DNA template. A final volume of 50 μL was adjusted with distilled water. Reactions were cycled in a PTC200 thermocycler (MJ Research, USA) at 94°C for 15 min, followed by 35 cycles of 94°C for 1 min; T_m for 1.5 min, with T_m denoting the corresponding melting temperature for hybridization between primers and template DNA; and 72°C for 1 min, with a final extension step at 72°C for 10 min. The amount of PCR product was determined by comparison to known concentrations of standards (Smartlader, Eurogentec, Belgium). PCR products were purified with the GFX PCR DNA purification kit (Amersham, UK).

Purified PCR products (600 to 700 ng) were digested with 12 units of enzyme *Hae*III or *Hin*6I (New England Biolabs, USA). The precise length of T-RFs from the digested PCR products was determined by capillary electrophoresis (ABI prism 310, Applied Biosystems, USA). About 50 ng of the digested DNA from each sample was mixed with 10 μL of deionized formamide and 0.25 μL of TAMRA size standard and then denatured at 94°C for 2 min and immediately chilled on ice prior to electrophoresis. After an injection step of 10 s, electrophoresis was carried out for up to 30 min applying a voltage of 15 kV. T-RFLP profiles were performed using GeneScan software (ABI).

Dominant T-RFs were selected by comparison of numerical values and electropherograms. The clustering values were analyzed with the T-RFLP similarity matrix on the RDP (Ribosomal Database Project) Web site (http://rdp.cme.msu.edu/) [56]. The obtained distance matrix was used to construct a dendrogram with MEGA version 2.1 [51] using the UPGMA method (Unweighted Pair Group Method with Arithmetic Mean).

T-RFLP profiles were also compared by Canonical Correspondence Analysis (CCA) according to Fromin et al. [25]. This test is based on the linear correlation between community data (abundance of each T-RF) and environmental parameters in the mat at light conditions (scalar irradiance at wavelengths of Chl *a* [676 nm] and BChl*a* [845 nm] absorption, depth, and O_2 concentration). The CCA were realized with MVSP v3.13d software (Rockware Inc., UK).

Results

Biomarkers in Waulkmill and Swanbister Bay Mats

The major lipid compounds in both Waulkmill and Swanbister beach mats were fatty acids, encompassing essentially C_{14}–C_{22} homologues dominated by *n*-hexadec-9(*Z*)-enoic and *n*-hexadecanoic acids (Fig. 1A, B). Other major compounds were *n*-octadec-9(*Z*)-enoic, *n*-eicosapentenoic, *n*-tetradecanoic, and *n*-pentadecanoic acids, which are generally representative of algal and microbial contributions. *N*-Octadec-9(*Z*)-enoic acid is abundant in photosynthetic algae and cyanobacteria [11]. *N*-Eicosapentenoic acid and other polyunsaturated *n*-eicosane and *n*-docosane acids are specific of inputs from diatom species [93]. *Iso*- and *anteiso*-pentadecanoic acids were the two main branched fatty acids present in significant proportions. These compounds are abundant in sulfate-reducing bacteria and sulfur-oxidizing bacteria such as *Thiomicrospira* [29].

The aliphatic hydrocarbon phyt-1-ene together with other phytene homologues occurred in both mats, but their presence was more pronounced in the Swanbister mat (Fig. 1C, D). These hydrocarbons are characteristic for methanogens [82] and may also be produced during the decomposition of phytol [18]. The presence of an isoprenoid compound specific of methanogenic origin, 2,6,10,15,19-pentamethylicosane [34, 75], in the Swanbister mat (Fig. 1C) suggests that at least in this mat the occurrence of the phytanes is due to inputs from these microorganisms. *N*-Heptadecane and *n*-heptadecenes were major compounds in both mats and especially abundant in the Waulkmill mat (Fig. 1D). These compounds are

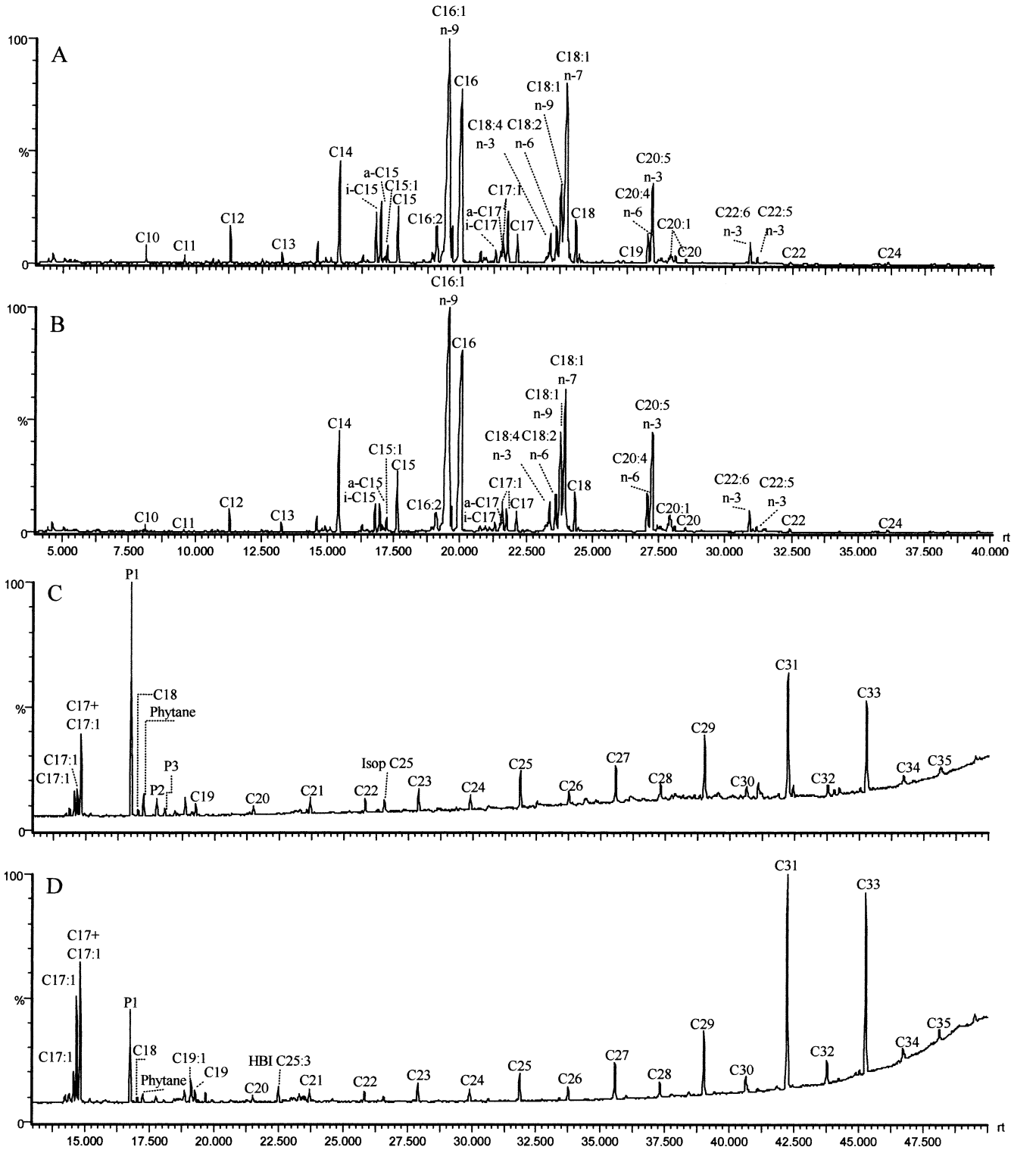

Fig. 1. Gas chromatographic profiles showing the major fatty acids (A, B) and the major hydrocarbons (C, D) in microbial mats from Swanbister (A, C) and Waulkmill (B, D) Bay. P1 denotes phyt-1-ene and P2 and P3 are phytenes. HBI C25, highly branched isoprenoid hydrocarbon. Isop C_{25}, 2,6,10,15,19-pentamethylicosane.

generally found in cyanobacteria [30, 67] or in phototrophic eukaryotes [7]. Other hydrocarbons specific for algal inputs such as C_{25} highly branched isoprenoid alkenes synthesized by diatoms [62] were also present in the

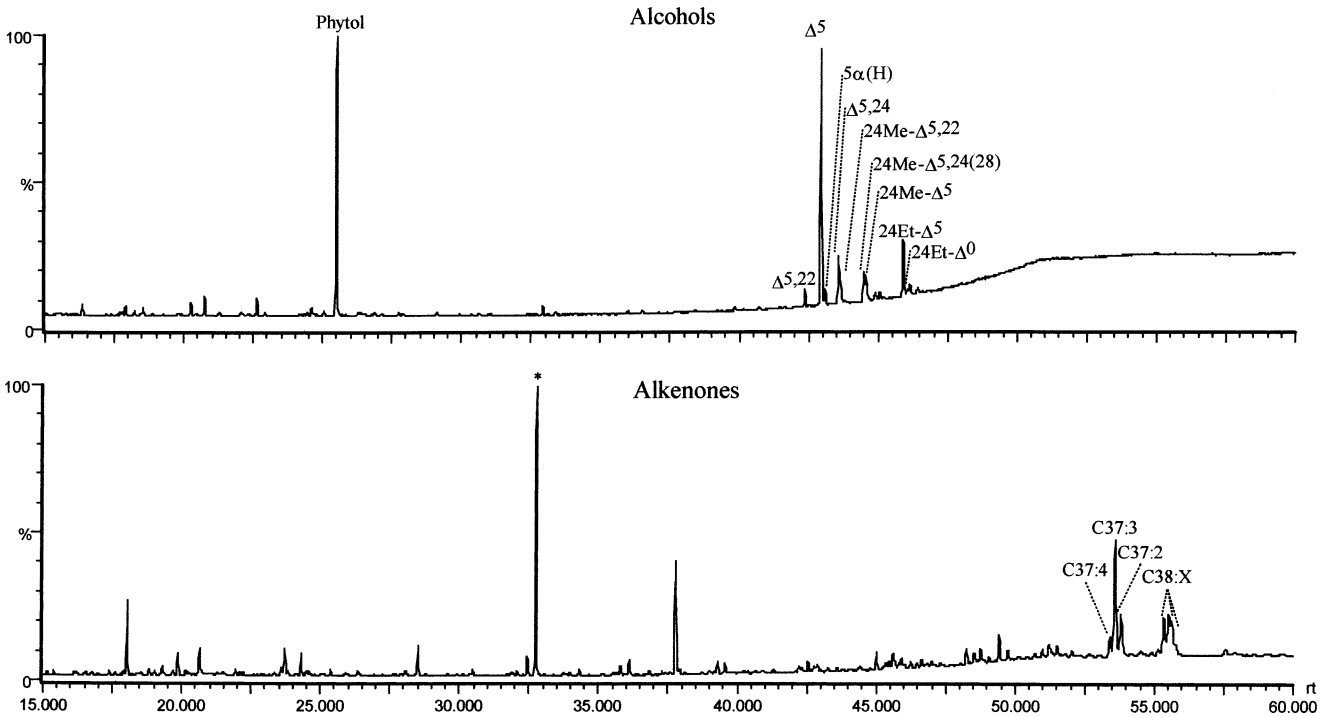

Fig. 2. Gas chromatographic profiles showing the major alcohols (upper graph) and alkenones (lower graph) in Waulkmill Bay mats.

Waulkmill mat. In addition to these hydrocarbons, a distribution of C_{23}–C_{35} *n*-alkanes predominated by the odd carbon numbered homologues, namely C_{29}, C_{31}, and C_{33}, representative for inputs from higher plants [20], were found in both mats. This distribution can also be found in other sediments in coastal environments [5], probably reflecting the influence of wind-transported materials from nearby higher plants.

A significant amount of phytol was found in the Waulkmill mat, representing contributions from algae (Fig. 2). Other lipids of algal origin, such as C_{37}–C_{38} di-, tri-, and tetraunsaturated alkenones specific for Haptophyceae [92, 57] and sterols, were also present. The sterol distribution in the Waulkmill mat was dominated by cholest-5-en-3β-ol and contains minor proportions of 24-ethylcholest-5-en-3β-ol, cholesta-5,24-dien-3β-ol, 24-methylcholesta-5,24(28)-dien-3-ol, and their homologues saturated at Δ^5 (Fig. 2, upper graph). Sterols unsaturated at positions Δ^5, Δ^{22}, and $\Delta^{5,22}$ can originate from cyanobacteria [67, 61, 63], green algae [68, 4] or diatoms [64, 41, 4]. 24-Methylcholesta-5,24(28)-dien-3β-ol is a common diatom marker [64, 41, 4], and its occurrence is consistent with the presence of highly branched isoprenoid hydrocarbons.

Spectral Scalar Irradiance and Cyanobacteria in Waulkmill Bay mats

From spectral scalar irradiance profiles the zonation of phototrophs in the mats could be inferred from the absorption characteristics of their pigments at specific wavelengths. In the Waulkmill mat, three main wavelength regions of pronounced absorption could be identified (Fig. 3). The pronounced minimum of scalar irradiance in the narrow region around 675 nm corresponds to Chl *a* absorption, indicating the presence of cyanobacteria and/or microalgae. A shoulder in the spectra measured over the upper 2 mm indicated some absorption at ~625 nm due to the presence of phycocyanin. The presence of purple bacteria throughout the upper millimeters of the mat was indicated by the pronounced minima in the region from 760 to 900 nm and at around 590 nm corresponding to BChl *a* absorption. The scalar irradiance in these wavelength regions was already at 1 mm depth less than 50% of the downwelling scalar irradiance at the mat surface and at 2.6 mm depth less than 1–2%. The strong absorption by Chl *a* and BChl *a* indicates the presence of dense populations of oxygenic and anoxygenic phototrophs in the upper 2.6 mm of the mat.

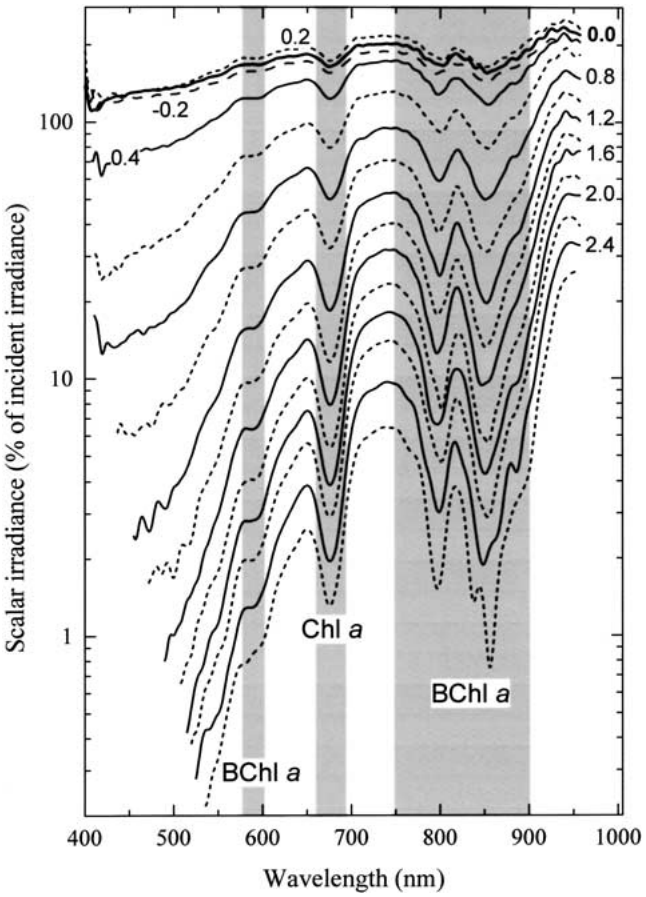

Fig. 3. Depth profile of spectral scalar irradiance in a Waulkmill Bay mat normalized to the downwelling spectral scalar irradiance at the mat surface. Numbers on curves indicate depth (mm). Depth 0 indicates the mat surface and increasing positive numbers indicate increasing depths in the mat.

Several different genera of filamentous and unicellular cyanobacteria were identified (Table 2), with cyanobacteria of the genera *Lyngbya* and *Oscillatoria* and of the *Pleurocapsa* and *Gloeocapsa* groups being the most abundant in the Waulkmill Bay mat as observed with CLSM and light microscopy. Some cyanobacteria occurred only at certain depths of the mat, whereas others were found in several or all mat slices investigated.

Spectral Scalar Irradiance and Cyanobacteria in Swanbister Bay Mats

In a Swanbister Bay mat, spectral scalar irradiance minima at characteristic Chl *a* and BChl *a* absorption wavelengths were found (Fig. 4). Pronounced light scattering was detected at the mat surface and in the uppermost mat layers. Wavelengths corresponding to Chl *a* absorption were more strongly attenuated in the Swanbister mat than wavelengths corresponding to BChl *a* absorption (Fig. 4), whereas in the Waulkmill mat both wavelength regions were almost equally attenuated throughout the mat (Fig. 3).

Spectral scalar irradiance profiles in another mat sample from Swanbister Bay, which was densely covered by purple bacteria and characterized by a pink-colored surface, showed a much more pronounced BChl *a* absorption (Fig. 5, upper graph). The spectral irradiance in the wavelength regions of Chl *a* and BChl *a* absorption was already at a depth of 0.8 mm <10% of the downwelling spectral scalar irradiance. From these profiles, the average attenuation spectrum of scalar irradiance over the depth interval of 0–0.8 mm was calculated (Fig. 5, lower graph). The vertical spectral attenuation coefficient (K_0) was highest in the wavelength region between 400 and 550 nm, the region of carotenoid and Chl *a* absorption. The attenuation coefficient of BChl *a* absorption wavelengths was higher than the attenuation coefficient of Chl *a* absorption, indicating higher densities of purple bacteria in this mat. Thus, mats from Swanbister Bay were very heterogeneous and patchy concerning zonation and population densities of oxygenic and especially anoxygenic phototrophs.

In Swanbister Bay mats covered by purple bacteria (pink surface), only a few genera of cyanobacteria, i.e., mainly unicellular morphotypes of the *Pleurocapsa* group and one filamentous type, were found in low numbers (Table 3).

Microbial Community Structure of Swanbister Bay Mats

To assess the microbial community structure of a Swanbister Bay mat, the universal primer pair 8f-926r targeting a partial sequence of the 16S rDNA gene of eubacteria was applied. After digestion with two different restriction enzymes (*Hae*III, *Hin*6I), the diversity of the amplified 16S fragments was analyzed by T-RFLP. The structure of the T-RFLP profiles, as characterized by the number and distribution of major bands (peaks of highest relative fluorescence intensity), varied from top to bottom of the mat (data not shown). Depending on the restriction enzyme used, different dominant T-RFs were observed. Degrees of similarity among the microbial communities of the different mat layers were quantified with the T-RFLP profile matrix program (RDP). The resulting similarity dendrogram (not shown) did not reveal any specific distribution of microbial communities in the analyzed mat layers, probably because several bacterial species may have terminal fragments of identical size.

Table 2. Filamentous and unicellular cyanobacteria in Waulkmill Bay mats tentatively identified according to Castenholz [10] and their characteristics and depth distribution as determined by CLSM and light microscopy

Genera (tentatively)	Diameter (µm)	Septation	Gas vacuoles	Sheath	Abundance	Depth (mm)
Filamentous cyanobacteria						
Lyngbya sp.	6.25–10.30	+	-	+	(+++)	0; 1.85
Oscillatoria sp.	12.5–14	-	-	+	(+++)	0; 1.85
Leptolyngbya sp.	0.94	-	-	+ (thin)	(++)	3.2
Pseudoanabena sp.	2.5	+	+	+ (thin)	(+)	1.85
Genera (tentatively)	**Diameter (µm)**	**Cell division**		**Sheath**	**Abundance**	**Depth (mm)**
Unicellular cyanobacteria						
Pleurocapsa group	2 × 3	Binary fissions in many different planes		+	(+++)	3.2
Gloeocapsa group	4–8	2 or 3 planes		+	(+++)	0; 1.85; 3.2
Microcystis sp.	1.9 × 1.9	Binary fissions in many different planes		+	(++)	0; 1.85; 3.2; 5.1
Aphanothece sp.	5 × 7	1 plane		+ (thin)	(++)	0
Pleurocapsa group	Diverse size and form	Binary fissions in several planes (pseudofilaments)		-	(+)	1.85

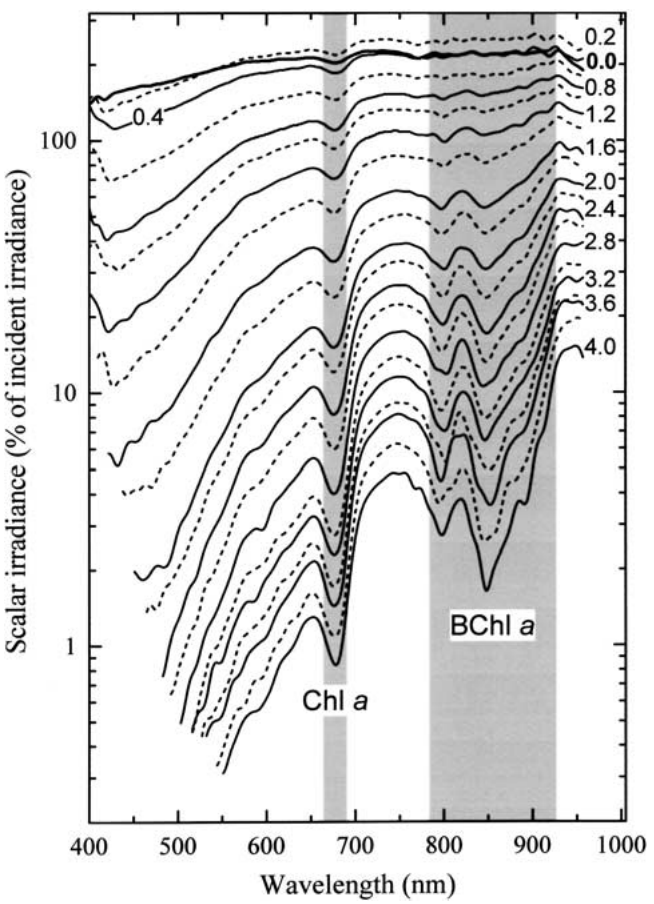

Fig. 4. Depth profile of spectral scalar irradiance in a Swanbister Bay mat normalized to the downwelling spectral scalar irradiance at the mat surface. Numbers indicate depth (mm).

More specific primers were used to analyze the sulfate-reducing and anoxygenic phototrophic microbial community. The biodiversity of the sulfate-reducing bacteria (SRB) was analyzed using the primers 8f-SRB385 and the combination of both restriction enzymes (*Hae*III, *Hin*6I). The resulting T-RFLP profiles contained almost 60 different peaks. In almost all mat layers fragments of 64, 189, 190, 191, 193, 200, 204 bp were found after digestion with *Hae*III, as well as dominant fragments of 64, 87, 89, 92, 337, 348, 350, 352, 371 bp using *Hin*6I (data not shown). Some T-RFs, however, showed a depth-dependent distribution, as T-RFs obtained with *Hae*III of 178, 181, 182, 209, 267, 314 and 317 bp were predominating only in the upper mat layers, whereas T-RFs of 268, 312, 315 bp were dominant in layers below 1 mm depth (data not shown). A similarity dendrogram was obtained by comparing all T-RFs observed with the two different restriction enzymes in each mat layer (Fig. 6A), which indicated a stratification of the SRB communities. The SRB communities in the upper mat layer (0–1 mm) seemed to be related and formed a distinct cluster, clearly differing from the ones at increasing depths. Two other closely related groups were located between 1 and 1.6 mm and between 2 and 3 mm depth, suggesting two different communities of SRB in these depth horizons. Furthermore, populations of SRB in the layer at 1.6–2 mm depth seem to form a divergent cluster.

The T-RFLP patterns were analyzed by Canonical Correspondence Analysis to reveal the variables, which influenced the organization of each SRB population.

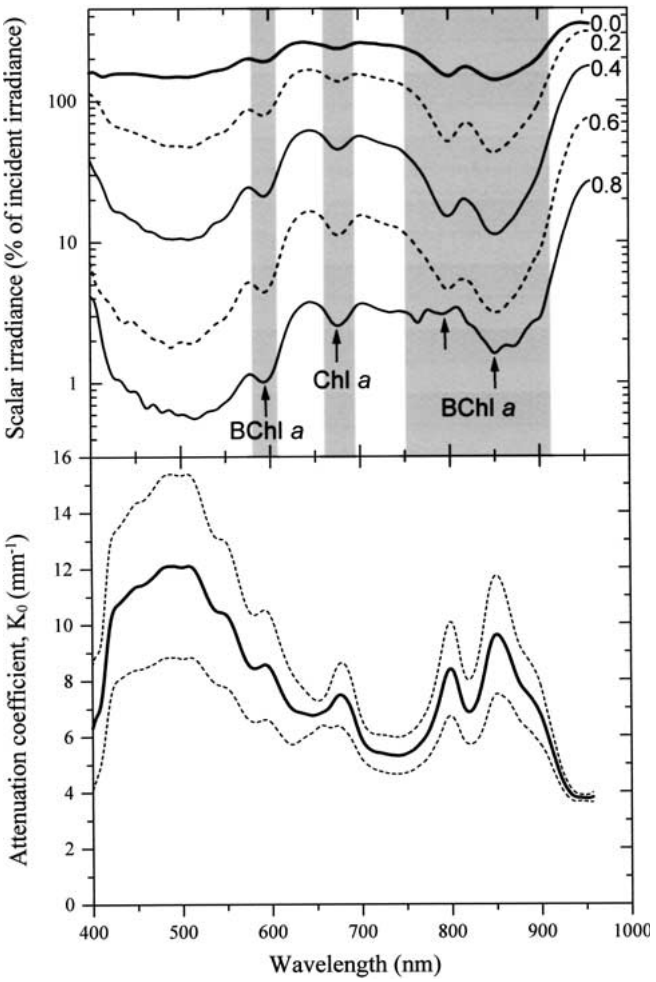

Fig. 5. Depth profile of spectral scalar irradiance (upper graph) in a Swanbister Bay mat densely covered by purple bacteria. The profiles of spectral scalar irradiance were normalized to the downwelling spectral scalar irradiance at the mat surface. Numbers indicate depth (mm). Average attenuation spectrum of scalar irradiance over the depth interval of 0–0.8 mm (lower graph), calculated from the spectral scalar irradiance profiles shown in the upper graph. Broken lines in the lower graph indicate the standard deviations of the attenuation coefficients, K_0.

Using the averaged microsensor O_2 profile at 1312 µmol photons $m^{-2}s^{-1}$ and scalar irradiance profiles at Chl *a* (676 nm) and BChl *a* (845 nm) absorption wavelengths in the top 3 mm of the mat (Figs. 4, 7C), this analysis showed that their dispersion was influenced mostly by irradiance and O_2 concentration (Fig. 6C). Two distinct groups appeared, one in the anaerobic zone and one in the aerobic zone exposed to light. This analysis showed a distribution of different SRB species with depth and thus that SRB were displayed according to depth.

The biodiversity of purple anoxygenic phototrophic bacteria (PAB) was assessed by using primers designed to target the *pufM* gene, which is encoding for a subunit of the photosynthetic reaction center in purple sulfur and purple nonsulfur bacteria. T-RFLP analysis of the amplified *pufM* fragments resulted in complex profiles containing about 30 peaks. Major T-RFs were observed, which allowed a comparison and distinction between the different mat layers. In the upper mat layers fragment peaks of 129, 187, 201, and 203 bp were found (*Hae*III), whereas the bottom layers were characterized by fragment peaks of 215 and 225 bp (data not shown).

Similarity dendrograms showed delineation of the profiles into clusters, indicating a stratification of purple phototrophic bacteria within the mat (Fig. 6B). Purple phototrophic communities from 1.4 to 2 mm and from 1–1.4/2–3 mm depth were closely related. These two community clusters were less closely related to the community in the upper mat layers than to the community below 3 mm depth. Furthermore, the similarity dendrogram also suggests that there were significant differences between the anoxygenic phototrophic communities in the uppermost millimeter of the mat.

Canonical correspondence analysis obtained from T-RFLP profiles showed that the phototrophic communities of the upper layers were clearly influenced by irradiance. In contrast, communities of the deep layers were negatively influenced by O_2 penetration (Fig. 6D). Surprisingly, predicted patterns of T-RFs from *pufM* sequences digested with *Hae*III or *Hin*6I obtained from the NCBI bank (data not shown) showed that the T-RFs specific of the upper layers could correspond to aerobic heterotrophic alphaproteobacteria, such as the genus *Sphingomonas*. Indeed, it has been recently demonstrated that this genus possesses the *pufM* gene [6]. T-RFs from deep layers of the mat could correspond to predicted T-RF patterns of purple sulfur bacteria from the genus *Thiocystis* and of purple nonsulfur bacteria from the genus *Rhodomicrobium*. The general T-RF fingerprints observed within the mat could be equivalent to predicted T-RF patterns of gamma-proteobacteria such as members of the genera *Rhodobacter* or *Allochromatium*.

Microenvironment of Swanbister Bay Mats

Profiles of O_2, gross photosynthesis, pH and H_2S were measured at different positions in a Swanbister Bay mat incubated in darkness and at an irradiance of 1312 µmol photons $m^{-2}s^{-1}$ (Fig. 7). During dark incubation, the average O_2 penetration was 0.8 mm and steep gradients of both H_2S and S_{tot} developed below this depth (Fig. 7A).

Table 3. Filamentous and unicellular cyanobacteria in Swanbister Bay mats tentatively identified according to Castenholz [10] and their characteristics and depth distribution as determined by CLSM and light microscopy

Genera (tentatively)	Diameter (μm)	Septation	Gas vacuoles	Sheath	Abundance	Depth (mm)
Filamentous cyanobacteria						
Borzia sp.	1.88 (short filaments)	+	-	+ (thin)	(+)	1.55
Genera (tentatively)	**Diameter (μm)**	**Cell division**		**Sheath**	**Abundance**	**Depth (mm)**
Unicellular cyanobacteria						
Pleurocapsa group (*Microcystis* sp.)	1.9 × 1.9	Binary fissions in many different planes		+	(+++)	0; 1.55; 3.35
Pleurocapsa group	Diverse size and form	Binary fissions in several planes (pseudofilaments)		-	(+++)	0; 1.55; 3.35
Pleurocapsa group (*Stanieria* sp.)	2 × 3	Multiple fissions or in combination with limited (1–3) binary fissions		-	(+)	3.35

A gradual decrease of pH was found in the dark incubated mat, accounting for a decrease of approximately 1 pH unit between the water and the mat at around 4 mm depth (Fig. 7B). Sulfate reduction rates were lowest in the upper centimeter of dark incubated Swanbister Bay mats and highest in the 1–2 cm depth interval (Table 4).

At an irradiance of 1312 μmol photons $m^{-2}s^{-1}$, gross oxygenic photosynthesis occurred in the upper 2.8 mm of the mat, leading to an increased O_2 penetration of 4 mm and a peak of O_2 concentration at 1.6 mm depth (Fig. 7C). As calculated from the profiles of spectral scalar irradiance measured in the same mat sample (Fig. 4), this O_2 maximum occurred in the depth layer of highest Chl *a* absorption, as indicated by the depth profile of the vertical attenuation coefficient, K_0, at 676 nm. Below that zone, both O_2 concentration and K_0 (676 nm) decreased, whereas the attenuation coefficient at 845 nm, indicative for BChl *a* absorption, increased. This indicates an increasing population density of BChl *a*–containing anoxygenic phototrophic bacteria in the anoxic mat layer. The presence of a population of anoxygenic phototrophs in the zone of highest O_2 concentration and Chl *a* absorption was indicated by a peak of K_0 (845 nm) in that zone, which was, however, less pronounced than the peak of K_0 (676 nm).

In the upper 5 mm of the light incubated mat, H_2S was undetectable; only in one position were very low concentrations of H_2S and sulfide detected below 3 mm depth (data not shown). Photosynthetic CO_2 fixation led to an increase of pH in the upper 2 mm of the mat by more than 0.5 pH unit, with the peak of pH located approximately in the layer of maximal O_2 concentration and K_0 (676 nm). At increasing depths the pH decreased to pH 7.5 (Fig. 7D).

Oxygen and Sulfide Cycling as a Function of Irradiance in Swanbister Bay Mats

In the same sediment core, O_2, gross photosynthesis, H_2S and pH profiles were measured at a fixed position at increasing downwelling irradiances (Fig. 8). Oxygen penetration increased in the mat with increasing irradiance from 0.8 mm during darkness to 1.4, 1.6, 2.2, and 2.6 mm at 43, 96, 183, and 349 μmol photons $m^{-2}s^{-1}$, respectively. At an irradiance of 96 μmol photons $m^{-2}s^{-1}$, a net production of O_2 was detected. The thickness of the photic zone increased gradually from 0.5 mm at 43 μmol photons $m^{-2}s^{-1}$ to 1.8 mm at 349 μmol photons $m^{-2}s^{-1}$ (Fig. 8, upper panel). The increase of gross oxygenic photosynthesis and of the photic zone thickness with irradiance led to a gradual increase of pH in the upper mat layers (Fig. 8, lower panel). The pronounced pH maximum in the upper mat layer at irradiances >43 μmol photons $m^{-2}s^{-1}$ affected the corresponding S_{tot} profiles (Fig. 8, upper panel). Profiles of S_{tot} were calculated from measured H_2S and pH profiles. The S_{tot} profiles at these irradiances showed a pronounced shoulder of S_{tot} concentration, which was not present in the corresponding H_2S profiles and was probably caused by the curvature of the pH profiles. Since H_2S and pH profiles could not be measured at exactly the same position, the unusual shape of the S_{tot} profiles was most probably caused by a pronounced microheterogeneity of the mat. These shoulders in the S_{tot} profiles thus represent overestimations of sulfide concentration and will not be discussed further. Compared to the H_2S profile in the dark incubated mat, the upper H_2S boundary moved downward in the mat at irradiances >96 μmol photons $m^{-2}s^{-1}$ (Fig. 8, upper panel).

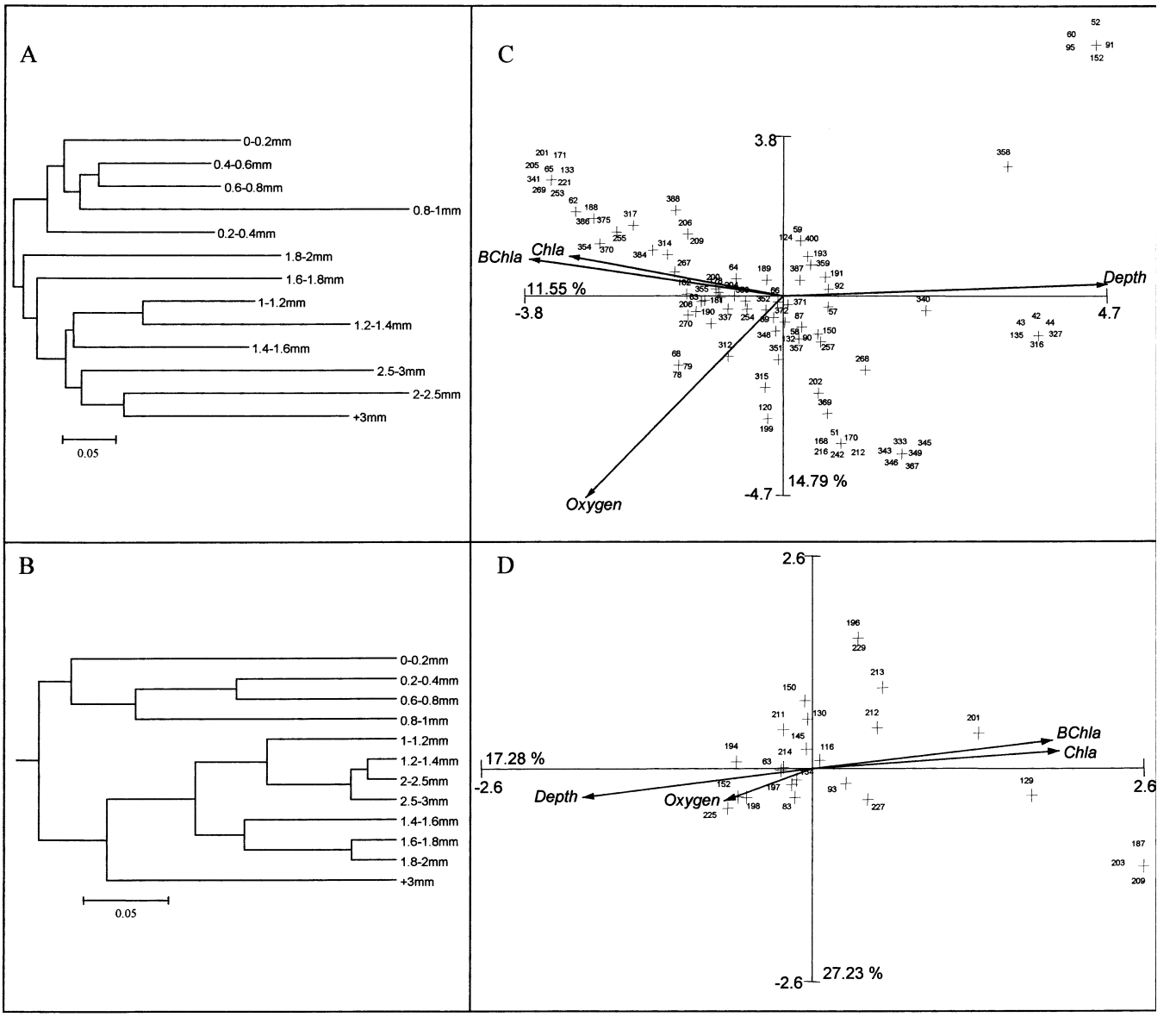

Fig. 6. The sulfate-reducing (SRB) (A) and the purple anoxygenic bacterial (PAB) (B) community relatedness of each layer of a Swanbister Bay mat based on the Jaccard coefficient. Each community was represented by a phylogenetic signature constructed by stacking two individual 5′ T-RFLP patterns corresponding to the *Hae*III and *Hin*6I digests of the 16S rRNA encoding gene for the SRB and the *pufM* gene for the PAB. Canonical correspondence analysis (CCA) between SRB (C) or PAB (D) (T-RF in base pairs) and environmental variables: scalar irradiance at characteristic Chl *a* (676 nm) and BChl *a* (845 nm) absorption wavelengths, O_2 concentration, and depth.

Areal rates of net oxygenic photosynthesis (P_n), calculated as the O_2 flux across the mat–water interface, rates of O_2 consumption in the aphotic zone (R_{aphot}), and rates of H_2S oxidation/production (H_2S fluxes) increased with irradiance and saturated at higher irradiances (Fig. 9). The determined H_2S fluxes, however, strongly underestimate sulfide fluxes, since pH also tends to increase in deeper layers at higher irradiance, which results in calculation of higher sulfide concentrations from H_2S data. Increasing H_2S fluxes will therefore translate to much stronger increases of sulfide fluxes.

Discussion

Microbial Community Composition of Waulkmill and Swanbister Bay Mats

In mats from both Waulkmill and Swanbister Bay, the presence of oxygenic phototrophs was evident (Figs. 1, 2,

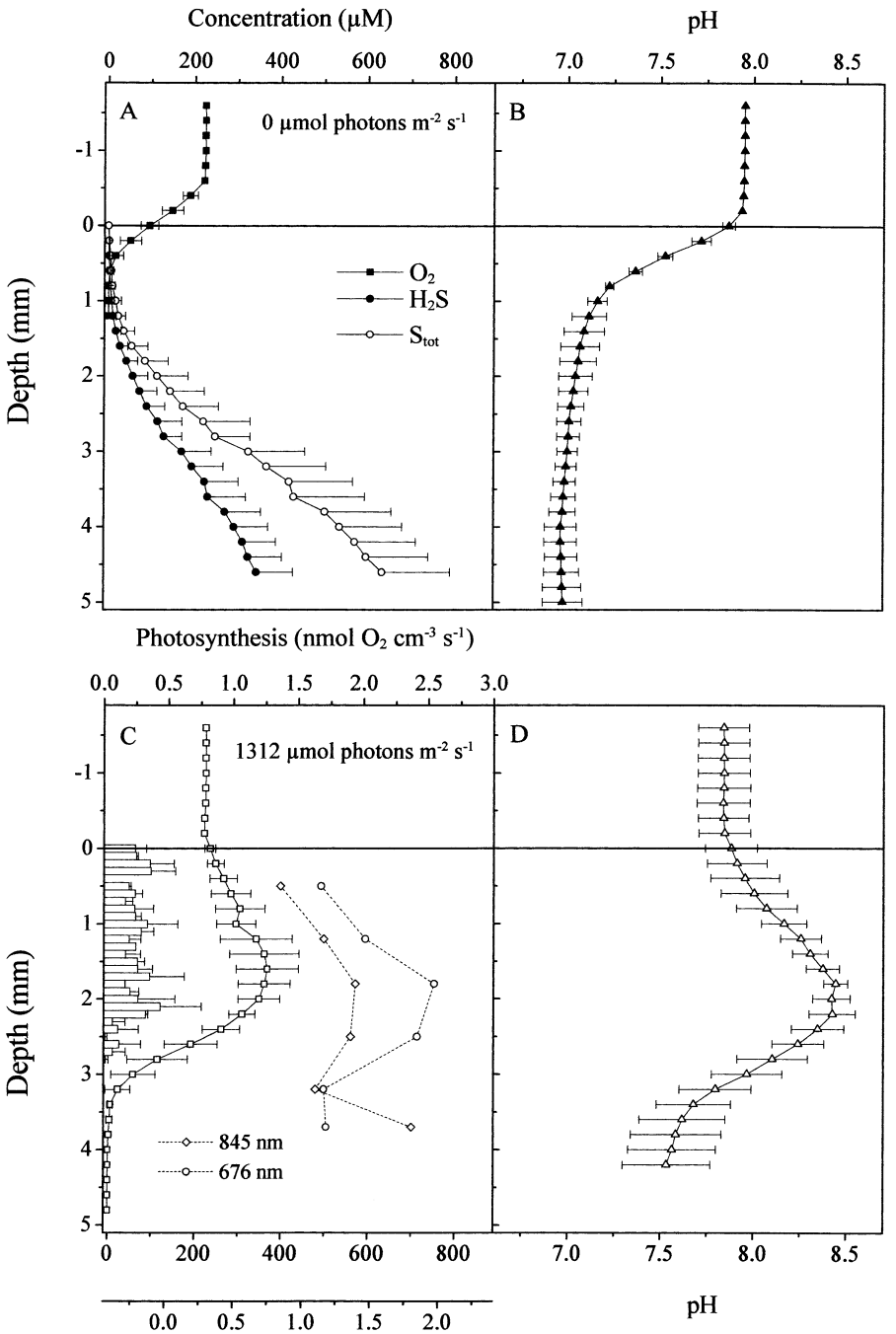

Fig. 7. Average profiles (n = 2–3) of gross photosynthesis (bars), O_2, H_2S, sulfide (S_{tot}) (A, C), and pH (B, D) measured at different positions in a Swanbister Bay mat at 0 (A, B) and 1312 µmol photons $m^{-2}s^{-1}$ (C, D). Error bars indicate standard deviation. Depth profiles of the vertical attenuation coefficient, K_0, at characteristic Chl *a* (676 nm) and BChl *a* (845 nm) absorption wavelengths as calculated from the depth profiles of spectral scalar irradiance measured in the same mat sample (profiles shown in Fig. 4).

3, 4, Tables 2, 3). Biomarker and CLSM analysis revealed a more pronounced abundance of cyanobacteria and high amounts of algal lipids (phytol, sterols, alkenones, highly branched isoprenoid hydrocarbons, heptadecane, and heptadecenes) in Waulkmill Bay mats. This indicates high contributions of oxygenic phototrophs in Waulkmill Bay mats, with specific contributions from diatoms and Haptophyceae. The latter were most probably of planktonic origin, buried in the sediment after settling on the sediment surface.

The bio-optical properties of two different Swanbister Bay mat samples revealed a strong heterogeneity concerning the phototrophic community (Figs. 4, 5), indicating a pronounced patchiness of the distribution of purple bacteria on Swanbister beach. A factor influencing the distribution and population densities of purple sulfur bacteria can be the availability of sulfide. The amount of sulfide present in the mat will limit the presence of oxygenic phototrophs to species able to cope with temporary exposure to sulfide. Environmental conditions on beaches

Table 4. Depth distribution of average sulfate reduction rates (n = 2–3) in Swanbister Bay mats

Depth (cm)	Sulfate reduction rate (nmol $cm^{-3}d^{-1}$)
0–1	234 ± 58
1–2	297 ± 33
2–3	245 ± 56

in Scapa Flow are restrictive for the development of cyanobacteria, as indicated by the low abundances and few genera found (Tables 2, 3). The production of sulfide by sulfate-reducing bacteria is, among other environmental parameters, controlled by the amount and quality of organic matter in the sediment (e.g., [78]). The main sources of organic matter are decomposing macroalgae buried in the sediment [31], resulting in a heterogeneous distribution of low molecular weight organic substrates for sulfate-reducing bacterial activity.

A pronounced microheterogeneity of sulfate reduction and sulfide distribution was found in Swanbister beach mats, as indicated by the standard deviations of measured sulfate reduction rates and sulfide microprofiles (Table 4, Fig. 7A). Thus, a heterogeneous distribution of sulfide could affect the distribution of the different phototrophs. A patchy distribution of sites virtually covered by purple bacteria (pink surface) was observed on Swanbister beach during sampling in July 2000, as well as a patchy distribution of macroalgae growing on the beach or deposited on the sediment surface. Additional to organic matter supply after decomposition, organic sulfur compounds such as dimethylsulfide (DMS) and dimethylsulfoniopropionate (DMSP) might be released from degrading macroalgae. Both compounds are potential substrates for purple bacteria [39], including *Thiocapsa roseopersicina* [90, 37, 38]. By providing such organic sulfur substrates, degrading macroalgae could also directly enhance growth of purple sulfur bacteria in their nearby surroundings, further contributing to their patchy distribution on these beaches.

Biomarker analysis showed that lipids reflecting the presence of methanogens (phytenes and 2,6,10,15,19-

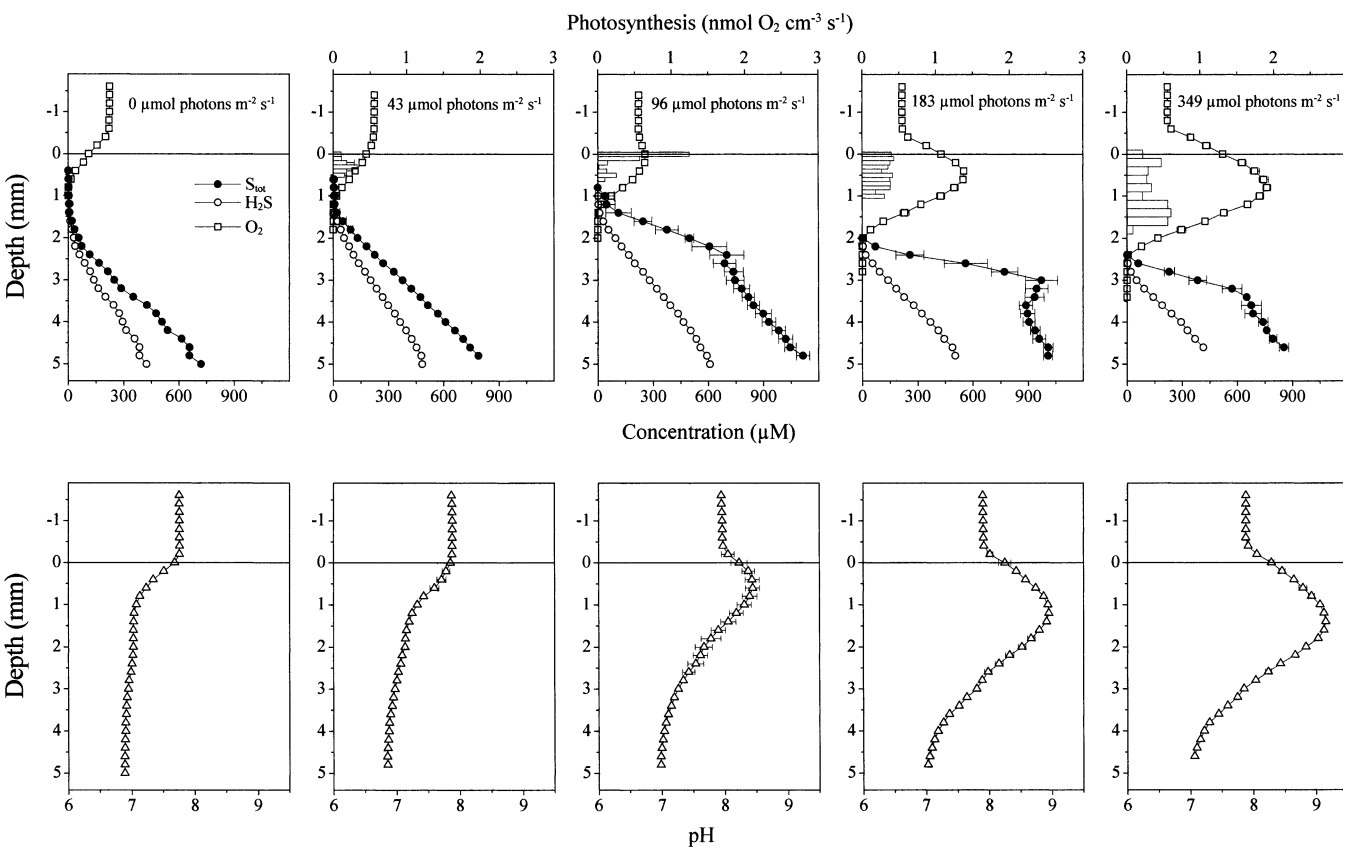

Fig. 8. Average profiles (n = 1–3) of gross photosynthesis (bars), O_2, H_2S, sulfide (S_{tot}) (upper panel) and pH (lower panel) measured at a fixed position in the same mat from Swanbister Bay at increasing downwelling irradiances. Error bars indicate standard deviation.

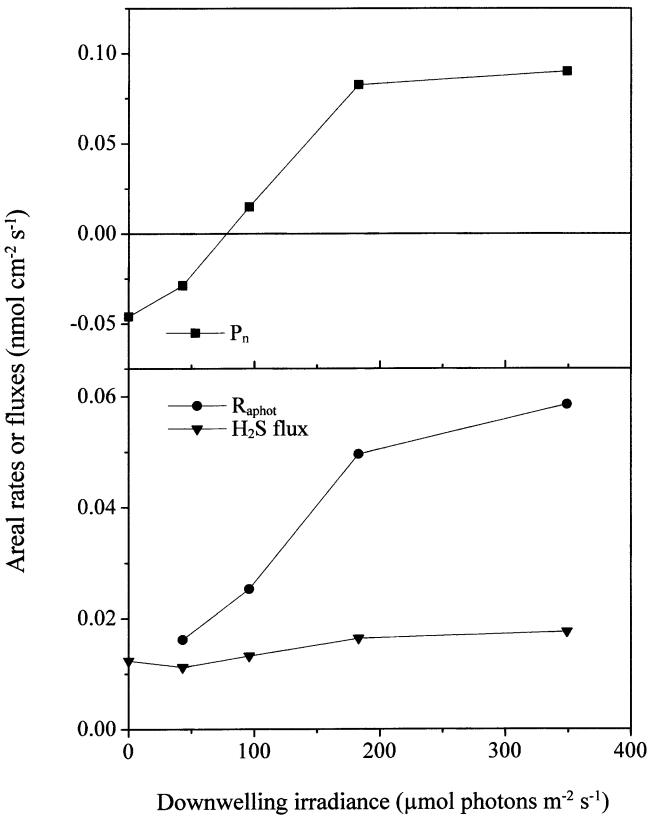

Fig. 9. Areal rates of net photosynthesis (P_n), O_2 consumption in the aphotic zone (R_{aphot}) and of net H_2S production/consumption (H_2S flux) vs irradiance in the Swanbister Bay mat.

pentamethylicosane), as well as fatty acids characteristic of sulfate-reducing bacteria (*iso*- and *anteiso*-pentadecanoic acids) were abundant especially in Swanbister Bay mats (Fig. 1). With our data we can, however, only speculate on the biogeochemical importance of methanogens in the mat. As has been shown in salt marsh sediments (e.g., [66, 76]), methane production in marine sediments is most probably due to utilization of noncompetitive substrates such as methylamines and DMS [43, 65]. Glycine betaine, one of the most widespread compatible solutes [94], and the osmoregulatory compound of marine algae, DMSP [42], present at high concentrations in microbial mats [39, 89], are precursors of trimethylamine and DMS [65]. Thus, these compounds could potentially play a role as substrates for methanogenesis in these mats.

Oxygen and Sulfur Cycling in Swanbister Bay Mats

Microsensor data showed a gradual increase of both O_2 concentration and penetration with irradiance due to increasing oxygenic photosynthesis by cyanobacteria and microalgae in Swanbister Bay mats (Figs. 8, 9). Furthermore, H_2S fluxes tended to increase with irradiance (Fig. 9), indicating higher sulfide turnover rates in light conditions. These include both higher production rates by sulfate reduction and higher sulfide consumption rates. Although (aerobic) chemolithotrophic sulfide oxidation by *T. roseopersicina* may occur in light conditions [70, 71], phototrophic oxidation (in the presence of O_2) seem to be preferred because of higher energetic yields by phototrophy than by chemotrophy [17, 84, 85]. The light dependency of the H_2S fluxes (Fig. 9) further suggests that anoxygenic photosynthesis by purple sulfur bacteria strongly affected net H_2S consumption in light-incubated Swanbister beach mats.

Microsensor data on sulfide cycling underestimate sulfur cycling in microbial mats, since fluxes calculated from microprofiles represent only net rates of sulfide turnover. As has been shown in light-incubated cyanobacterial mats [9, 88, 77], sulfate reduction can occur in the highly oxygenated surface layer. This activity, however, is not detectable with H_2S microsensors because of immediate reoxidation of the produced sulfide. Furthermore, other reduced sulfur compounds, such as polysulfides, elemental sulfur, and thiosulfate, which are present in Swanbister mats [86], may play a significant role in the sulfur cycle of these mats. The dominant purple sulfur bacterium in these mats, *T. roseopersicina*, is characterized by a high metabolic versatility [69, 84] and can use polysulfide [87], thiosulfate [17], and intracellular elemental sulfur [70, 71].

Oxygen consumption rates in the aphotic zone (R_{aphot}) increased with irradiance (Fig. 9). Although H_2S fluxes underestimate sulfide fluxes especially in light conditions (see Results), aerobic/oxic sulfide oxidation seemed not to have significantly contributed to R_{aphot} at higher irradiances. This points to a more important role of other O_2-consuming processes, such as aerobic respiration. T-RFLP analysis together with predicted patterns of T-RFs supplied from the NCBI Bank indicated the presence of aerobic, heterotrophic alpha-proteobacteria in the upper layers of the mat, which could have contributed to O_2 consumption in that zone. As mentioned by Nagashima et al. [60], the detection of these nonphototrophic bacteria with the primer set targeting specifically the *pufM* gene conserved among purple phototrophic bacteria could be due to horizontal gene transfer. T-RFLP analysis also revealed the presence of different communities of SRB in the uppermost layers of Swanbister Bay mats (Fig. 6A). Sul-

fate-reducing bacteria are also characterized by their capacity for aerobic respiration [47, 81] and could have directly contributed to O_2 consumption in these mat layers.

Communities of Sulfate-Reducing and Purple Bacteria in Swanbister Bay Mats

The populations of purple bacteria within the upper millimeters of the Swanbister mat (Figs. 4, 6B, 7C) experienced pronounced variations of microenvironmental conditions between dark–light transitions (Fig. 8). A minor population in the surface layer experienced highly oxic conditions during light periods and micro-oxic conditions during the night, with sulfide being available only during the night at low concentrations (Figs. 7A, 8). Populations in the depth interval between the surface layer and the permanently anoxic zone (Figs. 7C, 8) were only exposed to sulfide during darkness. In light, these populations experience, at least temporarily, simultaneously low O_2 and sulfide concentrations, since the depth of the oxygen–sulfide interface increased with increasing irradiance (Fig. 8). This condition is subsequently followed by exposure to either solely O_2 or sulfide at further increasing or decreasing irradiances. Populations present below this transition zone always experienced sulfide, but may have been light limited (Fig. 4). Thus, the full spectrum of metabolic versatility may be used by different populations of *T. roseopersicina* zonated in the mats. This includes chemolithotrophy during darkness using O_2 and sulfide as substrates, degradation of storage carbohydrates (glycogen) under anoxic dark conditions, photolithotrophy in the light in the presence of only sulfide, of both sulfide and O_2, or of only O_2 using intracellular elemental sulfur or other external reduced sulfur compounds [69, 84].

A pronounced diversity and a depth-dependent distribution of purple bacteria was found by T-RFLP analysis (Fig. 6B). From *pufM* T-RFLP profiles, a T-RF of 93 bp (restriction enzyme *Hae*III) was detected in all mat layers within the top 3 mm of the mat. The sequences of the *pufL* and *pufM* genes of *T. roseopersicina* strain T. ork were recently determined (A. Fourçans, R. Duran, P. Caumette, unpublished; accession number AJ544223), and a predictive T-RF of 92 bp was found for the *pufM* gene of *T. roseopersicina* digested with this restriction enzyme. So, the observed T-RF could correspond to the predominant purple sulfur bacterium *T. roseopersicina*.

The results also show that in Swanbister mats different communities of anoxygenic phototrophs are zonated within the mat in response to the microenvironmental conditions (Fig. 6D). The predominant T-RF of 214 bp obtained with restriction enzyme *Hin*6I represents the dominating anoxygenic phototrophic community in Swanbister beach mats, as deduced from the sequences and T-RFs of purple bacteria presently available. Although predictive digestions made *in silico* on the RDP Web site (TAP: T-RFLP Analysis Program) cannot be used for phylogenetic identification of communities based on their T-RFs [58], this T-RF could be related to the species *Allochromatium vinosum*. The presence of this major species seemed to be independent of depth, O_2 and irradiance (Fig. 6D) and was distributed all over the mat (data not shown). This species was also found by van Gemerden et al. [86]. Further determination of *pufM* gene sequences from isolated purple bacteria will be useful to obtain more information about the dominant members.

Two closely related community clusters of purple bacteria were found in the depth layer from 1 to 3 mm (Fig. 6B), i.e., in the transition layer of the mat. Communities present in this layer experienced pronounced variations, ranging from highly oxic during high light conditions to sulfidic conditions during darkness. These pronounced variations seem to select for versatile species of purple bacteria (also others than *T. roseopersicina*) able to thrive under these conditions. As indicated by T-RFLP analysis, these could include species of the genus *Allochromatium*, which are characterized by a pronounced metabolic versatility [40, 69].

Since microsensor and T-RFLP analyses were not performed in exactly the same Swanbister mat sample, some deviations concerning the localization of this transition layer might have occurred between both samples. Furthermore, the O_2 and sulfide microgradients measured in a laboratory under controlled conditions similar to the conditions during immersion periods might change during emersion periods as occurring *in situ* during low tide. However, our laboratory microsensor data compare relatively well to microsensor profiles measured *in situ* at low tide by van Gemerden et al. [86]. Furthermore, the fact that these two community clusters were less related to the community in the upper mat layers than to the community below 3 mm depth points to an O_2-dependent distribution of purple bacteria in Swanbister Bay mats. This is consistent with the CCA showing that O_2 is the most important variable influencing the distribution of purple bacteria. Thus, despite the predominance of *T. roseopersicina* in these mats, a variety of different

purple bacteria may have stratified in response to O_2 and sulfide gradients.

Also, the distribution and diversity of sulfate-reducing bacteria seemed to be partly influenced by O_2. A distinct and related SRB community cluster was found in the uppermost mat layer, clearly differing from the communities found at increasing depths (Fig. 6A). Thus, the almost permanent oxic conditions in the uppermost mat layer (Figs. 7, 8) may select for especially O_2-tolerant SRB species. Communities of SRB below this layer are exposed to anaerobic conditions at least during low light and dark periods (Figs. 7, 8). Several SRB, e.g., *Desulfovibrio* species and *Desulfonema*-related bacteria, possess adaptive strategies for survival under oxic conditions, enabling them to thrive in microbial mats. These strategies include aggregation, migration, aerotaxis, and O_2 respiration [46, 47, 81, 22, 59, 77, 14].

The CCA demonstrated that factors other than the presence of O_2 also influenced the depth distribution and diversity of SRB. The influence of irradiance at Chl *a* and BChl *a* absorption wavelengths (Fig. 6C) could be the result of interactions between phototrophs and SRB and might be considered as an indirect irradiance effect. The finding of some groups at different depths was not directly correlated with O_2 or sulfide gradients. Sulfate-reducing bacteria are characterized by a pronounced metabolic versatility and are apparently able to catalyze all reactions of a complete sulfur cycle [13, 14]. This includes the use of a variety of electron acceptors such as sulfite, sulfur, thiosulfate, nitrate, nitrite, O_2, and Fe(III), as well as their ability to perform disproportionation and oxidation of diverse sulfur compounds (sulfur, thiosulfate, sulfite), and aerobic respiration [3, 44, 19, 15, 12, 55, 45, 26, 95]. Thus, not only the presence of O_2 and the availability of organic substrates, but also the distribution of sulfur compounds like thiosulfate, sulfur, and sulfite could influence the distribution of SRB in this mat.

Microbial communities of coastal microbial mats on the Orkney Islands are apparently more diverse than previously described. Furthermore, although mats on Swanbister beach could be distinguished concerning population density and localization of the purple layer on or below the mat surface (Figs. 4, 5), a clear differentiation between different microbial mats as found and described earlier [86] was not possible in July 2000. In particular, sediments populated only by purple bacteria and characterized by an absence of Chl *a*–containing oxygenic phototrophs could not be found. This type of mat was previously described as one of the three types of mat systems developing especially on Swanbister beach [86]. The enforcement of strict waste discharge regulations has led to improved wastewater treatment in the area over the past decade, which has significantly reduced the amount of organic matter discharged onto the beaches. These changes have created environmental conditions less favorable for the exclusive development of purple sulfur bacteria, which would also account for the increased microbial diversity in these mat sediments.

Acknowledgements

We acknowledge the financial support by the EC (MAT-BIOPOL project, grant EVK3-CT-1999-00010) and the Danish Natural Science Research Council (M.K., contract no. 9700549). The staff and especially Alex Simpson, Director of the Orkney County Council Marine Unit laboratory, are gratefully acknowledged for providing excellent laboratory facilities. Anni Glud is acknowledged for the construction of the microsensors.

References

1. Achenbach LA, Carey J, Madigan MT (2001) Photosynthetic and phylogenetic primers for detection of anoxygenic phototrophs in natural environments. Appl Environ Microbiol 67:2922–2926
2. Amann RI, Binder BJ, Olson RJ, Chisholm SW, Devereux R, Stahl DA (1990) Combination of 16S rRNA-targeted oligonucleotide probes with flow cytometry for analyzing mixed microbial populations. Appl Environ Microbiol 56:1919–1925
3. Bak F, Cypionka H (1987) A novel type of energy metabolism involving fermentation of inorganic sulphur compounds. Nature 326:891–892
4. Ballantine JA, Lavis A, Morris RJ (1979) Sterols of the phytoplankton—effects of illumination and growth stage. Phytochemistry 18:1459–1466
5. Barbe A, Grimalt JO, Pueyo JJ, Albaigés J (1990) Characterization of model evaporitic environments through the study of lipid components. Org Geochem 16:815–828
6. Béjà O, Suzuki MT, Heidelberg JF, Nelson WC, Preston CM, Hamada T, Eisen JA, Fraser CM, DeLong EF (2002) Unsuspected diversity among marine aerobic anoxygenic phototrophs. Nature 415:630–633
7. Blumer M, Guillard RRL, Chase T (1971) Hydrocarbons of marine phytoplankton. Mar Biol 8:183–189
8. Broecker WS, Peng T-H (1974) Gas exchange rates between air and sea. Tellus 26:21–35

9. Canfield DE, Des Marais DJ (1991) Aerobic sulfate reduction in microbial mats. Science 251:1471–1473
10. Castenholz RW (2001) Phylum BX. Cyanobacteria. Oxygenic photosynthetic bacteria. In: Boone DR, Castenholz RW (Eds.) Bergey's Manual of Systematic Bacteriology. The Archea and the Deeply Branching and Phototrophic Bacteria, vol 1. Springer, Berlin, pp 473–599
11. Chuecas L, Riley JP (1969) Component fatty acids of the total lipids of some marine phytoplankton. J Mar Biol Assoc UK 49:97–116
12. Coleman ML, Hedrick DB, Lovley DR, White DC, Pye K (1993) Reduction of Fe(III) in sediments by sulphate-reducing bacteria. Nature 361:436–438
13. Cypionka H (1994) Novel metabolic capacities of sulfate-reducing bacteria, and their activities in microbial mats. In: Stal LJ, Caumette P (Eds.) Microbial Mats: Structure, Development and Environmental Significance, NATO ASI Series G, vol 35. Springer, Berlin, pp 367–376
14. Cypionka H (2000) Oxygen respiration by *Desulfovibrio* species. Ann Rev Microbiol 54:827–848
15. Dannenberg S, Kroder M, Dilling W, Cypionka H (1992) Oxidation of H_2, organic compounds and inorganic sulfur compounds coupled to reduction of O_2 or nitrate by sulfate-reducing bacteria. Arch Microbiol 158:93–99
16. de Wit R, Jonkers HM, van den Ende FP, van Gemerden H (1989) *In situ* fluctuations of oxygen and sulphide in marine microbial sediment ecosystems. Neth J Sea Res 23:271–281
17. de Wit R, van Gemerden H (1987) Chemolithotrophic growth of the phototrophic sulfur bacterium *Thiocapsa roseopersicina*. FEMS Microbiol Ecol 45:117–126
18. Didyk BM, Simoneit BRT, Brassell SC, Eglinton G (1978) Organic geochemical indicators of palaeoenvironmental conditions of sedimentation. Nature 272:216–222
19. Dilling W, Cypionka H (1990) Aerobic respiration in sulfate-reducing bacteria. FEMS Microbiol Lett 71:123–128
20. Eglinton G, Hamilton RJ (1967) Leaf epicuticular waxes. Science 156:1322
21. Epping EHG, Khalili A, Thar R (1999) Photosynthesis and the dynamics of oxygen consumption in a microbial mat as calculated from transient oxygen microprofiles. Limnol Oceanogr 44:1936–1948
22. Eschemann A, Kühl M, Cypionka H (1999) Aerotaxis in *Desulfovibrio*. Environ Microbiol 1:489–495
23. Fonselius SH (1983) Determination of hydrogen sulphide. In: Grasshoff K, Ehrhardt M, Kremling K (Eds.) Methods of Seawater Analysis. Verlag Chemie, Weinheim, pp 73–80
24. Fossing H, Jørgensen BB (1989) Measurement of bacterial sulfate reduction in sediments: evaluation of a single-step chromium reduction method. Biogeochemistry 8:205–222
25. Fromin N, Hamelin J, Tarnawski S, Roesti D, Jourdain-Miserez K, Forestier N, Teyssier-Cuvelle S, Gillet F, Aragno M, Rossi P (2002) Statistical analysis of denaturing gel electrophoresis (DGE) fingerprinting patterns. Environ Microbiol 4:634–643
26. Fuseler K, Krekeler D, Sydow U, Cypionka H (1996) A common pathway of sulfide oxidation by sulfate-reducing bacteria. FEMS Microbiol Lett 144:129–134
27. García HE, Gordon LI (1992) Oxygen solubility in seawater: Better fitting equations. Limnol Oceanogr 37:1307–1312
28. Grant J, Gust G (1987) Prediction of coastal sediment stability from photopigment content of mats of purple sulphur bacteria. Nature 330:244–246
29. Grimalt JO, de Wit R, Teixidor P, Albaiges J (1992) Lipid biogeochemistry of *Phormidium* and *Microcoleus* mats. Org Geochem 19:509–530
30. Han J, McCarthy ED, Calvin M, Benn MH (1968) Hydrocarbon constituents of the blue-green algae *Nostoc muscorum*, *Anacystis nidulans*, *Phormidium luridum* and *Chlorogloea fritschii*. J Chem Soc C:2785–2791
31. Herbert RA (1985) Development of mass blooms of photosynthetic bacteria on sheltered beaches in Scapa Flow, Orkney Islands. Proc Roy Soc Edinburgh 87B:15–25
32. Hershey JP, Plese T, Millero FJ (1988) The pK_1* for the dissociation of H_2S in various ionic media. Geochim Cosmochim Acta 52:2047–2051
33. Hoffmann C (1942) Beiträge zur Vegetation des Farbstreifen-Sandwattes. Kieler Meeresforschungen Sonderheft 4:85–108
34. Holzer G, Oro J, Tornabene TG (1979) Gas chromatographic–mass spectrometric analysis of neutral lipids from methanogenic and thermoacidophilic bacteria. J Chromatogr 186:795–809
35. Isaksen M, Finster K (1996) Sulfate reduction in the root zone of the sea grass *Zostera noltii* on the intertidal flats of a coastal lagoon (Arcachon, France). Mar Ecol Prog Ser 137:187–194
36. Jeroschewski P, Steuckart C, Kühl M (1996) An amperometric microsensor for the determination of H_2S in aquatic environments. Anal Chem 68:4351–4357
37. Jonkers HM, de Bruin S, van Gemerden H (1998) Turnover of dimethylsulfoniopropionate (DMSP) by the purple sulfur bacterium *Thiocapsa roseopersicina* M11: ecological implications. FEMS Microbiol Ecol 27:281–290
38. Jonkers HM, Jansen M, Van der Maarel MJEC, van Gemerden H (1999) Aerobic turnover of dimethyl sulfide by the anoxygenic phototrophic bacterium *Thiocapsa roseopersicina*. Arch Microbiol 172:150–156
39. Jonkers HM, Koopmans GF, van Gemerden H (1998) Dynamics of dimethyl sulfide in a marine microbial mat. Microb Ecol 36:93–100
40. Kämpf C, Pfennig N (1980) Capacity of Chromatiaceae for chemotrophic growth. Specific respiration rates of *Thiocystis violacea* and *Chromatium vinosum*. Arch Microbiol 127:125–135
41. Kates M, Tremblay P, Anderson R, Volcani BE (1978) Identification of the free and conjugated sterol in a non-photosynthetic diatom, *Nitzschia alba*, as 24-methylene cholesterol. Lipids 13:34–41

42. Kelly DP, Smith NA (1990) Organic sulfur compounds in the environment. Adv Microb Ecol 11:345–385
43. King GM (1984) Utilisation of hydrogen, acetate and "non-competitive" substrates by methanogenic bacteria in marine sediments. Geomicrobiol J 3:275–306
44. Krämer M, Cypionka H (1989) Sulfate formation via ATP sulfurylase in thiosulfate- and sulfite-disproportionating bacteria. Arch Microbiol 151:232–237
45. Krekeler D, Cypionka H (1995) The preferred electron acceptor of *Desulfovibrio desulfuricans* CSN. FEMS Microbiol Ecol 17:271–278
46. Krekeler D, Sigalevich P, Teske A, Cypionka H, Cohen Y (1997) A sulfate-reducing bacterium from the oxic layer of a microbial mat from Solar Lake (Sinai), *Desulfovibrio oxyclinae* sp. nov. Arch Microbiol 167:369–375
47. Krekeler D, Teske A, Cypionka H (1998) Strategies of sulfate-reducing bacteria to escape oxygen stress in a cyanobacterial mat. FEMS Microbiol Ecol 25:89–96
48. Kühl M, Fenchel T (2000) Bio-optical characteristics and the vertical distribution of photosynthetic pigments and photosynthesis in an artificial cyanobacterial mat. Microb Ecol 40:85–93
49. Kühl M, Jørgensen BB (1992) Spectral light measurements in microbenthic phototrophic communities with a fiber-optic microprobe coupled to a sensitive diode array detector. Limnol Oceanogr 37:1813–1823
50. Kühl M, Steuckart C, Eickert G, Jeroschewski P (1998) A H_2S microsensor for profiling biofilms and sediments: application in an acidic lake sediment. Aquat Microb Ecol 15:201–209
51. Kumar S, Tamura K, Jakobsen IB, Nei M (2001) MEGA2: Molecular evolutionary genetics analysis software, Bioinformatics
52. Lassen C, Ploug H, Jørgensen BB (1992) A fibre-optic scalar irradiance microsensor: Application for spectral light measurements in sediments. FEMS Microbiol Ecol 86:247–254
53. Li Y-H, Gregory S (1974) Diffusion of ions in sea water and in deep-sea sediments. Geochim Cosmochim Acta 38:703–714
54. Liu WT, Marsh TL, Cheng H, Forney LJ (1997) Characterization of microbial diversity by determining terminal restriction fragment length polymorphisms of genes encoding 16S rRNA. Appl Environ Microbiol 63:4516–4522
55. Lovley DR, Phillips EJP (1994) Novel processes for anaerobic sulfate production from elemental sulfur by sulfate-reducing bacteria. Appl Environ Microbiol 60:2394–2399
56. Maidak BL, Cole JR, Lilburn TG, Parker CTJ, Saxman PR, Farris RJ, Garrity GM, Olsen GJ, Schmidt TM, Tiedje JM (2001) The RDP-II (Ribosomal Database Project). Nucleic Acids Res 29:173–174
57. Marlowe IT, Brassell SC, Eglinton G, Green JC (1984) Long chain unsaturated ketones and esters in living algae and marine sediments. Org Geochem 6:135–141
58. Marsh TL, Saxman P, Cole J, Tiedje J (2000) Terminal restriction fragment length polymorphism analysis program, a web-based research tool for microbial community analysis. Appl Environ Microbiol 66:3616–3620
59. Minz D, Flax JL, Green SJ, Muyzer G, Cohen Y, Wagner M, Rittmann BE, Stahl DA (1999) Diversity of sulfate-reducing bacteria in oxic and anoxic regions of a microbial mat characterized by comparative analysis of dissimilatory sulfite reductase genes. Appl Environ Microbiol 65:4666–4671
60. Nagashima KVP, Hiraishi A, Shimada K, Matsuura K (1997) Horizontal transfer of genes coding for the photosynthetic reaction centers of purple bacteria. J Mol Evol 45:131–136
61. Nes WR, McKean ML (1977) Biogeochemistry of Steroids and Other Isoprenoids. University Park Press, Baltimore
62. Nichols PD, Volkman JK, Palmisano AC, Smith GA, White DC (1988) Occurrence of an isoprenoid C_{25} diunsaturated alkene and high neutral lipid content in Antarctic sea-ice diatom communities. J Phycol 24:90–96
63. Nishimura M, Koyama T (1977) The occurrence of stanols in various living organisms and the behaviour of sterols in contemporary sediments. Geochim Cosmochim Acta 41:379–385
64. Orcutt DM, Paterson GW (1975) Sterol, fatty acid and elemental composition of diatoms grown in chemically defined media. Comp Biochem Physiol 506:579–583
65. Oremland RS, King GM (1989) Methanogenesis in hypersaline environments. In: Cohen Y, Rosenberg E (Eds.) Microbial Mats: Physiological Ecology of Benthic Microbial Communities. American Society for Microbiology, Washington DC, pp 180–190
66. Oremland RS, Marsh LM, Polcin S (1982) Methane production and simultaneous sulfate reduction in anoxic, salt marsh sediments. Nature 296:143–145
67. Paoletti C, Pushparaj B, Florenzano G, Capella P, Lercker G (1976) Unsaponifiable matter of green and blue-green algal lipids as a factor of biochemical differentiation of their biomass: II. Terpenic alcohol and sterol fractions. Lipids 11:266–271
68. Patterson GW (1974) Sterols of some green algae. Comp Biochem Physiol 47B:453–457
69. Pfennig N, Trüper HG (1992) The family Chromatiaceae. In: Balows A, Trüper HG, Dworkin M, Harder W, Schleifer K-H (Eds.) The Prokaryotes. Springer, Berlin, pp 3200–3221
70. Pringault O, de Wit R, Caumette P (1996) A benthic gradient chamber for culturing phototrophic sulfur bacteria on reconstituted sediments. FEMS Microbiol Ecol 20:237–250
71. Pringault O, de Wit R, Kühl M (1999) A microsensor study of the interaction between purple sulfur and green sulfur bacteria in experimental benthic gradients. Microb Ecol 37:173–184
72. Revsbech NP (1989) An oxygen microelectrode with a guard cathode. Limnol Oceanogr 34:474–478
73. Revsbech NP, Jørgensen BB (1983) Photosynthesis of benthic microflora measured with high spatial resolution by the

oxygen microprofile method: Capabilities and limitations of the method. Limnol Oceanogr 28:749–756
74. Revsbech NP, Jørgensen BB (1986) Microelectrodes: Their use in microbial ecology. Adv Microb Ecol 9:293–352
75. Schouten S, van der Maarel MEJ, Huber R, Sinninghe Damsté JS (1997) 2,6,10,15,19-Pentamethylicosenes in *Methanolobus bombayensis*, a marine methanogenic archaeon and *Methanosarcina mazei*. Org Geochem 26:409–414
76. Senior E, Lindstrom EB, Banat I, Nedwell DB (1982) Sulfate reduction and methanogenesis in the sediment of a saltmarsh on the east coast of the United Kingdom. Appl Environ Microbiol 43:987–996
77. Sigalevich P, Meshorer E, Helman Y, Cohen Y (2000) Transition from anaerobic to aerobic growth conditions for the sulfate-reducing bacterium *Desulfovibrio oxyclinae* results in flocculation. Appl Environ Microbiol 66:5005–5012
78. Skyring GW (1987) Sulfate reduction in coastal ecosystems. Geomicrobiol J 5:295–374
79. Stal LJ, van Gemerden H, Krumbein WE (1985) Structure and development of a benthic marine microbial mat. FEMS Microbiol Ecol 31:111–125
80. Tabatabai MA (1974) Determination of sulfate in water samples. Sulfur Inst J 10:11–14
81. Teske A, Ramsing NB, Habicht K, Fukui M, Küver J, Jørgensen BB, Cohen Y (1998) Sulfate-reducing bacteria and their activities in cyanobacterial mats of Solar Lake (Sinai, Egypt). Appl Environ Microbiol 64:2943–2951
82. Tornabene TG, Langworthy TA, Holzer G, Oro J (1979) Squalenes, phytanes and other isoprenoids as major neutral lipids of methanogenic and thermoacidophilic "archaebacteria." J Mol Evol 13:73–83
83. Ullman WJ, Aller RC (1982) Diffusion coefficients in nearshore marine sediments. Limnol Oceanogr 27:552–556
84. van Gemerden H (1993) Microbial mats: a joint venture. Mar Geol 113:3–25
85. van Gemerden H, de Wit R, Tughan CS, Herbert RA (1989a) Development of mass blooms of *Thiocapsa roseopersicina* on sheltered beaches on the Orkney Islands. FEMS Microbiol Ecol 62:111–118
86. van Gemerden H, Tughan CS, de Wit R, Herbert RA (1989b) Laminated microbial ecosystems on sheltered beaches in Scapa Flow, Orkney Islands. FEMS Microbiol Ecol 62:87–102
87. Visscher PT, Nijburg JW, van Gemerden H (1990) Polysulfide utilization by *Thiocapsa roseopersicina*. Arch Microbiol 155:75–81
88. Visscher PT, Prins RA, van Gemerden H (1992) Rates of sulfate reduction and thiosulfate consumption in a marine microbial mat. FEMS Microbiol Ecol 86:283–294
89. Visscher PT, Quist P, van Gemerden H (1991) Methylated sulfur compounds in microbial mats: in situ concentrations and metabolism by a colorless sulfur bacterium. Appl Environ Microbiol 57(6):1758–1763
90. Visscher PT, van Gemerden H (1991) Photo-autotrophic growth of *Thiocapsa roseopersicina* on dimethyl sulfide. FEMS Microbiol Lett 81:247–250
91. Vogel AI (1978) Textbook of Practical Organic Chemistry. Longman, New York
92. Volkman JK, Eglinton G, Corner EDS, Sargent JR (1980) Novel unsaturated straight-chain C_{37}–C_{39} methyl and ethyl ketones in marine sediments and a coccolithophore *Emiliania huxleyi*. Adv Org Geochem 1979:219–227
93. Volkman JK, Jeffrey SW, Nichols PD, Rogers GI, Garland CD (1989) Fatty acids and lipid composition of 10 species of microalgae used in mariculture. J Exp Mar Biol Ecol 128:219–240
94. Welsh DT (2000) Ecological significance of compatible solute accumulation by microorganisms: from single cells to global climate. FEMS Microbiol Rev 24:263–290
95. Widdel F (1988) Microbiology and ecology of sulfate- and sulfur-reducing bacteria. In: Zehnder AJB (Eds.) Biology of Anaerobic Microorganisms. John Wiley, New York, pp 469–585
96. Wieland A, Kühl M (2000) Irradiance and temperature regulation of oxygenic photosynthesis and O_2 consumption in a hypersaline cyanobacterial mat (Solar Lake, Egypt). Mar Biol 137:71–85
97. Wieland A, Kühl M (2000) Short-term temperature effects on oxygen and sulfide cycling in a hypersaline cyanobacterial mat (Solar Lake, Egypt). Mar Ecol Prog Ser 196:87–102
98. Wieringa EBA, Overmann J, Cypionka H (2000) Detection of abundant sulphate-reducing bacteria in marine oxic sediment layers by a combined cultivation and molecular approach. Environ Microbiol 2:417–427

SCANNING VOL. 27, 176–180 (2005)

Received: December 1, 2004
Accepted with revision: May 6, 2005

Characterization of an Oil-Degrading *Microcoleus* Consortium by Means of Confocal Scanning Microscopy, Scanning Electron Microscopy and Transmission Electron Microscopy

ELIA DIESTRA, ANTONIO SOLÉ, MERCEDES MARTÍ,* TIRSO GARCIA DE OTEYZA,† JOAN O. GRIMALT,† ISABEL ESTEVE

Department of Genetics and Microbiology, Autonomous University of Barcelona, and *Microscopy Service, Autonomous University of Barcelona, Bellatera; †Department of Environmental Chemistry (IIQAB-CSIC), Barcelona, Spain

Summary: A consortium of microorganisms with the capacity to degrade crude oil has been characterized by means of confocal laser scanning microscopy (CLSM), transmission electron microscopy (TEM), and scanning electron microscopy (SEM). The analysis using CLSM shows that *Microcoleus chthonoplastes* is the dominant organism in the consortium. This cyanobacterium forms long filaments that group together in bundles inside a mucopolysaccharide sheath. Scanning electron microscopy and transmission electron microscopy have allowed us to demonstrate that this cyanobacterium forms a consortium primarily with three morphotypes of the heterotrophic microorganisms found in the *Microcoleus chthonoplastes* sheath. The optimal growth of *Microcoleus* consortium was obtained in presence of light and crude oil, and under anaerobic conditions. When grown in agar plate, only one type of colony (green and filamentous) was observed.

Key words: *Microcoleus* consortium, confocal laser scanning microscopy, transmission electron microscopy, scanning electron microscopy, crude oil

PACS: 07.78.+s, 0.7.79.-v, 61.16.Bg, 61.16. Ch, 87.64.Dz

Introduction

Microbial mats are benthic stratified microbial communities in which different microorganisms are closely packed in a very thin layer (15 mm) which covers the sediment. These mats are found throughout the world and are formed primarily by cyanobacteria (oxygenic phototrophic microorganisms), which are responsible for the primary production of these ecosystems (Stal 1995). Confocal laser scanning microscopy (CLSM), scanning electron microscopy (SEM), and transmission electron microscopy (TEM) have been used repeatedly to characterize the forming of these communities.

Confocal laser scanning microscopy has been used successfully for identifying filamentous cyanobacteria. Two-dimensional (2-D) and three-dimensional (3-D) images have been used for visualizing cyanobacetria filaments at depth. Cyanobacteria emit natural autofluorescence which makes it possible to examine the cells in situ, minimizing the samples treatment (Fourçans *et al.* 2004, Solé *et al.* 2001, Wieland *et al.* 2003).

Due to their high-resolution capabilities, SEM and TEM have often been used for characterizing the overall biodiversity of natural microbial communities (Esteve *et al.* 1994, Mir and Esteve 1992, Stolz 1994).

Although molecular techniques are also regularly applied to study biodiversity in microbial mats, these techniques may give rise to difficulties in the case of cyanobacteria with thick polysaccharide sheaths (López-Cortés *et al.* 2001). Cyanobacteria in natural environments usually form a consortium with different populations of microorganisms. Consortium interactions mediate mutually beneficial cycling of potentially limiting nutrients. The mutual benefits are also evident in culture experiments, in which cyanobacterial hosts and bacterial epiphytes promote each other's growth (Paerl *et al.* 1994) and could potentially improve degradation of complex environmental contaminants such as a crude oil.

Previous studies carried out by Al-Hasan *et al.* (1994, 1998) indicate that cyanobacterial microbial mats develop extensively after oil spills as seen in Kuwait following the first Gulf war.

In the wake of these studies, our group started a project to determine the role of cyanobacterial mats on oil degradation in natural environments. During this study, we established several microcosms in which the effect of oil pollution on the structure of the cyanobacterial communities was thoroughly studied. From these microcosms a consortium of microorganisms was isolated capable of degrading crude oil (Garcia de Oteyza *et al.* 2004).

This research was supported by Spanish grant DGICYT BOS2001-2033.

Address for reprints:

Elia Diestra
Department of Genetics and Microbiology
Autonomous University of Barcelona
08193 Bellaterra, Spain
e-mail: elia.diestra@uab.es

In the present study, we applied CLSM, SEM, and TEM to characterize the microorganisms that form the above-mentioned consortium.

Materials and Methods

Sample Treatment and Growth Conditions

Artificial microcosms, which simulate marine microbial mats, were prepared in polypropylene boxes according to the method described by Llirós *et al*. 2003. Some of these microcosms were polluted with crude oil after inoculation with samples of microbial mat obtained from the Ebro delta. After 2 months, samples were taken from these microcosms to obtain cyanobacteria cultures with the capacity to degrade crude oil.

Cyanobacteria enrichment cultures were obtained by introducing a portion of the microbial mat into mineral Pfenning medium (van Gemerden and Beeftink 1993) and containing 3% (v/v) of Maya crude oil. Cultures were grown in anoxic conditions and incubated in the light at 15 $\mu Em^{-2}s^{-1}$ and 27ºC. *Microcoleus* consortium cultures were obtained in liquid medium from the enrichment cultures, using the procedure described above. This consortium was also grown in a solid medium covered with 150 µl of crude oil. The plates were incubated in anaerobic jars under the conditions already mentioned.

To illustrate the role of the consortium in oil degradation, different experiments were carried out. Culture aliquots from the previously described consortium were growing both in presence and absence of light, carbonates, and crude oil. Aerobic and anaerobic conditions were also tested.

Colonies of the consortium obtained on agar plates as well as growth liquid medium were characterized by means of CLSM, SEM, and TEM.

Confocal Laser Scanning Microscopy

Samples were taken from liquid cultures and agar plates and analyzed by CLSM in accordance with the method described by Solé *et al.* (1998). Samples were viewed in a Leica true confocal scanner TCS 4d (Leica Laser-Technik GmbH, Heidelberg, Germany).These were excited with a 568 nm line from a laser argon krypton. The fluorescence was captured with a long-pass 590 filter. Twenty focal planes were obtained from 20 µm thickness. Later, applying the confocal software summa, projections and stereoscopic images were obtained (with 2-D and 3-D information, respectively). The 2-D and 3-D images were used to follow the filaments of *Microcoleus chthonoplastes* in depth.

Scanning Electron Microscopy

For SEM, samples were fixed in 2.5% glutaraldehyde and washed in buffer phosphate according to Miloning (1961). They were then centrifuged and dehydrated in successively increasing concentrations of acetone (30, 50, 70, and 100%). Subsequently, the samples were processed according to the method described by Nogués *et al*. (1994) (this method describes the use of specific capsules in which the sample is placed and then dehydrated without loss or alteration) and dried by critical-point drying. Finally, all samples were mounted on metal stubs, coated (thus avoiding charging the samples and ensuring good image quality) with a 96 nm layer of gold (this ensures better secondary-electron emission and, therefore, better image quality). The images were viewed with a Hitachi S-570 scanning electron microscope (Hitachi Ltd., Tokyo, Japan).

Transmission Electron Microscopy

For thin sectioning, samples from liquid and solid media were suspended in 2.5% glutaraldehyde sodium cacodylate buffer (0.1M; pH 7.4) for 2 h, according to Esteve *et al.* (1990). The samples were washed in the same buffer, post-fixed with 1% OsO_4 (at 4ºC for 2 h) and washed three times in the same buffer. Samples were centrifuged at 5,000 xg for 10 min and the pellet obtained was mixed with an equal volume of 2% pure agar. The agar was cut into small cubes, dehydrated in a graded series (30, 50, 70, 100%) of acetone, and then rinsed twice in 100% propylene oxide. Finally, samples were embedded in Spurr resin. An LKB ultramicrotome was used for sectioning (LKG, Bromma, Sweden). Ultrathin sections were mounted on carbon-coated grids, stained with saturated uranyl acetate and Reynolds lead citrate (Reynolds 1963) and viewed in a Hitachi H-7000 transmission electron microscope (Hitachi Ltd).

For size determination of heterotrophic bacteria, a total of 300 measurements were made, taken directly from the printed images at a final enlargement of ×4600.

Results and Discussion

Cultures of the consortium were obtained from samples taken from microcosms polluted with Maya crude oil, as described in Materials and Methods.

In Figure 1a, dense masses of the consortium can be seen fixed to the oil by means of a matrix of polysaccharides. In the same way, colonies of this consortium (irregular in shape and greenish in color) (Fig. 1b) and cell lawns (Fig.1c) were obtained by growing them in a solid medium polluted with oil.

Confocal laser scanning microscopy was used to characterize the cyanobacterium forming the consortium. Long trichomes can be observed between the droplets of oil (Fig. 1d). The trichomes can be seen to be made up of cells that are greater in length than width (3 µm in diameter), with visible constrictions at the cross walls; the mature end cells are conical. According to Castenholz (2001), this cyanobacterium has been identified as *Microcoleus*

chthonoplastes (Fig 1e). *Microcoleus chthonoplastes* was identified before and after adding oil.

In addition, electron microscopy techniques (SEM and TEM) were used to determine whether *Microcoleus chthonoplastes* was the only microorganism responsible for the formation of colonies, or whether this was found in association with other microorganisms inside the sheath. The images obtained by SEM indicate the presence of small bacilli attached to the exopolysaccharide (EPS) sheaths of the cyanobacterium (Fig. 2c). Ultrathin sections of the same samples show the presence of *Microcoleus chthonoplastes* and the thylakoids inside the cells (Fig. 2a), which are membranous structures containing the photosynthetic pigments. Although it is not a taxonomic characteristic, the presence of highly electrondense inclusions in the majority of the cells analyzed should also be noted (Fig. 2b). We have still not ascertained the nature of these inclusions, but some authors have described similar structures in other microorganisms growing in the presence of oil (Singer and Finnerty 1984).

In addition to *Microcoleus* filaments, SEM images also show the presence of three morphotypes of heterotrophic bacteria inside the cyanobacterial sheath (Fig. 2d). The average TEM diameters were type I (0.30 μm; standard deviation, 0.033); type II (0.22 μm; standard deviation, 0.026); and type III (0.50 μm; standard deviation, 0.060). Their relative abundance was 76.5, 15.5, and 8.0%, respectively.

The consortium described was grown under different culture conditions (Table I). As can been seen in this table, although the consortium may also grow in the absence of oil, the optimal growth occurred in the presence of light and crude oil, and under anaerobic conditions.

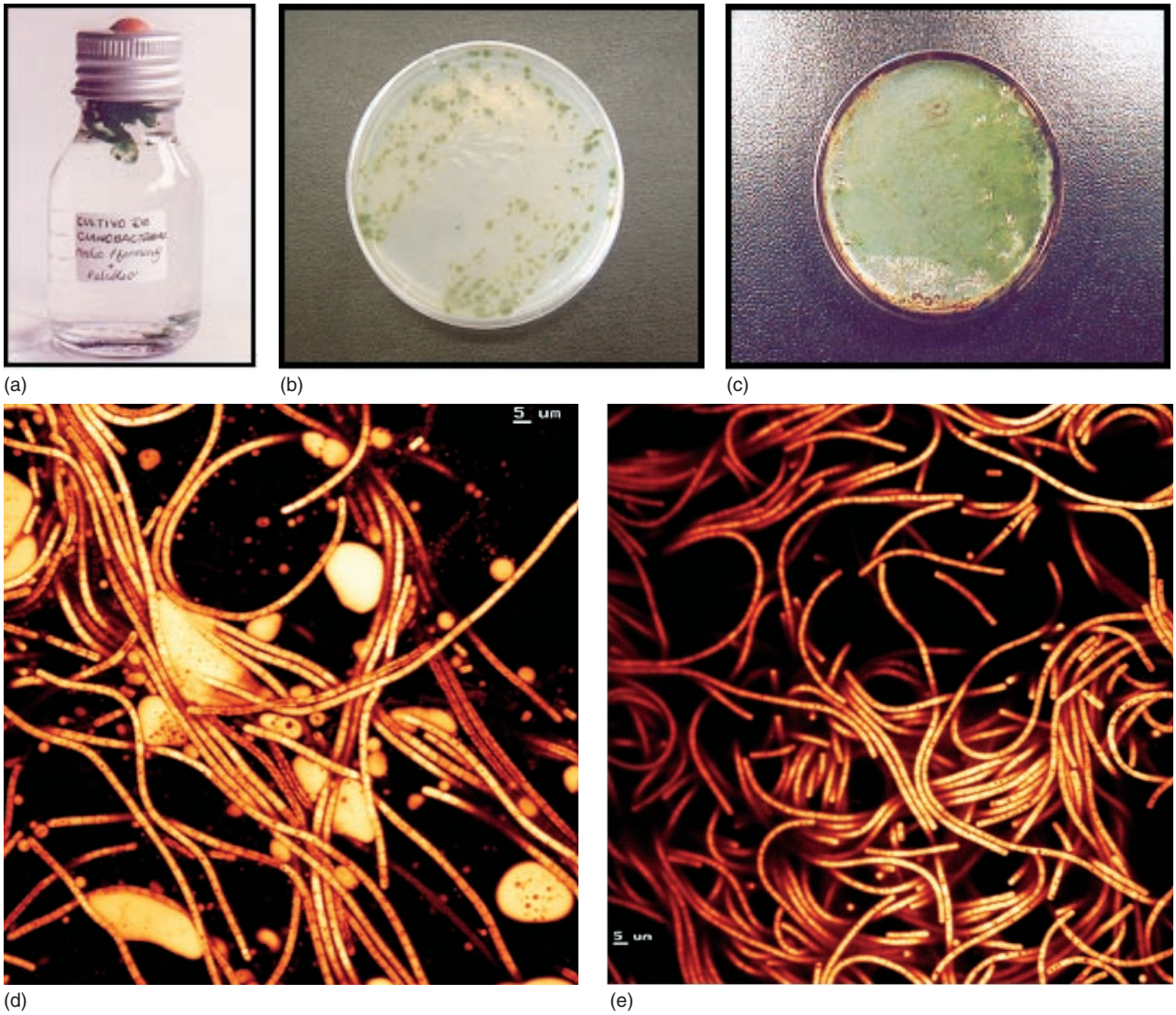

Fig. 1 (a) The *Microcoleus* consortium growing in liquid cultures attached to crude oil. (b) The *Microcoleus* consortium growing in agar plates, forming colonies. (c) Cell lawns of *Microcoleus chthonoplastes* in polluted solid media. (d) Confocal laser scanning microscopy (CLSM) image showing the filaments of *Microcoleus chthonoplastes* in polluted liquid media. (e) A CLSM image showing the filaments of *Microcoleus chthonoplastes.*

TABLE 1 Cultures of *Microcoleus* consortium under different growth conditions

Light	O_2	Carbon source		Growth
		CO_3	Crude oil	
+	–	–	+	++++
+	+	–	+	++
+	–	–	+	+
+	+	+	–	+
–	–	–	+	–
–	+	+	–	–
–	–	+	–	–
–	+	–	+	–

The consortium grew in the presence of light, which it means that the consortium's heterotrophic depended on the growth of *Microcoleus chthonoplastes* for its own growth. Furthermore, no growth whatsoever is detected in the absence of light.

Table I, also shows that the consortium can grow both aerobically and anaerobically. Similar studies into the growth of *Microcoleus chthonoplastes* in natural environments demonstrated that this cyanobacterium can carry out oxygenic and anoxygenic photosynthesis (Solé *et al.* 2003).

Concerning the carbon source, the consortium grew in the presence of carbonates as well as of crude oil; nevertheless, the oil provided the optimum growth for the con-

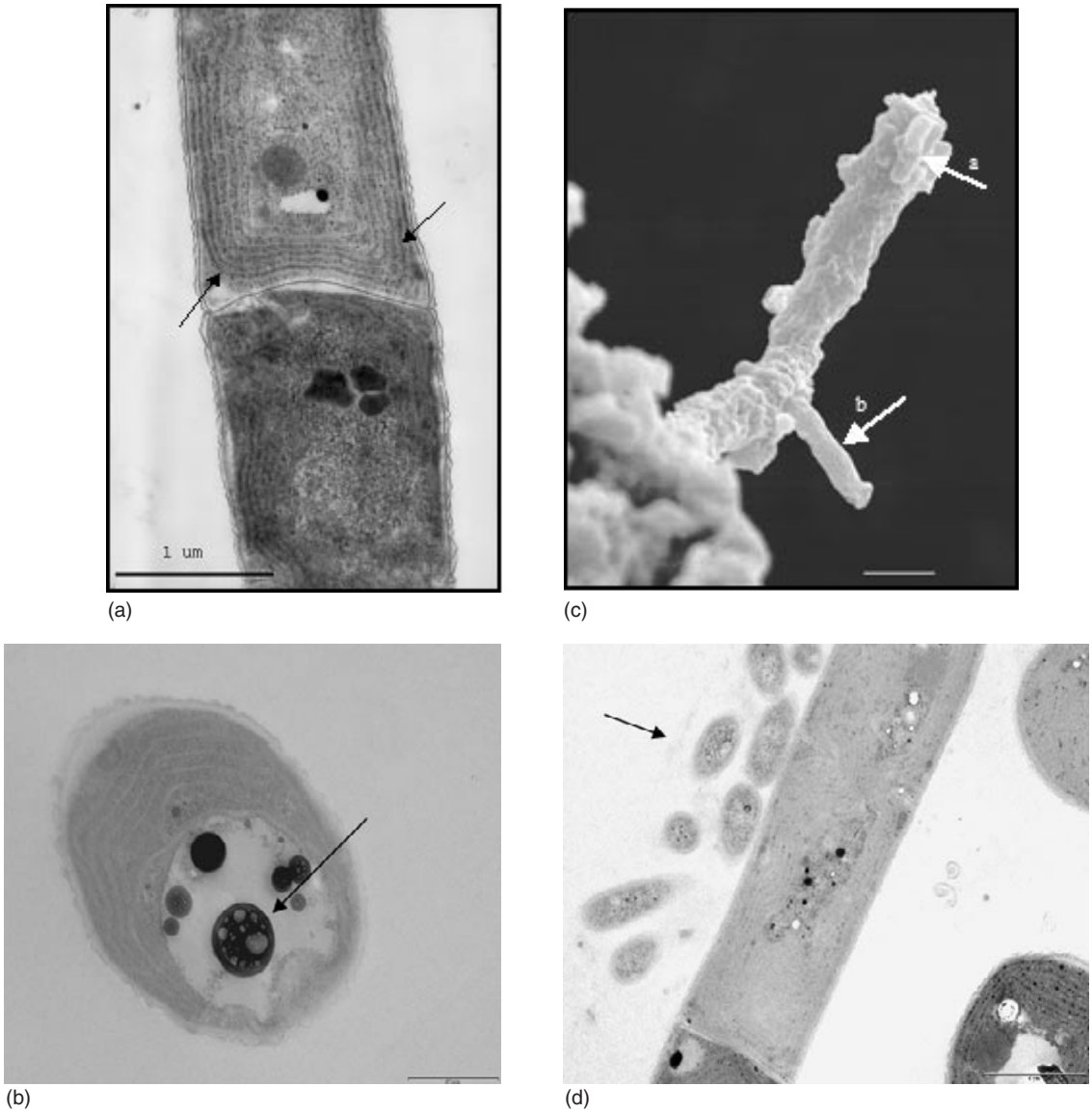

Fig. 2 (a) Ultrathin sections of *Microcoleus chthonoplastes*; the thylakoids are indicated by arrows. Scale bar = 1 µm. (b) Ultrathin sections of *Microcoleus chthonoplastes* from polluted liquid media. The electrondense inclusions organules inside the cell are indicated by arrows. Scale bar = 500 nm. (c) Scanning electron microscopy micrography of *Microcoleus chthonoplastes* surrounded by heterotrophic microorganisms (a and b). Scale bar = 1µm. (d) Ultrathin sections of *Microcoleus chthonoplastes* with the majority of heterotrophic bacteria surrounded by exopolysaccharide (indicated by arrow). Scale bar = 1µm.

sortium. We recently demonstrated that the consortium is essentially involved in degradation of aliphatic heterocyclic organo-sulphur compounds, such as alkylthiolanes and alkylthianes. Other groups of compounds, such as the alkylated monocyclic and polycyclic aromatic hydrocarbons carbazoles, benzothiophenes and dibenzothiophenes, also underwent some degree of transformation, involving only the more volatile and less alkylated homologues (Garcia de Oteyza *et al.* 2004).

The use of different high-resolution microscopy techniques allowed us not only to characterize the microorganisms that form the consortium but also to determine their position (inside the mucilages surrounding *Microcoleus chthonoplastes*), morphology, and relative abundance.

Confocal laser scanning microscopy has been acknowledged as especially suited to characterizing cyanobacteria, both in cultures and natural environments (Diestra *et al.* 2004, Solé *et al*. 2003), as the samples do not require any manipulation. On the other hand, SEM and TEM (most particularly the latter) allowed us to determine the relative abundance of each of the microorganisms in the consortium. The microorganisms were identified as heterotrophs through their morphometrical characteristics and through the absence of the intra-cytoplasmatic membranes that characterize phototrophic microorganisms.

This consortium has the added interest of being capable of degrading Maya crude oil, rich in sulphur and aromatic compounds, which is potentially more harmful to marine ecosystems than other oils (Garcia de Oteyza *et al.* 2004).

Acknowledgments

The authors express their thanks to the staff of the Servei de Microscòpia at the Autonomous University of Barcelona for technical assistance with the electron microscopy. They also thank J. Mas for his help in discussing this work.

References

Al-Hasan RH, Sorkhoh NA, Al-Bader D, Radwan, SS: Utilization of hydrocarbons by cyanobacteria from microbial mats on oily coasts of the Gulf. *Appl Microbiol Biotechnol* 41**,** 615–619 (1994)

Al-Hasan RH, Al-Bader D, Sorkhoh NA, Radwan S: Evidence for *n*-alkane consumption and oxidation by filamentous cyanobacteria from oil-contaminated coasts of the Arabian Gulf. *Mar Biol* 130, 521–527 (1998)

Castenholz RW: Phylum BX Cyanobacteria. Oxygenic Photosynthetic Bacteria. *In: Bergey's Manual Systematic Bacteriology. Vol 1. The Archea and Deeply Branching and Phototrophic Bacteria,* 2nd ed. (Eds. Boone DR, Castenholz RW, Garrity GM). Springer-Verlag, New York 1, (2001) 473–599

Diestra E, Solé A, Esteve I: A comparative study of cyanobacterial diversity in polluted microbial mats by means CLSM. *Ophelia* 58, 3, 151–156 (2004)

Esteve I, Montesinos E, Mitchell JG, Guerrero R: A quantitative ultrastructural study of *Chromatium minus* in the bacterial layer of Lake Cisó (Spain). *Arch Microbiol* 153, 316–323 (1990)

Esteve I, Ceballos D, Martínez-Alonso M, Gaju N, Guerrero R: Development of versicolored microbial mats: Succession environmental significance. In *Microbial Mats: Structure, Development and Environmental Significance*. NATO ASI Series G: Ecological Sciences (Eds. Stal L, Caumette P). Springer-Verlag, Heidelberg 35, (1994) 4165–4420

Fourçans A, Garcia de Oteyza T, Wieland A, Solé A, Diestra E, van Bleijswijk J, Grimalt JO, Kühl M, Esteve I, Muyzer G, Caumette P, Durán R: Characterization of functional bacterial groups in a hypersaline microbial mat community (Saline-de-Giraud, Camargue, France). *FEMS Microbial Ecol* 51/1, 55–70 (2004)

Garcia de Oteyza T, Grimalt JO, Diestra E, Solé A, Esteve, I: Changes in the composition of polar and apolar crude oil fractions under the action of *Microcoleus* consortium. *Appl Microbiol Biotechnol* 66, 226–232 (2004)

Llirós M, Munill X, Solé A, Martínez-Alonso M, Diestra E, Esteve I: Analysis of cyanobacteria biodiversity in pristine and non polluted microbial mats in microcosms by confocal laser scanning microscopy (CLSM). In *Science, Technology and Education of Microscopy*: An Overview (Ed. Mendez-Vilas A). FORMATEX Microscopy Book Series. Vol 1. (2003) 483–489

López-Cortés A, Garcia-Pichel F, Nübel U, and Vázquez-Juárez R: Cyanobacterial diversity in extremal environments in Baja California, México: a polyphasic study. *Int Microbiol* 4, 227–236 (2001)

Miloning G: Advantages of a phosphate buffer OsO_4 solutions in fixation. *J Appl Phys* 32, 1637 (1961)

Mir J, Esteve I: The SEM in microbial ecology. *Microsc Anal (Europe Ed)* 29, 31–33 (1992)

Nogués C, Martí M, Boada M, Ponsà M: A simple method for processing individual oocytes and embryos for electron microscopy. *J Microsc* 174, 51–54 (1994)

Paerl HW, Bebout BM, Currin CA, Fitzpatrick MW, Pinckney JL: Nitrogen fixation dynamics in microbial mats. In *Microbial mats: Structure, development and environmental significance* (Eds. Stal L, Caumette P). *NATO ASI Series G: Ecological Sciences,* Springer-Verlag, Heidelberg 35, (1994) 325–337

Reynolds ES: The use of lead citrate at high pH as an electron-opaque stain in electron microscopy. *J Cell Biol* 17, 208–212 (1963)

Singer ME, Finnerty NR: Microbial metabolism of straight-chain and branched alkanes. In *Petroleum Microbiology.* (Ed. Atlas RM). MacMillan Publishing Co., New York 1, (1984) 1–53

Solé A, Gaju N, Guerrero R, Esteve I: Confocal laser scanning microscopy of Ebro delta microbial mats. *Microsc Anal* 29, 13–15 (1998)

Solé A, Gaju N, Méndez-Alvarez S, Esteve I: Confocal laser scanning microcopy as a tool to determine cyanobacteria biomass in microbial mats. *J Microsc* 204, 3, *258*–262 (2001)

Solé A, Gaju N, Esteve I: The biomass dynamics of cyanobacteria in an annual cycle determined by confocal laser scanning microscopy. *Scanning* 25, 1–7 (2003)

Stal LJ: Physiological ecology of cyanobacteria in microbial mats and other communities. *New Phytol* 131, 1–32 (1995)

Stolz JF: Light and electron microscopy in microbial mat research: An overview. In *Microbial Mats: Structure, Development and Environmental Significance* (Eds. Stal L, Caumette P). *NATO ASI Series G: Ecological Sciences,* Springer-Verlag, Heidelberg 35, (1994) 173–182

van Gemerden H, Beeftink HH: Ecology of phototrophic bacteria, In *Studies in Microbiology.* (Ed. Ormerod JG) Blackwell Scientific Publications, Oxford (1983) 146–185

Wieland A, Kühl M, McGowan L, Fourçans A, Duran R, Caumette P, Garcia de Oteyza T, Grimalt JO, Solé A, Diestra E, Esteve I, Herbert R A: Microbial Mats on the Orkney Islands Revisited: Microenvironment and Microbial Community Composition. *Microbial Ecol* 46, 371–390 (2003)

Vertical migrations of phototrophic bacterial populations in a hypersaline microbial mat from Salins-de-Giraud (Camargue, France)

Journal:	*FEMS Microbiology Ecology*
Manuscript ID:	FEMSEC-05-08-0289
Manuscript Type:	Research Paper
Date Submitted by the Author:	12-Aug-2005
Complete List of Authors:	Fourçans, Aude; Univesrité de Pau, laboratoire Ecologie Moleculaire Solé, Antoni; Autonomous University of Barcelona, Department of Genetics and Microbiology Diestra, Elia; Autonomous University of Barcelona, Department of Genetics and Microbiology Ranchou-Peyruse, Anthony; Université de Pau, Laboratoire ecologie moleculaire Esteve, Isabel; Autonomous University of Barcelona, Department of Genetics and Microbiology Duran, Robert; Université de Pau, Laboratoire ecologie moleculaire Caumette, Pierre; Université de Pau, Laboratoire ecologie moleculaire
Keywords:	hypersaline mat, phototrophs , diel cycle , T-RFLP, CLSM, stratification

Vertical migrations of phototrophic bacterial populations in a hypersaline microbial mat from Salins-de-Giraud (Camargue, France)

Fourçans, A.[1], Solé, A.[2], Diestra, E.[2], Ranchou-Peyruse, A.[1], Esteve, I.[2], Caumette, P.[1] and Duran, R[1,*]

Running title: Vertical migration of phototrophs in microbial mat

[1] Laboratoire d'Ecologie Moléculaire EA 3525, Université de Pau et des Pays de l'Adour, avenue de l'Université, BP 1155, F-64013 Pau Cedex, France

[2] Department of Genetics and Microbiology, Autonomous University of Barcelona, E-08193 Bellaterra, Spain

[*] Corresponding author: Prof Robert DURAN - email: robert.duran@univ-pau.fr

Phone: +33 5 59 40 74 80 - Fax: +33 5 59 40 74 94

Keywords : hypersaline mat, phototrophs, diel cycle, T-RFLP, CLSM, stratification.

Abstract

The spatio-temporal distribution of phototrophic communities of the hypersaline photosynthetic Camargue microbial mat (Salins-de-Giraud, France) was investigated during a diel cycle by combining microscopic and molecular approaches. *Microcoleus chthonoplastes*, the dominant cyanobacterium of the oxyphototrophic community, was followed with Confocal Laser Scanning Microscopy. Its vertical distribution varied from a homogenous distribution during the night, when the oxic zone is restricted to the upper 0.5 mm, to a specific localization to the upper oxic zone of 1.5 mm during daytime. It is likely that thanks to a set of adaptative responses that include migration and metabolism shifts, *Microcoleus chthonoplastes* benefit from the diel fluctuation of environmental parameters. Terminal Restriction Fragment Length Polymorphism of PCR-amplified *pufM* gene fragments revealed three groups of anoxyphototrophic populations. The first group of at least fourteen populations specific for each period, the second group of at least four populations homogenously distributed whatever the period and the third group of at least six populations located at different horizons in function of the period considered. Thus, vertical migration, aggregate formation and metabolic switches were the most evident defense of the photosynthetic populations against adverse effects of sulfide and oxygen fluxes during a diel cycle.

1. Introduction

Microbial mats are cohesive microbial communities growing at solid-aqueous interfaces, in environments as diverse as intertidal coastal sediments [1-3], hypersaline ponds [4-6] , or thermal springs [7]. Oxygenic and anoxygenic phototrophic microorganisms play a dominant role in these structures. Cyanobacteria, located at the surface, have been described as the chief primary producers. They constitute the basic matrix and stabilize the microbial mat by forming an intertwined filamentous complex network [8]. The gliding cyanobacterium *Microcoleus chthonoplastes* was described as dominant in hypersaline environments [9, 10] , marine intertidal microbial mats [11] and in hot deserts [12]. In the deeper anoxic layers of the mat, phototrophic sulfur bacteria take part in the energy flow because they perform simultaneously detoxification of H_2S and photoassimilation of CO_2 [13]. During the diel cycle, the chemical gradients change dramatically exposing bacteria to variable environmental conditions [14, 15]. By migration, bacteria escape from extreme conditions and therefore can benefit from optimal habitats for their development [16, 17]. Although vertical migrations have been previously reported for bacteria inhabiting microbial mats such as sulfur-oxidizing bacteria [18-20], sulfate-reducing bacteria [21, 22] and cyanobacteria [18, 20, 22-27], it is still difficult to evaluate which depth-dependent parameters (light intensity and spectral composition, temperature, pH, electron donors and acceptors, carbon sources, etc.) control the vertical distribution. Recently, we reported a general description of bacterial communities from Camargue microbial mats [5] showing a correlation between the bacterial organization and the environmental parameters at micro-scale level. Further observations of phototrophic community migration are needed to fully understand the behavior of these populations in response to changing environmental conditions.

We report here on the spatio-temporal distribution of anoxygenic and oxygenic phototrophic populations in the Camargue microbial mat from Salins-de-Giraud during a diel

cycle. Because of the complex structure of microbial mats, we applied molecular and microscopic techniques to assess the phototrophic bacterial groups selectively at a micro-scale level. The complex structure of filamentous cyanobacteria with abundant mucilage makes DNA extraction difficult resulting in an underestimation of this population [28]. Making use of their pigment content, we identified and quantified the cyanobacteria by analysis of optical sections at high-resolution employing Confocal Laser Scanning Microscopy (CLSM), which is more precise than chemical techniques of pigment quantification. To specifically target anoxyphototrophs, Terminal Restriction Fragment Length Polymorphism (T-RFLP) analysis of PCR amplified *pufM* gene was performed. Because this technique is more sensitive than techniques involving measurement of extracted pigments, it made possible a resolution of bacterial diversity at the genus level. We thus determined the *in situ* distribution of the phototrophic community in a mat and correlated its migration with environmental parameters as determined by use of microsensors.

2. Materials and methods

2.1 General information

A microbial mat in the Salins-de-Giraud saltern was analyzed in parallel with *in situ*, microsensor measurements (O_2, H_2S, pH) during a diel cycle in June 2001 [29]. The mat existed at a salinity range between 70 and 110 ‰ (w/v) [5].

2.2 Sampling procedure

We sampled microbial mats in a large shallow pond in the saltern of Salins-de-Giraud, close to the sand barrier and seacoast (43°27’35’’ N, 04°41’28’’ E, Camargue, France). Several samples were collected at different times (9:40h, 15:00h, 18:00h, 22:00h, 4:00h and 7:30h) during a diel cycle from 11 to 12 June 2001 using falcon tubes as coring devices.

For T-RFLP, triplicate samples of mat cores (35 mm i.d.) were collected, at 15:00h and 4:00h. The upper 10 mm of the mat core was sliced off aseptically, transferred into sterile Petri dishes, frozen in liquid nitrogen, transported on dry ice and finally stored at –80°C until further analysis. These frozen samples were then sliced with a cryomicrotome (MICROM Gmbh, Walldorf, Germany). Slices of approximately 100 µm thickness for the two first millimeters, and 200 µm thickness for the next two millimeters were generated. Based on prior results from microsensor measurements [29], 11 horizons within the top fourth millimeters from the surface were chosen. Three replicates from each horizon were analyzed to characterize bacterial communities. Genomic DNA was extracted from these different slices and vertical distribution of microbial communities for each depth was determined by T-RFLP.

For CLSM analysis, sampled cores (18 mm in length) at each sampling time were placed in a small plastic tube containing 2,5 % (v/v) glutaraldehyde in a phosphate buffer (0,2 M, containing 90 ‰ NaCl), and stored at 4ºC until further processing. The different mat samples were analyzed by means of a Leica True Confocal Scanner TCS 4d (Leica Laser-Technik GmbH, Heidelberg, Germany) equipped with an argon-krypton laser. The use of this microscope facilitates the characterization and identification of cyanobacteria in microbial mats [30]. Subsamples were cut in vertical slices of defined dimensions taking into account the need to preserve the vertical stratification of the mat. Confocal images from three replicates, optical series and summa projections, were taken at every 250 µm depth in each vertical slice.

2.3 Cyanobacteria characterization

Characterization of the cyanobacterial diversity in every mat subsample by CLSM was performed directly on-screen in continuous mode and from the confocal images obtained.

Cyanobacteria were identified as previously described [5]. After cyanobacteria identification, the profiles of abundance for each of them were determined.

2.4 Biomass estimation of Microcoleus chthonoplastes

CLSM suma projection images corresponding to the different time profiles (three replicates at each 250 μm depth) were transformed to binary images (black/white) using Adobe Photoshop 6.0 for Windows. In these images, black contours of *M. chthonoplastes* were selected from among all other cyanobacteria contours, which were erased from them. The intercrossed black contours usually involve white areas. In the new image, a black, one-pixel wide line was also erased to avoid that these white areas were also count as *M. chthonoplastes.* Morphological data of the perimeter and area for every *M. chthonoplastes* outline were obtained through the UTHSCSA Image Tool 3.0, an image processing and analysis program, and exported to a Microsoft Excel 97 book. Values for length, width and biovolume were calculated in accordance with the expressions described in [31]. The quotient between the biovolume of *M. chthonoplastes* and the volume of sediment analyzed was multiplied by a factor of 310 fg C/μm^3 to convert these data to biomass. Averages of biomass data from three replicates and for each subsample studied were calculated. Results were expressed in mg C/cm^3 sediment. Finally, we determined the spatio-temporal biomass variations of *M. chthonoplastes*.

2.5 T-RFLP (Terminal Restriction Fragment Length Polymorphism)

From each selected horizon of the mat, genomic DNA was extracted with the UltraClean Soil DNA Isolation Kit (MoBio Laboratories, Carlsbad, USA), according to the recommendations of the supplier; except in the first step in which EDTA was added at a final concentration of 10mM, to avoid degradation of genomic DNA. All extracted genomic DNA

samples were stored at -20°C until further processing. For T-RFLP analysis, we specifically targeted the purple anoxygenic phototrophs with the primers set pb557f-pb750r, which amplifies a *pufM* DNA gene fragment [32]. For T-RFLP analysis, forward (f) and reverse (r) primers were fluorescently labeled with TET and HEX respectively. The restriction enzyme used in T-RFLP analysis was *Hae*III (New England Biolabs, Beverly UK). Fragment analysis was performed with an ABI Prism 310 (Applied Biosystems, Foster city, USA). Triplicates for each layer were analyzed to avoid analytical artifacts and assure the reproducibility of the method. Dominant terminal restriction fragments (T-RFs) greater than 100 fluorescent units in intensity and present in each replicate were selected. Predictive digestions were performed on all *PufM* sequences known in order to assign the different T-RFs to a certain genus or species.

T-RFLP profiles were normalized by calculating relative abundances from fluorescence intensity of each T-RFs. Normalized T-RFLP profiles were compared by correspondence factorial analysis (CFA).

2.6 Statistical analysis

All depth T-RFLP profiles were compared by Correspondence Factorial Analysis (CFA). We assessed the extend of correlation of diversity, with biomass of *Microcoleus chthonoplastes* estimated by CLSM, and with environmental parameters (oxygen, pH, H_2S, S_{tot}) determined in a previous study during the same diel cycle [29] by the use of Canonical Correspondence Analysis (CCA). These multivariable statistical analyses are ordination methods by similarity matrix that reduces in two or three dimensions the dispersion diagram of samples compared [5, 33]. Relatives T-RF values were calculated from each T-RFLP profile and listed in a table for statistical analysis. CFA and CCA were performed with MVSP v3.12d software (Kovach Computing Service, Anglesey, Wales) [34].

3. Results

3.1 Vertical distribution of oxygenic phototrophic bacteria in Camargue mat

Four major types of filamentous cyanobacteria were observed using CLSM. *Microcoleus chthonoplastes* and *Halomicronema excentricum* were the most abundant. The third type was an unidentified picocyanobacterium forming filaments of approximately 0.96 µm diameter. The fourth type was *Pseudanabaena* sp., which was the less abundant. In addition, some unicellular cyanobacteria were identified, which were members of the *Gloeocapsa* and *Pleurocapsa* groups. The relative abundances of these cyanobacteria at different depths of the mat were determined during a diel cycle (Fig. 1). *M. chthonoplastes* was distributed throughout the mat, more abundant near the surface during daytime. *Halomicronema excentricum*, typical of high salinity environments, was distributed throughout the mat during the day while it was mainly located between 0 and 1.5 mm depth during the night. The maximum abundance of the picocyanobacterium was observed in the deeper zone (between 2 and 4 mm). *Pseudanabaena* sp. was found at depth 3.25 mm only in the morning (9:40 h). Cyanobacteria of the *Gloeocapsa*-group were found at different depth, 0.5 and 2 mm (15:00 h), 0.25 mm (22:00 h) and 0.75 mm (4:00 h) whereas those of the *Pleurocapsa*-group were found at various depths at 4:00 h. Fig. 1 also reveals that *Microcoleus chthonoplastes*, the most widely distributed cyanobacterium, showed important temporal changes. Therefore, its migration within the mat during a diel cycle was followed by biomass analysis. *Microcoleus chthonoplastes* is characterized by typical bundles with several trichomes oriented in parallel with cells longer than wide and with visible constrictions at the cross-walls (Fig. 2). Its spatio-temporal distribution is presented in Fig. 3. At 9:40h, *M. chthonoplastes* was present in the entire mat showing its maximum biomass (39.7 mgC/cm^3 sediment) at 1 mm depth and at two other zones, 1.75 mm (24.27 mgC/cm^3 sediment) and 2.5 mm depth (29.53 mgC/cm^3 sediment). At 15:00h, the filaments were principally distributed in the surface part with a

concentration of 31.22 mgC/cm^3 sediment and at 1.75 mm depth (28.91 mgC/cm^3 sediment). At 18:00h, *M. chthonoplastes* reached the mat surface (0.5 mm) with a maximum concentration (52.80 mgC/cm^3 sediment), while its concentration was low at the deepest zone (3 mm). During the night (22:00h), after sunset *M. chthonoplastes* filaments were mainly localized at depths between 0 and 1.5 mm, and decreased to undetectable levels below 2.25 mm. At 4:00h, *M. chthonoplastes* filaments were homogeneously distributed throughout the 3 mm of the microbial mat. Finally at 7:30h, the distribution of *M. chthonoplastes* was similar to that at 9:40h, with a maximum biomass of 35.25 mg C/cm^3 sediment at depths between 0.75 mm and 1 mm, a 25.88 mg C/cm^3 sediment at depth of 1.75 mm, and 10.49 mg C/cm^3 sediment at a depth of 2.5 mm.

3.2 Vertical distribution of anoxygenic phototrophic bacteria in the Camargue mat

The distribution of the phototrophic anoxygenic bacteria (PAB) within the mat was analyzed during a diel cycle by T-RFLP targeting the functional *pufM* gene that encodes for a subunit of the photosynthetic center of purple bacteria. The study was performed at two contrasted hours (15:00h and 4:00h) showing opposite oxygen/sulfide gradients [29].

T-RFLP profiles revealed an important diversity of the PAB communities within the mat, with 24 different OTUs (Operational Taxonomic Unit) detected by digestion with *Hae*III. The overall organization of anoxyphototroph populations changed between daylight (15:00h) and early morning (4:00h) (Fig. 4). When the distributions of the OTUs were compared between day and night, the OTUs were dispatched in three groups. The first group formed by OTUs specific for each period (15:00h: OTUs 93, 119, 167, 202, 225 bp; 4:00h: OTUs 36; 46, 90, 125, 132, 156, 177, 197, 212 bp). The second group constituted by OTUs that had developed homogeneously within the 4 mm, independent of the diel cycle (OTUs 117, 129, 199, and 228 bp). *Hae*III predictive digestion of all *pufM* sequences available correlated the OTU of 129 bp

with the chemotrophic bacteria *Erythrobacter litoralis.* The third group constituted by OTUs present at both hours, but located in different horizons. Some of them showed important differences in their distribution. OTU of 104 bp was limited to the oxic zone (0-0.4 mm) at 15:00h, but at 4:00h it was also found in anoxic zones (1.2-1.3 mm and 3.8-4 mm) even though still abundant in the 0-0.4 mm layer. Interestingly, at 22:00h its zonation was in an intermediate horizon at 0 to 1.6 mm (data not shown). The OTU of 137 bp may be related to the purple non sulfur bacteria *Roseospira marina*, present in the whole 4 mm of the mat in daytime, was observed in the mid anoxic layer (1.2-1.3 mm) at 4:00h. OTU of 192 bp was present in an oxic zonation between 0.9-1.6 mm at 15:00h whereas it was just confined in the anoxic layer (1.5-1.6 mm) at 4:00h. Whereas OTUs of 114, 148, 187 bp were detected only in anoxic zones during the day, they were also found at the surface or spread throughout the mat at night.

Correspondence Factorial Analysis (CFA) obtained from T-RFLP data supported the observation that the distribution of the PAB populations in the mat depended on the diel period (Fig. 5), emphasizing three distinct clusters. Communities from each layer of the 4:00h situation were grouped together, except those from the two layers 0.3-0.4 mm and 1.2-1.3 mm. In contrast these PAB communities were close to a second cluster formed by most communities from the mat layers at 15:00h situation. The communities of the deep layer (3.4-3.6 mm) of the mat during the day appeared to be independent from the other two groups, mainly influenced by axis 2 showing a variance of 11.82 %. Among the OTUs corresponding to axis 2, the OTU of 199 bp (*Hae*III) may be related to the purple sulfur bacteria *Halochromatium salexigens* and to a purple non sulfur bacteria recently isolated from this marsh (data not shown).

The mat of 4:00h is characterized by the presence of OTUs of 114, 129 and 132 bp, part of axis 1, and OTU 148 bp, part of axis 2. The mat of 15:00h is influenced by others OTUs

corresponding to the T-RFs of 129, 137, 202, 228 bp and, 117, 199 bp composing axis 1 and 2 respectively. These OTUs could not be correlated to known PAB species.

4. Discussion

4.1. Diel migration of Microcoleus chthonoplastes

M. chthonoplastes, a typical inhabitant of hypersaline environments [4, 35], was the most abundant cyanobacterium showing large temporal changes. Its vertical distribution varied from a homogenous distribution (at 4:00h and at 7:30h) after a period of darkness (6-9 h) to a specific localization near the surface (at 18:00h) after an approximately 12 h illumination period (Fig. 3). These observations, consistent with the fact that *M. chtonoplastes* is a gliding bacterium, suggest that *M. chtonoplastes* has vertical migratory movements during a diel cycle. During the night, *M. chthonoplastes* was able to maintain its position in the mat probably by its capacity to carry out alternative metabolisms such as fermentation in the dark, or sulfur respiration [36]. During the day (from 9:40h to 18:00h), it was located in different zones indicating probably that this bacterium has a versatile metabolism that is consistent with previous studies [30, 37, 38]. It was not surprising to detect *M. chthonoplastes* in oxic and anoxic zones since this bacterium is able to perform both oxygenic and anoxygenic photosynthesis and to grow at sulfide concentrations lower than 974 µM [37] never reached in the Camargue mat [29]. This observation could also suggest that two distinct subpopulations with different metabolisms may coexist in an intermediate situation to take advantage of a large range of energy sources.

4.2. Diel migration of Anoxyphototrophs communities

Wieland and co-workers [29] have characterized the biogeochemistry of the Camargue mat during a diel cycle, describing two opposite periods. First, in the afternoon a clearly defined

upper oxic zone of 1.5 mm occurred above an anoxic region down to a depth of 4 mm. Second, in the night the oxic zone restricted to the upper 0.5 mm of the mat was penetrated with sulfide while below the mat (0.5 mm-4 mm) became completely anoxic. Changes in the Phototrophic Anoxygenic Bacteria (PAB) communities observed during the diel cycle can be explained by the variation of the physico-chemical gradients. The predominance of specific OTUs at each hour suggested that the type of bacterial metabolism operating may be specifically adapted to the prevailing environmental conditions. It is likely that some of these OTUs correspond to bacterial types with an ability to escape adverse conditions. To further understand their role in the general functioning of the mat it is of great interest to follow specifically their migration. Bacterial migration was also observed with OTUs found in both periods but localized in different horizons (OTUs 104, 114, 137, 148, 187, 192 bp). By vertical migration they reach optimal or tolerable conditions of growth. The migration probably results in a cluster formation in a specific zone of the mat when conditions are adverse as opposed to dispersion when conditions are favorable.

4.3. Dynamics of the microbial mat during a diel cycle

4.3.1. Parameters influencing the PAB distribution

A Canonical Correspondence Analysis (CCA; Fig. 6) correlated the data obtained in this study to biogeochemical data measured in parallel by Wieland et al. [29]. CCA revealed the influence of main parameters on the PAB community structure. In the afternoon (15:00h), it was mainly influenced at depth but not at the surface by sulfide. Indeed, in contrast to the early morning (4:00h), oxygen and sulfide gradients were well defined in the afternoon showing a well established oxygen-sulfide interface. Oxygen, pH, and biomass of *M. chthonoplastes* were defined as negative factors in the development of the PAB. *M. chthonoplastes* and other cyanobacteria may influence the PAB distribution both directly by

their presence as competitor and indirectly via their metabolic activities. Oxygenic photosynthesis in mat surface at day produces oxygen with a concomitant increase of pH up to 9.4 in the first 1.5 mm [29] producing adverse conditions for PAB. The decrease in oxygen and in pH to 6.8 during night, both of which result from the cessation of photosynthetic activity, favor maintenance of cell integrity of PAB as described for *Chromatium* sp. [39].

4.3.2. Behavior of photosynthetic communities

The diel fluctuations of the gradients of electron donors and acceptors at microscale across this microbial mat induces an important change on the distribution of photosynthetic communities. Few reports have described the behaviors of diverse phototrophic bacteria, oxygenic and anoxygenic, in response to changing environmental conditions [18, 30, 40-42,]. Bacteria are able to escape adverse conditions through mobility controlled by chemotatic mechanisms. Although phototaxis is the main mechanism controlling the position of cyanobacteria [18, 30], the overall cyanobacterial distribution across the mat may also depend on others taxis mechanisms such as oxygen or sulfide taxis. Sulfide may strongly influence the distribution of cyanobacteria since it is an inhibitor of oxygenic photosynthesis [41, 42] notwithstanding that cyanobacteria may vary in sulfide tolerance [43]. The Camargue mat is dominated by *M. chthonoplastes*, a versatile bacterium that is probably divided in two subpopulations. A subpopulation highly sensitive to sulfide was located in a mat area without sulfide and a second subpopulation tolerant to high sulfide concentration (around 200 µM) was observed at two-millimeter depth.

The changes of the PAB distribution revealed different behaviors of anoxyphototrophs in response to environmental changes during the diel cycle. First, several migration movements of PAB were observed resulting mainly in aggregate formation, probably in response to adverse conditions. Some OTUs formed aggregates at night (OTUs 137 and 192 bp)

migrating from oxic to a strongly anoxic zone of the mat. Recently we described the marine purple non sulfur bacteria *Roseospira marina* which may be related to OTU of 137 bp as highly motile and unable to respire or ferment in the dark under anaerobic conditions [44]. Thus, the aggregation by this bacterium may be a means by which it maintains its cell integrity. Other OTUs aggregate at daytime (OTUs 114, 148 and 187 bp) but they were always located in the anoxic zone of the mat whatever the time of day. Since oxygen is toxic for obligate anoxyphototrophic bacteria, they control their position by aero-taxis [40]. Therefore, the bacteria corresponding to these OTUs may react by a negative chemotactic response. In contrast, OTU of 104 bp, migrating from a sulfidic anoxic zone to a strongly oxic and non sulfidic zone during the day, exhibited a positive chemotactic response to oxygen. This OTU may correspond to aerobic heterotrophic bacteria containing a non active *pufM* gene such as *Sphingomonas* or *Erythrobacter* genus [45]. Secondly, OTUs were present in the whole mat at any time in a diel cycle (OTUs of 117, 129, 199, and 228 bp), suggesting that these bacteria may have a versatile metabolism capable of adapting to changes in environmental conditions. Located close to the oxygen-sulfide interface, they may be related to microorganisms capable of chemotrophy, or fermentation in dark oxic or microoxic conditions, like some purple non sulfur bacteria, small-sized *Chromatiaceae*, *Ectothiorhodospiraceae,* or aerobic anoxygenic phototrophic bacteria [46, 47].

5. Conclusions

Where Camargue microbial mat develops, environmental conditions can change dramatically on a short term [29]. The results presented here demonstrated that the fluctuation of environmental parameters during a diel cycle influenced the vertical stratification of phototrophic communities throughout the microbial mat. Thanks to a set of adaptative responses that include migration and metabolism shifts, *Microcoleus chthonoplastes* benefit

from the diel fluctuation of environmental parameters and therefore was the dominant cyanobacterium of the oxyphototrophic mat community. The distribution of the anoxyphototrophic community, was influenced directly by competition with the high abundance of *Microcoleus chthonoplastes* and indirectly by the metabolism of *M. chthonoplastes*. Vertical diel migration of the anoxyphototrophic community in response to variations in sulfide and oxygen concentrations was detectable at a fine depth scaling. Our observation of such migration indicated that aero- and energy taxis were the main mechanisms controlling the bacterial positioning in the mat. Aggregate formation and metabolic switches were the most evident defense of the photosynthetic populations against adverse effects of sulfide and oxygen fluxes during a diel cycle.

Acknowledgments

We acknowledge the financial support by the EC (MATBIOPOL project, grant EVK3-CT-1999-00010) and the "Conseil Régional d'Aquitaine". The authors are grateful to the Company of Salins-du-midi at Salins-de-Giraud for facilitating access to the salterns, sampling and field experiments. AF is partly supported by a doctoral grant from the "Conseil General des Pyrénées Atlantiques".

References

[1] Esteve, I., Martínez M., Mir J., and Guerrero R. (1992) Typology and structure of microbial mats communities in Spain: A preliminary study. Limnetica 8, 185-195.

[2] Guerrero, R., Urmeneta J., and Rampone G. (1993) Distribution of types of microbial mats at the Ebro Delta, Spain. Biosystems 31, 135-144.

[3] Wieland, A., Kühl M., Mcgowan L., Fourçans A., Duran R., Caumette P., Solé A., Diestra E., Esteve I., García De Oteyza T., Grimalt J.O., and Herbert R.A. (2003) Microbial mats

on the Orkney islands revisited: microenvironment and microbial community composition. Microb. Ecol. 46, 371-390.

[4] Caumette, P., Matheron R., Raymond N., and Relexans J.C. (1994) Microbial mats in the hypersaline ponds of Mediterranean salterns (Salins-de-Giraud, France). FEMS Microbiol. Ecol. 13, 273-286.

[5] Fourçans, A., García de Oteyza T., Wieland A., Solé A., Diestra E., van Bleijswijk J., Grimalt J.O., Kühl M., Esteve I., Muyzer G., Caumette P., and Duran R. (2004) Characterization of functional bacterial groups in a hypersaline microbial mat community (Salins-de-Giraud, Camargue, France). FEMS Microbiol. Ecol. 51, 55-70.

[6] Giani, D., Seeler J., Giani L., and Krumbein W.E. (1989) Microbial mats and physicochemistry in a saltern in the Bretagne (France) and in a laboratory scale saltern model. FEMS Microbiol. Ecol. 62, 151-162.

[7] Ferris, M.J., Muyzer G., and Ward D.M. (1996) Denaturing gradient gel electrophoresis profiles of 16S rRNA-defined populations inhabiting a hot spring microbial mat community. Appl. Environ. Microbiol. 62, 340-346.

[8] D'Amelio, E.D., Cohen Y., and Des Marais D.J. (1987) Association of a new type of gliding, filamentous, purple phototrophic bacterium inside bundles of *Microcoleus chthonoplastes* in hypersaline cyanobacterial mats. Arch. Microbiol. 147, 213-220.

[9] Stal, L.J. (1994) Microbial mats in coastal environments, p. 21-32. In L. J. Stal, and P. Caumette (eds), Microbial Mats. ed. Berlin Heidelberg: Springer-Verlag.

[10] Stal, L.J., and Krumbein W.E. (1985) Isolation and characterization of cyanobacteria from a marine microbial mat. Bot. Mar. 28, 351-365.

[11] García-Pichel, F., Prufert-Bebout L., and Muyzer G. (1996) Phenotypic and phylogenetic analysis show *Microcoleus chthonoplastes* to be a cosmopolitan cyanobacterium. Appl. Environ. Microbiol. 62, 3284-3291.

[12] Campbell, S.E. (1979) Soil stabilization by a prokaryotic desert crust: implications for Precambrian land biota. Orig. Life 9, 335-348.

[13] Pfennig, N. (1975) The phototrophic bacteria and their role in the sulfur cycle. Plant and Soil 43, 1-16.

[14] Revsbech, N.P., Jørgensen B.B., Blackburn T.H., and Cohen Y. (1983) Microelectrode studies of the photosynthesis and O2, H2S and pH profiles of a microbial mat. Limnol. Oceanogr. 28, 1062-1074.

[15] van Gemerden, H. (1993) Microbial mats: A joint venture. Mar. Geol. 113, 3-25.

[16] Alexandre, G., Greer-Phillips S., and Zhulin I.B. (2004) Ecological role of energy taxis in microorganisms. FEMS Microbiol. Rev. 28, 113-126.

[17] Taylor, B.L., Zhulin I.B., and Johnson M.S. (1999) Aerotaxis and other energy-sensing behavior in bacteria. Annu. Rev. Microbiol. 53, 103-128.

[18] García-Pichel, F., Mechling M., and Castenholz R.W. (1994) Diel migrations of microorganisms within a benthic, hypersaline mat community. Appl. Environ. Microbiol. 60, 1500-1511.

[19] Nelson, D.C., Jørgensen B.B., and Revsbech N.P. (1986) Growth pattern and yield of a chemoautotrophic *Beggiatoa* sp. in oxygen-sulfide microgradients. Appl. Environ. Microbiol. 52, 225-233.

[20] Thar, R., and Kühl M. (2001) Motility of *Marichromatium gracile* in response to light, oxygen, and sulfide. Appl. Environ. Microbiol. 67, 5410-5419.

[21] Krekeler, D., Teske A., and Cypionka H. (1998) Strategies of sulfate-reducing bacteria to escape oxygen stress in a cyanobacterial mat. FEMS Microbiol. Ecol. 25, 89-96.

[22] Teske, A., Ramsing N.B., Habicht K., Fukui M., Kuver J., Jørgensen B.B., and Cohen Y. (1998) Sulfate-reducing bacteria and their activities in cyanobacterial mats of solar lake (Sinai, Egypt). Appl. Environ. Microbiol. 64, 2943-2951.

[23] Bebout, B., and Garcia-Pichel F. (1995) UV B-induced vertical migrations of cyanobacteria in a microbial mat. Appl. Environ. Microbiol. 61, 4215-4222.

[24] Nelson, D.C., Revsbech N.P., and Jørgensen B.B. (1986) Microoxic-anoxic niche of *Beggiatoa* spp.: microelectrode survey of marine and freshwater strains. Appl. Environ. Microbiol. 52, 161-168.

[25] Richardson, L.L. (1996) Horizontal and vertical migration patterns of *Phormidium corallyticum* and *Beggiatoa* spp. associated with black-band disease of corals. Microb. Ecol. 32, 323-335.

[26] Richardson, L.L., and Castenholz R.W. (1987) Diel vertical movements of the cyanobacterium *Oscillatoria terebriformis* in a sulfide-rich microbial mat. Appl. Environ. Microbiol. 53, 2142-2150.

[27] Whale, G.F., and Walsby A.E. (1984) Motility of the cyanobacterium *Microcoleus chthonoplastes* in mud. Phycol. J. 19, 117-123.

[28] López-Cortés, A., García-Pichel F., Nübel U., and Vázquez-Juárez R. (2001) Cyanobacterial diversity in extrem environments in Baja California, Mexico: a polyphasic study. Int. Microbiol. 4, 227-236.

[29] Wieland, A., Zopfi J., Benthien M., and Kühl M. (2005) Biogeochemistry of an iron-rich hypersaline microbial mat (Camargue, France). Microb. Ecol. 49, 34-49.

[30] Solé, A., Gaju N., and Esteve I. (2003) The biomass dynamics of cyanobacteria in an annual cycle determined by confocal laser scanning microscopy. Scanning 25, 1-7.

[31] Solé, A., Gaju N., Mendez-Alvarez S., and Esteve I. (2001) Confocal laser scanning microscopy as a tool to determine cyanobacteria biomass in microbial mats. J. Microscopy 204, 258-261.

[32] Achenbach, L.A., Carey J., and Madigan M.T. (2001) Photosynthetic and phylogenetic primers for detection of anoxygenic phototrophs in natural environments. Appl. Environ. Microbiol. 67, 2922-2926.

[33] Gauch, J.H.G. (1982) Multivariate Analysis in Community Ecology, New York, p. 298.

[34] Kovach, W. L. (1999) MVSP - a Multivariate Statistical Package for Windows. In. Wales U.K.: Kovack Computing Services.

[35] Abed, R.M., Garcia-Pichel F., and Hernández-Mariné M. (2002) Polyphasic characterization of benthic, moderately halophilic, moderately thermophilic cyanobacteria with very thin trichomes and the proposal of *Halomicronema excentricum* gen. nov., sp. nov. Arch. Microbiol. 177, 361-370.

[36] Moezelaar, R., Bijvank S.M., and Stal L. (1996) Fermentation and sulfur reduction in the mat-building cyanobacterium *Microcoleus chthonoplastes*. Appl. Environ. Microbiol. 62, 1752-1758.

[37] De Wit, R., and Van Gemerden H. (1987) Oxidation of sulfide to thiosulfate by *Microcoleus chthonoplastes*. FEMS Microbiol. Lett. 45, 7-13.

[38] Decho, A.W. (1990) Microbial exopolymer secretions in ocean environments: their role(s) in food webs and marine process. Oceanogr. Mar. Biol. Ann. Rev. 28, 73-153.

[39]van Gemerden, H., and Beeftink H.H. (1981) Coexistence of *Chlorobium* and *Chromatium* in a sulfide-limited continuous culture. Arch. Microbiol. 129, 32-34.

[40] Armitage, J.P., Keighley P., and Evans M.C.W. (1979) Chemotaxis in photosynthetic bacteria. FEMS Microbiol. Lett. 6, 99-102.

[41] Miller, S.R., and Bebout B.M. (2004) Variation in sulfide tolerance of photosystem II in phylogenetically diverse cyanobacteria from sulfidic abitats. Appl. Environ. Microbiol. 70, 736-744.

[42] Oren, A., Padan E., and Malkin S. (1979) Sulfide inhibition of Photosystem II in cyanobacteria (blue-green algae) and tobacco chloroplasts. Biochimica et Biophysica Acta (BBA) - Bioenergetics 546, 270-279.

[43] Cohen, Y., Jørgensen B.B., Padan E., and Shilo M. (1986) Adaptation to hydrogen sulfide of oxygenic and anoxygenic photosynthesis among cyanobacteria. Appl. Environ. Microbiol. 51, 398-407.

[44] Guyoneaud, R., Moune S., Eatock C., Bothorel V., Hirschler-Rea A., Willison J., Duran R., Liesack W., Herbert R., Matheron R., and Caumette P. (2002) Characterization of three spiral-shaped purple nonsulfur bacteria isolated from coastal lagoon sediments, saline sulfur springs, and microbial mats: emended description of the genus *Roseospira* and description of *Roseospira marina* sp. nov., *Roseospira navarrensis* sp. nov., and *Roseospira thiosulfatophila* sp. nov. Arch. Microbiol. 178, 315-324.

[45] Béjà, O., Suzuki M.T., Heidelberg J.F., Nelson W.C., Preston C.M., Hamada T., Eisen J.A., Fraser C.M., and DeLong E. F. (2002) Unsuspected diversity among marine aerobic anoxygenic phototrophs. Nature 415, 630–633.

[46] Pfennig, N., and Truper H.G. (1983) Taxonomy of phototrophic green and purple bacteria: a review. Ann Microbiol (Paris) 134B, 9-20.

[47] Yurkov, V.V., and Beatty J.T. (1998) Aerobic anoxygenic phototrophic bacteria. Microbiol. Mol. Biol. Rev. 62, 695-724.

Figures

Fig. 1. Relative Abundance in depth of the different cyanobacteria characterized by CLSM during the diel cycle in Camargue mat. The relative abundance is expressed in %.

Fig. 2. Confocal image of *Microcoleus chthonoplastes* forming bundles of filaments. Scale bar = 5 µm.

Fig. 3. Biomass profiles of *Microcoleus chthonoplastes* during the diel cycle. The biomass is expressed in mgC/cm^3 sediment.

Fig. 4. Relative abundance of T-RF for each horizon of the mat at 4:00h and 15:00h. Data were obtained from 5' end T-RFLP profiles by *Hae*III digestion of *pufM* amplified fragments.

Fig. 5. Correspondence Factorial Analysis (CFA) of the purple anoxygenic bacterial communities (PAB) of each layer of the mat at 15:00h (closed symbol) and 4:00h (open symbol). Each community was represented by a 5'end T-RFLP pattern corresponding to the *Hae*III digest of the *pufM* encoding gene.

Fig. 6. Canonical Correspondence Analysis (CCA) between the PAB communities of each layer of the mat at 15:00h (closed symbol) and 4:00h (open symbol), and environmental variables measured at these two hours: biomass of *Microcoleus chthonoplastes* (Biomass), pH, and concentration of O_2, H_2S and S_{tot} (sulfide total).

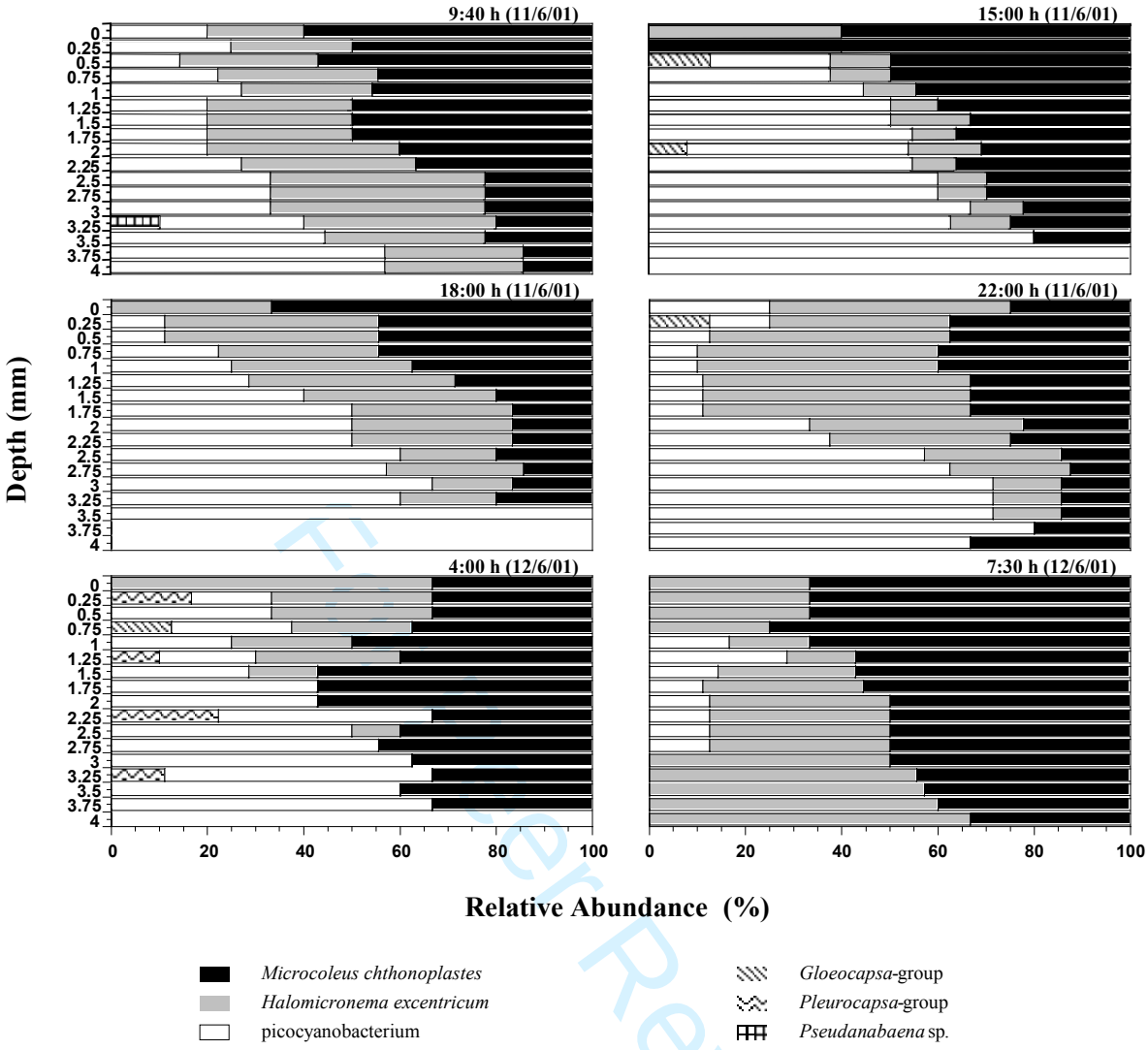

Fig. 1

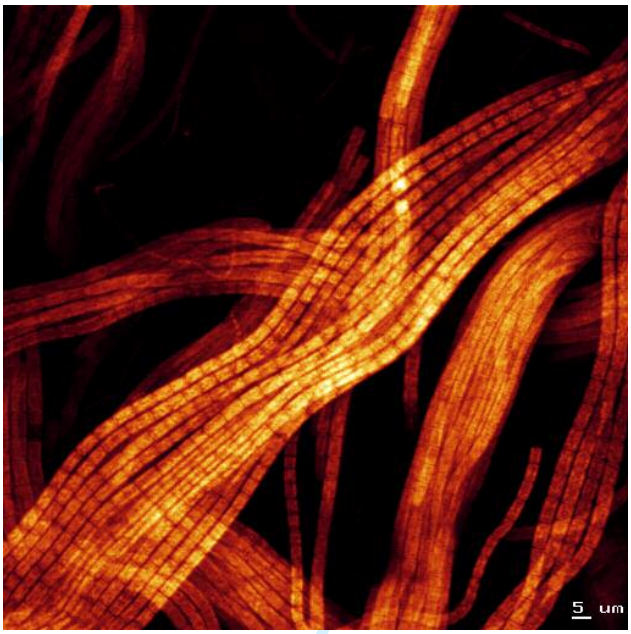

Fig. 2

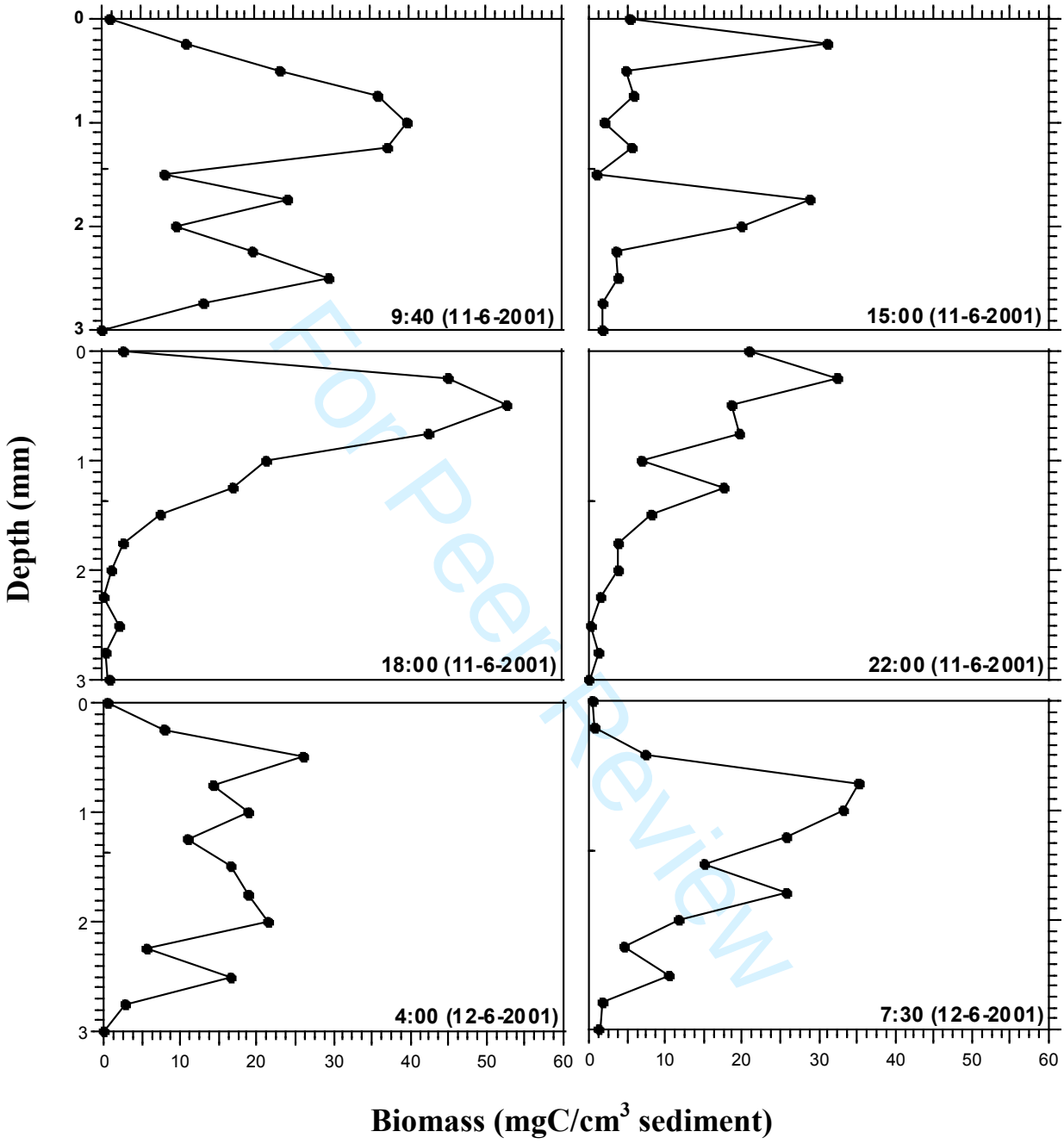

Fig. 3

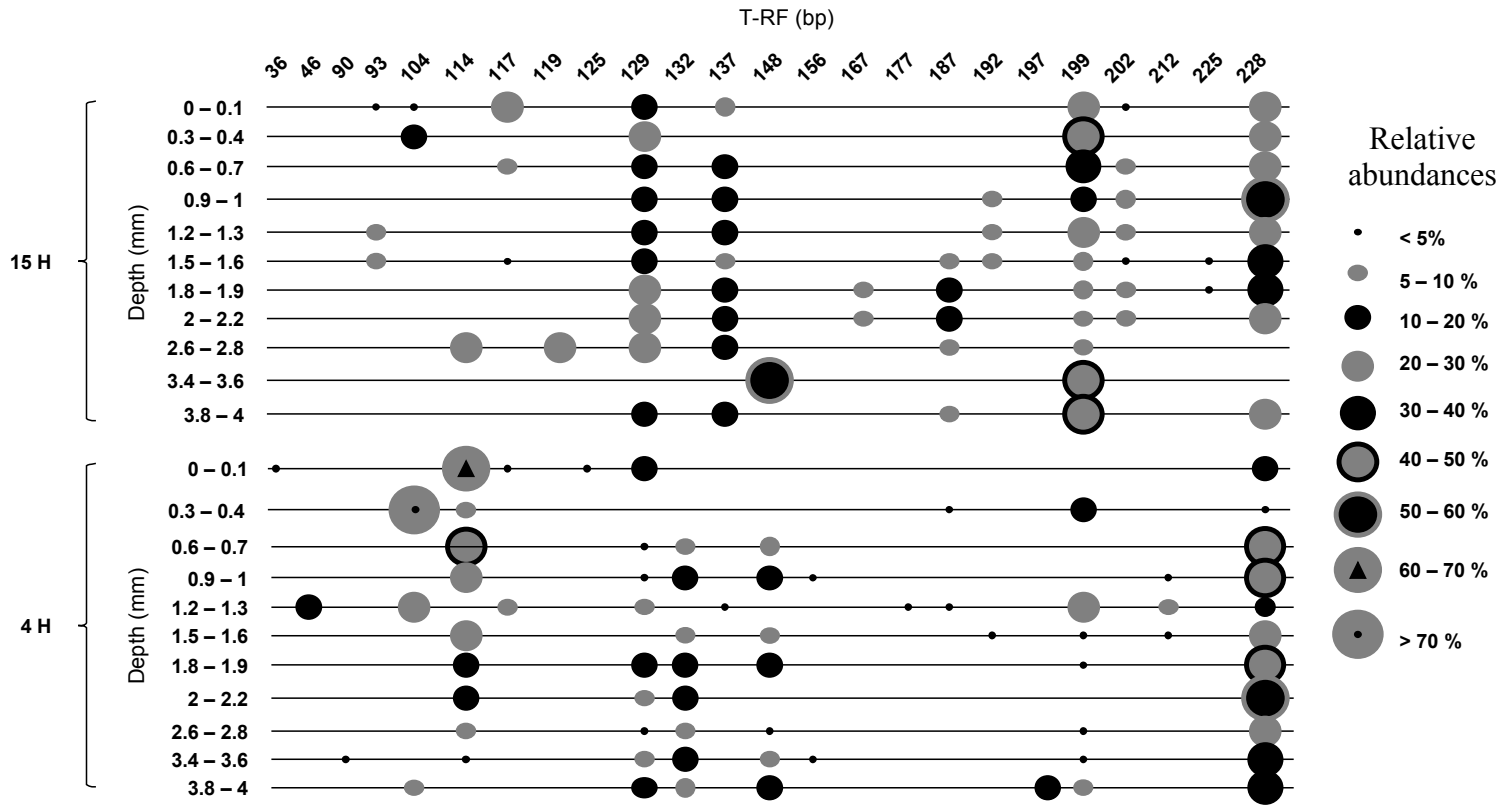
T-RF (bp)
36 46 90 93 104 114 117 119 125 129 132 137 148 156 167 177 187 192 197 199 202 212 225 228
15 H
4 H
Depth (mm)
0 – 0.1
0.3 – 0.4
0.6 – 0.7
0.9 – 1
1.2 – 1.3
1.5 – 1.6
1.8 – 1.9
2 – 2.2
2.6 – 2.8
3.4 – 3.6
3.8 – 4
Relative abundances
< 5%
5 – 10 %
10 – 20 %
20 – 30 %
30 – 40 %
40 – 50 %
50 – 60 %
60 – 70 %
> 70 %

Fig. 4

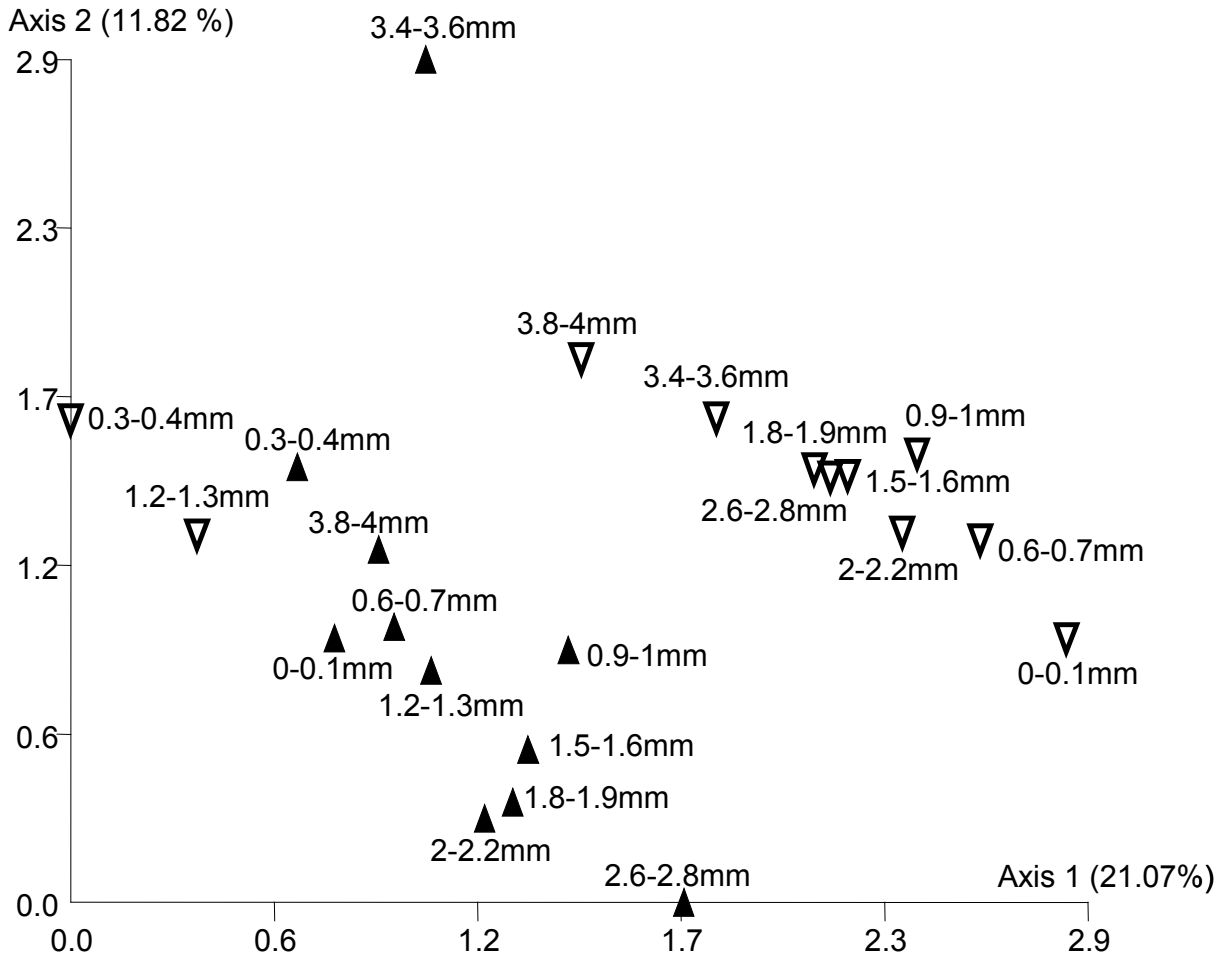
Axis 2 (11.82 %)
2.9
2.3
1.7
1.2
0.6
0.0
0.0
0.6
1.2
1.7
2.3
2.9
Axis 1 (21.07%)
3.4-3.6mm
3.8-4mm
3.4-3.6mm
0.3-0.4mm
0.3-0.4mm
1.8-1.9mm
0.9-1mm
1.5-1.6mm
1.2-1.3mm
3.8-4mm
2.6-2.8mm
2-2.2mm
0.6-0.7mm
0.6-0.7mm
0-0.1mm
0.9-1mm
0-0.1mm
1.2-1.3mm
1.5-1.6mm
1.8-1.9mm
2-2.2mm
2.6-2.8mm

Fig. 5

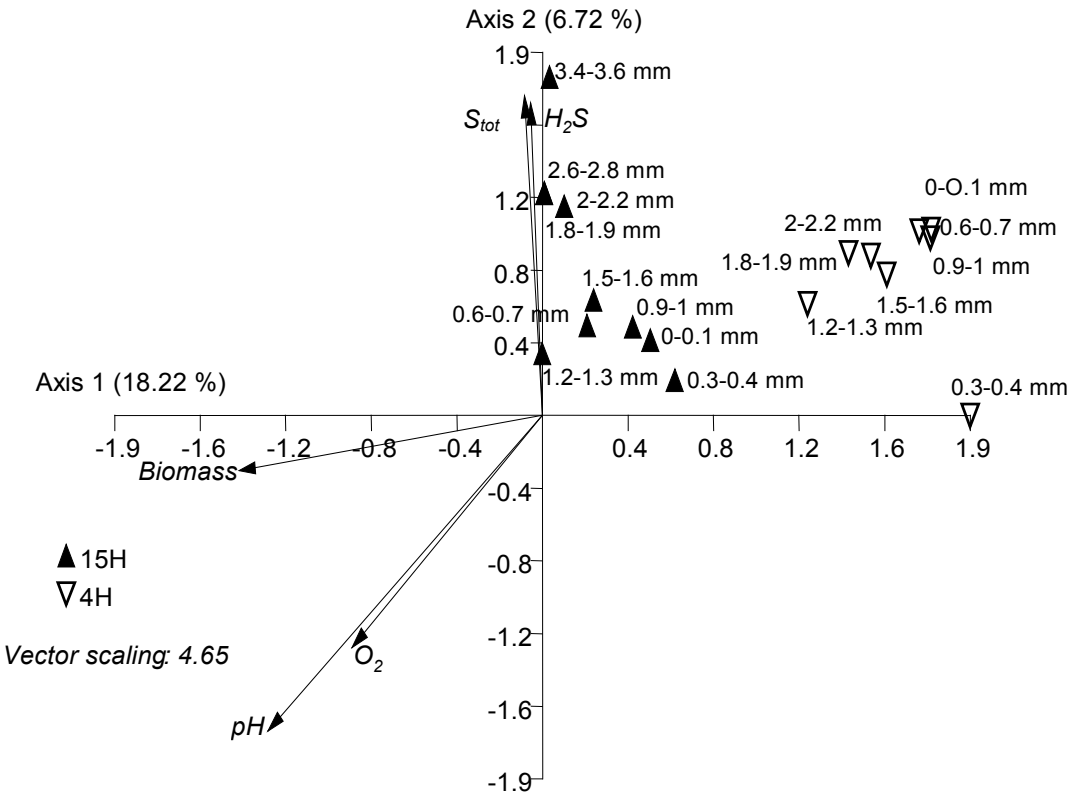

Fig. 6